uOttawa

L'Université canadienne
Canada's university

FACULTÉ DES ÉTUDES SUPÉRIEURES ET POSTOCTORALES

uOttawa

L'Université canadienne
Canada's university

FACULTY OF GRADUATE AND POSDOCTORAL STUDIES

Nilesh Patel

AUTEUR DE LA THÈSE / AUTHOR OF THESIS

Ph.D. (Chemical Engineering)

GRADE / DEGREE

Department of Chemical Engineering

FACULTÉ, ÉCOLE, DÉPARTEMENT / FACULTY, SCHOOL, DEPARTMENT

Influence of Process Parameters on the Morphology and Enzyme Production of Trichoderma Reesei

TITRE DE LA THÈSE / TITLE OF THESIS

Jules Thibault

DIRECTEUR (DIRECTRICE) DE LA THÈSE / THESIS SUPERVISOR

CO-DIRECTEUR (CO-DIRECTRICE) DE LA THÈSE / THESIS CO-SUPERVISOR

EXAMINATEURS (EXAMINATRICES) DE LA THÈSE / THESIS EXAMINERS

Gordon Hill

André Tremblay

Boguslaw Kruczek

Jason Zhang

Gary W. Slater

Le Doyen de la Faculté des études supérieures et postdoctorales / Dean of the Faculty of Graduate and Postdoctoral Studies

INFLUENCE OF PROCESS PARAMETERS ON THE MORPHOLOGY AND ENZYME PRODUCTION OF *Trichoderma reesei*

Nilesh Patel

Thesis Submitted to the

Faculty of Graduate and Postdoctoral Studies

In Partial Fulfillment of the Requirements for the Degree of

Doctorate in Philosophy

In

Department of Chemical and Biological Engineering

UNIVERSITY OF OTTAWA

Your file Votre référence
ISBN: 978-0-494-48411-1
Our file Notre référence
ISBN: 978-0-494-48411-1

ABSTRACT

The production of cellulase from the filamentous fungus *Trichoderma reesei* is a critical step in the industrial process leading to cellulose ethanol as it represents a major part of the cost. A research project was initiated in order to understand the intimate relationship that exists between the key process parameters and the morphological characteristics of *T. reesei* during the course of fermentation and to improve the production of enzymes. Experiments were performed using three types of bioreactors with completely different mixing system: (1) stirred tank bioreactor (STB) with Rushton turbines, (2) reciprocating plate bioreactor (RPB) with six perforated plates, and (3) Couette flow bioreactor (CFB) with outer wall rotating. Fermentations normally followed the protocol that is currently used industrially. It consists of two phases: a growth phase to generate the necessary biomass and the secretion phase where the desired enzymes are produced. A semiautomatic image analysis protocol was developed to characterize the mycelium morphology during the fermentation process. To evaluate the performance of STB and RPB in *T. reesei* fermentation, series of fed-batch experiments at different agitation speeds were conducted. Due to the limitation in evaluating the effect of shear in conventional bioreactors such as STB, a 5-L Couette flow bioreactor was designed and built to grow the microorganism in a uniform and defined shear conditions. Experiments in CFB were successfully performed in a continuous mode.

Oxygen mass transfer coefficient is an important process parameter in fungal fermentation. Therefore, first a review of available techniques to estimate K_La was done. Two new techniques based on neural network, and varying agitation and/or flow rate are presented. Also, two new methods based on image analysis and DNA quantification are developed to estimate the biomass concentration during *T. reesei* fermentation in the presence of an insoluble substrate.

The findings from this study provide new insight into the *T. reesei* fermentation. Also, the techniques developed can be implemented in large scale industrial bioreactors to better understand and monitor the *T. reesei* fermentation.

RÉSUMÉ

La production de la cellulase à partir du champignon filamenteux *Trichoderma reesei* est une étape critique du procédé industriel menant à l'éthanol issu de la cellulose puisqu'elle constitue une partie important du coût de production. Un projet de recherche a été initié pour mieux comprendre la relation intime existant entre les paramètres du procédé et les caractéristiques morphologiques de *T. reesei* durant la fermentation et pour améliorer la production d'enzymes. Des expériences ont été faites dans trois types de bioréacteurs ayant des mécanismes de mélange distincts: (1) un bioréacteur mélangé (STB) avec trois turbines de Rushton, (2) un bioréacteur à plateaux mobiles (RPB) muni de six plateaux, et (3) un bioréacteur Couette (CFB) avec le cylindre extérieur en rotation. Les fermentations ont été menées suivant le protocole couramment utilisé en industrie. Il consiste en deux phases: une phase de croissance pour produire la biomasse nécessaire et la phase de sécrétion dans laquelle les enzymes désirées sont produites. Un protocole semi-automatique d'analyse d'image a été développé pour caractériser la morphologie de *T. reesei* durant la fermentation. Pour évaluer la performance du STB et du RPB pour la fermentation de *T. reesei*, plusieurs séries d'expériences en semi-continues à différentes vitesses d'agitation ont été faites. Compte tenu des contraintes pour évaluer l'effet du cisaillement dans des bioréacteurs conventionnels, tel le STB, un bioréacteur Couette de 5 L a été conçu et construit pour soumettre le microorganisme à des conditions uniformes et définies de cisaillement. Les expériences dans le CFB ont été effectuées avec succès en mode continu.

Le coefficient de transfert d'oxygène est un facteur important pour les fermentations utilisant des champignons filamenteux. Ainsi, une revue des techniques disponibles pour estimer le K_La a été faite. Deux nouvelles techniques basées sur les réseaux neuronaux et sur la variation de l'agitation et/ou du débit de gaz sont présentées. En plus, deux nouvelles méthodes basées sur l'analyse d'image et la quantification de l'ADN ont été développées pour estimer la concentration de la biomasse durant la fermentation de *T. reesei* dans un milieu où le substrat est non soluble.

Cette recherche a permis d'avancer dans la compréhension des fermentations impliquant *T. reesei*. De plus, les techniques développées peuvent être mises en œuvre à une échelle industrielle pour mieux comprendre et surveiller les fermentations impliquant ce microorganisme.

DEDICATION

To my grandmother (Ma) and late grandfather (Bapa, "Masterji")

STATEMENT OF CONTRIBUTIONS OF COLLABORATORS

I hereby declare that I am the sole author of this thesis. I have performed the experimental design, all experiments and the associated data analysis.

My supervisor, Dr. Jules Thibault, provided continual guidance throughout this work and made editorial comments and corrections to my written work.

Véronique Lecault worked as part of her undergraduate thesis under my supervision on the development of a semi-automatic image analysis protocol. She is the first author for the papers presented in Chapters 5 and 6.

Raseeka Rahumathulla did her undergraduate thesis under my supervision working on the development of the DNA analysis protocol. She is the first author of the paper presented in Chapter 7.

The image analysis and the protein activity of all the fermentation samples presented in this thesis were performed by Viviane Choy. She is the coauthor for the papers presented in Chapters 8 and 9.

In Chapter 8, Philippe Malouf is also a coauthor for his work in the rheological characterization of samples and also for his help in the fermentation set-up.

In Chapter 10, Amanollah Baloochzehi is a coauthor for his work in biomass analysis of the samples and for his help in performing few fermentation.

Signature: _____ Date: 21/August/2008

ACKNOWLEDGEMENT

Many people have contributed to my thesis. First and foremost I would like to thank my supervisor, Professor Jules Thibault. He not only provided valuable suggestions and criticism throughout my graduate program but also took genuine interest to see that my life during the graduate studies was as productive and trouble-free as possible.

Fruitful discussions with Dr. Theresa White, Dr. Glenn Munkvold and their team at Iogen Corporation, Canada helped in the successful design of project and also in setting-up of the sample analysis protocols used in this study. This project would not exist without their collaboration and support.

I would like to thank all the professors and support staff at the Department of Chemical and Biological Engineering particularly Dr. Kruczek for his recommendations, Dr. Kumar, Dr. Matsuura and Dr. Tremblay for their help in membrane selection and Dr. Zhang for the use of his laboratory equipment.

I am deeply grateful to our department technicians, Louis Tremblay, Franco Ziraldo and Gerard Nina for their technical help in successfully running my experiments.

I had fortunate experience to work with my lab mates and friends (not in any particular order): Véronique Lecault, Vivane Choy, Philippe Malouf, Yun Lin, Raseeka Rahumathulla, Amanollah Baloochzehi and Deepak Rana. I will always cherish the countless hours spent working together.

Finally, I would like to express my grateful thanks to my family and friends. My dear friend, Gabriela Fonseca, has always been there when I needed any help. I am grateful for her thoughtful input in the preparation of this theis.

I am indebted to my parents, aunt and uncle who have made a lot of sacrifice for my future. Without them as well as my sisters and brothers, I would not have been able to pursue my dream.

I truly appreciate my wife, Meena, for her unselfish patience while I worked on my thesis. I spent the time which I should have spent with her to complete my thesis.

TABLE OF CONTENTS

LIST OF TABLES

LIST OF FIGURES

CHAPTER 1

INTRODUCTION

During the 1980's when the oil prices dropped after the upsurge of the 1970's, it seemed like there would be no shortage of oil supply in the near future. However, this decade has broken all records in oil prices and still demand keeps increasing mainly due to the emergence of developing countries such as China and India. Apart from the high cost of oil, which affects the economy, the use of oil causes a significant increase in greenhouse gases (GHG). The fast increase in CO_2 accumulation and other GHG's in the atmosphere is gravely endangering the ecological balance of the Earth. Therefore, due to the energy shortage and the environmental damage caused by use of conventional fuels, considerable research is being done in finding an alternative to gasoline which could offset some of the demand for oil and could also be environmentally friendly. One of the alternatives to gasoline is the use of bioethanol from cellulose since it is the most abundant renewable resource. Although CO_2 is produced during the production and combustion of bioethanol, some of this CO_2 is reutilized to grow new biomass. Therefore, the net CO_2 added to the atmosphere is less when compared to the release due to the utilization of fossil fuels such as oil. However, currently most of the bioethanol production is from corn and sugarcane, which causes huge upward pressure on the food prices. Therefore, production of bioethanol using lignocellulosic material such as bagasse, waste paper and wheat straw are obviously going in a better direction. A major challenge in the production of lignocellulosic ethanol is the efficient extraction of sugars from cellulose. Furthermore, conventional methods for hydrolysis such as acid treatment lead to lower ethanol yield and higher by-product formation (Shin et al., 2000).

The structural complexity and rigidity of cellulosic materials has forced nature to produce a large diversity of degradative enzymes/proteins (cellulases), which act synergistically on their substrate. The complete degradation of cellulose can be achieved only by the synergistic action of various enzymes which make up the cellulase enzyme. There are three main components of cellulase enzyme: cellobiohydrolases (CBH),

endoglucanases (EG) and β-glucosidase (BG). EG randomly attacks the amorphous regions of cellulose fiber by breaking the β-glucosidic bonds. The end of the chain is attached by CBH to produce cellobiose, a dimer of glucose. The cellobiose is further broken down to produce glucose by the BG enzyme. Many microorganims, both bacterial and fungal species, are known to produce cellulase. Bacterial species such as *Clostridium* and *Bacillus* and filamentous species such as *Aspergillus* and *Trichoderma* are well known producers of cellulase. However, the cellulase produced by *Trichoderma reesei* (*T. reesei*) is stable (Sternberg, 1976) and is considered as an efficient enzyme system for the complete hydrolysis of cellulosic substrates into fermentable sugars (Ryu and Mandels, 1980). Further, *T. reesei* Rut C-30 strain, which is used in this study, is not repressed by glucose to the same extent as others (Montenecourt and Eveleigh, 1977).

A fungal fermentation is recognized as a complex multiphase, multicomponent process. Cell growth and product formation are influenced by a large number of operating parameters: culture broth composition, temperature, pH, shear stress, initial inoculum, dissolved oxygen and fungal morphology. All these parameters are varying during the course of fermentation and are influencing each other. For example, the intimate relationship between morphology, broth rheology, dissolved oxygen level and mixing intensity is a prime example of the complexity of this fermentation process. Due to this complex interrelationship of operating parameters, it is important to take into account morphology, enzyme production and process performance simultaneously (Schügerl et al., 1998).

Compared to unicellular microbes, the unique morphology of filamentous fungi presents special challenges during the optimization and scale-up of fermentation. An understanding of the growth and morphological complexity of the filamentous fungi is paramount for developing consistent, scalable, productive and efficient fungal fermentation processes (Wang, 2002). Morphological characteristics of submerged mycelial cultures have therefore been established as one of the key bioprocess parameters (Žnidaršic and Pavko, 2001). Even though substantial increases in overall protein production have been realized by classical mutation and selection approaches, it is important to have a good grasp of the morphology during the fermentation to optimize the enzyme production.

Another important process parameter to consider, especially in fungal fermentation, is the oxygen mass transfer coefficient (K_La). Oxygen mass transfer is an important design consideration in submerged fermentation due to the low solubility of oxygen. The solubility is further decreased due to the presence of dissolved salts. In addition, K_La normally decreases with an increase in viscosity. The most common techniques to increase oxygen transfer are to increase either agitation or air flow rate. Both of these techniques lead to higher costs of operation. Moreover, high agitation rates have shown to affect the growth of microorganism and product formation. Therefore, it is important to select optimum agitation and air flow rate to achieve adequate oxygen mass transfer. Oxygen mass transfer becomes more difficult when aerobic fungal fermentations such as *T. reesei* are performed due to the highly viscous and non-Newtonian nature of the broth. Higher power input is required to achieve good mixing and impellers are easily flooded decreasing the stirring efficiency (Schüegerl, 1981). Bubble coalescence causes an increase in bubble size reducing the gas/liquid interfacial area and bubble residence time in the bioreactor. Based on these considerations, a comprehensive study on the oxygen mass transfer was also conducted and, new techniques to measure or estimate K_La were developed and applied in submerged fermentation such as *T. reesei* fermentation.

1.1 OBJECTIVES

The main objective of this research project is to develop a set of interrelated tools for the complete analysis of the physiological and morphological state of the microorganism *T. reesei* during the course of fermentation in view of optimizing the production of enzymes. In order to achieve this objective, the following steps were taken:

(1) Perform a comprehensive review of oxygen mass transfer coefficient estimation techniques and develop new techniques.

(2) Develop an image analysis protocol, using Light Microscopy (LM) to relate the morphological and physiological information on *T. reesei* to the operating conditions and the production of enzymes.

(3) Design and build a 5-L Couette flow bioreactor to conduct fermentation runs under a constant shear field to investigate the influence of shear rate on the morphology of *T. reesei* and production of enzymes at different stages of fermentation.

(4) Investigate the influence of the type of bioreactors (stirred tank, reciprocating plate and Couette flow) on the biomass growth, protein production, rheology, and morphology of *T. reesei*.

1.2 RESEARCH METHODOLOGY

This research project consists of a series of submerged fermentations conducted in different types of bioreactors and under different modes of operation in view of developing an efficient, fully automated and well controlled, economically viable process for the production of enzymes by fermentation using filamentous fungi. This study will also bring essential information on the influence of process parameters on the morphology characteristics of *T. reesei* and the production of enzymes.

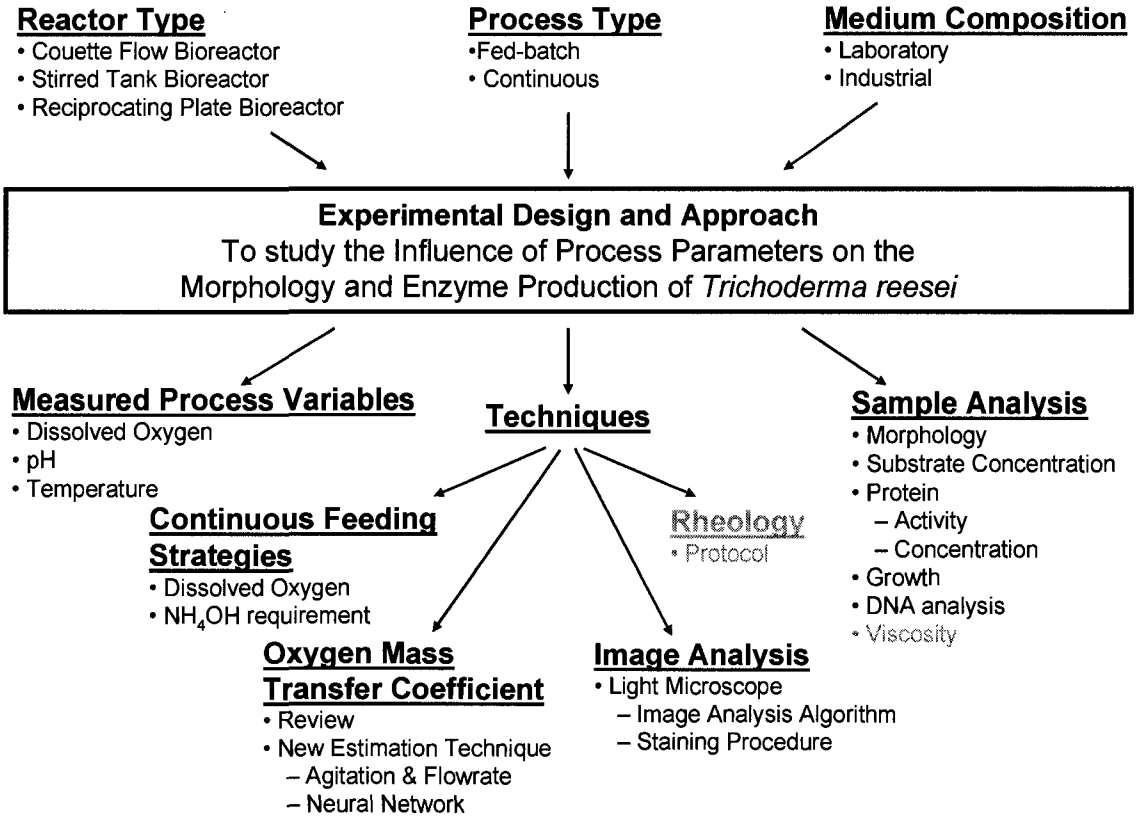

Figure 1.1 – Schematic overview of the research project.

Figure 1.1 provides a schematic overview of the relationship that exists between the various facets of this research project. Each topic will now be discussed in turn. The development of the technique for rheological analysis (topic in light gray) is part of the

overall objective but was performed under a different research project and therefore further details on this technique and the results can be found in Malouf (2008).

1.3 MATERIALS AND METHODS

1.3.1 Bioreactors

In a paper on the effect of agitation on growth of *T. reesei* and enzyme production, Lejeune and Baron (1995) have shown that, in a 20-L stirred tank bioreactor, the optimal agitation rate for enzyme activity was 200 rpm whereas it was 300 rpm for fastest growth. They also found that, at 400 rpm, the extracellular protein concentration was at its lowest. Ganesh et al. (2000) clearly showed that a loss in cellulase enzyme activity increased with an increase in agitation speed in a stirred tank bioreactor. These results point to the delicate compromise between the necessary shear that is required for homogenization of the fermentation broth and high oxygen mass transfer coefficient (K_La), and its detrimental impact on the morphology and physiology (functions of the cell) of the microorganism. Therefore, three bioreactor configurations are used in this research project to clearly characterize the effect of shear on the growth, protein production and morphology of *T. reesei*. A brief description of the bioreactors is given below but a more thorough description is provided in subsequent chapters.

1.3.1.1 STIRRED TANK BIOREACTOR

The laboratory-scale Stirred-Tank Bioreactor (STB) has a total volume of 22.5 L with a working volume of 17-18 L. A schematic diagram of the STB is shown in Appendix A.1. The bioreactor, built in our laboratory, is made of stainless steel and has an inner diameter of 228 mm and a column height of 550 mm. Three identical Rushton turbines, mounted on the central shaft, are used for mixing. Four baffles are placed inside the mixing vessel to achieve uniform mixing. Due to foaming problems in *T. reesei* fermentation, a mechanical foam breaker was built and placed on the centre shaft above the liquid medium during the operation in continuous mode.

1.3.1.2 RECIPROCATING PLATE BIOREACTOR

A Reciprocating Plate Bioreactor (RPB), built in our laboratory with the identical dimensions as the STB, was used. A schematic diagram of the RPB is shown in Appendix A.1. The RPB is particularly well suited for highly viscous fermentations (Lounes and

Thibault, 1994). It consists of a stack of perforated plates mounted on a vertically reciprocating shaft to agitate the vessel contents. The reciprocating plates occupy the whole cross-sectional area of the bioreactor and, as a result, energy is imparted more gently and uniformly throughout the fermentation medium. The plate stack consists of 6 perforated stainless steel plates, 221-mm diameter and 1.25-mm thick. Each plate is spaced 50 mm apart from one another. The perforations have a diameter of 19 mm.

1.3.1.3 COUETTE FLOW BIOREACTOR

A 5-L Couette Flow Bioreactor (CFB), designed as part of this project is used to perform fermentation runs under a relatively uniform and defined shear environment. CFBs have been successfully used in the past by researchers (O'Connor et al., 2002, Sahoo et al., 2003, Sun and Linden, 1999) to study the effect of shear on the growth of microorganism during fermentation. But these bioreactors were small in size, typically less than 1 L, and usually run in batch mode. The novelty in the current design of CFB is its larger size (5 L) and is designed such that it can be operated in batch, fed-batch and continuous mode. In a CFB, the fermentation broth is entrapped in the small annular section of two concentric cylinders. The outer cylinder is rotated at constant speed whereas the inner cylinder remains stationary. Aeration is provided by allowing air to diffuse through a membrane fixed to the outside surface of the inner cylinder. A picture of CFB in operation is shown in Appendix A.2.

1.3.2 Mode of Operation

Fermentations normally follow the protocol that is currently used industrially. It consists of two phases: a growth phase to generate the necessary biomass and a secretion phase where the desired enzymes are produced. Operating only in batch mode throughout the fermentation will lead to significant reduction in productivity (McLean et al., 1985). Fermentations are started in batch mode, with sugar and other nutrients, in a sterile bioreactor sparged with air. After inoculation from a flask culture, the fermentation is allowed to proceed in batch mode for 24-48 h, until the initial sugar concentration is reduced to a very low level, typically less than 1 g/L. An inducing feed, lactose, (Domingues et al., 2001) is then introduced to the fermentation in fed-batch mode. Little to no extracellular protein is produced during the initial batch operation prior to switching to the inducer feed.

During the experiments performed using STB and RPB to evaluate the effect of agitation, fermentation runs are performed following the industrial protocol that uses a combination of batch and fed-batch modes, respectively for the growth and production phases. This will also ensure to produce results that are as relevant as possible to industry. To obtain information on the influence of different substrate feeding strategies on the growth and protein production of *T. reesei*, experiments are performed in continuous mode (chemostat). In particular, the CFB is designed to also operate in chemostat mode in order to measure the steady state morphological state and protein production under conditions of uniform shear and where morphology will not be affected by the age distribution of cells. An approximate time to complete each experimental run including sample and data analysis is given in Table 1.1.

Table 1.1 – Time to complete one experimental run.

Tasks	Duration (days)
• Preparing Inoculum & Setting-up Bioreactor	2-3
• Experimental Run	7-8
• Sample and Data Analysis	3-4
Total Time to Complete One Experiment	12-15

1.3.3 Control and Measurement System

In this project, it is very important to have a robust, flexible control and measurement system. This system should be able to have the following characteristics:

1) Ability to be used in three different types of bioreactors.
2) Capacity to measure and store process parameters such as pH, DO, temperature, feed rate (using weighing balance) and off-gas analysis (using mass spectrometer).
3) Control agitation rate (STB and CFB) and process parameters such as pH (using acid/base addition) and DO (agitation rate or substrate feeding).
4) Flexibility to include new feeding strategies.

A single commercial available system cannot satisfy all these objectives. Therefore, a system was developed based on Labview® measurement and automation software (National Instrument, Austin, USA). Further data acquisition was performed using DT-906 card (Data Translation, Marlboro, USA). The main panel of the Labview® program

developed is shown in Appendix A.3. A schematic diagram and picture of the complete bioreactor set-up with the control and measurement system is shown in Appendix A.4 and A.5 respectively.

1.3.4 Operating Conditions

The strain used throughout this work was *T. reesei* RUT C-30 (ATCC 56765) and was either supplied by Iogen Corporation, Ottawa or purchased from ATCC. The initial volume of the fermentation medium for the fed-batch and continuous mode was 10 L. Temperature (ca. 28°C) and pH (ca. 3.5 or 4.5) were controlled throughout the run. The DO was not controlled during the batch phase. However, during the protein production phase (fed-batch and continuous), the DO was maintained above the critical concentration of 20% air saturation during the *T. reesei* fermentation (Schell et al., 2001) either by controlling the lactose feeding or agitation rate.

1.3.5 Medium Selection

The medium selected in this project was based both on industrial ingredients and that used in previous studies. A summary of various medium compositions used in *T. reesei* fermentations is presented in Appendix B.1. Although cellulose is the best inducer of cellulase production, there are many operational difficulties associated with using a solid medium. For that reason, this project utilizes lactose, which also induces cellulase and offers many advantages such as less catabolite repression compared to other soluble sugars (e.g. glucose). When using lactose, cell growth does not depend on cellulose hydrolysis; it also produces a complete set of cellulase (Esterbauer et al., 1991) and, most importantly, it can be easily fed into the bioreactor during the continuous mode (Chaudhuri and Sahai, 1994). As well, corn steep solids were replaced in the continuous operation by protease peptone and yeast extract, which were found to be beneficial in improving cellulase productivity (Gallo et al., 1981).

1.3.6 Sample Analysis

1.3.6.1 BIOMASS ANALYSIS AND PROTEIN CHARACTERIZATION

Biomass concentration as a function of time was measured by dry weight analysis. Glucose and lactose concentrations (substrates) were measured by a YSI glucose analyzer (YSI Incorporated, USA) and an enzymatic kit (Boehringer Mannheim, Germany), respectively. The protein concentration was measured by the Bradford method (Bradford,

1976) using bovine serum albumin (BSA) as a standard. The enzymatic activity was estimated using filter paper assay method and carboxymethyl cellulose assay as per the IUPAC protocol (Ghose, 1987).

1.3.6.2 IMAGE ANALYSIS

Many studies have shown the effect of morphology on the productivity and the rheology of fermentation broth (Paul et al., 1999). Consequently, a detailed quantitative study on the morphology of the microorganism is necessary to understand the relationship between morphology and productivity. Image analysis to study morphology includes two basic steps: (1) the image of the fermentation broth sample is captured using an image acquisition device attached to a microscope and (2) the captured image is processed using image analysis software for measurements and calculations of morphological properties. The use of image analysis to study the morphology of microorganisms is limited for industrial applications due to the labour-intensive work required to obtain statistically reliable results, which are representative of an industrial-scale reactor. Therefore, in order to be able to analyze a large number of samples, a semi-automatic image analysis technique needed to be developed. The technique can be automated by using a motorized stage and a controllable illumination system with autofocus capability. Additionally, the software should allow writing an algorithm to automate the procedure and measure the required morphological parameters.

The first task in this part of the project was to select appropriate microscope and image analysis software, which could satisfy the requirements for a successful development of a semi-automated image analysis technique. A detailed evaluation of available software and microscopes was done. A monochrome camera (CoolSnap ES, Roper Scientific, Tucson, AZ) mounted on an Olympus IX81 microscope (Olympus, Melville, NY) was selected for the image analysis measurements. The automated stage of the microscope as well as the image analysis was controlled and performed, respectively, by the Image-Pro® Plus software (Image-Pro® Plus version 5.1, Media Cybernetics, Silver Spring, MD). Macros allowing the semiautomatic analysis of multiple images were written in Visual Basic code. Each captured image was saved in a TIFF format for further analysis. Further details on the image analysis procedure and morphological parameters analyzed are provided in subsequent chapters. The various steps involved in a semi-automatic image

analysis procedure are shown in Appendix C. For a detailed statistical analysis on the image analysis procedure refer to Choy (2008).

1.3.6.3 RHEOLOGY ANALYSIS

Rheological analysis of the fermentation broth samples were performed with the AR-G2 Rheometer controlled by a computer with AR Instrument Control and Data Analysis software (TA Instruments, New Castle, Delaware, USA). For a more detailed explanation of the procedure and results refer to Malouf (2008).

1.4 STRUCTURE OF THESIS

This thesis is divided into three main sections. Each section is dedicated to a particular topic and chapters in each section are presented in journal article format. There are 9 journal articles in total (3 in each section).

1.4.1 Section I – Oxygen Mass Transfer Coefficient (K_La)

The chapter 2 is dedicated to the review of various techniques to estimate K_La, both in submerged and solid state fermentation. In chapters 3 and 4, two new techniques are presented and applied in submerged fermentations.

1.4.3 Section II – Sample Analysis

This section is devoted to the developed image analysis and biomass estimation technique. The importance of image analysis in fungal fermentations is discussed earlier as well as the need for an automated image analysis technique. Chapter 5 presents the image analysis technique for the morphological characterization and viability assessment during the *T. reesei* fermentation. Two techniques for estimating biomass in presence of insoluble substrate were developed. Chapter 6 presents the correlation developed to estimate biomass using the biomass density estimation acquired from image analysis. Estimation of biomass using DNA quantification is based on the knowledge that the DNA content of the microorganism remains constant at every phase of fermentation process. Chapter 7 presents the extraction and DNA quantification technique, both in presence of soluble and insoluble substrates (corn steep solids and solka floc).

1.4.2 Section III – *Trichoderma reesei* Rut C-30 Fermentations

Chapter 8 presents the results of the study on the effect of agitation rate on the growth, protein production and rheology of the fermentation broth. Design of the CFB and

experiments at different shear rates are provided in Chapter 9. It has been shown by a number of researchers that switching between growth and starvation cycle is better for cellulase production than continuous feeding. Therefore, those experiments using different feeding strategies based on the dissolved oxygen and base requirement were performed in STB and the data is presented in Chapter 10.

1.5 REFERENCES

Bradford, M. M., A Rapid and Sensitive Method for the Quantification of Microgram Quantities of Protein Utilizing the Principle of Protein-Dye Binding. Analytical Biochemistry, *72*: 248-254, 1976.

Chaudhuri, J. B. and Sahai, V., Comparison of Growth and Maintenance Parameters for Cellulase Biosynthesis by *Trichoderma reesei* - C5 With Some Published Data. Enzyme and Microbial Technology, *16*: 1079-1083, 1994.

Choy, V., Influence of Agitation on the Morphology of *Trichoderma reesei* and its Correlation with the Protein Production. MASc Thesis, University of Ottawa, Ottawa, Canada, 2008.

Domingues, F. C., Quiroz, J. A., Cabral, J. M. S., and Fonseca, L. P., Production of Cellulases in Batch Culture Using a Mutant Strain of *Trichoderma reesei* Growing on Soluble Carbon Source. Biotechnology Letters, *23*: 771-775, 2001.

Esterbauer, H., Steiner, W., Labudova, I., Hermann, A., and Hayn, M., Production of *Trichoderma* Cellulase in Laboratory and Pilot Scale. Bioresource Technology, *36*: 51-65, 1991.

Gallo, B., Tassinari, T., Spano, L., and Ryu, D. D. Y., Cellulase Process Improvement and its Economics. *In* M. Moo-Young (ed.), Advances in Biotechnology, Vol. 3, pp. 281-288, Pergamon Press, 1981.

Ganesh, K., Joshi, J. B., and Sawant, S. B., Cellulase Deactivations in Stirred Reactor. Biochemical Engineering Journal, *4*: 137-141, 2000.

Ghose, T. K., Measurement of Cellulase Activity. Pure & Applied Chemistry, *59*: 257-268, 1987.

Lejeune, R. and Baron, G. V., Effect of Agitation on Growth and Enzyme Production of *Trichoderma reesei* in Batch Fermentation. Applied Microbiology and Biotechnology, *43*: 249-258, 1995.

Lounes, M. and Thibault, J., Mass Transfer of Reciprocating Plate Bioreactor. Chemical Engineering Communications, *127*: 169-189, 1994.

Malouf, P. Relationship Between Morphology and Rheology during *Trichoderma reesei* RUT C-30 Fermentations, MASc Thesis, University of Ottawa, Ottawa, Canada, 2008.

McLean, D. D., Abear, K., and Podruzny, M. F., Fed-Batch Production of Cellulases Using *Trichoderma reesei* Rutgers C-30. Canadian Journal of Chemical Engineering, *64*: 588-597, 1985.

Montenecourt, B. S. and Eveleigh, D. E., Preparation of Mutants of *Trichoderma reesei* With Enhanced Cellulase Production. Applied and Environmental Microbiology, *34*: 777-782, 1977.

O'Connor, K. C., Cowger, N. L., De Kee, D. C. R., and Schwarz, R. P., Prolonged Shearing of Insect Cells in a Couette Bioreactor. Enzyme and Microbial Technology, *31*: 600-608, 2002.

Paul, G. C., Priede, M. A., and Thomas, C. R., Relationship Between Morphology and Citric Acid Production in Submerged *Aspergillus niger* Fermentations. Biochemical Engineering Journal, *3*: 121-129, 1999.

Ryu, D. D. Y. and Mandels, M., Cellulases: Biosynthesis and Application. Enzyme and Microbial Technology, *2*: 91-102, 1980.

Sahoo, S., Verma, R. K., Suresh, A. K., Rao, K. K., Bellare, J., and Suraishkumar, G. K., Macro-Level and Genetic-Level Responses of *Bacillus subtilis* to Shear Stress. Biotechnology Progress, *19*: 1689-1696, 2003.

Schell, D. J., Farmer, J., Hamilton, J., Lyons, B., McMillan, J. D., Saez, J. C., and Tholudur, A., Influence of Operating Conditions and Vessel Size on Oxygen Transfer During Cellulase Production. Applied Biochemistry and Biotechnology, *91-93*: 627-642, 2001.

Schügerl, K., Oxygen Transfer into Highly Viscous Media. Advances in Biochemical Engineering, *19*: 71-174, 1981.

Schügerl, K., Gerlach, S. R., and Siedenberg, D., Influence of the Process Parameters on the Morphology and Enzyme Production of *Aspergilli*. Advances in Biochemical Engineering and Biotechnology, *60*: 195-266, 1998.

Shin, C. S., Lee, J. P., Lee, J. S., and Park, S. C., Enzyme Production of *Trichoderma reesei* Rut C-30 on Various Lignocellulosic Substrates. Applied Biochemistry and Biotechnology, *84-86*: 237-245, 2000.

Sternberg, D., Production of Cellulase by *Trichoderma*. Biotechnology and Bioengineering Symposium, *6*: 35-53, 1976.

Sun, X. and Linden, J. C., Shear Stress Effects on Plant Cell Suspension Cultures in a Rotating Wall Vessel Bioreactor. Journal of Industrial Microbiology and Biotechnology, *22*: 44-47, 1999.

Wang, L. Enhanced Production of Heterologous Protein by Recombinant *Aspergillus niger* through Bioprocessing Strategies in Submerged Cultures. Thesis, Russ College of Engineering and Technology, Ohio University, USA, 2002.

Žnidaršic, A. and Pavko, A., The Morphology of Filamentous Fungi in Submerged Cultivations As Bioprocess Parameter. Food Technology and Biotechnology, *39*: 237-252, 2001.

SECTION - I

OXYGEN MASS TRANSFER COEFFICIENT

CHAPTER 2

Review of Oxygen Mass Transfer Measurement Methods

Nilesh Patel and Jules Thibault

Department of of Chemical and Biological Engineering

University of Ottawa

Ottawa (ON), K1N 6N5, Canada

Abstract

The oxygen mass transfer coefficient (K_La) is undoubtedly one of the most important parameters in aerobic fermentations. This chapter reviews the various methods for measuring K_La in fermentation processes. Methods used for model fluids, submerged fermentations and solid state fermentations can be classified as steady-state or dynamic methods. A brief description of the most important methods along with their advantages and disadvantages is provided.

In the last decade, no significant development on the methods to measure K_La has occurred but established methods were modified in a way to estimate more accurately the oxygen mass transfer phenomena occurring in a fermenter. Recent advances in the development of new mathematical techniques, determination of K_La in small scale bioreactors and modifications of existing methods for animal cell cultures are also discussed.

2.1 INTRODUCTION

In most aerobic fermentation, oxygen mass transfer coefficient (K_La) is often the limiting factor for both growth and higher productivity. This is mainly due to the low solubility of oxygen in aqueous system. Therefore, an important goal in most aerobic fermentations is to maintain an optimal level of dissolved oxygen (DO) concentration by

continuously supplying oxygen into the bioreactor to provide an environment to the microorganisms that is conducive to high growth and/or production rates. A continuous and accurate determination of K_La will help to better control the fermentation process. But it is not easy to predict K_La values throughout the fermentation process since the broth rheology, and the concentration of cells and products are changing continuously.

The advantages and disadvantages of the methods for the measurement of the oxygen transfer rates and coefficients in the absence and presence of microorganisms were reviewed by Sobotka et al. (1982) and Van't Riet (1979). Since then, many new methods have been proposed: bioluminescence method (Vashitz et al., 1989), pseudo-random pulses (Gauthier et al., 1990), reaction time (Denis et al., 1990), step changes in the headspace pressure of the bioreactor (Linek et al., 1989), frequency response technique (Varder and Lilly, 1982), changes in the inlet oxygen concentration using oxygen enriched air (Kim and Chang, 1989), using Krypton (Pedersen et al., 1993), and many others. Therefore, the objective of this chapter is to review important methods that are used to determine K_La and examine the advances that have occurred in that field.

2.1.1 Oxygen Mass Transfer Coefficient (K_La)

The rate at which oxygen is transferred from the gas phase to the liquid phase is dependent on the bioreactor design, the type of mixing devices, the operating conditions, and the fluid physical properties. Therefore, all these parameters need to be taken into consideration while determining the efficiency of aeration processes in fermentation systems. This is commonly achieved by estimating the overall volumetric oxygen mass transfer coefficient, K_La, which reflects the impact of all these parameters on the aeration efficiency.

In submerged fermentations, microorganisms usually consume oxygen in its dissolved form. To achieve its dissolved state, oxygen must overcome different transport resistances, starting from the diffusion from bulk gas phase to the liquid medium and finally penetrating the cell envelope for the intracellular reaction rate (Bailey and Ollis, 1986). The main transfer resistance is attributed to the liquid film resistance such that K_La usually corresponds to liquid volumetric mass transfer coefficient. K_La is the product of the liquid mass transfer coefficient and the volumetric interfacial surface area between gas and the liquid phase. Early works were done to either calculate the volumetric gas-

liquid interfacial area 'a', or the liquid phase mass transfer coefficient 'K_L', or the overall volumetric oxygen mass transfer coefficient 'K_La'. Due to difficulties in measuring 'K_L' and 'a' separately, K_La is usually calculated as a way to characterize the aeration capacity of a fermentation system. The volumetric interfacial surface area (a) is defined per unit volume of liquid or per unit volume of fermentation broth, thereby leading to two different values of K_La related by the factor (1 - ε) where ε isgas void fraction. In the literature, the former definition is used because it is easier to measure the initial and non-aerated liquid volume even though the rigorous definition for 'a' should be the surface interfacial area per unit volume of fermentation broth.

The rate of oxygen transfer (OTR) from the gas to the liquid phase can be calculated by multiplying K_La by the concentration driving force. Therefore, the oxygen transfer rate is given by:

$$OTR = N_{O_2} = K_L a \left(C_L^* - C_L \right) \tag{2.1}$$

where C_L is the dissolved oxygen (DO) concentration and C_L^* is the saturated DO concentration, i.e. the concentration that would be in equilibrium with the concentration in the gas phase. C_L^* can be calculated using Henry's law.

$$C_L^* = \frac{p_G}{H} \tag{2.2}$$

where H is the Henry's law constant and p_G is the oxygen partial pressure in the gas phase. It is also possible to correct the DO concentration to account for the presence of substrate (Schumpe, 1978). However in large bioreactors, due to the change in concentration of oxygen as gas bubbles move up in the bioreactor and the hydrostatic pressure difference, a logarithmic mean driving force needs to be calculated (Sobotka et al., 1982). Also, sometimes the bulk of the DO concentration does not represent the actual oxygen available for microorganism to consume because microbial cells might adsorb at the gas-bubble-liquid interface (Bailey and Ollis, 1986).

Equation (2.1) provides the oxygen transfer rate in the absence of oxygen consumption. This equation needs to be modified when microorganisms are present and are consuming oxygen. Equation (2.1) can be rewritten to include the rate of oxygen consumption:

$$\frac{dC_L}{dt} = K_L a \left(C_L^* - C_L\right) - Q_{O_2} X \tag{2.3}$$

Here, X is biomass concentration and $Q_{O_2} X$ is the oxygen uptake rate.

2.1.2 Mixing Devices

To increase the oxygen transfer rate, it is required to increase either the mass transfer coefficient or the oxygen concentration driving force. To enhance the oxygen transfer rate, an oxygen-enriched gas stream can be used instead of air but this is rarely done because it is not economically feasible. The easiest way is to increase the mass transfer coefficient by increasing both K_L and a using a proper mixing device. A mixing device provides the necessary shear to increase the convective mass transfer and to increase the interfacial surface area. The surface area of contact is increased in two ways: by maintaining a high population of small gas bubbles and increasing the gas holdup.

The $K_L a$ depends on several factors such as the geometry of the bioreactor, the type of mixing devices, the fluid rheology and the operating conditions. The estimation of $K_L a$ is commonly reported as a function of the power input ($\overline{P_G}$) per unit volume (V_L) and the superficial gas velocity (U_G), using the following relationship:

$$K_L a = \gamma \left(\overline{P_G} / V_L\right)^{\alpha} U_G^{\beta} \tag{2.4}$$

Where γ, α and β are parameters of model. Additional terms are sometimes added to include the effect of the apparent viscosity of the medium, the surface tension and/or the concentration of a species of the medium that affects $K_L a$. Different values of the coefficients α, β and γ have been found by different authors depending on the type of bioreactors, types of mixing devices and the nature of the medium. Typical values of γ, α and β in a stirred tank are respectively 2.6×10^{-2}, 0.4 and 0.5 for coalescing water and 2.0×10^{-3}, 0.7 and 0.2 for noncoalescing water system (Bailey and Ollis, 1986). Other types of correlations have been published for specific applications. Equation (2.4) states that $K_L a$ increases with higher mixing intensity and/or higher gas flow rate. However, there is an economic penalty associated with increasing these parameters. In addition, too vigorous agitation can subject the microorganisms to high shear stress, which can be

detrimental to their growth and ability to produce the desired product. Finding an optimum operating point for these parameters therefore becomes an important issue.

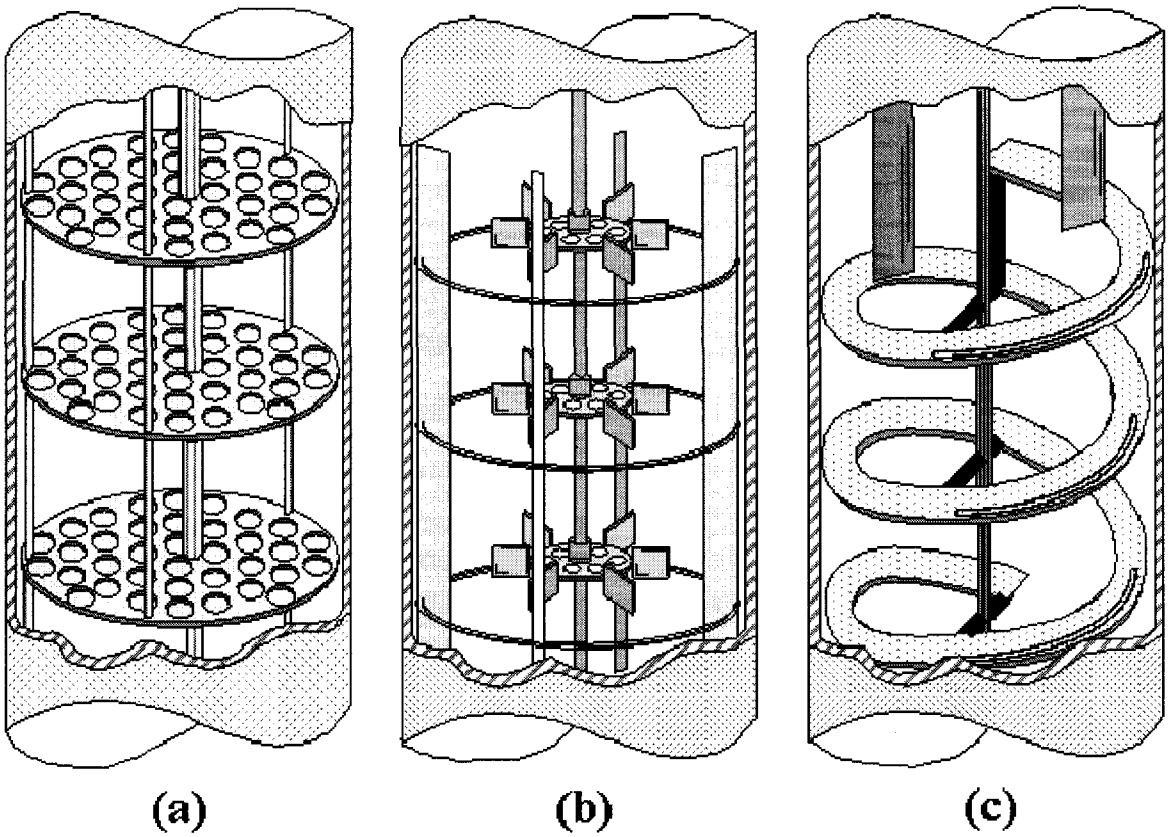

Figure 2.1 – Different types of mixing devices: (a) Reciprocating Plate Bioreactor (RPB); (b) Stirred Tank Bioreactor (STB); (c) Helical Ribbon Impeller (HRI).

Depending on the type of microorganism and fermentation broth, different types of mixing devices are used. Some of them are presented in Figure 2.1. For highly viscous fermentation broths, the use of traditional mixing devices such as Rushton turbines leads to non-uniform K_La within the stirred tank bioreactor (STB) (Lounes et al., 1995). It is important to choose a mixing device that can significantly reduce or even eliminate stagnant zones while providing a better and homogeneous overall volumetric oxygen mass transfer coefficient. Several unconventional mixing devices have been designed and studied. Some of them are the reciprocating plate mixer (Lounes et al., 1995), the helical ribbon mixer (Jolicoeur et al., 1992), and the helical ribbon screw mixer (Tecante and Choplin, 1993). Helical ribbon mixers are good for mixing but relatively poor for oxygenation. Therefore, any mixing device should have the following characteristics:

provide high K_La, low energy consumption, low shear stress, homogeneity of fermentation broth and easy to scale-up.

2.1.3 Measuring Instruments

2.1.3.1 DISSOLVED OXYGEN PROBE

DO probes are most commonly used in industrial bioreactors to measure the broth DO concentration. To properly measure the DO, it is important to consider a suitable location of the probe, the type of probe and the probe dynamics. These aspects will be discussed later when describing the dynamic method. Linek et al. (1985) discussed in detail the methods to take into account the various resistances affecting the probe dynamics. In addition, for a better accuracy, a fast response probe is necessary because the probe response time (τ_P) should be much smaller than the dynamics of oxygenation that is equal to the inverse of the oxygen mass transfer coefficient ($1/K_La$). Van't Reit (1979) concluded that probes with τ_P equal to 2 or 3 s can be used to measure K_La up to 0.1 s^{-1}. In the section discussing the gassing-out method, the equation to account for the probe response dynamics is presented and incorporated into the model to estimate K_La.

Fibre Optic probes based on the principle of fluorescent quenching has been used to measure the DO (Wang et al., 1999). Although, fibre optic probes have a very quick response time, preliminary test performed in our laboratory using Foxy-R Fibre Optics probes (Ocean Optics Inc, USA) found it not suitable for use in fermentation. It is not suitable for sterilization by both autoclaving or UV sterilization. It was observed that after each sterilization cycle, by maintaining constant the integration time, the count for the fluorescent peak, the intensity, and the range of intensity from 0%-100% kept decreasing. Further, the fibre optic cable is very sensitive to movement and greatly affects the probe response. A slight movement will cause the DO reading to spike because a light path occurred.

2.1.3.2 GAS ANALYZER

Determination of K_La using gas balance method requires measuring the concentration of the inlet and outlet gas streams. This is usually done using gas analyzers such as mass spectrometers, gas chromatographs, infrared analysers, paramagnetic analyzers and others. In fermentation with slowly metabolized microorganisms, some appreciable errors could occur due to the very small difference in oxygen concentration between the inlet

and outlet streams. In fact, according to Ruffieux et al. (1998) the only analyzer which can be used for animal cell culture is the mass spectrometer. The gas balance method used commonly in culture conditions requires corrections for temperature, pressure and humidity (Spriet et al., 1982). As noted by Spriet et al. (1982), the precision of the static method depends on the precision of the oxygen analyzer.

2.2 METHODS FOR THE DETERMINATION OF K_La

In the following section, different methods for the measurement of K_La both in model fluids and fermentation systems are presented. Due to ever-changing properties of the fermentation broth such as the viscosity, it is difficult to make a reliable estimation of K_La during the course of fermentation. To overcome this problem, many authors have measured K_La for model fluids instead of fermentation broths. Model fluids such as water (Baird and Rama Rao, 1998, Linek et al., 1987), aqueous solutions of carbomethyl cellulose (Popovic and Robinson, 1989), and dextran (Audet et al., 1996) were chosen to mimic the rheological behaviour of fermentation broths at different stages of fermentation. Model fluids have distinct advantage that they can be precisely characterized and their physical properties remain the same during the entire experimental test. Therefore, the methods applicable to model fluids are presented below and later to the actual fermentation. Some of the methods used with fluid models can be adapted to be used during fermentation.

2.2.1 Model Fluids

2.2.1.1 STEADY STATE METHODS

Steady-state methods rely on the absorption of oxygen from the gas phase simultaneously with the removal of oxygen from the liquid phase normally through a chemical or enzymatic reaction to maintain a constant, usually low, level of DO.

According to Linek (1990), difficulties in the determination of the driving force for the non ideal gas flow can be avoided by using pure oxygen for absorption during the steady state methods. Provided that the difference between the inlet and the outlet gas oxygen concentrations is small, the oxygen concentration in the dispersed gas phase is insensitive to the character of the gas phase flow, well mixed or plug flow, through the fermenter. For this reason, K_La values measured by steady-state methods are considered as the most

reliable methods (Linek, 1991). In addition, with steady-state methods, the overall mass transfer rate is evaluated whereas with dynamic methods, local K_La values are measured.

The steady-state methods are based either on a global oxygen balance or a global carbon dioxide balance in the gas phase of the bioreactor. The accuracy of steady-state methods relies strongly on the ability to measure precisely small oxygen gas concentration differences between the inlet and the outlet gas streams. The sensitivity to oxygen gas concentration differences can explain the relatively scattered K_La values obtained with the various steady-state methods.

The addition of an electrolyte to water reduces significantly the average size of bubbles, resulting in an increase in the gas-liquid contact area and in K_La (Imai et al., 1987, Van't Riet, 1979). K_La values obtained for an electrolyte solution are larger than those obtained for distilled water. The larger the level of agitation, the larger is the gap between K_La values obtained for the electrolyte solution and pure water. This is in agreement with the data reported by Van't Riet (1979).

With steady-state techniques, great care must be exercised to make sure that the oxidation rate is not enhanced by the chemical reaction. Steady-state methods are slow and expensive. They cannot provide accurate determination of K_La at low oxygen conversions (Vashitz et al., 1989).

2.2.1.1.1 Sodium Sulfite Method

Based on a technique first proposed by Cooper et al. (1944) where the oxidation of sodium sulfite, with copper or cobalt ions as a catalyst, serves to keep a low level of oxygen in the liquid phase. Oxygen entering the liquid phase is immediately consumed to oxidize the sulfite, so that the rate of oxidation is equivalent to the oxygen transfer rate. The rate of oxidation is normally evaluated by titration of the sulfite ions remaining in the solution.

The next four methods described in subsequent sections are all based on the sulfite oxidation method initially proposed by Cooper et al. (1944) which consists of (1) removing the DO from the liquid medium, (2) adding a known concentration of sodium sulfite, (3) sparging the liquid medium with a known flow rate of oxygen gaseous mixture, and (4) monitoring the sulfite concentration as a function of time. The stoichiometry of the reaction in aqueous solution is as follows:

$$SO_3^{2-} + H_2O \rightarrow SO_4^{2-} + 2H^+ + 2e^- \quad (2.5)$$

$$\frac{1}{2}O_2 + H_2O + 2e^- \rightarrow 2OH^- \quad (2.6)$$

The sulfite oxidation method does not require that the mechanism of the rather complex chain of sulfite oxidation reaction be known in detail (Linek and Vacek, 1981c). The effect of copper catalyst is very complex. Cupric ion has a catalytic action whereas cuprous ion has an inhibiting effect (Linek and Vacek, 1981a). For cobalt catalyst concentration greater than 10^{-6} kmol/m^3, the oxygen transfer rate is enhanced by chemical reaction (Thibault et al., 1990). The same critical cobalt concentration was obtained by Dussap et al. (1985). Moreover, this is also in agreement with the findings of Linek and Vacek (1981a), who reported that cobalt catalyst gives about twelve times faster reaction rate than copper catalyst. The higher K_La values obtained through the sulfite oxidation method over that of water are due to the strong ionic state of the sulfite solution provided that no chemical reaction enhancement occurs. Indeed, as observed by many researchers (Dussap et al., 1985, Linek and Vacek, 1981c, Van't Riet, 1979), there exists a cobalt concentration, at which the accompanying reaction is sufficiently rapid to keep a zero DO concentration in the bulk liquid but which does not enable to any significant extent the reaction to proceed in the liquid film at the gas-liquid interface, that would then chemically enhance the mass transfer coefficient.

However, as pointed out by Linek and Benes (1978), the reaction of DO with sulfite ions is catalytically sensitive to impurities contained in reagents. Therefore critical catalyst concentration should not be taken for granted but one should resort to experimentation to determine the experimental conditions for which the chemical reaction will not enhance the oxygen absorption.

Ogut and Hatch (1988) used a $CoSO_4$ catalyst concentration of 10^{-3} kmol/m^3, which is much higher than the required minimum concentration for chemical enhancement. This explains the reasons for their relatively high values of K_La observed for lower values of the gassed power per unit volume $\bar{P}_G/V_L$ than reported by others.

2.2.1.1.2 Iodometry Method

Iodometry is the traditional sulfite oxidation method as initially proposed (Cooper et al., 1944) and used by others (Douglas and West, 1965). It consists of removing a small

known volume of the medium and immediately neutralizes the remaining sulfite ions with aqueous iodine. The appearance of a yellow colour attests the complete neutralization of the remaining sulfite. The excess iodine is then titrated with sodium thiosulfate ($Na_2S_2O_3$), which allows the calculation of the sulfite concentration. The oxygen transfer rate is obtained by following the rate of oxidation of sodium sulfite. For constant operating conditions, the oxidation of sulfite is a linear function of time (Figure 2.2). It is therefore possible to calculate the K_La using the following equation:

$$K_La = \frac{1}{V_L\left(C_L^* - C_L\right)} \frac{\left[SO_3^{-2}\right]_{t_1} - \left[SO_3^{-2}\right]_{t_2}}{(t_1 - t_2)} \frac{1 \text{ mole of } O_2}{2 \text{ moles of } SO_3^{-2}} \qquad (2.7)$$

Until sulfite ions are present in the solution, the DO concentration (C_L) remains at zero. The sulfite oxidation method is an accurate method provided that the oxygen transfer rate is not enhanced by the chemical reaction and that sampling and titration are done under an inert atmosphere. It is, however, time consuming.

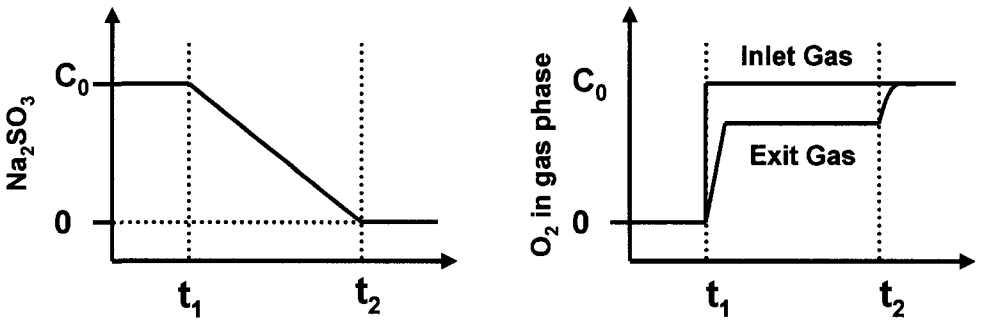

Figure 2.2 – Change in concentration of Na_2SO_3 and oxygen gas concentration in sulfite oxidation method.

2.2.1.1.3 Gas Balance Method

Siegell and Gaden (1962) proposed a modification to the sulfite oxidation method that consists in measuring oxygen concentration, flow rate, pressure and temperature of the inlet and exit gas streams while the sulfite method is being performed. This is a combination of the gas balance method and the sulfite oxidation method. This method was also used by Ogut and Hatch (1988) and Denis et al. (1990). The same procedure is used except that the iodometry is replaced by a simple oxygen mass balance. The difference in the gaseous oxygen concentration across the liquid medium is a measure of the overall oxygen transfer rate (OTR) and K_La is calculated with the following equation:

$$K_L a = \frac{Q_1 C_1 - Q_2 C_2}{V_L \left[C_L^* - C_L \right]} \tag{2.8}$$

This method is significantly more rapid than the traditional sulfite method (approximately 15 minutes) and offers the advantage of being able to determine numerous $K_L a$ values under various operating conditions (flow rate, agitation) in the same experiment. On the other hand, this method relies heavily on the ability to measure accurately small oxygen concentration difference and gas flow rates. In addition, the precision in the calculation of $K_L a$ relies on the assumption that the flow of gas through the fermenter is ideal i.e., well mixed. Pressure and temperature are also measured to perform a proper oxygen material balance.

2.2.1.1.4 Na_2SO_3 Feeding Method

To alleviate the enhancement of the physical absorption caused by the sodium sulfite and by the modification of the electrolytic properties of the solution, Imai et al. (1987) proposed a simple method for feeding sodium sulfite in the fermenter as it is consumed to maintain a low concentration of electrolyte in the liquid medium. They used sulfite concentration of less than 5.5 mol/m^3 so that the oxygen absorption is physical since sulfite oxidation occurs only in the bulk liquid. They used the following equation to calculate $K_L a$:

$$K_L a = \frac{Q_{Na_2SO_3} \left[(C_{BF} - C_{BS}) - (C_{AF} - C_{AS}) \right]}{2 V_L \, C_{Ai} (1 - C_{AS}/C_{Ai})} \tag{2.9}$$

Here, Q is the volumetric feed rate of Na_2SO_3 solution, C_{As} and C_{Bs} are the concentration of DO and residual sulfite in steady state, respectively. C_{AF} is the concentration of DO in the Na_2SO_3 feed solution, C_{BF} is the sulfite concentration in the feed solution and C_{Ai} is the equilibrium concentration of dissolved gas at the gas-liquid interface. The feeding of Na_2SO_3 was continued until the DO reaches steady state and the liquid level was maintained constant using an overflow pipe. This method has the advantage that it can be used quickly to measure $K_L a$ even in large fermenters without requiring excessive amount of sodium sulfite concentration. However, Linek et al. (1990) found that this method gave correct values of $K_L a$ only when pure oxygen was used.

2.2.1.1.5 Reaction Time Method

This method was proposed by Denis et al. (1990) and is similar to the mass balance method. In this modified method, it is necessary to maintain constant all operating variables and to know the exact initial concentration of sulfite ions in the liquid medium. The overall oxygen transfer rate is then calculated with the time required to completely oxidize sulfite to sulfate. A known initial concentration of Na_2SO_3 is added at time t_1 and the final time t_2 is recorded when the oxidation of sulfite is completed. The completeness of reaction or the value of t_2 is observed when the DO begins to return to saturation concentration.

$$K_L a = \frac{1}{V_L \left(C_L^* - C_L\right)} \frac{\left[SO_3^{-2}\right]_{t_1}}{\left(t_2 - t_1\right)} \frac{1 \text{ mole of } O_2}{2 \text{ moles of } SO_3^{-2}} \tag{2.10}$$

2.2.1.1.6 Hydrazine Method

This method relies on the catalytic reaction of hydrazine with oxygen to give nitrogen and water:

$$N_2H_2 + O_2 \xrightarrow{\text{Catalyst}} N_2 + H_2O \tag{2.11}$$

To be sure that hydrazine is not present in excess, a solution of hydrazine is gradually added continuously. The steady state DO level enables determining $K_L a$ because the feeding rate of hydrazine is equal to the absorption rate of oxygen in the liquid phase (Equation 2.1).

$K_L a$ is determined when no net accumulation of hydrazine is observed. The DO is significantly lower than the saturation concentration but not zero; this is possible by delaying the addition to slightly increase the DO to a known concentration. Both products, nitrogen and water, do not modify the physical and chemical properties of the medium. Thus, this method can be utilised for a coalescent system contrary to sulfite method. However, this method must be operated under specific conditions of pH (pH>11), catalyst and oxygen concentration. Zlokarnik (1978) used a mixture of copper hydroxide and copper oxides where as Weiland et al. (1986) used copper tetrasulphophtalocyanine (CuTeSP) as catalyst. However, Linek et al., (1987) do not recommend this method because a chemical enhancement of oxygen absorption was observed thereby affecting the determination of $K_L a$.

2.2.1.1.7 Krypton Method

This method was proposed by Pedersen et al. (1993) and it is based on a volatile, radioactive isotope ^{85}Kr. K_La is determined for Krypton using a gas balance of inlet gas containing the radioactive isotope and radioactivity is measured in the exhaust gas. K_La for oxygen is found by using following ratio (Tsivoglou et al., 1965):

$$\frac{(K_La)_{Kr}}{(K_La)_{O_2}} = 0.82 \tag{2.13}$$

Radioactive isotope ^{85}Kr is a volatile isotope that is inert to model fluids as well as to fermentation broths. Therefore, this method can be applied to actual fermentation broth. Pedersen et al. (1993) applied this method to measure the K_La during the growth of *Aspergillus oryzae*.

2.2.1.1.8 Glucose Oxidase Method

Linek et al. (1981b) used another steady-state method based on the oxidation of glucose in the presence of the enzymes glucose oxidase and catalase. This method follows the enzymatic oxidation of glucose into gluconic acid. This method was used recently by Juraščik et al. (2007). The enzymes, glucose oxidase and an excess of catalase react in following way:

$$\text{Glucose} + O_2 \xrightarrow[H_2O]{\text{Glucose oxidase}} \text{Gluconic acid} + H_2O_2 \tag{2.14}$$

$$H_2O_2 \xrightarrow{\text{Catalase}} H_2O + \frac{1}{2}O_2 \tag{2.15}$$

The rate of oxygen consumption in the enzymatic reaction can be calculated using the rate equation for oxygen transfer under steady-state conditions. One advantage of this method is that the reaction does not accelerate the oxygen transfer and also has a high specificity of the catalytic action. This method has also the advantage that the liquid medium can have properties that can resemble those of fermentations systems.

2.2.1.2 DYNAMIC METHODS

Dynamic methods are the most popular methods for measuring K_La and they are being used in a large number of applications. It normally consists of lowering the oxygen concentration of the solution by substituting the oxygen rich stream with nitrogen or by using a small quantity of sodium sulfite in presence of a catalyst such as cobalt. The

deoxygenated liquid is then aerated and agitated, and the increase in DO monitored with a DO probe. This method is also popularly known as unsteady state gassing-out method. By recording the DO concentration as a function of time, it is possible to calculate the oxygen transfer coefficient K_La.

K_La determined based on the dynamic method varies from the simple first order model to more complex analyses such as the dynamic model moment analysis proposed by Dang et al. (1977), as well as numerous other models to compensate for the dynamic response of the oxygen probe itself, the effect of the liquid film resistance in the vicinity of the membrane and the dynamics of the gas and liquid phases (Dunn and Einsele, 1975, Dussap and Gros, 1984, Gibilaro et al., 1985, Kok and Zajic, 1975, Linek et al., 1984).

There are numerous problems with the dynamic method. Linek et al. (1987) in an excellent review article discussed the potential problems in using the dynamic method. Neglecting the oxygen electrode response time, the effect of liquid hydrodynamics and gas phase mixing are common sources of errors in K_La measurements (Dunn and Einsele, 1975). When gas bubbles impinge against the electrode membrane, the recorded signal corresponds to the average partial pressure of oxygen in the vicinity of the membrane. Merta and Dunn (1976) found that errors of 20% in DO concentrations could be caused by either bubble contact or liquid turbulence. To alleviate this problem, it has been suggested to place the probe with a 45° angle (Nienow et al., 1978). Linek and Vacek (1978) suggested using a protective gauge or to place probe in a bypass or place the probe facing upwards to prevent bubbles interacting with the membrane. However for a standard commercial fermenter, the probe location and orientation are fixed and as a result K_La values determined with the dynamic methods during the fermentation might also be incorrect.

Many authors observed an unexpected decrease in K_La with an increase in dissipated power. Linek et al. (1982) showed that this was due to the use of air for the measurement of K_La. Especially at high mixing intensity the dynamic method showed a drop in K_La with increasing power provided to system. Linek et al. (1989) recommends that only two dynamic methods (pure oxygen and dynamic pressure method - discussed later) are not affected by experimental conditions and for these two methods the driving force is also well defined.

2.2.1.2.1 Gassing-Out Method

In this method, the liquid medium is deaerated by using nitrogen with the same gas rate and agitation conditions as the experimental run to be performed. This procedure serves to deplete the liquid of oxygen and insures that the gas hold-up remains constant (Chapman et al., 1982). In addition, with this procedure it is not necessary to consider the influence of the simultaneous inter-phase nitrogen transport since it has no appreciable effect on the determination of K_La values (Linek et al., 1981a, 1982). To obtain the correct value of the oxygen transfer coefficient, it is necessary to compensate for the dynamics of the DO probe, the resistance to the liquid film in the vicinity of the membrane and the dynamics of the gas and liquid phases. Assuming first-order dynamics for all of these contributions, the following set of equations are obtained (Dang et al., 1977):

Oxygen probe dynamic model:

$$\tau_P \frac{dC_P}{dt} = C_F - C_P \tag{2.16}$$

Diffusion film dynamic model:

$$\tau_F \frac{dC_F}{dt} = C_L - C_F \tag{2.17}$$

Well-mixed gas phase dynamic model:

$$V_G \frac{dC_2}{dt} = [Q_1C_1 - Q_2C_2] - K_La\ V_L \left(C_L^* - C_L\right) \tag{2.18}$$

Well-mixed liquid phase dynamic model:

$$\frac{dC_L}{dt} = K_La \left(C_L^* - C_L\right) \tag{2.19}$$

The mean oxygen concentration in the liquid in equilibrium with the oxygen concentration in the gas phase, C_L^*, can be calculated using Henry's law for experiments performed with distilled water and the correlation published by Linek and Vacek (1981a) for sodium sulfate solutions. It is possible to solve this set of first-order differential equations by Laplace transform (Dang et al., 1977) or by finite differences to determine the overall oxygen transfer coefficient. Values of K_La can be obtained from the nonlinear least-square fit (Denis et al., 1990, Lounes and Thibault, 1994) of the experimental

response curves. It is possible to let the curve fitting routine to determine the value of the electrode and the film diffusion time constants along with the values of the oxygen transfer coefficient. However, it is better to determine the time constants of the electrode and the film diffusion through separate experiments to reduce the number of degrees of freedom in the evaluation of K_La.

According to Linek et al. (1987), the correct variant of the dynamic method for the determination of K_La is when pure oxygen is introduced as a step input to the liquid batch freed from any desorbed gas (with vacuum desorption or sodium sulfite) otherwise there is difference in the expected driving force and the actual driving force. The disadvantage is that K_La is measured from the start of the liquid aeration, which means calculating K_La when dispersion is not in steady state (Linek et al., 1987).

2.2.1.2.2 Dynamic Pressure Method

Another dynamic method recommended by Linek et al. (1989) involves changing the concentration of oxygen in the gas phase by a step in pressure in the reactor. In this method, the aerated reactor is submitted to a change of approximately 20% in the total pressure, which leads to a simultaneous and uniform change in the gas phase oxygen concentration. This method has the advantage that it is not affected by non-ideal gas phase mixing and it can also be used for large fermenters since the pressure change is very small. It was also used for pilot plant fermenter by Linek et al. (1994).

2.2.1.2.3 Pseudo-Random Pulse Method

This method proposed by Gauthier et al. (1990) uses a pseudorandom binary sequence which consists in switching in a pseudorandom fashion the inlet gas stream with air and nitrogen during a finite time interval. A typical random perturbation in the inlet gas and the associated DO response are presented in Figure 2.3.

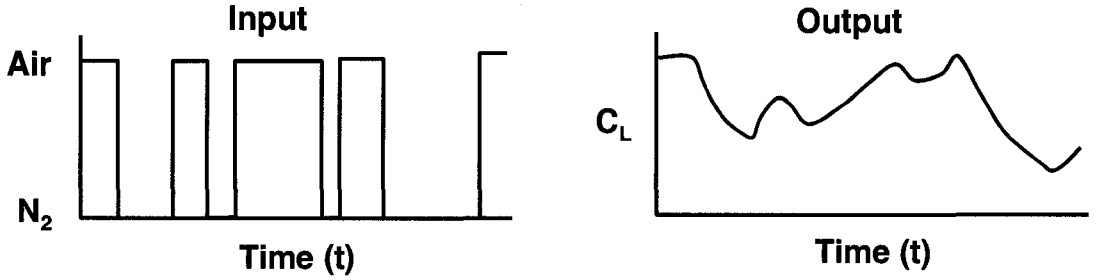

Figure 2.3 – Perturbation sequence in the inlet gas and associated DO concentration output.

The whole system of equations is solved with respect to time to determine K_La. The principal advantage of the pulsed dynamic method as compared with the gassing out method is that it induces little perturbation to the process and it can be done on-line without stopping either gas flow or agitation. This procedure reduces the influence of non-ideal mixing gas phase on the K_La value. In addition, this method requires much less nitrogen than the standard gassing-out method, implying a potential application for large-scale systems.

2.2.1.2.4 Frequency Response Method

In this method, Varder and Lilly (1982) changed the concentration of DO by sinusoidal pressure input which will change the saturation DO concentration. The system transfer function, defined in the Laplace domain, used for this study was:

System transfer function:

$$G(s)=\frac{C_L(s)}{C_L^*(s)}=\frac{1}{1+\frac{s}{K_La}} \tag{2.20}$$

Input Function:

$$C_L^*(s)=\frac{K\omega}{s^2+\omega^2} \tag{2.21}$$

Output Function:

$$C_L(s)=\frac{K\omega}{s^2+\omega^2}\frac{K_La}{s+K_La} \tag{2.22}$$

This method could also be used in an actual fermentation broth because it does not require any changes in composition of the liquid medium and it can also be done under sterile conditions. This method is similar to the pulsed dynamic method except that one frequency at the time is explored in the frequency method and the procedure must be performed at numerous frequencies to construct the Bode plots (amplitude ratio and phase angle) in order to determine the value of K_La. The authors proposed this method to easily incorporation other dynamic contributions such as the dissolved oxygen probe but failed to include it in their experience such that the system, as shown in Equation (2.2) is a simple first order system. At higher frequencies, the dynamics of the dissolved oxygen

probe cannot be neglected and the amplitude ratio becomes increasing small such that it would be difficult to obtain data over an extended frequency domain.

2.2.2 Submerged Fermentation

In a submerged fermentation, oxygen is sparged into the liquid medium and then oxygen diffuses from the gas phase to the liquid phase where microorganisms are present. It is assumed that the gaseous and DO concentration is homogeneous outside the gas and liquid films. The rate of oxygen absorption in a fermentation system is affected by the presence of cells, product formation and antifoam addition. Thus K_La values in fermenters often differ substantially from values predicted from correlation for oxygen absorption into water or simple aqueous solution from sulfite oxidation even when differences in liquid physical properties such as viscosity and diffusivity are taken into account. Therefore, there is a real need to have a reliable on-line method for measuring K_La in fermentation systems.

Calculating K_La during the course of aerobic fermentations is not an easy task because of the severe limitations that are imposed to the addition of chemicals to the broth and the necessity to keep an adequate good level of DO into the broth. There are only few dynamic methods (Bandyopadhyay and Ghose, 1976) and steady state methods (Mukhopadhayay et al., 1976) that can be used in actual fermentation broth. These will be briefly covered in this section.

The determination of oxygen absorption from air into the fermentation broth should be assessed under actual operating conditions of fermenters since their rate of oxygen absorption into a culture medium can be greatly affected by the presence of microorganisms, substrate, substances excreted by microorganisms and antifoam (Yagi and Yoshida, 1974).

2.2.2.1 STEADY STATE METHODS

2.2.2.1.1 Stationary Method

The oxygen uptake rate (OUR or $Q_{O2}X$) can be calculated (Shuler and Kargi, 1992) by performing a gaseous oxygen mass balance across the fermenter using a gas analyzer or using the OUR obtained from dynamic method (Taguchi and Humphrey, 1966). Under steady-state, Equation (2.3) is reduced to:

$$K_L a = \frac{\text{OUR}}{C_L^* - C_L^0} \tag{2.23}$$

2.2.2.1.2 Gas Balance Method

Under steady state conditions, the oxygen deficit of the gas stream across the fermenter must be equal to the oxygen uptake rate. To determine $K_L a$ by the gaseous oxygen mass balance technique the following equation is used (Patel and Thibault, 2004, Pouliot et al., 2000):

$$K_L a = \frac{1}{V_L} \frac{\left((P_1/RT_1)Q_{1,G}y_{1,O_2} - (P_2/RT_2)Q_{2,G}y_{2,O_2}\right)}{\left(C_L^* - C_L^0\right)} \tag{2.24}$$

The gaseous carbon dioxide production rate can also be used as described by the following equation:

$$K_L a = \frac{1}{RQ}\frac{1}{V_L} \frac{\left((P_2/RT_2)Q_{2,G}y_{2,CO_2} - (P_1/RT_1)Q_{1,G}y_{1,CO_2}\right)}{\left(C_L^* - C_L^0\right)} \tag{2.25}$$

However, to use the carbon dioxide production rate, an estimation of the respiratory quotient (RQ) must be available a priori. A good estimate of RQ is available for a large number of fermentations or can also be estimated from past fermentations.

2.2.2.1.3 Bioluminescence Method

Based on the study performed by Hastings (1952) where it was determined that the rate of oxygen supply to the cells is sensitive to the bioluminescence, Vashitz et al. (1989) has proposed a method to measure $K_L a$ in a viscous *Xanthomonas campestris* fermentation. A bioluminescent strain of *X. campestris* is used to measure the oxygen mass transfer. When the oxygen concentration declined below 1% (critical value), the luminescence declined sharply. This decline in luminescence was used to determine the oxygen transfer rate.

2.2.2.2 DYNAMIC METHOD

The dynamic method has been widely used in fermentation systems to determine the respiration rate of the culture using the response curve during the deoxygenation period and the $K_L a$ value using the response curve of the reaeration period thus allowing to measure the oxygen transfer coefficient under realistic fermentation conditions (Taguchi and Humphrey, 1966, Bandopadhyay et al., 1967, Paca and Gregr, 1977, Koizumi and

Aiba, 1984). When the dynamic method is used, it is necessary to perform an accurate modeling of the oxygen probe dynamics if correct values of K_La are to be obtained.

2.2.2.2.1 Taguchi and Humphrey Method

In the course of fermentation, Equation (2.3) represents the rate of change in the DO concentration in a batch reactor as a function the rate of oxygen transfer from the gas phase and the rate of utilization. The method, elaborated by Taguchi and Humphrey (1966), consists of first evaluating the oxygen consumption by the interruption of the gas flow rate (Figure 2.4). The decrease in the DO concentration in the bioreactor can be attributed entirely to the oxygen consumption by the microorganism. Therefore, Equation (2.3) becomes:

$$\frac{d C_L}{d t} = - Q_{O_2} X \qquad (2.26)$$

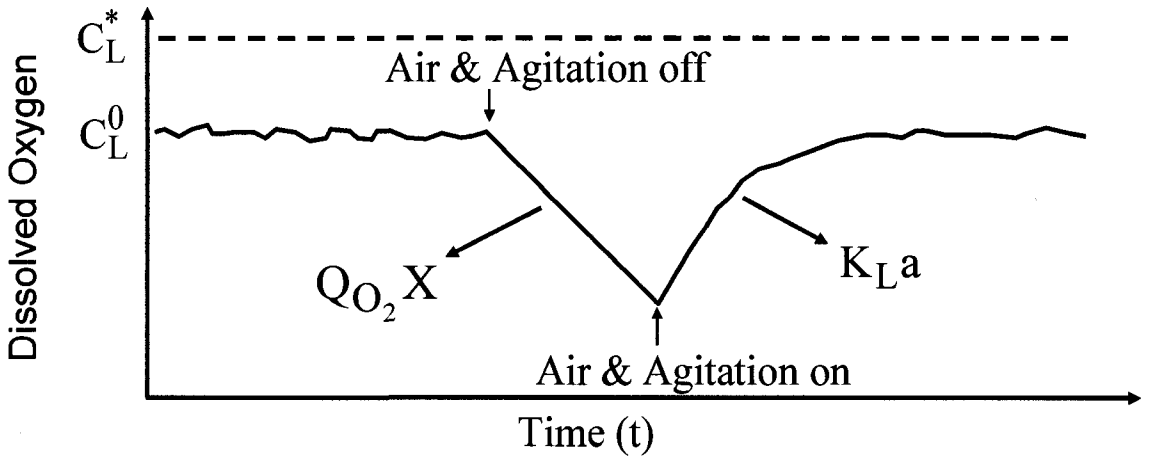

Figure 2.4 – Profile of the DO concentration while determining K_La using the Taguchi and Humphrey method.

This equation suggests that a plot of the DO concentration as a function of time gives a slope equal to the oxygen uptake rate $\left(- Q_{O_2} X\right)$. Before the DO reaches its critical value (C_{crit}), the gas is reintroduced into the bioreactor and agitation is resumed (Figure 2.4). The DO concentration is recorded until it returns to a constant value. The second portion of the dynamic test allows the calculation of the mass transfer coefficient. With some manipulations of equation (3), a plot of the DO concentration as a function of $\left(dC_L/dt + Q_{O_2} X\right)$ for the aeration part gives a slope equal to the reciprocal of K_La value

(Figure 2.5). The second portion of the DO profile can also be solved numerically and has the advantage of allowing the incorporation of the dynamics of the DO probe. Appreciable errors, especially for higher values of K_La, may result if the probe dynamics is neglected.

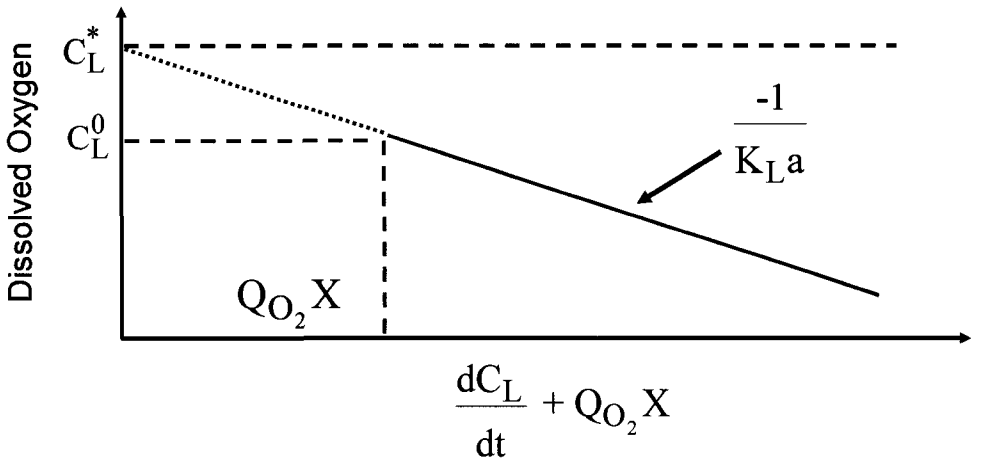

Figure 2.5 – Determination of K_La using slope obtained by plotting the DO concentration as a function of $\left(dC_L/dt + Q_{O_2}X\right)$.

The rate of respiration can be treated as zero order with respect to the DO concentration, C_L, for the range of C_L above the critical oxygen concentration C_{crit} and first order when C_L is very small, viz. C_L much less than C_{crit} (Yagi and Yoshida, 1975). It is important to point out that the estimate of K_La using the dynamic method does not depend on the estimation of $\left(Q_{O_2}X\right)$. Indeed, it can easily be shown that the dynamic response, after aeration and agitation are resumed, is independent of $\left(Q_{O_2}X\right)$ apart from having an influence on the final level of the DO concentration.

Pouliot et al. (2000) made a small change to the above method by keeping a small agitation when the aeration was cut to prevent cell sedimentation and avoid higher oxygen consumption in the lower part of the fermenter. It has been shown that low agitation has a negligible effect on K_La and surface aeration (Gagnon et al., 1998).

2.2.3 Solid State Fermentation (SSF)

Oxygen mass transfer coefficient (K_La) has been widely studied in submerged fermentation but has received little attention for solid state fermentation (SSF). In a SSF,

microorganisms grow around the solid particles or within the particle. A thin layer of liquid film surrounds the solid particle and also the biofilm growing on its surface. New mathematical models describing the performance of SSF bioreactors have been developed in last few years. Due to difficulties in determining the model parameters because of lack of experimental data, the validation of these models is difficult. Mitchell et al. (2002, 2004) have recently published a two-part review of the current state of SSF. The first part examines the techniques used to model heat and mass transfer phenomena and the second part reviews both empirical models and microscale models to model the microbial growth kinetics and intraparticle phenomena in SSF.

In a SSF, oxygen has to pass through the film of biomass at the surface of the pellet. Therefore, researchers (Rajagopalan and Modak, 1995) have concluded that although the oxygen concentration might be higher in the gaseous phase, it is still possible that the growth is limited by oxygen rather than substrate concentration at least during the early and middle stage of fermentation. Further, oxygen diffusion becomes more difficult at high moisture concentration because the pores are filled with liquid. Therefore, it is very important to estimate the oxygen mass transfer coefficient (K_La) in a SSF.

However, applying directly the techniques used in submerged fermentation to calculate K_La in SSF might lead to large errors since there is no convection on the liquid side of the medium and the oxygen is consumed in the liquid film (Thibault et al., 2000). Different models have been developed to represent the oxygen diffusion and reaction (Oostra et al., 2001, Rahardjo et al., 2002, Thibault et al., 2000). Thibault et al. (2000) developed a model where they suggested using a conductive biofilm coefficient (K_Fa) instead of K_La which is used in submerged fermentation because in a SSF there is no uniformly mixed bulk liquid on the gas-liquid interface and therefore the biofilm is the limiting step in the oxygen transfer. Using this model they compared the rate of oxygen transfer across the gas-liquid interface at the surface of the biofilm with the rate of diffusion across the biofilm.

2.2.3.1 ESTIMATION OF OXYGEN MASS TRANSFER IN SSF

Durand et al. (1988) estimated K_La using a modified sulfite oxidation method in a packed bed fermentation system. Gowthaman et al. (1995) used an overall gas balance method to estimate K_La in a SSF using a packed-bed reactor. They assumed that

microorganisms grow only on the liquid film surrounding the particle and mass transfer is only due to liquid film. Therefore, Equation (2.1) can be written for a SSF as:

$$N_{O_2} = K_L a \left(C_{L,r2} - C_{L,r1}\right) \tag{2.27}$$

where, r_1 is the radius of solid particle alone and r_2 is the radius of the solid particle with the surrounding liquid film. From above equation, $C_{L,r2}$ is in thermodynamic equilibrium with the gas phase immediately outside the particle and the DO concentration within the solid particle is uniform and equal to $C_{L,r1}$.

Thibault et al. (2000) argued that above equation is not valid for SSF since it does not follow the assumption taken while determining $K_L a$ in submerged fermentation where convection occurs on both the gas and liquid films. Indeed in SSF, the three mechanisms are: convection at the gas-liquid boundary, oxygen diffusion across the liquid film and oxygen being consumed within the liquid film by the microorganism. Therefore, they modified Equation (2.27) and a using mass balance suggested the following equation to determine the oxygen concentration profile.

$$N_{O_2} = \left(\frac{D_{O_2,L}}{\delta}\right) a \left(C_{L,r2} - C_{L,r1}\right) \tag{2.28}$$

They also suggested instead of using $K_L a$ in Equation (2.27), to use $K_F a$, a conductive biofilm coefficient, which takes the three physical parameters, $D_{O_2,L}$, δ and a, to describe the oxygen mass transfer in SSF. Then, K_F is the ratio of the DO diffusivity and the biofilm thickness.

2.3 RECENT ADVANCES

2.3.1 New Approach

2.3.1.1 DATA RECONCILIATION

It is now more common for fermentation systems to be equipped with an O_2/CO_2 monitor system such as mass spectrometer. This allows the estimation of $K_L a$ using four methods, thereby leading to four different estimates: one from dynamic method, one from stationary method and two from gas balance methods. At any time during fermentation, all methods should give identical values of $K_L a$, but this is rarely the case. The difference in the estimation of $K_L a$ is due to the reliability of measured variables but also because

the mass balance models are not perfect representations of the conditions prevailing in the fermentation broth. At the beginning of the fermentation process when the DO concentration is high, the dynamic method can give a good estimate of K_La but as the fermentation progresses and DO decreases, the accuracy of the dynamic method decreases. On the other hand, the gas balance method depends on the measurement of inlet and outlet gas concentrations and therefore, at the beginning of fermentation due to small biomass concentration, the difference in the inlet and outlet concentrations of oxygen in the gas stream are small. Therefore, K_La obtained using the gas balance method is not very accurate, but as the fermentation progresses and the amount of biomass increases, the difference between the inlet and outlet gas concentrations increases. As a result, the gas balance technique can provide a good estimate of K_La. However, as some methods are more accurate than others at different stages of fermentation, averaging K_La is not the best method to achieve a precise value. Instead, a data reconciliation technique (Pouliot et al., 2000, Patel and Thibault, 2004) can be used to improve the reliability of measurements in order to obtain a more accurate and consistent value of K_La.

Data reconciliation mainly consists of solving the K_La estimation problem by taking into account both the reliability of all measured variables and the accuracy of all mass balance equations. Patel and Thibault (2004) minimized an objective cost function involving 12 measured process variables and 4 mass conservation models using a quasi-Newton optimization routine to estimate K_La in *Aspergillus niger* fermentation. Weighting factors of each measurement terms can be easily determined. To determine the weighting factors of each oxygen conservation model, a Monte Carlo simulation was used considering the accuracy of all process variables.

$$J = \sum_{i=1}^{m} \varphi_i \left(\pi_i^{\text{estimated}} - \pi_i^{\text{measured}} \right)^2 + \sum_{j=1}^{n} \varphi_j \left(K_L a_j^{\text{estimated}} - K_L a_j^{\text{calculated}} \right)^2 \qquad (2.31)$$

Here, J is the objective function, ϕ are the weights, π_i is the measured variable i, m is equal to number of measured variables and n is equal of mass conservation models used to estimate K_La. Patel and Thibault (2004) also did a sensitivity analysis to show that data reconciliation provides more accurate estimates of K_La and relying on more than one method can help to give a better estimate of K_La.

2.3.2 Advances in Measuring Instruments

Small-scale bioreactors such as shake flasks, test tubes and microtiter plates (mini bioreactors) are extensively used to screen aerobic and anaerobic microorganisms. However, in such small scale bioreactors it is difficult to know if there is sufficient mixing, enough oxygen supply to microorganism or information on removal of carbon dioxide. Therefore, it is difficult to use data obtained from small-scale bioreactors to scale-up for large scale production.

To overcome these difficulties, researchers have recently used optical sensors to characterize small-scale bioreactors such as shake flasks and microtiter plates.

2.3.2.1 OPTICAL SENSORS

In the last decade, optical sensors are widely used to measure the DO concentration both in large and small scale bioreactors. Although developed recently, the principle behind the working of optical sensors is not new. It is based on the principle of dynamic fluorescence quenching developed by Kautsky in 1939. According to this principle, oxygen has the ability to quench the fluorescence and phosphorescence of certain luminophores such as a ruthenium complex.

In an optical sensor, a light source bombards a luminophore at around 475 nm emitting energy at around 600nm. This energy is transferred to oxygen molecules in the vicinity of luminophore. The degree of fluorescence quenching is measured by a detector. The degree of fluorescence quenching can be related to the level of the DO concentration. The optical sensors are calibrated using Stern-Volmer equation:

$$\frac{I_0}{I} = 1 + k\, p_{O_2} \tag{2.30}$$

A two-point calibration is performed by first placing the optical sensor in a liquid depleted with oxygen usually by purging nitrogen and then in a saturated liquid for the second point. Since Stern-Volmer equation is not linear at high concentration of oxygen, it is better to use more than two points to calibrate and use a second order polynomial algorithm.

If these sensors are to be used in a biological system, they should be able to withstand cycles of autoclave. Whitmaan et al. (2003) investigated the long term stability of their optical sensor by subjecting it to 80 autoclave cycles of 15 min each at 121°C. They

concluded that their sensor was not affected by autoclave procedure and also needs to be calibrated only once after the first autoclave. However, optical sensors provided by Ocean Optics are not recommended for autoclaving.

Another important parameter to consider before using any device to measure the DO concentration in fermentation system is the response time. Whitmann et al. (2003) found a time constant of 6 s for their sensor but Gupta and Rao (2003) used a sensor with a time constant of 30 s. Therefore, it is very important to know the time constant of the sensor used to measure the DO concentration and, if significant, it should be incorporated while calculating K_La as done by Gupta and Rao (2003).

Optical sensors using a luminophore is not the only technique recently developed to study the oxygen mass transfer phenomenon in microtiter plates. Herman et al. (2001, 2002) have used an optical method based on the sulfite oxidation method. They calculated the reaction time by monitoring the change in colour using a CCD camera from blue to yellow due to the pH drop at the end of reaction. If the length of sulfite-oxidation reaction is known, then the constant oxygen transfer rate can be calculated by knowing the initial concentration of Na_2SO_3 added.

2.3.3 Applications

2.3.3.1 SHAKE FLASK

Shake flasks are used in both research and industry for wide ranges of applications such as to prepare inoculum, screen microorganisms and study process operating conditions. But in the past, there has been little work done to quantify important information such as oxygen supply, effect of mixing and even oxygen diffusion through the plugs which are used to cover the shake flasks. It is generally assumed that there is sufficient oxygen supply and microorganisms are growing under near optimal conditions. Nikakhtari and Hill (2006) studied the mass transfer of oxygen through closure and headspace of the shake flasks. The geometry of the shake flask such as narrow neck of the holder and the type of closure were found to have a significant effect on the oxygen transfer in the shake flask. Therefore, there is a need to devise methods which can measure important parameters such as K_La for aerobic microorganism in shake flask.

The main difficulty in obtaining this information in shake flask is measuring the DO concentration with traditional DO probes or recently with fiber-optic technology.

Nikakhtari and Hill (2005) measured K_La in shake flask cultures using a 12-mm DO probe (Hach Company, Loveland) with 7.9 ± 0.5s probe response time. Further they developed an empirical equation for the prediction of K_La in shake flask cultures which was function of two parameters: (1) the stationary liquid surface and turbulence factor and (2) a factor defined as the ratio of the flask volume to the liquid volume multiplied by the shaker agitation speed.

These probes are difficult to operate under aseptic conditions, affect the flow conditions and may fail due to shaking at high speed. To overcome these problems, optical sensors have been used recently (Wittmann et al. 2003, Gupta and Rao, 2003) at the bottom of shake flask where a patch containing oxygen sensitive dye is placed. Then, the flask is placed on top of a coaster which contains a light source and a detector. This set-up is shown in Figure 2.6.

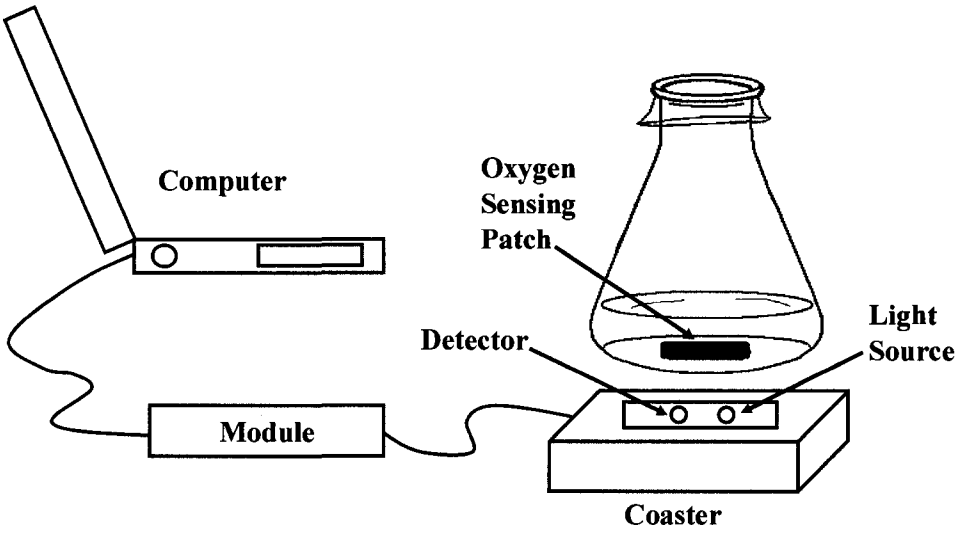

Figure 2.6 – Typical set-up of shake flask with optical sensor to monitor the DO concentration.

As discussed previously, the DO can be measured using the Stern-Volmer equation. The gassing-out method was used by both Wittmann et al. (2003) and Gupta and Rao (2003) to calculate K_La. Gupta and Rao (2003) took two resistances into consideration to determine two transfer coefficients: a gas-liquid mass transfer coefficient and a plug transfer coefficient. This technique was then applied to shake flask cultivating microorganism. Gupta and Rao (2003) further compared the K_La values obtained from

shake flasks to stirred tank fermenters and obtained similar growth and product formation kinetics proving that information obtained from shake flasks can be used for scale-up.

2.3.3.2 MICROTITER PLATES

Microtiter plates are widely used as a first step in screening microorganism for large-scale production. Difficulties encountered during shake flask experiments in obtaining experimental data become more profound in microtiter plates due to the very small size of reactor vessels (mini-bioreactors). Recently, with the help of optical sensors, it has become possible to follow the oxygen concentration in microtiter plates and by using the traditional methods such as the sulfite method and the dynamic method, K_La has been determined in such small size bioreactors. Figure 2.7 shows a single well in which flurophore was immobilized at the bottom. The flurophore is excited and the intensity read in a microplate reader.

John et al. (2003) developed 96-well microtiter plate with fluorophores immobilized at the bottom. For the first set of experiments, K_La was determined using the dynamic method using a microtiter plate reader with an integrated shaker. Zero DO concentration was achieved by adding sodium dithionite solution. Due to aeration, dithionite was first completely consumed and then excess oxygen starts accumulating in the medium. This increase in oxygen concentration in the medium was measured using a microtiter plate reader. Using Equation (2.3), K_La was estimated from the slope of the curve $\ln\left(C_L^* - C_L\right)$ versus time.

John et al. (2003) also performed a second set of experiments where the shaking intensity of the plate was much higher and *Corynebacterium glutamicum* were cultivated in both microtiter plates and in a stirred tank bioreactor. It was not possible to use the dynamic method because the change in oxygen concentration was not very fast compared to the measurement technique. However, the measurements were fast enough to keep the difference in DO small. Also, the oxygen transfer conditions in the well will change when moving between the measurement and shaking position. Therefore, to calculate K_La using Equation (2.3), DO measurements were taken from microtiter plates but OUR was calculated from cells growing at same density and growth rate in the stirred tank bioreactor.

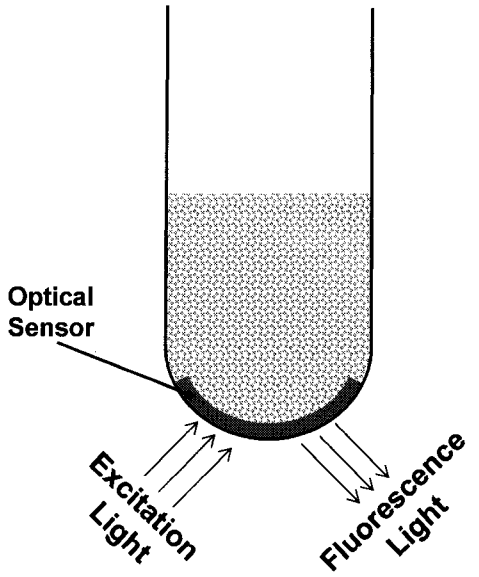

Figure 2.7 – Diagram of a single well in a microtiter plate with flurophores immoblized at the bottom.

2.3.4 Modification of Existing Methods

2.3.4.1 ANIMAL CELL CULTURES

Determination of K_La in animal cell culture becomes more difficult because of the absence of cell wall and their large size. They are therefore prone to cell damage due to sparging, bubble formation and foaming. Also animal cells have a high sensitivity to variation in DO concentration and also have low specific oxygen consumption rate.

Ruffieux et al. (1998) reviewed different techniques which are used to measure K_La in animal cell cultures. They classified the methods into global mass balance and dynamic methods. Global mass balance technique requires the use of a costly mass spectrometer since the difference in the inlet and outlet gas stream is very small due to very low specific oxygen consumption rate. On the other hand, to use the dynamic method the system needs to be disturbed and also it cannot be easily automated.

To avoid cell damage due to gas sparging, membrane aeration have been used. Dorresteijn et al. (1994) circulated the medium from the fermenter through a silicon tubing and then through a stripping vessel which was continuously flushed with nitrogen. Applying mass balance between liquid phase and headspace and also in the fermenter and the stripping vessel allowed them to determine simultaneously solubility of oxygen and K_La in a stirred tank bioreactor. Ruffieux et al. (1998) also recommended that the optimal

method for the determination of the OUR is the stationary liquid phase balance method. In this method, oxygen is continuously supplied using a PID controller such that the DO level remains constant. Therefore, the OUR becomes equal to the OTR which is given by Equation (2.1). The problem with this method is that K_La needs to be known throughout the fermentation process.

Ducommun et al. (2000) suggested a new technique where the K_La was kept constant throughout the fermentation process by using polytetrafluoroethylene (PTFE) membrane for aeration. To determine K_La, the reactor was deaerated using nitrogen and then air was introduced without and with animal cells. Using a membrane for aeration and for the determination of the OUR and K_La in animal cell culture seems to be a good choice considering the shear sensitive character of animal cells.

2.4 SUMMARY & CONCLUSION

The main aim of this chapter was to review different methods available for the measurement of K_La in fermenter with and without microorganism. Therefore, along with a brief introduction on oxygen mass transfer in fermentation system, various methods of K_La determination were reviewed. This list is however not complete but represents the most important ones. Some recent developments on oxygen mass transfer measurement methods have also been reviewed.

In the last decade with the increase in computing power, researchers are more able to develop and solve complex models. With further increase in this technology, more complex models can be developed for systems such as SSF where both macroscale and particle-level phenomena needs to be included to better understand the growth in SSF system. Due to difficulties in measurement in a SSF, currently most of the models used are simple kinetic models which do not describe completely the phenomena in SSF. With the development of new biomonitoring techniques, more experimental data will be available to validate the models and thus help in the scale-up which is currently very difficult in SSF.

With the advancement in technology (measuring instruments) and better methods being developed, it will be possible to estimate a more precise value of K_La during fermentation processes. Moereover, techniques such as data reconciliation can be used to

obtain a better estimate of K_La. However, early methods such as the dynamic method and the sulfite oxidation method will still be used to measure K_La either in the same form or modified since they provide reliable estimates of K_La when proper mass transfer models are applied.

2.5 NOMENCLATURE

a	gas-liquid volumetric surface area (m^2/m^3)
C	concentration (mol/m^3)
C_A	concentration of DO in vessel liquid (mol/m^3)
C_{AF}	DO concentration in feed Na_2SO_3 solution (mol/m^3)
C_{AS}	DO concentration under steady state (mol/m^3)
C_{BF}	sulfite concentration in feed solution (mol/m^3)
C_{BS}	concentration of residual sulfite under steady state (mol/m^3)
C_{crit}	critical or minimum DO concentration for normal growth (mol/m^3)
C_F	DO concentration in the liquid film (mol/m^3)
C_G	DO concentration in the gas phase(mol/m^3)
C_L	DO concentration in the liquid phase (mol/m^3)
C_L^0	pseudo-steady-state DO concentration recorded at the initiation of the dynamic method (mol/m^3)
C_L^*	saturated DO concentration in the solution (mol/m^3)
C_P	DO concentration recorded by the oxygen probe (mol/m^3)
DO	dissolved oxygen
H	Henry's law constant
I	fluorescence intensity at the oxygen concentration
I_0	fluorescence intensity in the absence in oxygen
K	Stern-Volmer paramter
K_Fa	biofilm mass transfer overall conductance (s^{-1})
K_G	mass transfer coefficient in gas phase (m/s)
K_L	mass transfer coefficient in liquid phase (m/s)
K_La	overall oxygen mass transfer coefficient (s^{-1})
J	objective function

N_{O_2} oxygen transfer rate (mol/m^3 s)

OTR oxygen transfer rate (mol/m^3.s)

OUR oxygen uptake rate (mol/m^3.s)

P pressure (Pa)

P_G partial pressure of gas (Pa)

$\overline{P_G}$ average power input (Pa)

p_{O2} partial pressure of oxygen (Pa)

Q flow rate (m^3/s)

$Q_{O_2}X$ oxygen uptake rate (mol/m^3 s)

R gas constant (8.306 Pa m^3/(mol K))

RPB reciprocating plate bioreactor

RQ respiratory quotient (–)

SSL solid state fermentation (–)

STB stirred tank bioreactor (–)

t time (s)

T temperature (K)

U_G superficial gas velocity (m/s)

V_L total liquid volume in the fermenter (m^3)

y gaseous mole fraction

GREEK LETTERS

α parameter in Equation (2.4) (–)

β parameter in Equation (2.4) (–)

γ parameter in Equation (2.4) (–)

ε gas void fraction (-)

ϕ weighting factor associated to each term in the objective function (–)

ω cycle frequency

π measured variables during fermentation process (–)

τ_F time constant of liquid film (s)

τ_P time constant of the DO probe (s)

σ standard deviation (–)

SUBSCRIPTS

1 inlet stream

2 outlet stream

CO_2 carbon dioxide

G Gas

i interface

L Liquid

m equal to number of measured variables

n equal to number of available K_La measuring methods

O_2 oxygen

r_1 particle radius (m)

r_2 particle radius with its biofilm (m)

SYMBOLS

^ estimated values

2.6 REFERENCES

Audet, J., Thibault, J., and LeDuy, A., Polysaccharide Concentration and Molecular Weight Effects on the Oxygen Mass Transfer in a Reciprocating Plate Bioreactor. Biotechnology and Bioengineering, *52*: 517, 1996.

Bailey, J. E. and Ollis, D. F. Biochemical Engineering Fundamentals, 2nd ed., McGraw Hill, New York, 1986.

Baird, M. H. I. and Rama Rao, N. V., Characteristics of Countercurrent Reciprocating Plate Bubble Column. II Axial Mixing and Mass Transfer. The Canadian Journal of Chemical Engineering, *66*: 222-231, 1988.

Bandyopadhyay, B., Humphrey, A. E., and Taguchi, H., Dynamic Measurement of the Volumetric Oxygen Transfer Coefficient in Fermentation Systems. Biotechnology and Bioengineering, *9*: 533-544, 1967.

Chapman, C. M., Gibilaro, L. G., and Nienow, A. W., A Dynamic Response Technique for the Estimation of Gas-Liquid Mass Transfer Coefficients in a Stirred Vessel. Chemical Engineering Science, *37*: 891-896, 1982.

Cooper, C. M., Fernstrom, G. A., and Miller, S. A., Performance of Agitated Gas-Liquid Contactors. Industrial and Engineering Chemistry, *36*: 504-509, 1944.

Dang, N. D. P., Karrer, D. A., and Dunn, I. J., Oxygen Transfer Coefficients by Dynamic Model Moment Analysis. Biotechnology and Bioengineering, *19*: 853-865, 1977.

Denis, A., Thibault, J., and LeDuy, A., On the Methods for the Determination of the Oxygen Transfer Coefficient in Mechanically Agitated Vessels. Chemical Engineering Communications, *94*: 35-51, 1990.

Dorresteijn, R. C., Degooijer, C. D., Tramper, J., and Beuvery, E. C., A Method for Simultaneous Determination of Solubility and Transfer Coefficient of Oxygen in Aqueous Media Using Off-Gas Mass Spectrometry. Biotechnology and Bioengineering, *43*: 149-154, 1994.

Douglas, S. A. and West, D. M. Analytical Chemistry, An Introduction. Holt, Rinehart and Winston, Inc., New York, 1965.

Ducommun, P., Ruffieux, P.-A., Furter, M.-P., Morison, I., and von Stockar, U., A New Method for on-Line Measurement of the Volumetric Oxygen Uptake Rate in Membrane Aerated Animal Cell Cultures. Journal of Biotechnology, *78*: 139-147, 2000.

Dunn, I. J. and Einsele, A., Oxygen Transfer Coefficients by the Dynamic Method. Journal of Applied Chemistry Biotechnology, *25*: 707-720, 1975.

Durand, A., Pichon, P., and Desgranges, C., Approaches to K_La Measurement in Solid State Fermentation. Biotechnology Techniques, *2*: 11-16, 1988.

Dussap, C. G. and Gros, J.-B., Interpretation of Static and Dynamic Responses of a Dissolved Oxygen Electrode in Viscous Broths. Analytica Chimica Acta, *163*: 151-160, 1984.

Dussap, C. G. and Gros, J.-B., Power Input, K_La Values in Pneumatically Agitated Fermentors With Extracellular Microbial Polysaccharides. Biotechnology '85 (Europe), 691-692, 1985.

Foust, H. C., Mack, D. E., and Rushton, J. H., Gas-Liquid Contacting by Mixers. Industrial and Engineering Chemistry, *36*: 517-522, 1944.

Fukuda, H., Sumino, Y., and Kanzaki, T., Scale-Up of Fermentors (I) Modified Equations for Volumetric Oxygen Transfer Coefficient. Journal of Fermentation Technology, *46*: 829-837, 1968.

Gagnon, H., Lounes, M., and Thibault, J., Power Consumption and Mass Transfer in Agitation Gas-Liquid Columns: A Comparative Study. Canadian Journal of Chemical Engineering, *76*: 379-389, 1998.

Gauthier, L., Thibault, J., and LeDuy, A., Measuring K_La With Randomly Pulsed Dynamic Method. Biotechnology and Bioengineering, *37*: 889-893, 1991.

Gibilaro, L. G., Davies, S. N., Cooke, M. C., Lynch, M., and Middelton, J. C., Initial Response Analysis of Mass Transfer in a Gas Sparged Stirred Vessel. Chemical Engineering Science, *40*: 1811-1816, 1985.

Gowthaman, M. K., Raghava Rao, K. S. M. S., Ghildyal, N. P., and Karanth, N. G., Estimation of K_La in Solid-State Fermentation Using a Packed-Bed Bioreactor. Process Biochemistry, *30*: 9-15, 1995.

Gupta, A. and Rao, G., A Study of Oxygen Transfer in Shake Flasks Using a Non-Invasive Oxygen Sensor. Biotechnology and Bioengineering, *84*: 351-358, 2003.

Hastings, J. W., Oxygen Concentration and Bioluminescence Intensity. I: Bacteria and Fungi. Journal of Cellular and Comparative Physiology, *39*: 1-30, 1952.

Hermann, R., Walther, N., Maier, U., and Büchs, J., Optical Method for the Determination of the Oxygen-Transfer Capacity of Small Bioreactors Based on Sulfite Oxidation. Biotechnology and Bioengineering, *75*: 355-363, 2001.

Hermann, R., Lehmann, M., and Büchs, J., Characterization of Gas-Liquid Mass Transfer Phenomena in Microtiter Plates. Biotechnology and Bioengineering, *81*: 178-186, 2002.

Hill, G. A. and Robinson, C. W., Measurement of Aerobic Culture Maximum Specific Growth Rate and Respiration Coefficient Using a Dissolved Oxygen Probe. Biotechnology and Bioengineering, *16*: 531-538, 1974.

Imai, Y., Takei, H., and Matsumura, M., A Simple Na2SO3 Feeding Method for K_La Measurement in Large-Scale Fermentor. Biotechnology and Bioengineering, *29*: 982-993, 1987.

John, G. T., Kilmant, I., Wittmann, C., and Heinzle, E., Integrated Optical Sensing of Dissolved Oxygen in Microtiter Plates: A Novel Tool for Microbial Cultivation. Biotechnology and Bioengineering, *81*: 829-836, 2003.

Jolicoeur, M., Chavarie, C., Carreua, P. J., and Archambault, J., Development of a Helical-Ribbon Impeller Bioreactor for High-Density Plant Cell Suspension Culture. Biotechnology and Bioengineering, *39*: 511-521, 1992.

Juraščik, M., Sikula, I., Rosenberg, M., and Markos, J., Measurement of Mass Trasnfer Coefficients in Airlift Reactors With Internal Loop Using the Glucose Oxidase. Methods in Chemical and Biochemical Engineering, *21*: 207-212, 2007.

Kim, D. J. and Chang, H. N., Dynamic Measurement of K_La With Oxygen-Enriched Air During Fermentation. Journal of Chemical Technology and Biotechnology, *45*: 39-44, 1989.

Koizumi, J. and Aiba, S., Reassessment of the Dynamic K_La Method. Biotechnology and Bioengineering, *26*: 1131-1133, 1984.

Kok, R. and Zajic, J. E., Dynamic Response of a Polarographic Oxygen Probe. Biotechnology and Bioengineering, *17*: 527-539, 1975.

Linek, V. and Benes, P., Enhancement of Oxygen Absorption into Sodium Sulfite Solutions. Biotechnology and Bioengineering, *20*: 697-707, 1978.

Linek, V., Benes, P., and Hovorka, F., The Role of Interphase Nitrogen Transport in the Overall Volumetric Mass Transfer Coefficient in Air-Sparged System. Biotechnology and Bioengineering, *23*: 301-319, 1981 (a).

Linek, V., Benes, P., Hovorka, F., and Holecek, O., Use of Glucose Oxidase System in Measuring Aeration Capacity of Fermentors. Comparison of the Dynamic and Steady-State Methods of K_La Measurement. Biotechnology and Bioengineering, *23*: 1467-1484, 1981 (b).

Linek, V. and Vacek, V., Chemical Engineering Use of Catalysed Sulfite Oxidation Kinetics for the Determination of Mass Transfer Characteristics of Gas-Liquid Contactors. Chemical Engineering Science, *36*: 1768, 1981 (c).

Linek, V., Benes, P., Vacek, V., and Hovorka, F., Analysis of Differences in K_La Values Determined by Steady-State and Dynamic Methods in Stirred Tanks. The Chemical Engineering Journal, *25*: 77-88, 1982.

Linek, V., Benes, P., and Vacek, V., An Experimental Study of Oxygen Probe Linearity and Transient Characteristics in the High Oxygen Concentration Range. Journal of Electroanalytical Chemistry, *169*: 233-257, 1984.

Linek, V., Sinkule, J., and Vacek, V., Dissolved Oxygen Probes. Comprehensive Biotechnology, *4*: 363-394, 1985.

Linek, V., Vacek, V., and Benes, P., A Critical Review and Experimental Verification of the Correct Use of the Dynamic Method for the Determination of Oxygen Transfer in Aerated Agitated Vessels to Water, Electrolyte Solutions and Viscous Liquids. Chemical Engineering Journal, *34*: 11-34, 1987.

Linek, V., Benes, P., and Vacek, V., Dynamic Pressure Method for K_La Measurement in Large-Scale Bioreactors. Biotechnology and Bioengineering, *33*: 1406-1412, 1989.

Linek, V., Benes, P., and Sinkule, J., Critical Assessment of the Steady-State Na_2SO_3 Feeding Method for K_La Measurement in Fermentors. Biotechnology and Bioengineering, *35*: 766-770, 1990.

Linek, V., Sinkule, J., and Benes, P., Critical Assessment of Gassing-in Methods for Measuring K_La in Fermentors. Biotechnology and Bioengineering, *38*: 323-330, 1991.

Linek, V., Moucha, T., Dousova, M., and Sinkule, J., Measurement of K_La by Dynamic Pressure Method in a Pilot-Plant Fermentor. Biotechnology and Bioengineering, *43*: 477-482, 1994.

Lounes, M. and Thibault, J., Mass Transfer in a Reciprocating Plate Bioreactor. Chemical Engineering Communications, *127*: 169-189, 1994.

Lounes, M., Audet, J., Thibault, J., and LeDuy, A., Description and Evaluation of Reciprocating Plate Bioreactors. Bioprocess Engineering, *13*: 1-11, 1995.

Merta, K. and Dunn, I. J., Oxygen Electrode Characteristics. Biotechnology and Bioengineering, *18*: 591-593, 1976.

Mitchell, D. A., von Meien, O. F., and Krieger, N., Recent Developments in Modeling of Solid-State Fermentation: Heat and Mass Transfer in Bioreactors. Biochemical Engineering Journal, *13*: 137-147, 2002.

Mitchell, D. A., von Meien, O. F., Krieger, N., and Dalsenter, F. D. H., A Review of Recent Deelopments in Modeling of Microbial Growth Kinetics and Intraparticle Phenomena in Solid-State Fermentation. Biochemical Engineering Journal, *17*: 15-26, 2004.

Mukhopadhyay, S. N. and Ghose, T. K., A Simple Method of K_La Determination in Laboratory Fermenter. Journal of Fermentation Technology, *54*: 406-419, 1976.

Nienow, A. W. and Wisdom, D. J., 2nd European Conference on Mixing. F1-1, BHRA, Cranfield. 30-3-1977, Cambridge, England, 1988.

Nikakhtari, H. and Hill, G. A., Closure Effects on Oxygen Transfer and Aerobic Growth in Shake Flasks. Biotechnology and Bioengineering, *95*: 15-21, 2006.

Nikakhtari, H. and Hill, G. A., Modelling Oxygen Transfer and Aerobic Growth in Shake Flasks and Well-Mixed Bioreactors. Canadian Journal of Chemical Engineers, *83*: 493-499, 2005.

Ogut, A. and Hatch, R. T., Oxygen Transfer into Newtonian and Non-Newtonian Fluids in Mechanically Agitated Vessels. The Canadian Journal of Chemical Engineering, *66*: 79-85, 1988.

Oostra, J., le Comte, E. P., van der Heuvel, J. C., Tramper, J., and Rinzema, A., Intra-Particle Oxygen Diffusion Limitation in Solid-State Fermentation. Biotechnology and Bioengineering, *75*: 13-24, 2001.

Patel, N. and Thibault, J., Evaluation of Oxygen Mass Transfer in *Aspergillus Niger* Fermentation Using Data Reconciliation. Biotechnology Progress, *20*: 239-247, 2004.

Pịca, J. and Grégr, V., Method for the Determination of Oxygen Transfer Coefficients (K_La) With the Correction for the Actual Cultivation Conditions. Journal of Applied Chemical Biotechnology, *27*: 155-164, 1977.

Pederson, A. G., Anderson, H., Nielsen, J., and Villadsen, J., A Novel Technique Based on Kr for Quantification of Gas-Liquid Mass Transfer in Bioreactors. Chemical Engineering Science, *49*: 803-810, 1994.

Popovic, M. K. and Robinson, C. W., Mass Transfer Studies of External-Loop Airlifts and a Bubble Column. AIChe Journal, *35*: 393-405, 1989.

Pouliot, K., Thibault, J., Garnier, A., and Acuña Leiva, G., K_La Evaluation During the Course of Fermentation Using Data Reconciliation Techniques. Bioprocess Engineering, *23*: 565-573, 2000.

Rahardjo, Y. S. P., Weber, F. J., le Comte, E. P., Tramper, J., and Rinzema, A., Contribution of Aerial Hyphae of *Aspergillus Oryzae* to Respiration in a Model Solid-State Fermentation System. Biotechnology and Bioengineering, *78*: 539-544, 2002.

Rajagopalan, S. and Modak, J. M., Modeling of Heat and Mass Transfer for Solid State Fermentation Process in Tray Bioreactor. Bioprocess Engineering, *13*: 161-169, 1995.

Ruffieux, P.-A., von Stockar, U., and Marison, I. W., Measurement of Volumetric (OUR) and Determination of Specific (QO2) Oxygen Uptake Rates in Animal Cell Cultures. Journal of Biotechnology, *63*: 85-95, 1998.

Schumpe, A., Adler, I., and Deckwer, W.-D., Solubility of Oxygen in Electrolyte Solutions. Biotechnology and Bioengineering, *20*: 145-150, 1978.

Shuler, M. L. and Kargi, F. Bioprocess engineering – basic principles. Prentice Hall PTR, New Jersey, 1992.

Siegell, S. D. and Gaden Jr, E. L., Automatic Control of Dissolved Oxygen Levels in Fermentations. Biotechnology and Bioengineering, *4*: 345-356, 1962.

Sobotka, M., Votruba, J., and Prokop, A., A Two-Phase Oxygen Uptake Model of Aerobic Fermentations. Biotechnology and Bioengineering, *23*: 1193-1202, 1981.

Sobotka, M., Prokop, A., Dunn, I. J., and Einsele, A. Review of methods for the measurement of oxygen transfer in microbial systems. Annual Reports on Fermentation Processes 5, 127-210. 1982.

Spriet, J. A., Botterman, J., de Buyser, D. R., de Visscher, P. L., and Vandamme, E. J., A Computer-Aided Noninterfering On-Line Technique for Monitoring Oxygen-Transfer Characteristics During Fermentation Processes. Biotechnology and Bioengineering, *24*: 1605-1621, 1982.

Taguchi, H. and Humphrey, A. E., Dynamic Measurement of the Volumetric Oxygen Transfer Coefficient in Fermentation Systems. Journal of Fermentation Technology, *14*: 881-889, 1966.

Tecante, A. and Choplin, L., Gas-Liquid Mass Transfer in Non-Newtonian Fluids in a Tank Stirred With a Helical Ribbon Screw Impeller. The Canadian Journal of Chemical Engineering, *71*: 859-865, 1993.

Thibault, J., LeDuy, A., and Denis, A., Chemical Enhancement in the Determination of K_La by the Sulfite Oxidation Method. The Canadian Journal of Chemical Engineering, *68*: 324-326, 1990.

Thibault, J., Pouliot, K., Agosin, E., and Perez-Correa, R., Reassessment of the Estimation of Dessolved Oxygen Concentration Profile and K_La in Solid-State Fermentation. Process Biochemistry, *36*: 9-18, 2000.

Tsivoglou, E. C., O'Connor, R. L., Walter, C. M., Godsil, P. J., and Logsdon, G. S., Tracer Measurements of Atmospheric Reaeration. L. Laboratory Studies. Journal of WPCF, *37*: 1343-1362, 1965.

Van't Riet, K., Review of Measuring Methods and Results in Nonviscous Gas-Liquid Mass Transfer in Stirred Vessels. Industrial and Engineering Chemistry Process Design and Development, *18*: 357-364, 1979.

Vardar, F. and Lilly, M. D., The Measurement of Oxygen Transfer Coefficients in Fermentors by Frequency Response Techniques. Biotechnology and Bioengineering, *24*: 1711-1719, 1982.

Vashitz, O., Sheintuch, M., and Ulitzur, S., Mass Transfer Studies Using Cloned-Luminous Strain of *Xanthomonas campestris*. Biotechnology and Bioengineering, *34*: 671-680, 1989.

Votruba, J., Sobotka, M., and Prokop, A., Evaluation of Aeration Capacity From Cultivation Data Files: Application to Large-Scale Fermentation. Biotechnology and Bioengineering, *19*: 1553-1556, 1977.

Wang, W., Reimers, C. E., Wainright, S. C., Shahriari. M. R., and Morris, M. J., Applying Fiber-Optic Sensors for Monitoring Dissolved Oxygen. Sea Technology, *40*: No. 3, 69-74, March 1999.

Weiland, P., Sick, R., Osorio, C., and Onken, U., Oxidation of Hydrazine - A Reliable Method for the Determination of Volumetric Mass Transfer Coefficient in Gas/Liquid System. German chemical engineering, *9*: 143-148, 1986.

Whittmann, C., Kim, H. M., John, G., and Heinzle, E., Characterization and Application of an Optical Sensor for Quantification of Dissolved O_2 in Shake Flasks. Biotechnology Letters, *25*: 377-380, 2003.

Yagi, H. and Yoshida, F., Oxygen Absorption in Fermenters: Effects of Surfactants, Antifoaming Agents, and Sterilized Cells. Journal of Fermentation Technology, *52*: 905-916, 1974.

Zlokarnik, M., Sorption Characteristics for Gas-Liquid Contacting in Mixing Vessels. Advances in Biochemical Engineering, *8*: 133-151, 1978.

CHAPTER 3

Enhanced In Situ Dynamic Method for Measuring K_La in Fermentation Media

Nilesh Patel and Jules Thibault

Department of Chemical and Biological Engineering

University of Ottawa

Ottawa (ON), K1N 6N5, Canada

Abstract

The overall oxygen mass transfer coefficient (K_La) is often used as scale-up factor of fermentation systems. In fermenter scale-up, it is desired to achieve the same K_La values at the larger scale that was obtained at a smaller scale during the development stage. It is therefore important to be able to measure K_La in situ during fermentation and to also determine the action to be taken to maintain its value at its design set point. These objectives can be obtained by measuring K_La using the dynamic method followed by a series of changes in agitation speed and/or aeration rate to determine the influence of these parameters on K_La. This enhanced dynamic method is demonstrated with two filamentous microorganisms: *Trichoderma reesei* for the production of cellulase and *Aspergillus niger* for the production of citric acid. Two different types of bioreactor were used: a reciprocating plate bioreactor and a stirred (Rushton) bioreactor. It is shown that the proposed method can provide a simple way to measure and to adjust K_La to its set point value during the course of fermentation.

Keywords: bioreactor, dynamic method, fermentation, oxygen mass transfer coefficient, scale-up

3.1 INTRODUCTION

The main objective of scale-up is to determine the operating conditions and mass transfer characteristics in a fermenter of different size in order to achieve the same process yield. Scale-up is the reproduction in a production-scale fermenter of results obtained from a successful fermentation carried out in laboratory or pilot-plant equipment. An important goal in most aerobic fermentations is therefore to maintain the operating conditions at the optimal level that were usually derived at a smaller scale. Many methods for scale-up have been proposed to ensure the same productivity when the scale of production is increased. Some of these methods, which have been applied successfully, are: (1) fixing K_La such that it is identical at both scales (Aiba et al., 1973, Bandaiphet and Prasertsan, 2006, Hensirisak et al., 2002); (2) keeping constant the power per unit volume (P_G/V_L) (Aiba et al., 1973); (3) keeping constant the tip speed of the agitator; (4) maintaining a constant dissolved oxygen concentration, and (5) keep equal mixing times in fermenters of different scales (Fox and Gex, 1956). Margaritis and Zajic (1978) considered only the first four scale-up methods and reported that they were used industrially in 30%, 30%, 20%, and 20% of the time, respectively.

For the scaling-up of aerobic fermentation, the effect of gas-liquid mass transport was found to be the most significant factor by Hubbard et al. (1994). The oxygen mass transfer coefficient (K_La) often serves to compare the efficiency of bioreactors and mixing devices and it is also considered as an important scale-up factor because it is desired to achieve a given oxygen mass transfer capability that can meet with the oxygen demand of the culture. Often, aeration and agitation are selected to achieve the desired oxygen mass transfer coefficient, since this is the controlling parameter in most fermentations (Blakebrough and Moresi, 1981).

The objective of this paper is to demonstrate how the in situ dynamic method to determine K_La during the course of fermentation can be easily extended to obtain information on the variation of K_La with agitation and aeration and therefore offer a way to use these measurements to manipulate the speed of agitation and/or the inlet gas flow rate to achieve the desired K_La value. It is important to realize that for filamentous microorganisms, the drastic increase in viscosity, associated with the growth and morphology of microorganisms, will affect K_La throughout the fermentation. This is the

case of *Aspergillus niger* which forms mycelia and/or pellets (Allen and Robinson, 1990) and of *Trichoderma reesei* which can adopt mainly four types of morphological states (Lecault et al., 2007). The oxygen mass transfer coefficient is significantly reduced as the concentration of the microorganism increases with time, this reduction being more important for some morphological states.

This paper is divided as follows. Materials and methods associated with experiments performed to demonstrate the enhanced dynamic method are first presented and followed by a description of the methods for the in situ determination of K_La including the proposed enhancement. Finally, results are presented and discussed.

3.2 MATERIALS AND METHODS

3.2.1 Bioreactors

The two bioreactors, a reciprocating plate bioreactor (RPB) and a stirred tank bioreactor (STB) with three Rushton turbines, were used in these experiments. These bioreactors, built in our laboratories, are identical except for the mixing mechanism. The two bioreactors have a total volume of 22 L and a working volume of 17 L. The bioreactors are made of stainless steel and have an inner diameter of 228 mm and a column height of 550 mm. The outer tube has an internal diameter of 236 mm that leaves an annular gap of 3.5 mm to form a jacket where water, at an appropriate temperature, is continuously circulated to maintain the temperature of the fermentation broth constant. The top of the bioreactor has ports for sampling, feeding, and to hold a dissolved oxygen probe, pH probe and a thermocouple. Compressed air is fed at the bottom of the bioreactor after passing through a rotameter, a mass flow meter and a sterile gas filter. The gas sparger at the bottom of the bioreactor is a thin plate perforated with one hundred uniformly distributed holes, 1 mm in diameter. The gas flow rate is controlled by a mass flow controller and a dissolved oxygen probe measures the dissolved oxygen (DO) at a point located 82 mm from the centre of the column and 255 mm from the bottom of the reactor for *A. niger* fermentation and 130 mm from the bottom for *T. reesei* fermentation. Positions of the probes are different due to different volume of the fermentation broth. The exit and inlet gas streams were dehumidified before analyzing their composition.

3.2.1.1 RECIPROCATING PLATE BIOREACTOR

A schematic view of the plate stack used in the RPB is shown in Appendix A.1 (a). The plate stack consisted of 6 perforated stainless steel plates, 221 mm in diameter and 1.25 mm thick. Each plate was spaced 50 mm apart from one another. The perforations have a diameter of 19 mm and holes are distributed on an equilateral triangular pitch. The plate fractional free area, including the 3.5 mm annular space between the plate edge and bioreactor wall, is 0.36. The driving unit consists of a connecting rod, which imparts the reciprocating motion, a tenfold reducing speed transmission and a variable speed motor controlled by a microcomputer. An aluminium disc, containing 100 uniformly distributed perforations and mounted on the output shaft of the reducing transmission, is used in conjunction with an infrared optical switch (HOA-2001, Honeywell) to measure and control, with a microcomputer, the frequency of the reciprocation by manipulating the power to the motor.

3.2.1.2 STIRRED TANK BIOREACTOR

A schematic view of the mixing device used in the stirred tank bioreactor is shown in Appendix A.1 (b). The three identical Rushton turbines were mounted on the central shaft. The location of the impellers, measured from the bottom of the column, is 56, 199 and 327 mm for *A. niger* fermentation and 54, 132 and 210 mm for *T. reesei* fermentation. As mentioned earlier, due to different volume of the fermentation broth, the impeller positions were adjusted so that all the impellers are immersed. Each turbine has 6 blades mounted on the periphery of a 50 mm diameter disk. Each blade is 25 mm long, 15 mm high and 1.5 mm thick. Four baffles were placed inside the mixing vessel.

3.2.2 Experimental procedure

The microorganisms used for the fermentation experiments were *Aspergillus niger* (ATCC 1015) and *Trichoderma reesei* RUT C-30 (ATCC 56765). For *A. niger*, the freeze-dried culture was rehydrated and grown on Petri dishes and subsequently transferred to an agar slant (SIGMA, Potato Dextrose Agar, P-2182). It was then used to inoculate 50 mL of culture medium. The composition of the culture medium (Atkinson and Mavituna, 1991) was identical for both bioreactors and composed of the following constituents (g/L): Sucrose, 140; NH_4NO_3, 2.5; KH_2PO_4, 2.5 and $MgSO_4 \cdot 7H_2O$, 0.25. Three days before the start of experiment, the microorganisms were transferred into two

730-mL Erlenmeyer flasks of culture medium. The bioreactors and its contents were autoclaved for a period of 20 min at 121°C. At the start of each experiment, the content of one Erlenmeyer was transferred into each bioreactor containing about 17 L of culture solution. A sample was collected daily from each bioreactor and was analyzed for biomass and pH. Samples were first centrifuged at 15 000 RPM for 20 minutes and then the supernatant was filtered using a pre-weighted 45 μm filter (Gelman Sciences Inc. glass fiber filter, Type A/E, 47 mm). The biomass was resuspended in distilled water to leach out residual sugars and nutrients, and centrifuged again. The supernatant and biomass were filtered. The filter and the biomass were placed in an oven (dryer) for 20 h at 85-90°C before measuring the dry weight of biomass. Each experiment ran for a period of 12-13 days.

Table 3.1 – Summary of operating conditions for both microorganisms.

Operating Condition	*A. niger* Fermentation	*T. reesei* Fermentation
Reactor	RPB & STB	STB
Agitation	0.75, 1.0 Hz, 300 RPM	350 RPM (Batch), 400 RPM (Continuous)
Air Flowrate	0.6 VVM	0.7 VVM
Temperature	30 °C	28 °C
pH	-	4.5
DO Probe	Ingold	Broadley James
pH Probe	-	Broadley James
Gas Analyzer	Paramagnetic and Infrared (Maihak, Multor 610)	Mass Spectrometer (Ametek, Proline)

For *T. reesei*, stock cultures were supplied by Iogen Corporation, Ottawa. The glycerol stock solutions of spores were maintained at -80°C and were transferred on potato dextrose agar plates. New plates were prepared every month and kept at 4°C. Experiments with this microorganism were performed only in the STB. The volume of the culture medium was 10 L and contained: glucose, 13 g/L; $(NH_4)_2SO_4$, 1.4 g/L;

KH_2PO_4, 2.0 g/L; $MgSO_4 \cdot 7H_2O$, 0.6 g/L; $CaCl_2 \cdot 2H_2O$, 0.3 g/L; $FeSO_4 \cdot 7H_2O$, 5.0 mg/L; $MnSO_4 \cdot 7H_2O$, 1.6 mg/L; $ZnSO_4 \cdot 7H_2O$, 1.4 mg/L; $CoCl_2 \cdot 6H_2O$, 2 mg/L, Peptone, 2 g/L and Yeast Extract, 0.5 g/L. The pH of the medium was initially adjusted to 5.5 using 10 N NaOH. Medium was autoclaved for 20 min at 121°C.

Shake flask cultures were performed with a volume of 500 mL in a 1-L Erlenmeyer flask with three baffles. A spore solution in sterilized water was prepared from the plates. The amount of biomass was quantified by dry weight analysis. A 25-mL sample of the culture broth was filtered through a pre-dried and pre-weighed glass fiber filter (grade A/E, Gelman Sciences, MI). One volume of the sample was washed with two volumes of deionized distilled water and oven-dried for 24 h at 95°C. The weight of the sample was measured after a 24-h period of cooling in a desiccator. A summary of the operating conditions for both microorganisms used is presented in Table 3.1.

3.3 K_La MEASUREMENT

The volumetric oxygen mass transfer coefficient was determined using the dynamic method (Taguchi and Humphrey,1966) and the overall gas balance method (Lounes and Thibault,1994). When the dissolved oxygen in the bioreactor was sufficiently high, it was possible to use both methods whereas for low dissolved oxygen concentration, it was only possible to use the gas balance method. These two methods are based on Equation (3.1), which states that the rate of change of the dissolved oxygen concentration in the fermentation medium is equal to the rate of oxygen transferred from the gas to the liquid phase minus the rate of the oxygen utilization rate by the microorganisms.

$$\frac{dC_L}{dt} = K_L a\left(C_L^* - C_L\right) - Q_{O_2} X \tag{3.1}$$

3.3.1 Dynamic Method

The dynamic method, first proposed by Taguchi and Humphrey (1966), is used to determine both the oxygen uptake rate and K_La at one instant during the fermentation. This method consists in stopping temporarily the gas flow into the bioreactor to eliminate the addition of oxygen to the liquid broth such that the decrease in dissolved oxygen concentration in the bioreactor can be attributed entirely due to its consumption by the microorganism. At the same time, the speed of agitation is completely stopped or reduced

to a minimum to prevent cells from settling at the bottom of the bioreactor (Gagnon et al.,1998). The slope obtained by plotting C_L versus time, which usually is a straight line, provides an estimate of the oxygen uptake rate ($Q_{O_2}X$). Before the dissolved oxygen reaches its critical value, the air is reintroduced into the bioreactor and agitation resumed.

Having an estimate of the oxygen uptake rate, the value of K_La can be determined from the rate of change of the dissolved oxygen up to its stationary value. K_La can be calculated by rearranging Equation (3.1).

$$C_L = C_L^* - \frac{1}{K_L a}\left(\frac{dC_L}{dt} + Q_{O_2}X\right) \tag{3.2}$$

K_La can be easily obtained graphically from the slope of Equation (3.2) or calculated by solving numerically Equation (3.1). A numerical solution has the advantage to easily allow incorporating the dynamics of the dissolved oxygen probe. Appreciable errors, especially for higher values of K_La, may result if the probe dynamics is neglected. It is worth noting that the estimation of K_La does not depend upon the quality of the estimation of the value of $Q_{O_2}X$, obtained in the first step (Dorresteijn et al., 1994).

3.3.2 Stationary Method

With the availability of more accurate gas analyzer or mass spectrometer, K_La can be calculated using three additional methods using the information obtained under stationary conditions. Under pseudo-steady-state conditions, Equation (3.1) can be rearranged to calculate K_La as follows:

$$K_L a = \frac{Q_{O_2}X}{C_L^* - C_L^0} \tag{3.3}$$

This equation requires an estimate of $Q_{O_2}X$ that can be easily obtained from the dynamic method as previously explained. This method is referred to as the stationary method. An estimate of $Q_{O_2}X$ can also be obtained using the difference in oxygen concentration between the inlet and exit gas streams since it represents the oxygen consumption by microorganisms. Therefore, this oxygen uptake rate can be used to calculate the K_La using Equation (3.4).

$$K_L a = \frac{\frac{1}{V_L}\left(\frac{P_1}{R T_1} Q_{1,G}\, y_{1,O_2} - \frac{P_2}{R T_2} Q_{2,G}\, y_{2,O_2}\right)}{(C_L^* - C_L^0)} \tag{3.4}$$

Similarly, if the respiratory quotient (RQ) is known, the carbon dioxide production rate can be used to calculate $K_L a$ using Equation (3.5).

$$K_L a = \frac{\frac{1}{RQ}\frac{1}{V_L}\left(\frac{P_2}{R T_2} Q_{2,G}\, y_{2,CO_2} - \frac{P_1}{R T_1} Q_{1,G}\, y_{1,CO_2}\right)}{(C_L^* - C_L^0)} \tag{3.5}$$

Usually, RQ is available for most of the common fermentation processes. Otherwise, it can easily be estimated from past fermentation experiments. All these four methods have their own strengths and limitations at different stages of the fermentation process. For example, the dynamic method can be used with relatively higher precision during the initial stages of fermentation as the oxygen consumption is low and the dissolved oxygen concentration in the medium is high. Because of the low oxygen consumption, the difference between the inlet and exit gas concentrations is consequently very small at that stage of fermentation, and the gas balance methods for $K_L a$ estimation lack accuracy. As fermentation progresses, the growth of biomass leads to an increase in oxygen consumption and a decrease in the concentration of dissolved oxygen. As a result, the gas balance methods provide more accurate $K_L a$ estimations. However, at one point, the dissolved oxygen concentration may become too low to allow using the dynamic method and one has to rely strictly on the gas balance methods. Fortunately, it is under these circumstances that the gas balance methods provide the most accurate estimates of the values of $K_L a$. Because the relative accuracy of the various methods constantly varies throughout the fermentation, averaging the values of $K_L a$ will not lead to the best estimate. To overcome this problem and to take into account the relative accuracy of all methods, a data reconciliation technique can be used (Patel and Thibault, 2004, Pouliot et al., 2000) to obtain a more reliable $K_L a$ estimate.

3.3.3 Variation of $K_L a$ with agitation and aeration rate

Once an estimate of $K_L a$ is available and its value does not correspond to the targeted value, two manipulated variables can normally be used to achieve the desired values dictated by scale-up: the intensity of agitation and the gas flow rate. Indeed, it has

traditionally been observed that K_La increases with the power input per unit volume (or speed of agitation) and the superficial gas velocity. This dependence has commonly been reported using the following relationship:

$$K_La = \gamma(P_G/V_L)^{\alpha} U_G^{\beta} \quad (3.6)$$

Sometimes, additional terms are added to include the effect of the apparent viscosity of the medium. Different values of coefficients α, β and γ have been found by different authors (Bailey and Ollis, 1986, Gagnon et al., 1998, Patel et al., 2004) depending on the type of bioreactors, agitation used and the nature of the medium.

A general trend for the variation of K_La with these two operating variables is observed for most mixing devices. Two distinct regimes of operation are usually observed. For low values of power input per unit volume or agitation speed, the oxygen mass transfer coefficient is a weak function of the power input per unit volume whereas it varies considerably with the superficial gas velocity. At lower agitation speeds, energy given to the gas-liquid mixture is not sufficiently high to break gas bubbles such that it is not able to increase significantly the volumetric surface area (a). Above a certain threshold of power input per unit volume, there is a significant increase of K_La with the power input per unit volume occurs. Previous works by Gagnon et al., (1998), Lounes and Thibault (1993), Perez and Sandall (1974) and Nishikawa et al. (1981) have all observed these two distinct regimes of operation.

In this paper, the objective is to show that the dynamic method can be enhanced to offer the possibility to determine at the same time the variation of K_La with the speed of agitation and the gas flow rate based on Equation (3.6). Upon completion of the dynamic experiment, it is possible to change the speed of agitation and/or the gas flow rate and record the resulting stationary value of the dissolved oxygen. Using Equation (3.3) it is possible to obtain an estimate of the K_La value corresponding to the new operating condition and then used the nominal K_La value and the new value to determine the required operating condition that would lead to the desired K_La value.

3.4 RESULTS AND DISCUSSION

The oxygen mass transfer coefficient (K_La) was measured using the data obtained during the dynamic method at different times during fermentation of *T. reesei* and *A.*

niger. Each time the dynamic method was used, a series of changes in the speed of agitation and/or aeration rate were also made in order to determine K_La under these conditions. Figure 3.1 presents a typical variation of the measured DO concentration as a function of time for a series of changes in the agitation speed for the fermentation broth of *T. reesei* at a given moment during the fermentation run.

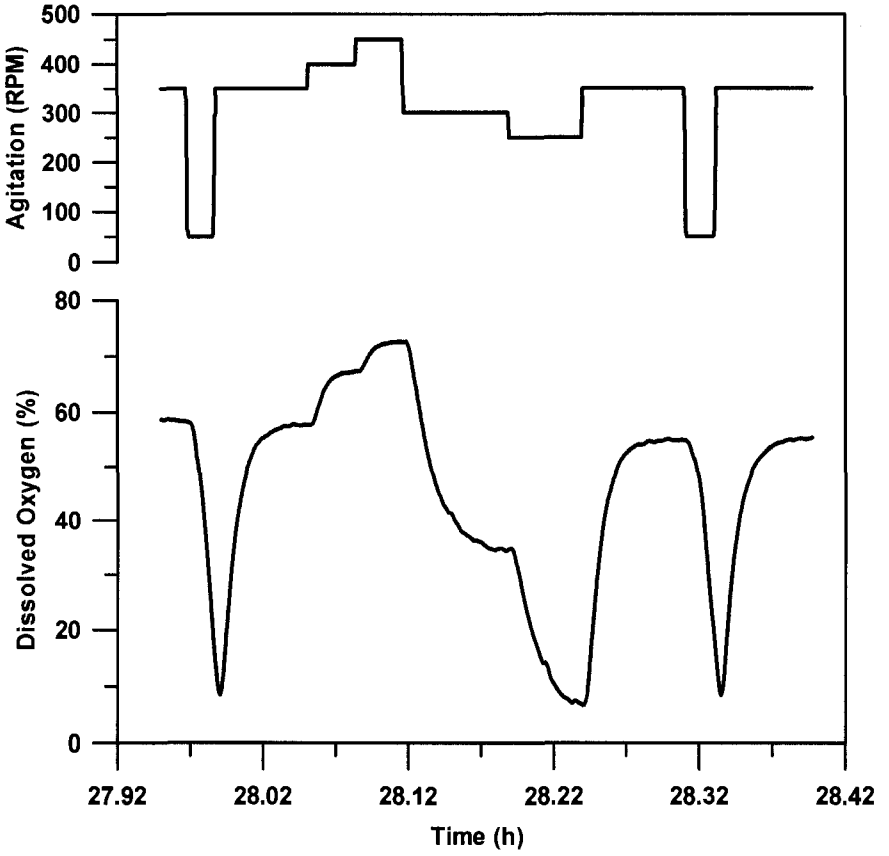

Figure 3.1 – Variation of the dissolved oxygen as a function of time for a sequence of changes in the agitation rate during a fermentation of *T. reesei*.

The first and last segments of the DO plot correspond to the dynamic method where the aeration rate was stopped and the agitation speed was lowered from 350 RPM to 50 RPM. The small agitation speed used when aeration was stopped has the objective to prevent the biomass from settling down and was shown previously to have no effect on the evaluation of K_La (Gagnon et al., 1998). For all the other segments of Figure 3.1, the aeration was constant. Hence, for each set of experiments performed at different fermentation time, K_La was determined both at the beginning and at the end, using the dynamic method, to ensure that the oxygen mass transfer coefficient did not change

during the period necessary to perform the sequence of variations in agitation and/or aeration. In all cases, K_La values were well within experimental errors.

In this investigation, the data reconciliation algorithm mentioned in the previous section was used to obtain the best values of K_La taking into account all measurements and their respective accuracies. Figure 3.2 presents the comparison of the experimental probe response with the predicted DO concentration and predicted DO probe response obtained with the data reconciliation algorithm for the first segment of Figure 3.1.

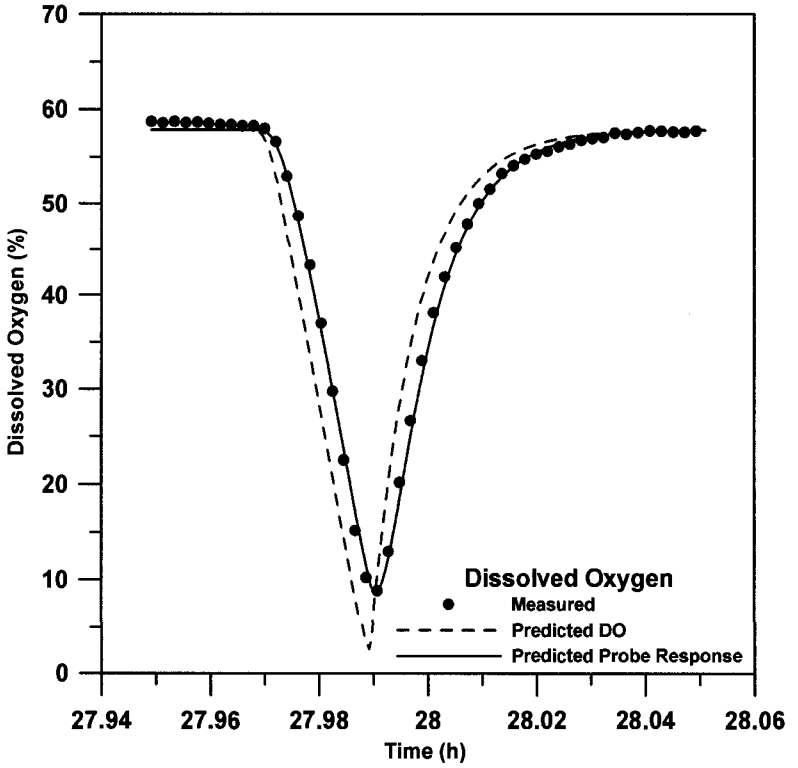

Figure 3.2 – Comparison of the experimental probe response with the predicted DO concentration and the predicted probe response obtained using the data reconciliation algorithm.

This graph clearly shows that it is important to include the dynamics of the DO probe in order to be able to predict the actual DO concentration and determine an accurate value of K_La. However, the use of the probe dynamics has no impact on the determination of $Q_{O2}X$ as the rate of decrease of both the probe response and predicted DO is identical after the initial transient period has elapsed. On the other hand, a significant error would be observed if K_La were determined using the probe response without correcting for the probe dynamics (Van't Riet, 1975).

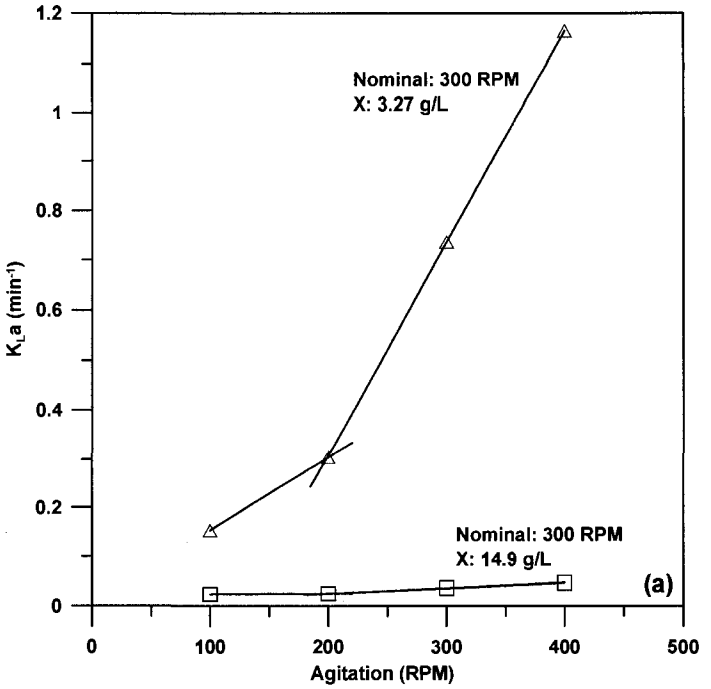

Figure 3.3 – K_La versus agitation speed at two different stages of fermentation of *A. niger* in the STB.

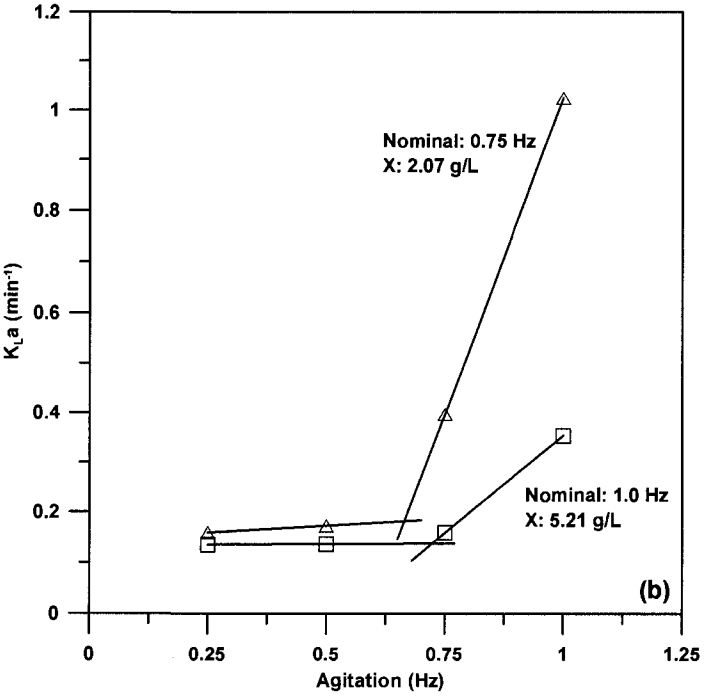

Figure 3.4 – K_La versus agitation speed at two different stages of fermentation of *A. niger* in the RPB.

Figures 3.3 and 3.4 present the results of the variation of K_La as a function of the agitation rate at different stages of fermentation of *A. niger* in stirred tank and reciprocating plate bioreactors, respectively. Because for each dynamic experiment, the oxygen uptake rate is determined, it is possible to use the stationary method and the steady-state DO concentration obtained for each agitation speed to estimate the values of K_La that prevail under new conditions of agitation. Figure 3.3 shows that for the STB, operating at a nominal speed of agitation of 300 RPM, the rate of increase of K_La with agitation is smaller at low agitation speed and much higher beyond an agitation threshold in the vicinity of 200 RPM. A similar shape for the variation of K_La with agitation has been previously observed for model fluids (Gagnon et al., 1998, Nishikawa et al., 1981, Perez and Sandall, 1974). The results of Figure 3.3 also clearly show the influence of biomass concentration on K_La, lower values of K_La being observed for a high biomass concentration. Indeed, K_La has decreased by more than one order of magnitude when the biomass concentration increased from 3.27 to 14.9 g/L. Similar results were obtained with the RPB (Figure 3.4) except that agitation has a negligible influence until a threshold value in the vicinity of 0.70 Hz is reached. Again the influence of biomass is clearly shown in Figure 3.4.

Figure 3.5 presents the variation of K_La determined in the STB at different stages of fermentation for *T. reesei*. For this experiment, four dynamic tests were performed followed by a sequence of changes in the agitation speed similar to the sequence of Figure 3.1. Since it is not expected to operate the fermenter below 200 RPM, it was decided to determine K_La in the range of agitation varying between 200 and 500 RPM, which is in the region above the threshold observed in Figure 3.3 where the variation of agitation is the greatest and where the mixing device can significantly influence the K_La. The results show the significant increase of K_La with agitation and the decrease of K_La with increasing biomass.

For the same set of experiments, a sequence of aeration flow rates was also performed to determine in situ the variation of K_La with agitation rate. The results of this sequence of aeration for the four tests that were performed are presented in Figure 3.6. The results show that K_La increases nearly linearly with the inlet gas flow rate. This increase is due to the larger gas holdup at higher inlet gas flow rate. The rate of increase in K_La with inlet

gas flow rate is larger at a higher speed of agitation and at a lower biomass concentration. These results also confirm that lower K_La is obtained as the concentration of biomass increases.

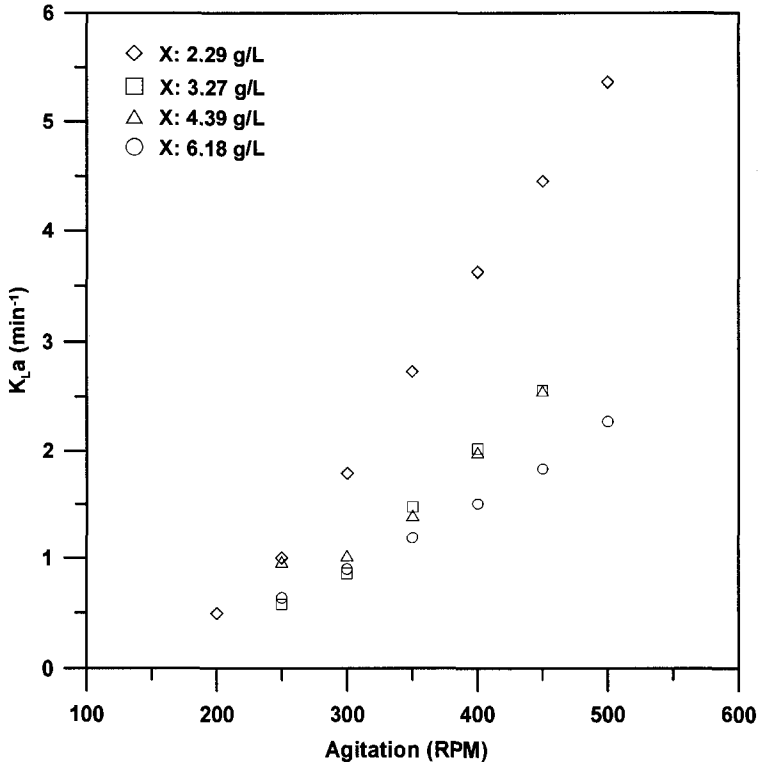

Figure 3.5 – K_La versus the speed of agitation at different stages of fermentation of *T. reesei* in stirred tank bioreactor.

The various results presented in this investigation rely heavily on the accurate determination of the oxygen utilization rate. Indeed, for each change of agitation and aeration, following a dynamic method, only the DO concentration obtained at each plateau (Figure 3.1) and the oxygen utilization rate are required for each K_La determination. Fortunately, the oxygen utilization rate can be determined very accurately such that the level of confidence in determining K_La is high. The same results were also analyzed strictly with the traditional dynamic method considering only the probe dynamic correction instead of the full data reconciliation and the results were nearly identical.

With respect to scaling, the enhancement of the dynamic method would allow to perform similar tests, albeit in a more restricted range than performed in this investigation, to obtain the necessary information to manipulate either the agitation speed or aeration rate in order to maintain K_La constant. Since it is known that K_La will change

throughout fermentation, the method described in this investigation allows determining the appropriate action to be taken in order for the system to operate in the vicinity of the targeted K_La. The selection of the manipulated variable (agitation, inlet gas flow rate or a combination of both) needs to be decided by the person in charge of fermentation. Some additional considerations are shear effect on microorganism or product and the tendency of the fermentation broth to foam.

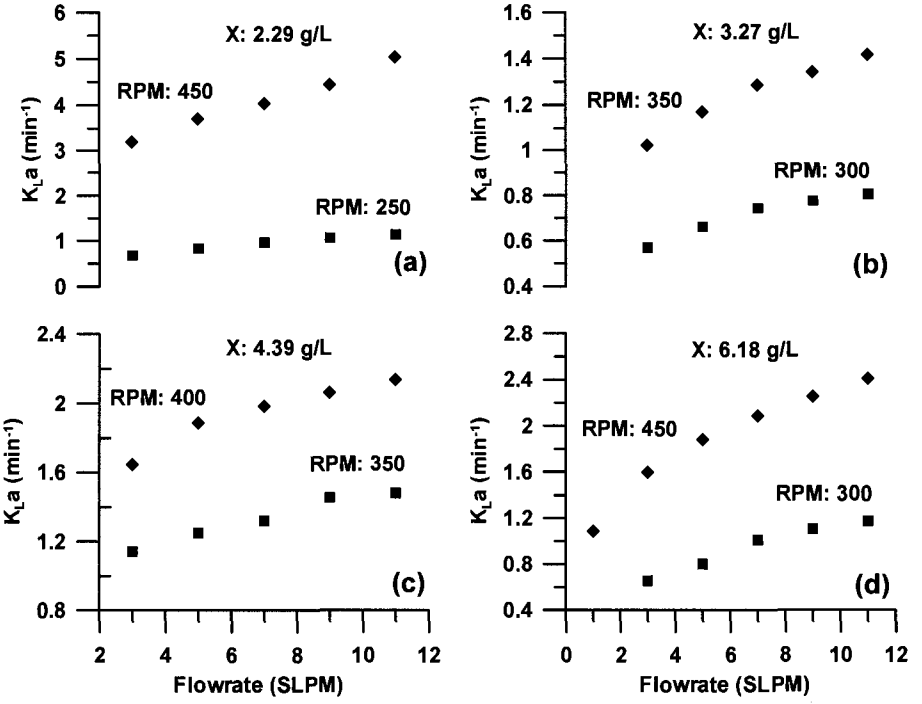

Figure 3.6 – K_La versus the air flow rate at different stages of fermentation of *T. reesei* in stirred tank bioreactor and under different conditions of agitation.

3.5 CONCLUSIONS

In this investigation, an extension to the dynamic method for the in situ determination of K_La has been presented whereby the traditional dynamic method is first performed and then immediately followed by either a variation of the agitation rate or the aeration rate. The additional information can be directly used to control K_La to the target value that is dictated by the scale-up method.

Even though a data reconciliation algorithm has been used in this investigation, similar results can be obtained with the traditional dynamic method provided the DO probe dynamics is taken into account in the calculation of K_La. However, the probe dynamics

has no impact on the determination of K_La during the sequence of tests performed following the initial dynamic method as it relies more heavily on the accuracy of the oxygen utilization rate.

3.6 NOMENCLATURE

C_L dissolved oxygen concentration (mol/m^3)

C_L^0 pseudo-steady-state dissolved oxygen concentration recorded at the initiation of the dynamic method (mol/m^3)

C_L^* dissolved oxygen concentration in equilibrium with mean gaseous oxygen concentration (mol/m^3)

K_La overall oxygen mass transfer coefficient (s^{-1})

P pressure (Pa)

P_G average gassed power input (W)

Q_G gas flow rate (m^3/s)

$Q_{O_2}X$ oxygen uptake rate (mol/m^3 s)

R gas constant (8.306 Pa m^3/(mol K))

RPB reciprocating plate bioreactor

RPM revolution per minute

RQ respiratory quotient

STB stirred tank bioreactor

SLPM standard litre per minute

t time (s)

T temperature (K)

U_G gas superficial velocity (m/s)

V_L liquid volume in the fermenter (m^3)

X biomass concentration (g/L)

y gaseous mole fraction

GREEK LETTERS

α parameter in Eq. (3.6) (–)

β parameter in Eq. (3.6) (–)

γ parameter in Eq. (3.6) (–)

SUBSCRIPTS

1 inlet stream

2 outlet stream

CO_2 carbon dioxide

G gas

O_2 oxygen

3.7 REFERENCES

Aiba, S., Humphrey, A. E., and Millis, N. F. Biochemical Engineering. Academic Press, New York, 1973.

Allen, D. G. and Robinson, C. W., Measurement of Rheological Properties of Filamentous Fermentation Broth. Chemical Engineering Science, *45*: 37-48, 1990.

Atkinson, B. and Mavituna F., Biochemical Engineering and Biotechnology Handbook, Stockton Press, p337, 1991.

Bailey, J. E. and Ollis, D. F., Biochemical Engineering Fundamentals. 2nd ed. McGraw Hill, New York, 1986.

Bandaiphet, C. and Prasertsan, P., Effect of Aeration and Agitation Rates and Scale Up on Oxygen Transfer Coefficient, K_La, in Exopolysaccharide Production from *Enterobacter cloacae* WD7. Carbohydrates Polymers, *66*: 216-228, 2006.

Blakebrough, N. and Moresi, M., Scale-Up of Whey Fermentation in a Pilot-Scale Fermenter. European Journal of Applied Microbiology and Biotechnology, *12*: 173-178, 1981.

Dorresteijn, R. C., de Gooijer, C. D., Tramper, J., and Beuvery, E. C., A Simple Dynamic Method for On-Line Determination of K_La During Cultivation of Animal Cells. Biotechnology Techniques, *8*: 675-680, 1994.

Fox, F. A. and Gex, V. E., Single-Phase Blending of Liquids. AIChE Journal, *2*: 539-544, 1956.

Gagnon, H., Lounes, M., and Thibault, J., Power Consumption and Mass Transfer in Agitation Gas-Liquid Columns: A Comparative Study. Canadian Journal of Chemical Engineering, *76*: 379-389, 1998.

Hensirisak, P., Parasukulsatid, P., Abblevor, F. A., Cundiff, J. S., and Velander, W. H., Scale-Up of Microbubble Dispersion Generator for Aerobic Fermentation. Applied Biochemistry and Biotechnology, *101*: 211-227, 2002.

Hubbard, D. W., Ledger, S. E., and Hoffman, J. A. Scaling-up Aerobic Fermentation which Produce Non-Newtonian, Viscoelastic Broths. *In* Advances in Bioprocess Engineering, Kluwer Academic Publishers, Netherlands, 1994.

Lecault, V., Patel, N., and Thibault, J., Morphological Characterization and Viability Assessment of *Trichoderma reesei* by Image Analysis. Biotechnology Progress, *23*: 734-740, 2007.

Lounes, M. and Thibault, J., Hydrodynamics and Power Consumption of a Reciprocating Plate Gas-Liquid Column. Canadian Journal of Chemical Engineering, *71*: 497-506, 1993.

Lounes, M. and Thibault, J., Mass Transfer of Reciprocating Plate Bioreactor. Chemical Engineering Communications, *127*: 169-189, 1994.

Margaritis, A. and Zajic, J. E., Mixing, Mass Transfer, and Scale-Up of Polysaccharide Fermentations. Biotechnology and Bioengineering, *20*: 939-1001, 1978.

Nishikawa, M., Makamura, M., Yagi, H., and Hashimoto, K., Gas Absorption in Aerated Mixing Vessel. Journal of Chemical Engineering of Japan, *14*: 219-226, 1981.

Patel, N., Goudreault, J., Bagchee, S., and Thibault, J., Wood Pulp as Model Fluid to Study the Oxygen Mass Transfer in *Aspergillus niger* Fermentation. Canadian Journal of Chemical Engineering, *82*: 1-8, 2004.

Patel, N. and Thibault, J., Evaluation of Oxygen Mass Transfer in *Aspergillus niger* Fermentation Using Data Reconciliation. Biotechnology Progress, *20*: 239-247, 2004.

Perez, J. F. and Sandall, O. C., Gas Absorption by Non-Newtonian Fluids in Agitated Vessels. AIChE Journal, *20*: 770-775, 1974.

Pouliot, K., Thibault, J., Garnier, A., and Acuña Leiva, G., K_La Evaluation During the Course of Fermentation Using Data Reconciliation Techniques. Bioprocess Engineering, *23*: 565-573, 2000.

Taguchi, H. and Humphrey, A. E., Dynamic Measurement of the Volumetric Oxygen Transfer Coefficient in Fermentation Systems. Journal of Fermentation, *44*: 881-889, 1966.

Van't Riet, K., Review of Measuring Methods and Results in Nonviscous Gas-Liquid Mass Transfer in Stirred Vessels. Industrial and Engineering Chemistry Process Design and Development, *18*: 357-364, 1979.

CHAPTER 4

Data Reconciliation Using Neural Networks for the *in situ* Determination of K_La in Fermentation Systems

Nilesh Patel and Jules Thibault

Department of Chemical and Biological Engineering

University of Ottawa

Ottawa (ON), K1N 6N5, Canada

Abstract

The oxygen mass transfer coefficient (K_La) is of paramount importance in conducting aerobic fermentation. K_La also serves to compare the efficiency of bioreactors and their mixing devices as well as being an important scale-up factor. In submerged fermentations, four methods are available to estimate the overall oxygen mass transfer coefficient (K_La): the dynamic method, the stationary method based on a previous determination of the oxygen uptake rate ($Q_{O2}X$), the gaseous oxygen balance and the carbon dioxide balance. Each method provides a distinct estimation of the value of K_La. Data reconciliation can be used to obtain the most probable value of K_La by minimising an objective function that includes measurement terms and oxygen conservation models, each being weighted according to their level of confidence. Another alternative, for a more rapid determination of K_La, is using a neural network which has been previously trained to predict K_La from the series of oxygen conservation models. Results obtained with this new approach show that K_La can be predicted rapidly and gives values that are equivalent to those obtained with the complete data reconciliation algorithm.

Keywords: Data reconciliation, Fermentation, K_La, Neural network, Oxygen mass transfer.

4.1 INTRODUCTION

The supply of oxygen is a critical factor in all aerobic fermentations. Indeed, aeration is one of the bottlenecks when operating aerobic fermentation because of the low solubility of oxygen and the constraint on the intensity of mixing due to the limiting shear stress that the cells can sustain. An insufficient oxygen transfer leads to a decrease of microbial growth and product formation. To assess if particular equipment would be able to supply oxygen at a non-limiting rate, it is essential to have a good estimate of the overall oxygen mass transfer coefficient (K_La). In submerged fermentations, K_La serves to compare the efficiency of bioreactors and their mixing devices to provide the right level of oxygenation. K_La is also one of the most important scale-up factors (Jarai, 1979, Moo-Young and Blanch, 1995).

Many methods have been proposed for the determination of K_La for submerged fermentations. The majority of the investigations have however been performed with water and other model fluids, in an attempt to mimic as closely as possible conditions encountered in fermentation systems. These investigations are very useful because conditions are well defined and can be rigorously controlled, providing relatively good estimates of K_La that can be used in design calculations. It is nevertheless preferable to determine K_La *in situ* under actual operating conditions since microorganisms, substrates, metabolites, viscosity and antifoam have an impact on the oxygen transfer rate (Yagi and Yoshida, 1974). In fact, K_La values in fermenters may differ substantially from values predicted for oxygen absorption into water or simple aqueous solutions even when differences in liquid physical properties such as viscosity and diffusivity are taken into account (Gauthier et al., 1991).

The two most common methods for K_La determination during the course of fermentation are the dynamic method (Taguchi and Humphrey, 1966) and the gaseous oxygen mass balance (Siegel and Gaden, 1962, Shuler and Kargi, 1992). Using the information of these two methods, two other methods can be easily defined: the stationary method and the carbon dioxide production rate method (Pouliot et al., 2000, Patel and Thibault, 2004). For the dynamic method, and subsequently the stationary method, only a fast response dissolved oxygen probe is required to obtain the necessary data. The two gaseous methods, which require oxygen and carbon dioxide sensors, use

global oxygen and carbon dioxide balances in the gas phase across the bioreactor, respectively.

K_La is obviously independent of the method employed to estimate its value. However, the four methods will invariably give four different estimates of K_La due to errors in measurements (Brown, 1991) and inaccuracy in the mass balance equations. Therefore, data reconciliation techniques could be used with advantage to obtain the most probable value of K_La where both the reliability of data measurements and the accuracy of each estimation method are taken into consideration. Data reconciliation essentially consists of writing and minimising an objective function that considers the level of confidence on the various measurements and the mass conservation models. Pouliot et al. (2000) defined an objective function comprised of the weighted contribution of twelve measurements and four mass conservation models to estimate the value of K_La at various fermentation times during the production of *Saccharomyces cerevisae*. Patel and Thibault (2004) used the same technique to determine K_La during the production of citric acid using *Aspergillus niger*. Data reconciliation involves the minimization of an objective function while taking into account the accuracy of each mass balance equation and each measurement involved in the mass balance equations (Hodouin et al., 1993).

In the present investigation, it is proposed to evaluate K_La using a feedforward neural network that is trained strictly using the theoretical mass balance models prevailing during the growth phase of typical aerobic fermentations. The mass conservation models include the dynamic method, the stationary method and the two gas balance methods. It is desired to define a series of simple variables of a fermentation that could be used jointly to estimate rapidly the value of K_La. Because the feedforward neural network uses input data based on the simulation of the four conservation mass balances, data reconciliation is implicitly imbedded and used to determine s single value of K_La. Cruz et al. (1999) have used a neural network to estimate K_La during the growth phase of *Cephalosporium acremonium* whereas Rao and Kumar (2007) used a neural network to model the mass transfer rate in an unbaffled surface aeration tank. Djebbar and Narbaitz (2002) used successfully a neural network to analyze the mass transfer characteristics in air stripping towers and to simulate K_La. To fit the neural network model, they assembled a large database of pertinent air stripping towers. All these applications used past process data to

fit a neural network that was used to estimate K_La in subsequent experiments. In this investigation, the neural network is used as a metamodel to encapsulate four fermentation mass balance equations that are simulated over a wide range of operating conditions and K_La values such that it is not specific to one type of fermentation. The training of the neural network is performed without resorting to actual experimental data but only using data that were generated from basic principles over a wide range of K_La values. Most variables used for the training of the neural network are defined from simulated fermentations. When the artificial neural network has been defined, it can be used directly without requiring optimization to estimate K_La values.

This chapter is divided as follows. A brief description of the experimental system is presented, followed by a brief review description of the different methods for measuring K_La during fermentation and the associated data reconciliation technique. This is followed by a description of the proposed neural network methodology to estimate K_La and, finally, the main results are presented, compared and discussed.

4.2 MATERIALS AND METHODS

The performance of data reconciliation for the determination of K_La using artificial neural networks and its comparison to the more conventional data reconciliation method will be evaluated for three different microorganisms: *Saccharomyces cerevisiae*, *Aspergillus niger* and *Trichoderma reesei*. The three different microorganisms were used at different time over a period of ten years such that conditions of fermentation and measurement equipment differed. Nevertheless, K_La determination was performed using the same methods. Since the general K_La neural network estimator derived in this investigation is not dependent on the strain, these differences should not matter. On the contrary, despite these differences, the validity of the reconciliation method proposed in this investigation will be reinforced.

4.2.1 Microorganisms and Fermentation Mediums

The first strain used in this study was *Saccharomyces cerevisiae*. The culture medium composition was: 0.5 g peptone, 3 g yeast extract, 1.25 g KH_2PO_4, 1.25 g K_2HPO_4, 0.45 g $MgSO_4 \cdot 7H_2O$, 5.33 g $(NH_4)_2SO_4$, and 1.1 g glucose per litre of water. Two bags of 8 g of Fleischmann's quick-rise yeast were used as inoculum and were added to an Erlenmeyer

flask containing 750 mL of the medium given above. The cells were incubated on an orbital shaker at 25°C for 1.5 h before being added to the fermenter. Glucose was used as the carbon source. The growth behaviour of *Saccharomyces cerevisiae* is strongly influenced by glucose concentration. To avoid the Crabtree effect, glucose solution (200 g/L glucose) was fed using a predetermined exponential feeding scheme in order to maintain a low concentration within the bioreactor. Fedbatch operation is important since one of the methods used to estimate the K_La value is based on the carbon dioxide production rate because the Crabtree effect would induce a systematic error in the K_La evaluation (Yamane et al., 1984). The objective of the feeding strategy was to maintain the respiratory quotient (RQ) around unity (Copella and Dhurjati, 1989, Wand et al., 1977).

The second microorganism was *Aspergillus niger* obtained from American Type Culture Collection (ATCC 1015). The freeze-dried culture was rehydrated and grown on Petri dish and subsequently transferred to an agar slant (SIGMA, Potato Dextrose Agar, P-2182). It was then used to inoculate a 50 mL of culture medium. The composition of the culture medium was composed of the following constituents (Atkinson and Mavituna, 1991): Sucrose, 140 g/L; NH_4NO_3, 2.5 g/L; KH_2PO_4, 2.5 g/L and $MgSO_4 \cdot 7H_2O$, 0.25 g/L. Three days before the start of experiment, the microorganisms were transferred into two 730-mL Erlenmeyer flasks of culture medium. At the start of each experiment, one Erlenmeyer was transferred into the bioreactor containing about 17 L of culture solution. Each experiment ran for a period of 12-13 days.

The third microorganism was *Trichoderma reesei* RUT C-30 (ATCC 56765). Stock cultures were supplied by Iogen Corporation, Ottawa. The glycerol stock solutions of spores were maintained at -80°C and were transferred on potato dextrose agar plates. New plates were prepared every month and kept at 4°C. The culture contained: glucose, 13 g/L; $(NH_4)_2SO_4$, 1.4 g/L; KH_2PO_4, 2.0 g/L; $MgSO_4 \cdot 7H_2O$, 0.6 g/L; $CaCl_2 \cdot 2H_2O$, 0.3 g/L; $FeSO_4 \cdot 7H_2O$, 5.0 mg/L; $MnSO_4 \cdot 7H_2O$, 1.6 mg/L; $ZnSO_4 \cdot 7H_2O$, 1.4 mg/L; $CoCl_2 \cdot 6H_2O$, 2 mg/L, Peptone, 2 g/L and Yeast Extract, 0.5 g/L. The pH of the medium was initially adjusted to 5.5 using 10N NaOH. Medium was autoclaved for 20 min at 121°C. Shake flask cultures were performed with a volume of 500 mL in a 1-L Erlenmeyer flask with three baffles. A spore solution in sterilized water was prepared from the plates.

4.2.2 Experimental system

Two types of bioreactors as shown in Appendix A.1 were used: a stirred tank bioreactor (STB) and a reciprocating plate bioreactor (RPB). These bioreactors, built in our laboratories, are identical except for the mixing mechanism. The STB was used for fermentations performed with the three types of microorganisms whereas the RPB was also used for fermentations with *Aspergillus niger*.

The STB has a total volume of 22.5 L and is made of two concentric stainless steel columns. The bioreactor has an inner diameter of 228 mm and a column height of 550 mm. The outer tube has an internal diameter of 236 mm that leaves an annular gap of 3.5 mm to form a jacket where water, at an appropriate temperature, is continuously circulated to maintain constant the temperature of the fermentation broth. The top cover plate of the bioreactor has ports for sampling, feeding, and to hold a dissolved oxygen probe, pH probe and a thermocouple. Compressed air is fed at the bottom of the bioreactor after passing through a rotameter, a mass flow meter and a sterile gas filter. The gas sparger at the bottom of the bioreactor contains one hundred uniformly distributed holes, 1 mm in diameter. The gas flow rate is controlled by a mass flow meter. The exit and inlet gas streams were dehumidified before analyzing their oxygen and carbon dioxide compositions with a gas analyzer (Maihak, Multor 610) or a mass spectrometer (Amatek. Proline). The mixing device consists of three identical Rushton turbines mounted on the central shaft. Each turbine consists of 6 blades mounted on the periphery of a 50 mm diameter disk. Each blade is 25 mm long, 15 mm high and 1.5 mm thick. Four baffles were placed inside the mixing vessel.

The RPB is identical to the STB except for the reciprocating plate stack used as the mixing device. The plate stack consisted of 6 perforated stainless steel plates, 221 mm in diameter and 1.25 mm thick. Each plate was spaced 50 mm apart from one another. The perforations have a diameter of 19 mm and holes are distributed on an equilateral triangular pitch. The plate fractional free area, including the 3.5 mm annular space between the plate edge and bioreactor wall, is 0.357. The driving unit consists of a connecting rod, which imparts the reciprocating motion, a tenfold reducing speed transmission and a variable speed motor controlled by a microcomputer. An aluminum disc, containing 100 uniformly distributed perforations and mounted on the output shaft

of the reducing transmission, is used in conjunction with an infrared optical switch (HOA-2001, Honeywell) to measure and control, with a microcomputer, the frequency of reciprocation by manipulating the power to the motor. A summary of the operating conditions for each fermentation is provided in Table 4.1.

Table 4.1 – Summary of operating conditions and some instrumentation

Variables	*S. cerevisiae*	*A. niger*	*T. reesei*
Temperature (°C)	30	30	28
Air flow rate (L/min)	10	10	7
Broth volume (L)	15-19	17	10
Agitation speed:			
STB (RPM)	400	100-400	350-400
RPB (Hz)	-	0.25-1.00	-
Gaseous O_2 measurement	Paramagnetic	Paramagnetic	Mass spectrometer
Gaseous CO_2 measurement	Infrared	Infrared	Mass spectrometer

4.3 METHODS FOR MEASURING K_La DURING THE COURSE OF A FERMENTATION

Pouliot et al. (2000) and Patel and Thibault (2004) have used four methods to estimate K_La during the course of a fermentation. These methods are based on the oxygen mass balance in the liquid phase or the oxygen and carbon dioxide concentration in the gas phase. These methods will be briefly described in turn.

4.3.1 Dynamic method

The dynamic oxygen mass balance within the fermenter is given by the following equation:

$$\frac{dC_L}{dt} = K_La\left(C_L^* - C_L\right) - Q_{O2}X \qquad (4.1)$$

This equation states that the rate of change of the dissolved oxygen in the fermenter is equal to the rate of oxygen mass transfer from the gas to the liquid phase minus the rate of oxygen utilisation by the microorganisms.

In the dynamic method, first reported by Taguchi and Humphrey (1966), the oxygen uptake rate (OUR or $Q_{O2}X$) and K_La are determined using the following procedure. As illustrated in Figure 4.1, the gas supply and the agitation are stopped momentarily to cut the oxygen supply to the liquid phase so that the rate of decrease of dissolved oxygen is caused entirely by the OUR. The decrease in dissolved oxygen is usually linear and the slope of the plot of C_L as a function of time provides a direct estimate of the oxygen uptake rate. The underlying hypothesis is that the rate of oxygen utilisation is unaffected by the absence of air bubbling and agitation, and lower dissolved oxygen concentration. Before the dissolved oxygen concentration reaches its critical lower limit, aeration and agitation are resumed and the dissolved oxygen concentration normally returns to its initial level. K_La can be estimated using Equation (4.1) and a graphical method or the finite difference method. The advantage of the latter is the possibility to easily include the dynamics of the dissolved oxygen probe, which could induce an important bias for higher values of K_La. It is important to point out that the estimate of K_La using the dynamic method does not depend on the estimation of $Q_{O2}X$.

A small variant of this method has been used whereby aeration was cut momentarily whereas the agitation was reduced to 30 RPM in order to prevent cell sedimentation. This small modification does not affect the estimation of K_La (Gagnon et al., 1998).

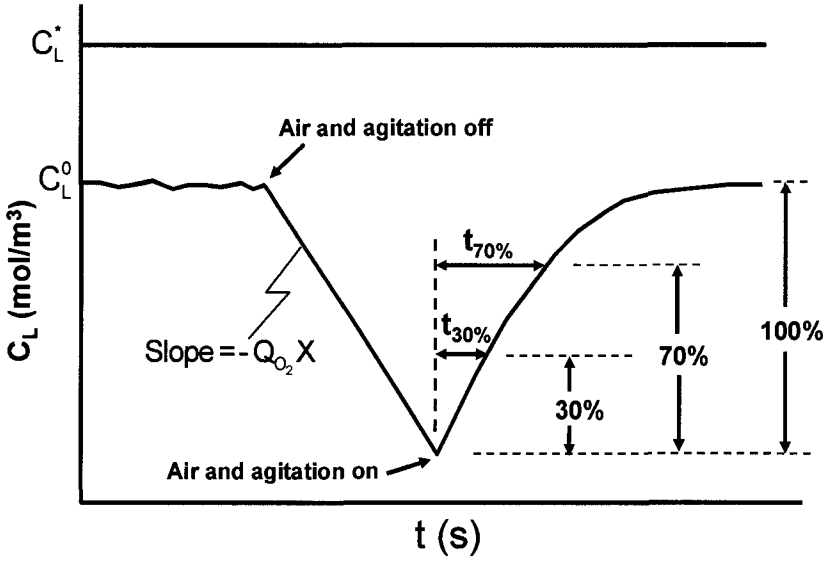

Figure 4.1 – Dissolved oxygen probe response during the dynamic method.

4.3.2 Stationary method

Once the estimation of $Q_{O2}X$ is available, it is possible to use Equation (4.1) along with the information prevailing in the pseudo-stationary phase preceding the dynamic test to directly calculate K_La:

$$K_La = \frac{Q_{O2}X}{C_L^* - C_L^0} \tag{4.2}$$

4.3.3 Oxygen mass balance method

Under pseudo-stationary conditions, the oxygen deficit of the gas stream across the fermenter is equal to the oxygen uptake rate (OUR). The OUR in Equation (4.2) can be replaced by the gaseous oxygen mass balance to estimate K_La:

$$K_La = \frac{\frac{1}{V_L}\left(\frac{P_1}{RT_1} Q_{1,G}\, y_{1,O_2} - \frac{P_2}{RT_2} Q_{2,G}\, y_{2,O_2}\right)}{(C_L^* - C_L^o)} \tag{4.3}$$

4.3.4 Carbon dioxide gas balance method

The gaseous carbon dioxide production rate can also be used to estimate K_La provided that an estimation of the respiratory quotient (RQ) is available. Similar to Equation (4.3), K_La is obtained as follows:

$$K_La = \frac{\frac{1}{RQ}\frac{1}{V_L}\left(\frac{P_2}{RT_2} Q_{2,G}\, y_{2,CO_2} - \frac{P_1}{RT_1} Q_{1,G}\, y_{1,CO_2}\right)}{(C_L^* - C_L^o)} \tag{4.4}$$

Good estimate of RQ is available for a large number of fermentations or can also be estimated from past fermentations. All these four methods have their own strengths and limitations at different stages of the fermentation process. For example, the dynamic method can be used with relatively higher precision during the initial stages of fermentation as the oxygen consumption is low and the dissolved oxygen concentration in the medium is high. Because of the low oxygen consumption, the difference between the inlet and exit gas concentrations is consequently very small at that stage of fermentation, and the gas balance methods for K_La estimation lack accuracy. As the fermentation progresses, the growth of biomass leads to an increase in oxygen consumption and to a decrease in the dissolved oxygen concentration. As a result, the gas balance methods become more accurate. Furthermore, at one point, the dissolved oxygen

concentration may become too low to allow using the dynamic method and one has to rely strictly on the gas balance methods. Fortunately, it is under these circumstances that the gas balance methods provide the most accurate estimates of the values of K_La. Because the relative accuracy of the various methods constantly varies throughout the fermentation, averaging the values of K_La will not lead to the best estimate. To overcome this problem and to take into account the relative accuracy of all methods, a data reconciliation technique was used. This technique, in addition to considering the precision of each method, takes into account the reliability of all measurements involved in the estimation of K_La values.

4.4 DATA RECONCILIATION TECHNIQUE

4.4.1 Conventional data reconciliation technique

Since it is now common for fermentation systems to be equipped with an O_2/CO_2 monitor or mass spectrometer (Heinzle, 1992), up to four methods are available to determine K_La, thereby leading to four different estimates. A simple average of the four values could be taken to give a unique and more precise value of K_La. However, as some methods are more accurate than others at different stages of fermentation, averaging K_La is not the best method to achieve a more precise value. Instead, a data reconciliation technique can be used with advantage to resolve this problem. This technique, briefly reviewed in the next section, considers the precision of each measurement and each estimation method to provide the best estimate of the K_La value. A more detailed description may be found in Pouliot et al. (2000).

Equations (4.1) to (4.4) involve twelve measured or estimated process variables (P, T, τ_P, C_L^*, C_L^0, V_L, RQ, Q_G, $y_{1,O2}$, $y_{2,O2}$, $y_{1,CO2}$, $y_{2,CO2}$) for which their measurements are generally subject to random and non-random errors. Data reconciliation can be used to minimize the impact of these errors in order that the adjusted or reconciled values of the process measurements obey mass conservation laws as well as other constraints. It is important to point out that, to perform process data reconciliation, the measured data must be redundant; that is, there exist more measured data than are necessary to satisfy system balances (Crowe, 1989, Hodouin and Everell, 1980). In addition, the mass balance models are never perfect representations of the underlying behaviour of the process due

to the many modelling assumptions that have to be made. Some of these assumptions are: the liquid and gas phases within the bioreactors are perfectly mixed, K_La is uniform at all locations within the bioreactor and the oxygen utilization rate is identical before and after the in situ dynamic test. As a result, data reconciliation has to be performed by taking into account both the measurement errors and the process modelling errors. To achieve this dual objective, general criteria for data reconciliation can be defined to take simultaneously into consideration all measured variables and all conservation models, written in the form of a weighted summation, whereby each term is being affected by a weight that corresponds to the level of confidence that one has in each measurement and each conservation model. This dual objective has been used successfully for many applications (Hodouin et al., 1993, Liebman et al., 1992, Mah, 1990, Makni et al., 1995).

The data reconciliation objective function was formulated with (1) the twelve process variables associated with their respective level of accuracy and (2) the four mass conservation balance equations with an estimate of their level of confidence. This objective function is minimized to determine a unique value of K_La. The dynamics of the dissolved oxygen probe, represented as a first order system, was also incorporated. In the objective function, the weighting factor for each measurement term was set equal to the inverse value of the variance associated to that measurement. Weighting factors of conservation models were determined considering the individual precision of each measured variable using a Monte Carlo simulation method (Patel and Thibault, 2004).

4.4.2 Data reconciliation via a feedforward neural network

The conventional data reconciliation algorithm requires mathematical artillery that is relatively extensive and that must be used for each K_La estimation. In order to simplify the procedure, it is proposed to use a feedforward neural network (FNN) to predict K_La using process information that can be easily obtained from dynamic experiments and gaseous oxygen and carbon dioxide concentrations. A feedforward neural network draws its analogy from human brain neuronal system which is able to learn by modifying the synaptic connections. It consists of a layer of input neurons, a layer of output neurons and one or more hidden layers. In this investigation, a three-layer FNN was used, that is a network with a single hidden layer as shown in Figure 4.2. A FNN can simply be viewed as a general nonlinear model that relates a set of independent variables (inputs) and

dependent variables (outputs). The inputs and outputs of the neural network are usually scaled into the range of 0 to 1. The neurons in the input layer simply store the coded information of the input variables and fan out this information to the functional neurons of the hidden layer. The hidden layer contains functional neurons (except for the bias in the hidden layer) which perform a nonlinear transformation of the weighted sum of the outputs of the neurons of the previous layer. The output neurons perform a similar operation whereby it transforms the weighted sum of the outputs of the hidden neurons to calculate the normalized output variables. To adequately represent the underlying phenomenon that the neural network is trying to model, it is necessary to train the model with representative data. In the training phase, an optimization algorithm is used to find a suitable set of parameters (connecting weights) that will minimize the prediction errors for the entire training data set. For a more comprehensive description of all aspects of neural networks including the underlying equations, the reader is referred to the introductory paper of Lippmann (1987) and Thibault et al. (1990).

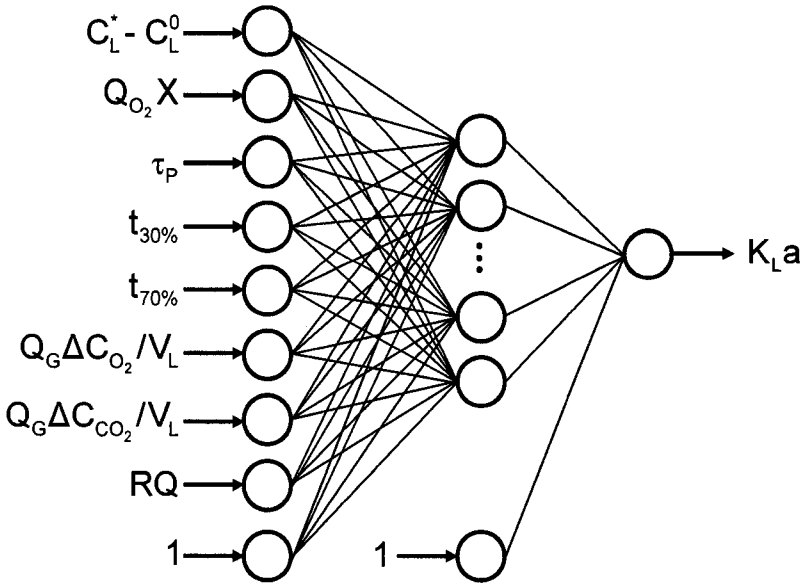

Figure 4.2 – Architecture of the feedforward neural network used for the estimation of $K_L a$.

In this investigation, it is assumed that the system of mass conservation Equations (4.1 – 4.4) applies for all three fermentation systems such that it is desired to derive a single neural network that will implicitly perform data reconciliation to calculate the most probable value of $K_L a$. To train the neural network to perform this task, the dynamic

method was simulated with different values of K_La, $Q_{O2}X$ and of the other twelve process variables. A series of 500 simulations was performed with all these process variables chosen randomly, some calculated from other process variables, over a relatively wide, yet realistic, range of variation. The range of variation of these variables in the simulation is presented in Table 4.2. For each simulation, some process parameters were directly selected or defined to be used as inputs to the neural network for the estimation of K_La. This set of parameters was then used to train the feedforward neural network of Figure 4.2 as a predictor for K_La.

Table 4.2 – Ranges of variation of each process variable to generate the training data set.

Variable	Range	Variable	Range
P (Pa)	99 300 – 103 300	Q_G (10^4 m^3/s)	1.00 – 1.67
T (K)	299 - 303	$y_{1,O2}$	0.1992 – 0.2092
τ_P (s)	5 - 15	$y_{2,O2}$	0.189 – 0.205
C_L^* (mol/m^3)	0.23 – 0.25	$y_{1,CO2}$ (10^4)	4.0 – 6.0
C_L^0 (mol/m^3)	0.001 – 0.24	$y_{2,CO2}$ (10^4)	5.72– 229.3
V_L (m^3)	0.008 – 0.017	$Q_{O2}X$ (10^4)	14.3 – 991.5
RQ	0.80 – 1.50	K_La (s)	0.001 – 0.10

The neural network of Figure 4.2 has eight process inputs that were defined from the simulation of Equations (4.1) - (4.4) and were selected because they are correlated with the value of K_La that prevails at any point during the fermentation. These variables are (see also Figure 4.1):

1. C_L^* - C_L^0 is the difference between the dissolved oxygen (DO) concentration at saturation and the pseudo-stationary DO concentration prior to the initiation of the dynamic test.
2. $Q_{O2}X$ is the oxygen utilization rate (also referred to as OUR) that is determined from the slope of the DO response when agitation and aeration are stopped. This value is not influenced by the dynamics of the DO probe so that the linear portion of the curve can be used directly for its evaluation.

3. τ_P is the time constant of the DO probe that was determined separately by fitting a first-order model to the response of the probe after its rapid transfer from a nitrogen-sparged medium to an oxygenated solution.
4. $t_{30\%}$ is the time required for the measured DO concentration to regain 30% of the range between the lowest DO concentration and the pseudo-stationary DO concentration. This time is influenced directly by K_La and the time constant of the DO probe. It is important to mention that the estimation of K_La is independent of the value of $Q_{O2}X$. Indeed, $Q_{O2}X$ only affects the final pseudo-stationary DO level but not the rate of change of the DO concentration while the system is returning to this final value after agitation and aeration have been resumed.
5. $t_{70\%}$, similar to $t_{30\%}$, is the time required for the measured DO concentration to regain 70% of the range of variation of the DO concentration. These two times are obviously directly impacted by the value of K_La as they represent the rise to the steady DO value when aeration and agitation are resumed.
6. $Q_G\Delta C_{O2}/V_L$ is the product of the gas flow rate and the change in concentration between the inlet and the exit of the fermenter divided by the liquid volume. This term represents the rate of oxygen consumption per unit volume of the fermentation broth.
7. $Q_G\Delta C_{CO2}/V_L$ is similar to previous term for the concentration of carbon dioxide. It represents the rate of carbon dioxide production per unit volume of the fermentation broth. When the value of the respiration quotient (RQ) is known, these two expressions would ideally be equivalent.
8. RQ is the respiration quotient and is usually fairly constant during a major part of the fermentation. Values of past experiments are usually used as an estimate.

This neural network performs data reconciliation using information pertaining to each mass conservation models to estimate a unique value of K_La. Once the neural network has been trained, it can be used rapidly to estimate K_La from the determination of the eight parameters. In addition to the nine input neurons, the neural network used 7 hidden neurons and one output neuron. Training was performed using a quasi-Newton optimisation algorithm (Powell, 1975). The parity plot of the theoretical (or simulated) K_La versus the predicted K_La using the neural network is presented in Figure 4.3. As can

be observed, the neural network is able to represent very well the 500 values of K_La that were determined over a relatively wide range of the numerous process variables. The neural network has been trained with 400 values taken randomly and the remaining 100 values were used for validation.

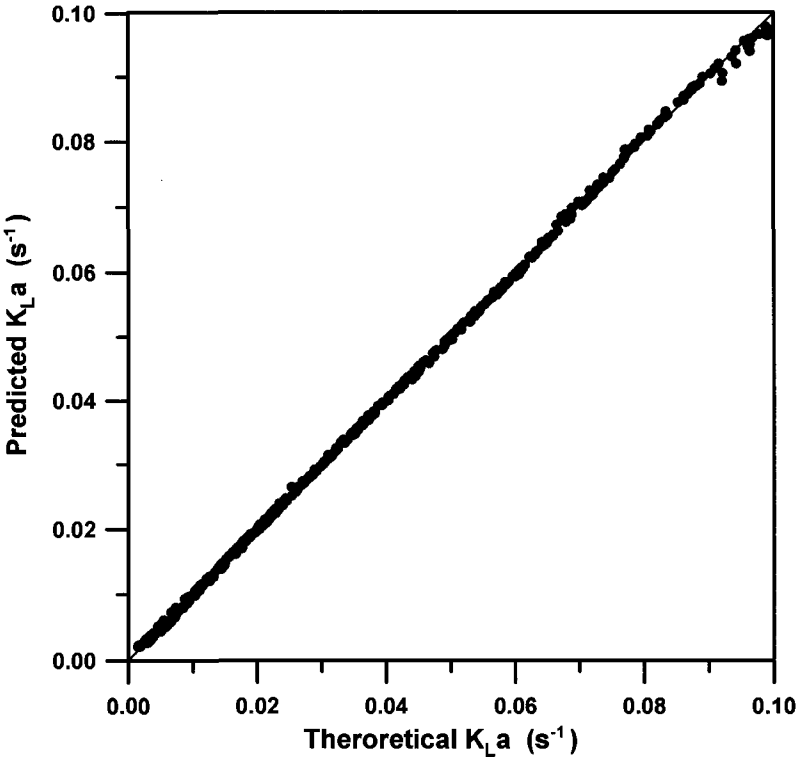

Figure 4.3 – Theoretical K_La versus predicted K_La for 500 simulations.

4.5 RESULTS AND DISCUSSION

The data obtained during the various dynamic K_La tests performed during the fermentations of *Saccharomyces cerevisiae*, *Aspergillus niger* and *Trichoderma reesei*, were used to test the ability of the neural network of Figure 4.2 to predict K_La values. The neural network predictions were compared with the K_La values obtained with the conventional data reconciliation method. These results are presented in Figure 4.4. The range of K_La for the three fermentation systems is different. For the production of baker's yeast, the fermentation has a relatively low viscosity and K_La is higher. As the viscosity of the fermentation broth increases, K_La decreases as observed for the fermentations with the two filamentous microorganisms, *Aspergillus niger* giving by far a more viscous fermentation broth. The average difference in the estimation of K_La between the two

methods lies well within the two dotted lines that represent the ±20% variation in K_La prediction. The scatter in the difference of K_La for *S. cerevisiae* and *A. niger* is greater than for *T. reesei*. This difference is mainly attributed to the precision of the equipment used to measure the gas phase concentration. For *T. reesei*, a mass spectrometer was used which provided a significantly greater accuracy than the O_2 paramagnetic and CO_2 infrared measurements for fermentations performed with the other two microorganisms.

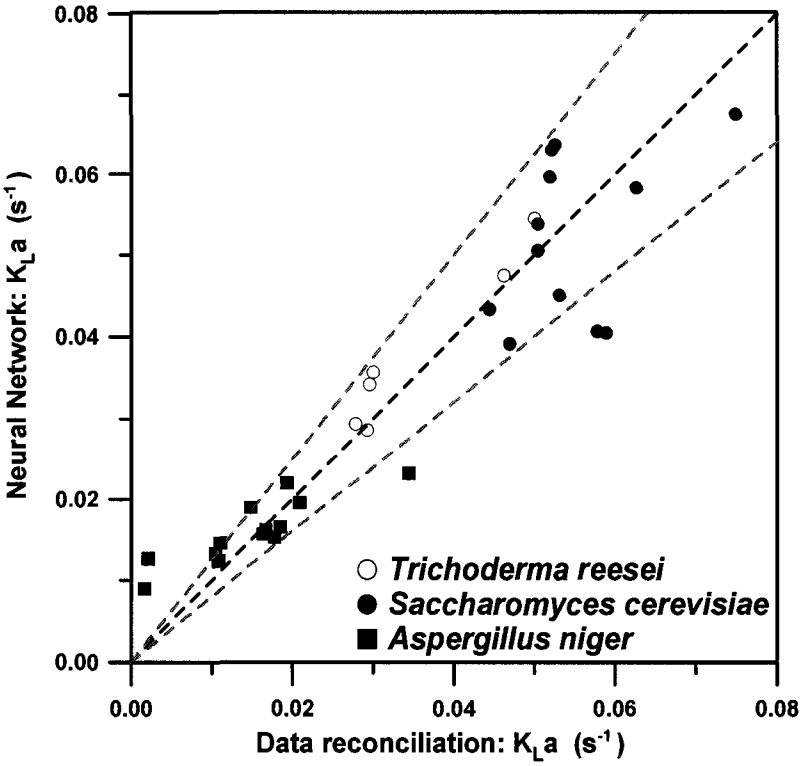

Figure 4.4 – Plot of the K_La values obtained with the neural network versus values obtained with the conventional data reconciliation technique. The two dotted lines from each side of the 45° line represent the range of ±20%.

The real value of K_La is obviously unknown and the four different methods discussed above and given in Equations (4.1 – 4.4) provide different estimates of K_La. It is only possible to compare predictions among themselves. It is assumed in this investigation that the conventional data reconciliation method provides the most probable value of K_La because it takes into account each of the twelve measurements as well as the four conservation models along with their respective accuracy (Pouliot et al., 2000, Patel and Thibault, 2004). In the case of the conventional data reconciliation, the accuracy of each model was determined by performing a Monte Carlo simulation at the point of operation

for each dynamic test in order to find the weighting factor to be used in the objective function. On the other hand, for the neural network, the underlying relationship that is developed depends only on the set of eight input variables of Figure 4.2 that were derived from simulations. Therefore, it is not possible to change, as in the case of the conventional data reconciliation, the weighting factor of a particular input variable to adapt to its current relative accuracy. Despite this limitation, the results of Figure 4.4 clearly show that the predictions of K_La using the artificial neural network are similar to those obtained by the conventional data reconciliation method.

The points on the parity plot of Figure 4.4 appear to be relatively well distributed around the 45^o line and there is no apparent systematic bias for any of the three fermentations. The level of accuracy observed in this comparison is relatively good and well within typical errors that are commonly seen in K_La estimation (Ruchti, 1981, Djebbar and Narbaitz, 2002). These results are very interesting, since a unique neural network was used for estimating K_La for the three types of microorganisms. To increase the sensitivity of the estimation, it could be possible to use training data generated over a more restricted range of operation that would be encountered in the actual fermentation. The input vector of the neural network could also be reduced in the case of a specific application. For example, if the time constant of the DO probe was known, a constant value could be used while generating the data and its value would be removed from the input vector of the neural network. It would also be advantageous to perform a correlation analysis between a series of inputs and K_La in the training data set to determine the inputs that have the most impact on the estimation of K_La, thereby allowing choosing the best input vector to construct the neural network.

Different versions of the neural network could be used depending on the operating points. For example, at the beginning of the fermentation, the differences of oxygen and carbon dioxide concentrations between the inlet and the outlet gas streams are generally low. The accurate estimation of K_La by these two methods strongly relies on the precision of the O_2 and CO_2 sensors, and of the mass flow meter. In this case, K_La could be estimated very reliably with the dynamic and stationary methods such that a neural network without the two gaseous terms and RQ value (last three elements of the input vector) could be constructed and an enhanced prediction could be obtained. The reverse

is true when the dissolved oxygen is very low and it is not possible to perform a dynamic test. In this case, the differences in gaseous concentrations would be closed to their maximum values and a greater accuracy in the estimation of K_La could be achieved considering only the gaseous terms. In that particular case, a neural network could be constructed with only four inputs because it is impossible to evaluate input variables $Q_{O2}X$, τ_P, $t_{30\%}$ and $t_{70\%}$. As a result, the latter four inputs could be safely eliminated from the network of Figure 4.2. For the simulations performed to generate the data to train the neural network, values of $Q_{O2}X$, $t_{30\%}$ and $t_{70\%}$ were set to zero whenever the stationary DO level was less than 20% and a dynamic method could not be performed in practice. The neural network was nevertheless able to integrate this information.

4.6 CONCLUSION

In this investigation, the *in situ* estimation of K_La in fermentation using a neural network trained strictly on theoretical mass conservation equations was examined and compared with the estimation obtained with the more conventional data reconciliation algorithm. It was found that the neural network has the ability to estimate the value of K_La from process variables defined from the response of the dynamic method of Taguchi and Humphrey (1966) and the gas balance methods. The values obtained were close to those obtained by the more conventional data reconciliation method.

The results obtained clearly showed that a single artificial neural network could be used for the estimation of K_La for different fermentation systems. Dedicated neural networks could be developed over a narrower range of K_La and for specific situations where not all the conservation models could be used. This would improve the estimation accuracy of K_La. However, results show that, given the typical estimation error normally associated with K_La determination, the unique artificial neural network of Figure 4.2 is adequate.

4.7 NOMENCLATURE

C_L dissolved oxygen concentration (mol/m^3)

C_L^0 pseudo-steady-state dissolved oxygen concentration recorded at the initiation of the dynamic method (mol/m^3)

C_L^* dissolved oxygen concentration in equilibrium with mean gaseous oxygen concentration (mol/m^3)

K_La overall oxygen mass transfer coefficient (s^{-1})

P pressure (Pa)

Q_G gas flow rate (m^3/s)

$Q_{O_2}X$ oxygen uptake rate (mol/m^3 s)

R gas constant (8.306 Pa m^3/(mol K))

RQ respiratory quotient

t time (s)

T temperature (K)

V_L liquid volume in the fermenter (m^3)

y gaseous mole fraction

SUBSCIPTS

1 inlet stream

2 outlet stream

CO_2 carbon dioxide

G gas

O_2 oxygen

4.8 REFERENCES

Atkinson, B. and Mavituna, F., Biochemical Engineering and Biotechnology Handbook. 2nd Ed., Stockton Press, pp 337, 1991.

Brown, D. E., Bioprocess Measurements and Control. Chemistry & Industry, *16*: 678-681, *September* 1991.

Crowe, C. M., Observability and Redundancy of Process Data for Steady State Reconciliation. Chemical Engineering Science, *44*: 2909-2917, 1989.

Cruz, A. J. G., Silva, A. S., Araujo, M. L. G. C., Giordano, R. C., and Hokka, C. O., Estimation of the Volumetric Oxygen Transfer Coefficient (K_La) From the Gas Balance and Using a Neural Network Technique. Brazilian Journal of Chemical Engineering, *16*: 179-183, 1999.

Copella, S. J. and Dhurjati P., A Detailed Analysis of *Saccharomyces cerevisiae* Growth Kinetics in Batch, Fed-batch, and Hollow-fiber. Bioreactors. The Chemical Engineering Journal, *41*: B27-B35, 1989.

Djebbar, Y. and Narbaitz, R. M., Neural Network Prediction of Air Stripping K_La. Journal of Environmental Engineering, *128*: 5, 451-460, 2002.

Gagnon, H., Lounes, M., and Thibault, J., Power Consumption and Mass Transfer in Agitation Gas-Liquid Columns: a Comparative Study. Canadian Journal of Chemical Engineering, *76*: 379-389, 1998.

Gauthier, L., Thibault, J., and LeDuy, A., Measuring K_La With Randomly Pulsed Dynamic Method. Biotechnology and Bioengineering, *37*: 889-893, 1991.

Heinzle, E., Present and Potential Applications of Mass Spectrometry for Bioprocess Research and Control. Journal of Biotechnology, *25*: 81-114, 1992.

Hodouin, D., Bazin, C., and Makni, S. On-line Reconciliation of Mineral Processing Data. Proc. of the AIME/SME Symposium - Emerging Computer Techniques for the Mineral Industry, Reno, Nevada, 1993.

Hodouin, D. and Everell, M. D., A Hierarchical Procedure for Adjustment and Material Balancing of Mineral Process Data. International Journal of Mineral Processing, *7*: 91-116, 1980.

Jarai, M., Factors Affecting the Scale-Up of Aerated Fermentation Processes. International Chemical Engineering, *19*: 701-708, 1979.

Liebman, M. J., Edgar, T. F., and Lasdon, L. S., Efficient Data Reconciliation and Estimation for Dynamic Processes Using Nonlinear Programming Techniques. Computers and Chemical Engineering, *16*: 963-986, 1992.

Lippmann, R. P., An Introduction to Computing With Neural Nets. IEEE ASSP Magazine, pp. 4, April 1987.

Mah, R. S. H. Chemical Process Structures and Information Flows. Batterworths, Boston, 1990.

Makni, S., Hodouin, D., and Brazin, C., A Recursive Node Imbalance Method Incorporating a Model of Flowrate Dynamics for On-Line Material Balance of Complex Flowsheets. Mineral Engineering, *8*: 753-766, 1995.

Moo-Young, M. and Blanch, H. W., Design of Biochemical Reactors – Mass Transfer Criteria for Simple and Complex Systems. Advances in Biochemical Engineering/Biotechnology, *19*: 1-69, 1981.

Patel, N. and Thibault, J., Evaluation of Oxygen Mass Transfer in *Aspergillus Niger* Fermentation Using Data Reconciliation. Biotechnology Progress, *20*: 239-247, 2004.

Pouliot, K., Thibault, J., Garnier, A., and Acuña Leiva, G., K_La Evaluation During the Course of Fermentation Using Data Reconciliation Techniques. Bioprocess Engineering, *23*: 565-573, 2000.

Powell, M. J. D., Some Global Convergence Properties of a Variable Metric Algorithm for Minimization Without Exact Line Searches. ASM/SIAM Symposium on Non-linear Programming, New York, 1975.

Rao, A. R. and Kumar, B., Predicting Re-Aeration Rates Using Artificial Neural Networks in Surface Aerators. International Journal of Applied Environmental Science, *2*: 155-166, 2007.

Ruchti, G., Dunn, I. J., and Bourne J. R., Comparison of Dynamic Oxygen Electrode Methods for the Measurement of K_La. Biotechnology Bioengineering, *23*: 277-290, 1981.

Shuler, M. L. and Kargi, F. Bioprocess Engineering – Basic Principles. Prentice Hall PTR, New Jersey, 1992.

Siegel, S. D. and Gaden Jr, E. L., Automatic Control of Dissolved Oxygen Levels in Fermentations. Biotechnology and Bioengineering, *4*: 345-356, 1962.

Taguchi, H. and Humphery, A. E., Dynamic Measurement of the Volumetric Oxygen Transfer Coefficient in Fermentation Systems. Journal of Fermentation Technology, *14*: 881-889, 1966.

Thibault, J., Van Breusegem, V., and Chéruy, A., On-line Prediction of Fermentation Variables Using Neural Networks. Biotechnology Bioengineering, *36*: 1041-1048, 1990.

Yagi, H. and Yoshida, F., Oxygen Absorption in Fermenters: Effects of Surfactants, Antifoaming Agents, and Sterilized Cells. Journal of Fermentation Technology, *52*: 905-916, 1974.

Yamane, T. and Shimizu, S., Fed-batch Techniques in Microbial Processes. Advances in Biochemical Engineering/Biotechnology, *30*: 147-194, 1984.

SECTION - II

SAMPLE ANALYSIS

CHAPTER 5

Morphological Characterization and Viability Assessment of *Trichoderma reesei* by Image Analysis

Véronique Lecault, Nilesh Patel, and Jules Thibault

Department of Chemical Engineering

University of Ottawa

Ottawa (ON), K1N 6N5, Canada

Abstract

The production of cellulase from the filamentous fungus *Trichoderma reesei* is a critical step in the industrial process leading to cellulose ethanol. Due to the lack of quantitative analysis tools, the intimate relationship that exists between the morphological and physiological states of the microorganism, the shear field in the bioreactor and the process performance is not yet fully understood. A semiautomatic image analysis protocol was developed to characterize the mycelium morphology and to estimate its percentage viability during the fermentation process based on four morphological types (unbranched, branched, entangled and clumped microorganisms). Pictures taken under bright field microscopy combined with images of fluorescein diacetate (FDA)-stained fungi were used to assess the morphological parameters and the percentage viability of microorganisms simultaneously. The method was tested during the course of fed-batch fermentation in a reciprocating plate bioreactor (RPB). The use of the image analysis protocol was found to be successful in quantifying the variations in the morphology and the viability of *T. reesei* throughout the fermentation.

Keywords: morphology, viability, *Trichoderma reesei*, filamentous fungi, image analysis

5.1 INTRODUCTION

Filamentous fungi such as *Trichoderma reesei* are widely employed in the production of proteins at the industrial scale. For instance, the laundry and the pulp and paper industries use degradative enzymes (cellulases) secreted by this microorganism for the hydrolysis of cellulosic substrates (Maras et al., 1999). Another application of these enzymes is the transformation of agricultural wastes into fermentable sugars for the production of bioethanol. Due to low specific activity and high manufacturing costs of the enzyme, this step of the process represents one of the major expenses in the production of ethanol from agricultural wastes. Therefore, it is critical to achieve low-cost cellulase production for the development of a sustainable bioethanol process (Schell et al., 2001). Efforts have been made to reduce enzyme manufacturing cost by utilizing agricultural wastes as a substrate for the microorganisms through solid state fermentation (Tengerdy and Szakacs, 2003). However, the scale-up of this process leads to many engineering challenges and submerged cultures are still predominantly used in industrial processes partly because of the pressure of increasing industrial rationalization and standardization (Hölker and Lenz, 2005).

Fungal fermentations are complex systems into which the operating conditions, the broth rheology, the enzyme production, the morphology of the microorganisms and their physiological state are all interrelated (Schügerl et al., 1998). It is necessary to understand the relationship between these parameters in order to improve the enzyme production. It has been reported that the morphology of filamentous mycelia was related to the protein secretion (Amanullah et al., 2002, Paul et al., 1999). It is also well known that the morphology is affected by the agitation conditions (Amanullah et al., 1999, Jüsten et al., 1996) and that it has an influence on the rheological properties of the system (Riley et al., 2000, Sinha et al., 2001).

The mycelial morphology can be classified into dispersed and pelleted forms. Under the operating conditions leading to the production of cellulase, *T. reesei* is found mainly in the dispersed form. The latter includes freely dispersed mycelia (comprising unbranched, branched and entangled morphologies) and clumped mycelia (Paul and Thomas, 1998). Various semiautomatic and fully automatic image analysis methods for analyzing dispersed filamentous fungi have been developed. The first algorithms were

restricted to the analysis of freely dispersed morphology (Adams and Thomas, 1988). Subsequently, the characterization of clumps was studied since mycelial aggregates occupy a significant fraction of the biomass and can affect the rheology of the system (Packer and Thomas, 1990). Further developments in the field led to the fully automatic and detailed analysis of morphological parameters for each morphological class of *Streptomyces clavuligerus*, *Penicillium chrysogemun*, *Aspergillus niger* and other filamentous species (Schügerl et al., 1998, Tucker et al., 1992). However, very few studies were done on the morphological kinetics of *T. reesei* during the course of fermentation. Lejeune et al. (1995) studied the morphology of *T. reesei* QM9414 in submerged culture, but their analysis was limited to freely dispersed mycelia.

Filamentous microorganisms are formed from spores and go through various differentiation steps. Healthy regions are initially filled with cytoplasm. Larger vacuoles are progressively formed until all the cytoplasm is lost and the cells become degenerated (Packer et al., 1992). Therefore, standard plating techniques such as colony forming unit count cannot be used to determine the percentage viability since the same hyphae can contain both viable and degenerated compartments. It would result in an overestimation of the viability. Various methods were tested to study the physiology of filamentous organisms by image analysis. Vanhoutte et al. (1995) have used methylene blue in combination with Ziehl fuschin to characterize six different physiological states of *P. chrysogenum*. Also, the occurrence of empty zones in *Streptomyces ambofaciens* was assessed using Carbol Gentian Violet staining (Drouin et al., 1997). Sebastine et al. (1999) measured the percentage viability of *actinomycete* mycelia by image analysis using a bacterial viability stain. The percentage viability was defined as the ratio of the projected area of regions with intact membrane over the total projected area of microorganisms. The viability of filamentous fungi was also assessed using fluorescein diacetate (3',6'-diacetylfluorescein (FDA)) and was shown to be related to the growth rate of the biomass (Hassan et al., 2002). This dye is hydrolyzed by the intracellular esterases to form fluorescein, a compound which exhibits fluorescence. Membrane integrity is required to maintain the dye inside the cell (Breeuwer and Abee, 2000). Therefore, not only degenerated regions have no active enzymes to catalyze the

hydrolysis, but they do not have intact membrane to retain fluorescein. It results in active regions exhibiting bright green fluorescence and degenerated regions appearing black.

The morphology and viability of the filamentous bacteria *Streptomyces clavuligerus* were studied simultaneously by image analysis (Pinto et al., 2004) but no attempt has been done on filamentous fungi. This work proposes a semiautomatic image analysis protocol allowing the detailed analysis of the morphological parameters of unbranched, branched, entangled and clumped microorganisms as well as the assessment of the percentage viability of biomass using FDA. The method is tested on *T. reesei* during fed-batch fermentation in a reciprocating plate bioreactor (RPB). In doing so, it is possible to assess physiological changes according to each morphological class during the fermentation.

5.2 MATERIALS AND METHODS

5.2.1 Microorganism and Maintenance

The strain used throughout this work was *T. reesei* RUT C-30 (ATCC 56765) supplied by Iogen Corporation, Ottawa. The glycerol stock solutions of spores were maintained at -80°C and were transferred on potato dextrose agar plates. New plates were prepared every month and kept at 4°C.

5.2.2 Shake Flask Cultures

The culture medium contained: glucose, 13 g/L; $(NH_4)_2SO_4$, 1.4 g/L; KH_2PO_4, 2.0 g/L; $MgSO_4 \cdot 7H_2O$, 0.6 g/L; $CaCl_2 \cdot 2H_2O$, 0.3 g/L; $FeSO_4 \cdot 7H_2O$, 5.0 mg/L; $MnSO_4 \cdot 7H_2O$, 1.6 mg/L; $ZnSO_4 \cdot 7H_2O$, 1.4 mg/L; $CoCl_2 \cdot 6H_2O$, 2 mg/L and corn steep solids, 6.0 g/L. The pH of the medium was initially adjusted to 5.5 using 10N NaOH. A solution containing crushed corn steep solids was first autoclaved separately for 45 min to eliminate possible contamination. The complete medium was then autoclaved for 20 minutes. Shake flask cultures were performed with a volume of 450 mL in a 1-L Erlenmeyer flask with three baffles. A spore solution in sterilized water was prepared from the plates. The spore concentration was calculated using a Petroff Hausser counting chamber (Hausser Scientific, Horsham, PA) and an appropriate volume was inoculated in the flask to obtain an initial concentration of 5×10^3 spores/mL. Flasks were kept in an

orbital shaker at 200 rpm and 28°C (model 3535CC Incubator shaker, Lab-Line Instrument Inc., Melrose Park, IL).

5.2.3 Bioreactor Culture

Laboratory-scale batch fermentation was performed in a reciprocating plate bioreactor (RPB) to test the image analysis protocol. A schematic representation of the RPB is shown in Appendix A.1 (a). This bioreactor consisted of a stack of perforated plates mounted on a vertical shaft. The reciprocating vertical movement of the plate stack provided the agitation. The stainless steel bioreactor had a total volume of 22.5 L with a working volume of 17 L. The inner diameter was 228 mm and the column height was 550 mm. Six stainless steel perforated plates (221-mm diameter and 1.25-mm thickness) were spaced 50 mm apart from one another and contained perforations having a 19-mm diameter. A 9-L fermentation was performed with the same culture medium as the shake flasks, except that 2 mL of antifoam was added. A 55-h old shake flask culture (450 mL) was used as inoculum. The fermentation was held at a constant agitation frequency of 0.25 Hz and a temperature of 28°C. A one-sided pH control was performed by the addition of NH_4OH (15% v/v) to prevent the pH to decrease below 4.5. The pH was measured on-line by a pH FermProbe (Broadley-James Corporation, Irvine, CA) whereas the dissolved oxygen (DO) was continuously monitored by a DO Sensor (Broadley-James Corporation, Irvine, CA). The DO level was controlled to 30% by feeding a 150 g/L lactose solution to the culture. A Proline mass spectrometer (Ametek, Pittsburgh, PA) was used to measure the concentration of CO_2 in the exhaust gas. Samples were taken daily and triplicates were analyzed. The fed-batch fermentation was stopped after 202 h.

5.2.4 Biomass Quantification

The amount of biomass was quantified by dry weight analysis. A 25-mL sample of the culture broth was filtered through a predried and preweighted glass fibre filter (grade A/E, Gelman Sciences, MI). One volume of the sample was washed with two volumes of deionised distilled water and oven dried for 24 h at 100°C. The weight of the sample was measured after a 24-h period of cooling in a desiccator.

5.2.5 Viability Control

To test the reliability of the viability protocol, a 40-h old sample was taken from the fermentor. Half of the sample was autoclaved for 20 minutes. Aliquots containing 0%,

20%, 40%, 60%, 80% and 100% v/v of the initial sample were mixed with the autoclaved sample. Samples were analyzed for morphology and viability using the staining procedures and the image analysis protocol presented below.

5.2.6 Staining

A solution of 70 mg FDA in 100 mL acetone was prepared and stored in the dark at 4°C. Before each analysis, 15 µL of the stock solution was added to 285 µL of a 0.1 M phosphate-citrate buffer, pH 4.5. If necessary, the sample was diluted with phosphate-citrate buffer to a final concentration of 0.4 to 4 g/L, yielding a density of approximately 0 to 10 microorganisms per frame. One volume of the diluted sample was added to three volumes of the FDA solution. The sample was agitated mildly during 5 min in the dark at 30°C. A 7.5-µL aliquot of each diluted sample was placed on a microscope slide and covered with an 18-mm x 18-mm coverslip for analysis.

5.2.7 Image Acquisition

For image analysis measurements, a monochrome camera (CoolSnap ES, Roper Scientific, Tucson, AZ) mounted on an Olympus IX81 microscope (Olympus, Melville, NY) was used. The automated stage of the microscope was controlled by the Image-Pro® Plus software (Image-Pro® Plus version 5.1, Media Cybernetics, Silver Spring, MD). The slide was divided into 567 frames and the automated stage prevented the same frame to be taken twice. Each frame was grabbed first under bright field. A UV light generated by a mercury lamp was then applied with a filter (490 nm excitation and 520 nm emission) and a second picture was taken. At least 60 sets of frames on each slide were taken randomly. The exposure time of both pictures was 32 ms throughout the experiment. To reduce fading issues, this value was chosen by taking the minimum exposure time allowing enough fluorescence throughout the image acquisition period.

5.2.8 Image Analysis

The image analysis was performed using the Image-Pro® Plus software. Macros allowing the semiautomatic analysis of multiple images were written in Visual Basic code. Each image to be analyzed was saved in a TIFF format. It was first transformed into an 8-bit grey scale image. Segmentation was then performed to create a binary image. All the pixels below a threshold value were set to black (0) whereas pixels above were set to white (255). To make thresholding independent of the luminosity of the

picture, the threshold value was set to be 6 tones below the mean value of the pixels on the image. All subsequent processing was made on the binary image.

Since only entire microorganisms were analyzed, all the objects touching the frame of the picture were removed. A filter was applied to also remove objects that had an area smaller than 100 pixels and roundness smaller than two. The roundness was calculated using the following equation:

$$\frac{\text{Perimeter}^2}{4\pi \times \text{Projected area}} \tag{5.1}$$

Since corn steep solids have various shapes and sizes, it was not possible to remove them all from the picture. Moreover, some large particles were touching microorganisms and it could have biased significantly the results. For this reason, the operator was prompted to select the microorganisms to be analyzed. This step was the only non automatic part of the protocol but it did not slow down dramatically the process since approximately five minutes per sample were required.

Selected microorganisms were automatically classified into unbranched, branched, entangled and clumped categories. Each object was put on a separate picture to make the classification. The microorganism was first skeletonized, i.e. transformed into a one pixel thick object based on the pixels median between the edges of the object. A filter was then applied to the skeleton to show the end and branching points. End point pixels were given a binary value of 32, branching points pixels were given a value of 64 or 128 whereas the rest of the skeleton had a value of 16. The branching points were subtracted from the skeleton and tips smaller than 3 μm were removed from it. The purpose of the last step was to avoid the count of small solid particles touching the mycelia as tips. If the number of tips at this point was two, the object was classified as unbranched mycelia. If not, the number of holes within the area of the objects was counted. As proposed by Paul and Thomas (1998), microorganisms without holes were classified as branched, objects having between one and three holes were classified as entangled and mycelia having more than four holes were classified as clumped.

For the analysis of unbranched mycelia, the area, the area/box ratio, the aspect ratio, the perimeter, the convex perimeter, the perimeter ratio and the roundness were

measured. Each object was skeletonized and the total length was measured. From the area and the total length, the mean diameter was calculated.

To measure the viability, the corresponding fluorescent image was opened. An automatic threshold was performed to transform the picture into a binary image. The threshold value was selected to be 3 tones over the mean of the distribution of pixels. Another automatic thresholding techniques based on the variance of the binomial pixel distribution was also tested but found to be unsuccessful due do variations in microorganism intensity on the same frame. The mask of the bright field image was subtracted from the fluorescent image to isolate the objects being analyzed. To adjust for variations in fluorescence intensity and obtain a consistent ratio of viable versus total area, a restricted dilation was applied to the resulting image. The diameter of viable regions was grown up to the boundaries of the corresponding objects on the bright field mask and the viable area was measured. From the total area and the viable area, the percentage of viability was calculated.

The analysis of branched mycelia included the same parameters as for unbranched mycelia. However, after skeletonization the number of tips, the mean, the minimum and maximum branch lengths as well as the mean, minimum and maximum internodal distances and the number of internodal units were also measured. The branching order was determined by calculating the number of iterations required to subtract all the end points. From the number of tips, the total length and the diameter, the hyphal growth unit (HGU) per length and the HGU per volume were measured.

The analysis of entangled mycelia was the same as for branched mycelia, except for the fact that the branching order could not be measured but the fullness was calculated. The same analysis was performed for clumped microorganisms. All data were sent to an Excel spreadsheet in a tabulated form.

5.3 RESULTS

5.3.1 Viability Measurement

Figure 5.1 shows a typical set of pictures of *T. reesei* taken with bright field and fluorescence microscopy after FDA staining. The distinction between viable and dead

hyphal regions can be observed since active mycelia exhibit bright fluorescence whereas dead mycelia appear dark on the picture taken under fluorescence microscopy.

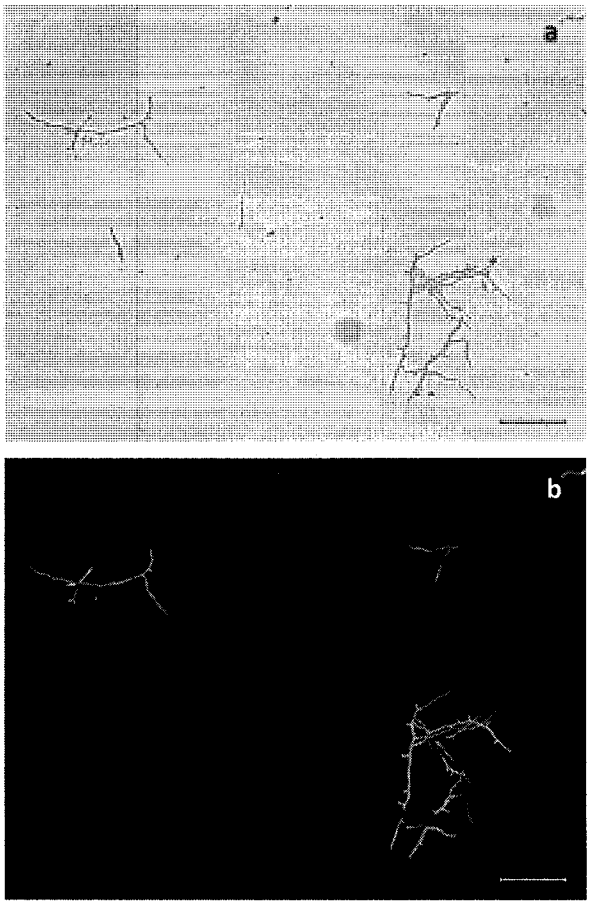

Figure 5.1 – Typical images of *T. reesei* (original magnification x10) stained with fluorescein diacetate (FDA) seen with (a) light microscopy and (b) fluorescence microscopy. Bar: 100 μm.

The efficiency of the viability algorithm has been tested on an actively growing sample from the RPB by mixing different proportions of viable and autoclaved fractions of the sample. Figure 5.2 shows the percentage viability obtained by image analysis as a function of the volumetric percentage of non autoclaved sample. The linear relationship between the measurements is shown by the line of best fit through the data. This line has a slope of 1.005 and a correlation coefficient of 0.967.

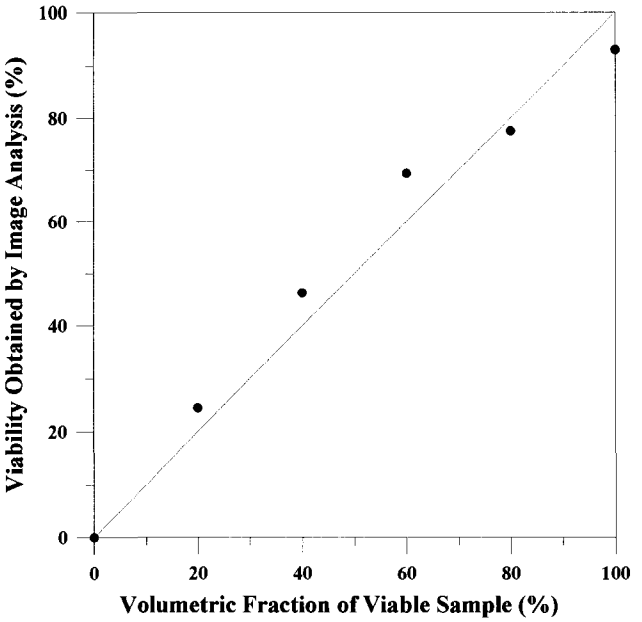

Figure 5.2 – Percentage viability estimated by image analysis as a function of the volumetric fraction of viable sample from a 40 h-old fermentation in a reciprocating plate bioreactor (RPB).

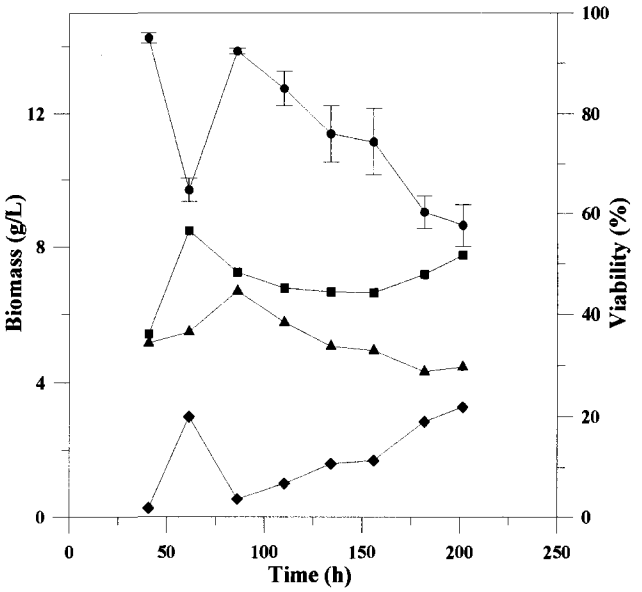

Figure 5.3 – Biomass concentration (■) and percentage viability (●) evolution during a fed-batch fermentation at 0.25 Hz in a RPB. The concentrations of viable (▲) and dead (♦) biomass are also shown.

The evolution of the biomass and its viability during fed-batch fermentation is shown on Figure 5.3. At the end of the initial growth batch phase, i.e. at 68 h, a lactose solution

was fed to the fermentation such as to maintain the dissolved oxygen level at 30% saturation. The biomass concentration reached a maximum value of 8.5 g/L and then decreased to 6.6 g/L. A drop from 95% to 65% in viability was observed at the end of the growth phase. The beginning of feeding resulted in an increase in viability followed by a decrease for the remaining of the fermentation. Toward the end of the fermentation, the viability went down rapidly to reach 58%. Consequently, the concentration of viable biomass decreased whereas a higher concentration of dead biomass was found in the medium. Image analysis was performed three times for each sample. Data points represent the mean from three replicates and error bars correspond to the standard deviation. The variation in viability never exceeded 10% of the mean value.

5.3.2 Morphological and Physiological Characterization

The simultaneous analysis of morphological and physiological parameters of *T. reesei* allowed the determination of the viability for each morphological type. Figure 5.4 shows the variation in viability for unbranched, branched, entangled and clumped mycelia. Throughout the fermentation, the viability of clumped mycelia was the highest whereas the percentage of viable unbranched mycelia was the lowest. The individual percentages of viability for each morphological type followed the same trend as the overall viability.

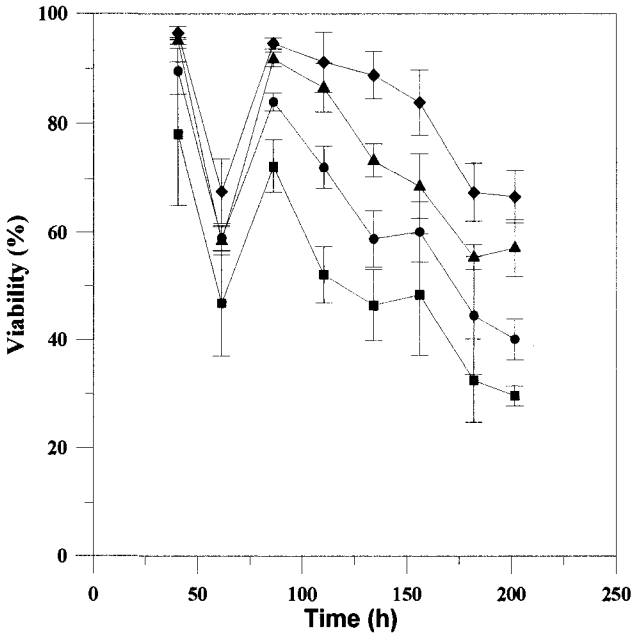

Figure 5.4 – Percentage viability of unbranched (■), branched (●), entangled (▲) and clumped (♦) microorganisms during a fed-batch fermentation at 0.25 Hz in a RPB.

In addition to the viability, the image analysis algorithm allowed the measurement of numerous morphological parameters. The mean projected area of freely dispersed mycelia (unbranched, branched and entangled) during the fed-batch fermentation is shown on Figure 5.5. Throughout the run, the area of unbranched microorganisms was the smallest, followed by the branched and entangled mycelia. A marked decrease in the projected area was observed after 175 h of fermentation which was concomitant to the drop in viability.

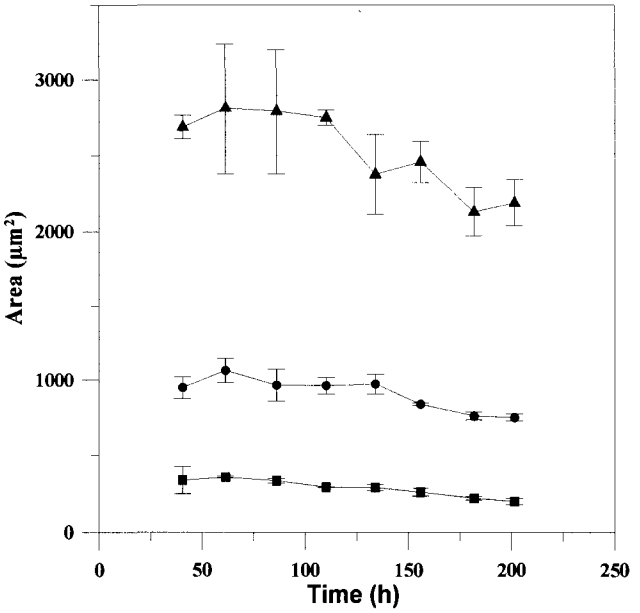

Figure 5.5 – Area of freely dispersed microorganisms during a fed-batch fermentation at 0.25 Hz in a RPB. Mean values for unbranched (■), branched (●) and entangled (▲) microorganisms are shown.

5.4 DISCUSSION

As reported previously (Hassan et al., 2002, Ingham and Klein, 1982, Söderström, 1977), FDA was successful to distinguish viable from dead regions in fungi species. It can be seen on Figure 5.1 that microorganisms exhibited null, partial or full fluorescence depending on their physiological state. Although FDA is known to fade rapidly (Hassan et al., 2002, Steward, 1995), photobleaching was not problematic during image acquisition. The exposure time for both images in a set of pictures was kept constant at 32 ms and the total time to take 60 pairs of pictures never exceeded 45 minutes. To avoid variation due to fading or light intensity, the threshold points were selected automatically

depending on the background intensity instead of being set to absolute values. The optimum parameters were determined to be 6 greyness levels below the mean density for the bright field image and 3 greyness levels over the mean density for the fluorescent pictures. The automation of this image processing step did not only reduce the time of analysis but also minimized variations caused by the operator's judgment. All viability measurements for individual hyphae were within the range of 0 to 100%. The subtraction of the bright field image from the fluorescent image followed by the dilation step allowed a perfect comparison of both projected areas independently of the variations in hyphal diameter caused by thresholding.

The accuracy of the viability measurement is verified on Figure 5.2. The sample used for this control was taken from a 40-h old fermentation while microorganisms were still in their initial growth phase. Although it was not possible to obtain a viability of a 100%, the sample chosen was very active with an initial percentage of FDA-stained area of 93%. Because of the dead hyphal regions in the initial sample, there was a slight overestimation in the expected viability from the volumetric proportion of viable sample. Results from triplicate analysis showed a standard deviation ranging from 0.5 to 7% for the overall viability determined by image analysis. Therefore, the error caused by the initial viability of the sample was not large enough to affect significantly the control. Although almost all fluorescent pictures appeared black, the autoclaved part of the sample exhibited a percentage viability of 0.003%. This was due to the entanglement of autofluorescent corn steep particles with the cells. A linear relationship with a slope of 1.005 was obtained, confirming the accuracy of the results obtained by image analysis. In previous studies, Ingham et al. (1982) correlated the percentage of FDA-stained area with the oxygen utilization, the glucose utilization and the biomass of fungi. Hassan et al. (2002) also found a linear relationship between the percentage of FDA-stained area and the biomass growth rate after different cell treatment. However, the accuracy of percentage viability value obtained by their image analysis algorithm was not verified. Here, it is shown that the percentage of FDA-stained hyphae measured by image analysis corresponds to the proportion between dead and viable microorganisms in a sample.

Knowing the percentage viability in the fermentor, it is possible to estimate the concentrations of viable and dead fungi. In the RPB experiment at 0.25 Hz, *T. reesei* was

grown for 68 h in batch mode then lactose feeding was initiated. The biomass reached a peak of 8.5 g/L at the end of the batch phase and decreased after feeding started. Previous studies of *T. reesei* RUT C-30 showed an increase in biomass concentration in fed-batch experiments (McLean et al., 1985). However in the present experiment, during fed-batch, the dissolved oxygen was maintained at 30% by manipulating only the rate of lactose addition. Therefore, the growth of microorganism was limited and biomass concentration initially decreased (due to cell lysis) to adapt to the growth at 30% dissolved oxygen and later increased slowly. This is a common strategy during the fed-batch process of *T. reesei* for production of cellulase. A higher protein production is achieved by maintaining a low concentration of substrate in the medium. As expected, a decrease in the viable biomass concentrations and an increase in the dead amount of cells were observed in the fed-batch part of the experiment. Similar results were reported for *T. hazarnium* (Breeuwer and Abee, 2000). A drop in viability, due to nutrient limitations, was noticed at the end of the batch mode (at 68 h) which led to a peak in dead biomass. Feeding rapidly resulted in an increased viable cell concentration and a better viability. The decreasing amount of dead biomass can be explained by the fact that when cell lysis occurs, microorganisms become hardly visible on the bright field picture and are not taken into account in the analysis.

The image analysis system was developed to analyze the morphological differences of *T. reesei* during fed-batch experiment. As explained by Paul and Thomas (1998), filamentous fungi go through a fragmentation step at the beginning of their growth. Prior to this step, microorganisms are found as large and elongated mycelia. Using an x10 objective and the microscopic system previously described, most of the microorganisms did not fit in one frame before the fragmentation phase. For this reason, the analysis was done after the fragmentation step at 40 h. This limitation in the image analysis protocol could be easily overcome by the use of an objective with smaller magnification if initial batch morphological data were required.

The simultaneous measurement of the morphology and the viability showed that unbranched cells always exhibited a lower viability than the other morphological classes (Figure 5.4). This observation supports the hypothesis of Paul et al. (1994) stating that

hyphal fragmentation is not due to shear only but also to degeneration of the mycelia. Old, vacuolated cells are less resistant to shear and tend to break more easily.

Although many morphological parameters are measured by the image analysis protocol, only the area of freely dispersed morphology is presented as an example (Figure 5.5). As the fermentation progressed, the projected area of all morphological types decreased. This observation concurs with the findings of Maazi et al. (2008). A similar trend was observed for the viability. Again, it supports the idea that there is a close relationship between the physiological state and the fragmentation of mycelia. The area of entangled hyphae was found to be higher than the area of branched mycelia. The first morphological class depends mostly on the positioning of the microorganisms on the slide. Longer branches have a higher probability of overlapping on each other. In contrast, unbranched hyphae often correspond to fragments from clumps or branched mycelia and therefore have a smaller area. The other morphological parameters will be useful to characterize the morphological differentiation steps. For instance, it is known that cultures exhibiting a high rate of differentiation from swollen hyphae to arthrospores tend to produce more antibiotics than fermentations adopting the filamentous shape (Bellgardt, 2000).

The morphological and physiological assessment of fungi by image analysis was relatively fast. It took 45 minutes for the operator to capture the 60 sets of pictures. Manual microorganism selection required 5 minutes. Then the image analysis macro ran automatically between 10 and 15 minutes depending on the number of objects being analyzed. Overall, each sample analysis took on an average 60 to 75 minutes.

5.5 CONCLUSIONS

Not only the presented technique is much faster than previously reported image analysis protocols (Tucker et al., 1992, Hassan et al, 2002) but as a major improvement, fungal morphology along with viability is measured. This rapid, accurate and reliable method combining bright field and fluorescence microscopy opens new possibilities to study the relationship between the morphology, the physiological state and the process parameters of *T. reesei*. It could also be easily extended to other filamentous fungi and

used as a tool for a better understanding of the parameters influencing production of protein and other valuable products.

5.6 REFERENCES

Adams, H. L. and Thomas, C. R., The Use of Image Analysis for Morphological Measurements on Filamentous Microorganisms. Biotechnology and Bioengineering, *32*: 707-712, 1988.

Amanullah, A., Blair, R., Nienow, A. W., and Thomas, C. R., Effects of Agitation Intensity on Mycelial Morphology and Protein Production in Chemostat Cultures of Recombinant *Aspergillus oryzae*. Biotechnology and Bioengineering, *62*: 434-446, 1999.

Amanullah, A., Christensen, L. H., Hansen, K., Nienow, A. W., and Thomas, C. R., Dependence of Morphology on Agitation Intensity in Fed-Batch Cultures of *Aspergillus oryzae* and Its Implications for Recombinant Protein Production. Biotechnology and Bioengineering, *77*: 815-826, 2002.

Bellgardt, K.-H. ß-Lactam antibiotics with *Penicillium chrysogenum* and *Acremonium chrysogenum*. *In* K. Schügerl and K.-H. Bellgardt (eds.), Bioreaction Engineering: Modelling and Control, pp. 391-431, Springer, Berlin, 2000.

Breeuwer, P. and Abee, T., Assessment of Viability of Microorganisms Employing Fluorescence Techniques. International Journal of Food Microbiology, *55*: 193-200, 2000.

Drouin, J. F., Louvel, L., Vanhoutte, B., Vivier, H., Pons, M. N., and Germain, P., Quantitative Characterization of Cellular Differentiation of *Streptomyces ambofaciens* In Submerged Culture by Image Analysis. Biotechnology Techniques, *11*: 819-824, 1997.

Hassan, M., Corkidi, G., Galindo, E., Flores, C., and Serrano-Carreón, L., Accurate and Rapid Viability Assessment of *Trichoderma* Harzianum Using Fluorescence-Based Digital Image Analysis. Biotechnology and Bioengineering, *80*: 677-684, 2002.

Hölker, U. and Lenz, J., Solid-State Fermentation - Are There Any Biotechnological Advantages? Current Opinion in Microbiology, *8*: 301-306, 2005.

Ingham, E. R. and Klein, D. A., Relationship Between Fluorescein Diacetate-Stained Hyphae and Oxygen Utilization, Glucose Utilization, and Biomass Growth of Submerged Fungal Batch Cultures. Applied and Environmental Microbiology, *44*: 363-370, 1982.

Jüsten, P., Paul, G. C., Nienow, A. W., and Thomas, C. R., Dependence of Mycelial Morphology on Impeller Type and Agitation Intensity. Biotechnology and Bioengineering, *52*: 672-684, 1996.

Lejeune, R., Nielsen, J., and Garon, G. V., Morphology of *Trichoderma reesei* QM 9414 in Submerged Cultures. Biotechnology and Bioengineering, *47*: 609-615, 1995.

Maazi, A., Pons, M. N., Vivier, H., Latrille, E., Corrieu, G., and Cosson, T. Morphological Characterization of Filamentous Growth. Proceeding of 2nd European Symposium on Biochemical Engineering Science, p. 234, Porto, Portugal, 2008.

Maras, M., van Die, I., Contreras, R., and van den Hondel, C. A., Filamentous Fungi As Production Organisms for Glycoproteins of Bio-Medical Interest. Glycoconjugate Journal, *16*: 99-107, 1999.

McLean, D. D., Abear, K., and Podruzny, M. F., Fed-Batch Production of Cellulases Using *Trichoderma reesei* Rutgers C-30. Canadian Journal of Chemical Engineering, *64*: 588-597, 1985.

Packer, H. L., Keshavarz-Moore, E., and Lilly, M. D., Estimation of Cell Volume and Biomass of *Penicillium chrysogenum* Using Image Analysis. Biotechnology and Bioengineering, *39*: 384-391, 1992.

Packer, H. L. and Thomas, C. R., Morphological Measurement on Filamentous Microorganisms by Fully Automatic Image Analysis. Biotechnology and Bioengineering, *35*: 870-881, 1990.

Paul, G. C., Kent, C. A., and Thomas, C. R., Hyphal Vacuolation and Fragmentation in *Penicillium chrysogenum*. Biotechnology and Bioengineering, *44*: 655-660, 1994.

Paul, G. C., Priede, M. A., and Thomas, C. R., Relationship Between Morphology and Citric Acid Production in Submerged *Aspergillus niger* Fermentations. Biochemical Engineering Journal, *3*: 121-129, 1999.

Paul, G. C. and Thomas, C. R., Characterization of Mycelial Morphology Using Image Analysis. Advances in Biochemical Engineering and Biotechnology, *60*: 1-59, 1998.

Pinto, L. S., Vivier, L. M., Pons, M. N., Fonseca, M. M. R., and Menezes, J. C., Morphology and Viability Analysis of *Streptomyces clavuligerus* in Industrial Cultivation Systems. Bioprocess Biosystem Engineering, *26*: 177-184, 2004.

Riley, G. L., Tucker, K. G., Paul, G. C., and Thomas, C. R., Effect of Biomass Concentration and Mycelial Morphology on Fermentation Broth Rheology. Biotechnology and Bioengineering, *68*: 160-172, 2000.

Schell, D. J., Farmer, J., Hamilton, J., Lyons, B., McMillan, J. D., Saez, J. C., and Tholudur, A., Influence of Operating Conditions and Vessel Size on Oxygen Transfer During Cellulase Production. Applied Biochemistry and Biotechnology, *91-93*: 627-642, 2001.

Schügerl, K., Gerlach, S. R., and Siedenberg, D., Influence of the Process Parameters on the Morphology and Enzyme Production of *Aspergilli*. Advances in Biochemical Engineering and Biotechnology, *60*: 195-266, 1998.

Sebastine, I. M., Stocks, S. M., Cox, P. W., and Thomas, C. R., Charactization of Percentage Viability of *Streptomyces clavuligerus* Using Image Analysis. Biotechnology Techniques, *13*: 419-423, 1999.

Sinha, J., Bae, J. T., Park, J. P., Kim, K. H., Song, C. H., and Yun, J. W., Changes in Morphology of *Paecilomyces japonica* and Their Effect on Broth Rheology During Production of Exo-Biopolymers. Appl. Microbiology & Biotechnology,*56*:88-92, 2001.

Söderström, B. E., Vital Staining of Fungi in Pure Cultures and in Soil With Fluorescein Diacetate. Soil Biology and Biochemistry, *9*: 59-63, 1977.

Steward, A., Vital Fluorochromes As Tracers for Fungal Growth Studies. Biotechnic and Histochemistry, *70*: 57-65, 1995.

Tengerdy, R. P. and Szakacs, G., Bioconversion of Lignocellulose in Solid Substrate Fermentation. Biochemical Engineering Journal, *13*: 169-179, 2003.

Tucker, K. G., Kelly, T., Delgrazia, P., and Thomas, C. R., Fully-Automated Measurement of Mycelial Morphology by Image Analysis. Biotechnology Progress, *8*: 353-359, 1992.

Vanhoutte, B., Pons, N. M., Thomas, C. R., Louvel, L., and Vivier, H., Characterization of *Penicillium chrysogenum* Physiology in Submerged Cultures by Color and Monochrome Image Analysis. Biotechnology and Bioengineering, *48*: 1-11, 1995.

CHAPTER 6

An Image Analysis Technique to Estimate the Cell Density and Biomass Concentration of *Trichoderma reesei*

Véronique Lecault, Nilesh Patel, and Jules Thibault

Department of Chemical and Biological Engineering

University of Ottawa

Ottawa (ON), K1N 6N5, Canada

Abstract

An automated image analysis protocol to estimate the cell volume fraction of filamentous fungi was developed. Using the projected area of lactophenol blue-stained hyphae and assuming a cylindrical shape for the microorganisms, the fraction occupied by the cells in a given volume was measured. Combined with the biomass dry weight obtained by filtration, the method was used to estimate the density of filamentous fungi. A value of 0.334 g dry weigth/cm^3 was found for *Trichoderma reesei* RUT C-30. Knowing the density of fungi, the algorithm was used to quantitatively assess the biomass evolution during the course of fermentation even in the presence of solid particles in the medium.

Keywords: biomass, image analysis, *Trichoderma reesei*, lactophenol blue, cell density, cell volume

6.1 INTRODUCTION

The use of microorganisms for the commercial production of proteins is widespread. The pharmaceutical, agricultural, food, and laundry industries employ filamentous fungi to produce many enzymes necessary to our everyday lives (Papagianni, 2004). For

instance, *Trichoderma reesei* is a microorganism secreting degradative enzymes such as cellulases that catalyze the hydrolysis of cellulosic substrates (Maras et al., 1999). Among other applications, cellulases are employed at industrial scale to transform agricultural wastes into fermentable sugars. To achieve high-yield and cost-effective enzyme production, a better understanding of the relationship that exists between the process parameters, the biomass concentration, the rheological properties of the culture and the protein secretion is necessary.

The biomass concentration is a key parameter that is related to the age, the productivity and the rheological properties of mycelial cultures (Riley et al., 2000). Conventional methods for estimating the biomass are the optical density and the dry weight filtration. In industrial fermentations, complex media such as corn steep liquor and cellulose are often used because of their low cost and high availability. However, these media contain solid particles that are unutilized by the cells, which makes the biomass estimation by conventional techniques difficult and inaccurate (Lynd et al., 2002). Other techniques such as DNA estimation (Lejeune et al., 1995) and capacitance-based probes (Sarra et al., 1996) have been tested as an alternative. Image analysis is also widely employed for determining the concentration of yeast (Bittner et al., 1998) and mammalian cells (Guez et al., 2004). However, few attempts have been made for filamentous microorganisms because their characteristic shape requires complex image analysis algorithms (Packer et al., 1992).

Along with the biomass concentration, the volume occupied by the cells is a useful parameter for the study of filamentous microorganisms. For instance, the rheological properties of filamentous suspension as a function of the cell volume fraction has been studied (Mohseni and Allen, 1995). Both the volume and biomass concentration are proportional and can be related to each other by the density of the cells. A filtration probe was developed to determine the density of *Penicillium chrysogenum* (Nestaas and Wang, 1981). Other techniques such as exclusion and dewatered cake volume have been used to determine the cell volume fraction of *Aspergillus niger* and *Streptomyces levoris* (Mohseni and Allen, 1995). The determination of cell density for filamentous fungi is complicated by the fact that mycelia can have various densities depending on their physiological state. Hyphae go through different steps of differentiation. At an early stage

of growth, cells are active and their membrane is intact. They are at that point classified as healthy cells. As aging occurs, large vacuoles are formed and regions eventually lose their cytoplasm to become degenerated. Therefore, the hyphal density varies with the age of fermentation (Nestaas and Wang, 2006, Oolman and Liu, 1991). An image analysis algorithm has already been developed to estimate the cell volume and biomass of *Penicillium chrysogenum* using greyness levels to differentiate healthy regions from degenerated regions (Packer and Thomas, 1990). The algorithm was successful at estimating cell volume and biomass but the processing was tedious and took as long as 7 h per sample.

Although the cell density has been estimated for various filamentous microorganisms, no attempt has been done for *T. reesei*. In this investigation, we present an image analysis algorithm for estimating the cell density of *T. reesei* based on hyphal staining using lactophenol blue. As shown on Figure 6.1, lactophenol blue was found to stain only healthy regions, leaving degenerated regions uncolored. Assuming a cylindrical shape of the filamentous microorganism, it is possible to estimate the cell volume using the following equation:

$$\text{Cell volume} = (\pi/4) \times (\text{hyphal diameter}) \times (\text{projected area}) \quad (6.1)$$

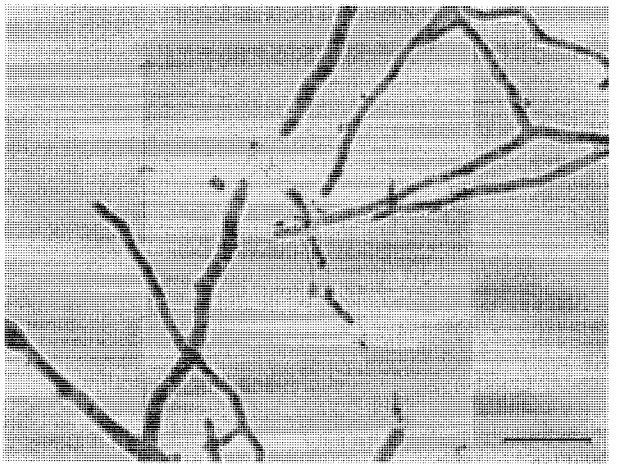

Figure 6.1 – Image of *T. reesei* stained with lactophenol blue. Healthy regions are fully stained while degenerated regions are partially stained. Bar: 20 μm.

The slope of the cell dry weight as a function of the cell volume at different concentrations during a batch experiment can therefore provide an estimate of the hyphal density of healthy cells. The same value can be used in combination with the image

analysis algorithm to estimate the biomass concentration in the presence of solid particles.

6.2 MATERIALS AND METHODS

6.2.1 Fermentation

T. reesei RUT C-30 (ATCC 56765) was supplied by Iogen Corporation, Ottawa and used throughout the experiment. Spores were kept on potato dextrose agar plates at 4°C and new plates were prepared every month. Inoculum was prepared in shake flasks containing 450 mL of culture medium in a 1-L Erlenmeyer flask with three baffles. The culture medium was composed of: glucose, 13 g/L; $(NH_4)_2SO_4$, 1.4 g/L; KH_2PO_4, 2.0 g/L; $MgSO_4 \cdot 7H_2O$, 0.6 g/L; $CaCl_2 \cdot 2H_2O$, 0.3 g/L; $FeSO_4 \cdot 7H_2O$, 5.0 mg/L; $MnSO_4 \cdot 7H_2O$, 1.6 mg/L; $ZnSO_4 \cdot 7H_2O$, 1.4 mg/L; $CoCl_2 \cdot 6H_2O$, 2 mg/L; peptone, 0.75 g/L; yeast extract, 0.25 g/L and urea, 0.3 g/L. The pH was adjusted to 5.5 by the addition of 10N NaOH and the medium was autoclaved for 20 minutes. A spore solution in sterilized water was prepared from the plates and the concentration was determined using a Petroff Hausser counting chamber (Hausser Scientific, Horsham, PA). An appropriate volume was added to the inoculum flask in order to obtain an initial concentration of 5×10^3 spores/mL. Fungi were cultured in an orbital shaker (model 3535CC Incubator shaker, Lab-Line Instrument Inc., Melrose Park, IL) for 62 h at 200 rpm and 28°C.

Laboratory-scale batch experiments were performed by adding 350 mL of the inoculum to a stirred tank bioreactor (Model D-415, New Brunswick Scientific, New Jersey, USA,) containing 7 L of medium. The bioreactor had a total volume of 15 L and a working volume between 3 to 10 L. The agitation was provided by three Rushton impellers at 300 rpm. The temperature was kept at 28°C throughout the experiment. To prevent foam formation and wall growth, 4 mL of antifoam was added daily to the culture. Samples of 30 mL were taken periodically and analyzed by dry weight measurement and image analysis. The batch fermentation was stopped after 68 h.

6.2.2 Dry Weight Measurement by Filtration

Dry weight biomass was quantified by filtering a 25-mL sample of the culture broth through a glass fibre filter (grade A/E, Gelman Sciences, MI) that has been predried and preweighted. The sample was washed with 50 mL of deionized distilled water and dried

for 24 h at 100°C. The biomass cake was cooled in a desiccator for another 24 h and weighed.

6.2.3 Staining

For every time point, a 1-mL sample was taken from the culture broth and homogenized by vortexing. If necessary, the sample was diluted in phosphate-citrate buffer, pH 4.5, to an approximate concentration of 0.1 to 1.0 g/L. One microliter of the homogenized sample was deposited on a glass slide and 4 μL of lactophenol blue were added directly in the droplet containing the fungi. The stained sample was covered by an 18-mm x 18-mm coverslip for analysis. To test the efficacy of the algorithm in the presence of solid particles, a 1 ml sample was centrifuged for 3 minutes at 2000 rpm at every time point. The supernatant was removed and replaced by an equal volume of culture media containing 6.0 g/L of corn steep solids. The sample was homogenized by vortex and stained using the same protocol.

6.2.4 Image Acquisition

The image acquisition was performed with a monochrome CCD camera (CoolSnap ES, Roper Scientific, Tucson, AZ) mounted on an Olympus IX81 microscope (Olympus, Melville, NY) in combination with an automated XY stage (Prior Scientific, Rockland, MA). All three components were controlled by the Image-Pro® Plus software (Image-Pro® Plus version 5.1, Media Cybernetics, Silver Spring, MD). A region of interest covering the entire coverslip area was selected and divided into 588 frames. A bright field image of each frame was grabbed at 10x magnification and saved in a folder for image processing.

6.2.5 Image Analysis

The image analysis was done by a custom macro subroutines written in Visual Basic and ran through the Image-Pro® Plus software. Images were first transformed from a TIFF format to an 8-bit grey scale format (Figure 6.2a) and segmented into a binary mask. Pixels below the threshold value were set to black (0) whereas pixels above were set to white (255) (Figure 6.2b). The threshold value was determined by minimizing the sum of the variance of the background and fungi distributions. A one-pass dilation using an 11 x 11 octagonal filtering kernel was performed to connect partially stained areas (Figure 6.2c). This stage was necessary to avoid eliminating small stained area when

applying subsequent size and roundness filters. Microorganisms that were cut by the edge of a frame were generally smaller and more circular than entire filamentous fungi. Therefore, cells touching the borders were separated from cells inside the frame and processed using two different algorithms. A mask of all objects located entirely inside the borders was created (Figure 6.2d). Regions that were bigger than 1000 μm^2 and had roundness higher than 2.5 were selected and transposed on a new image (Figure 6.2e). The roundness was calculated by the following equation:

$$\frac{\text{Perimeter}^2}{4\,\pi \times \text{Projected area}} \qquad (6.2)$$

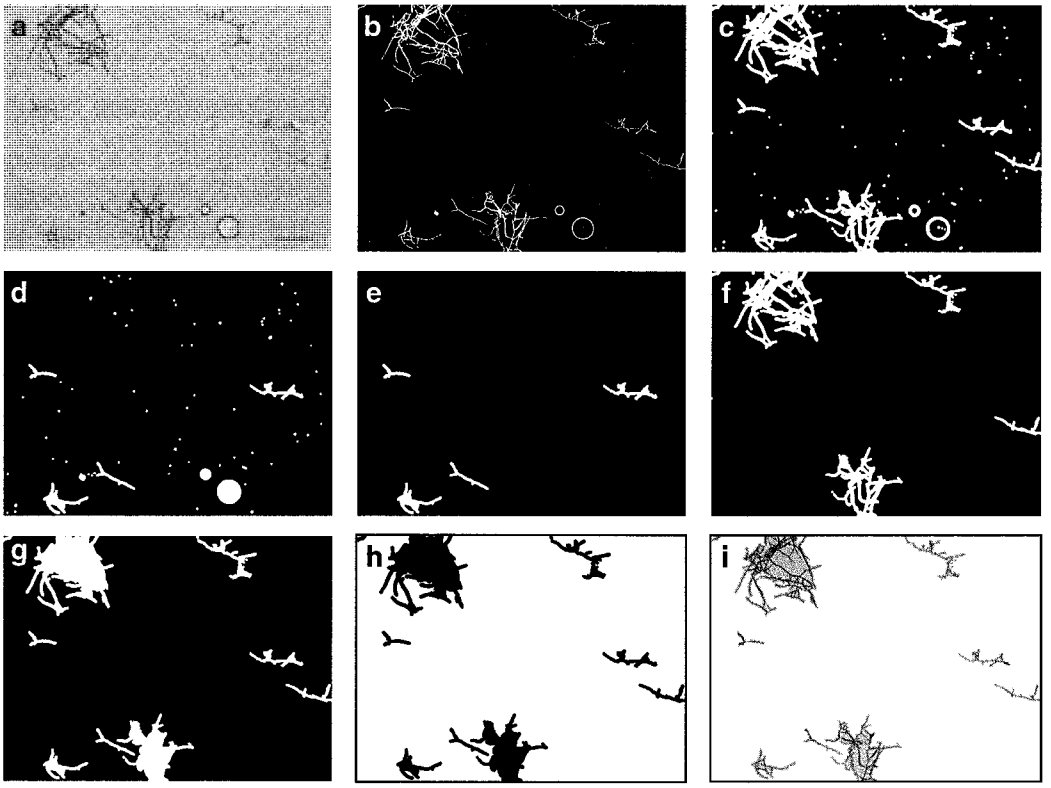

Figure 6.2 – Image analysis steps of the algorithm to determine the area of filamentous fungi stained with lactophenol blue. The image is (a) transformed to an 8-bit grey scale format, (b) segmented to a binary mask and (c) dilated. Objects inside the frame are (d) selected and (e) filtered for roundness and area. A mask containing objects touching the frame is (f) created, filtered and (g) added to the mask of microorganism inside the frame. The image is (h) inverted and (i) added to the initial picture where the projected area of the stained regions is measured. Bar: 100 μm.

Using this expression, a circular object would have a roundness of 1 whereas a less circular object would have a value greater than 1. The previous mask was subtracted from the binary image to create an image containing only objects that were partially cut by the edge of the frame (Figure 6.2f). Objects with an area bigger than 500 μm^2 and roundness greater than 1.4 were selected. Height and width limits of the size of the frame (1030 and 1380 μm, respectively) were also applied to remove the dark shadow produced by the edge of the coverslip. The mask of filtered objects touching the frame was added to the filtered objects inside the frame (Figure 6.2g). To take into account the fact that clumps of filamentous fungi occupying the entire frame could be removed by the height and width filters, eliminated objects were selected by subtracting the filtered objects touching the frame to the border mask. Only objects having a hole ratio greater than 0.9 were kept and added to the other filtered objects. The hole ratio was defined as the ratio of object area excluding holes to the total area of the object. The image containing all final objects was inverted to obtain dark objects on a white background (Figure 6.2h). Since dilated objects were much larger than the actual microorganisms, the mask was added to the initial 8-bit grey scale image, thereby hiding all particles that were not microorganisms. The high contrast of lactophenol blue compared to the background enabled the selection of stained fungi. To further improve the algorithm and eliminate remaining artefacts, the average optical intensity was limited to pixel values ranging from 70 to 150 (Figure 6.2i). Most background artefacts had higher values whereas solid particles contained in the media appeared to be darker. The total area of the stained fungi for each picture was sent to an Excel spreadsheet. To calculate cell volume, the diameter was estimated by taking the average of 50 measurements of the hyphal width in randomly selected pictures from each sample.

6.3 RESULTS AND DISCUSSION

6.3.1 Determination of Cell Density

The cell density of *T. reesei* was determined by comparing the cell volume obtained from image analysis to the biomass concentration determined by dry weight filtration at different cell concentrations. Figure 6.3 shows the correlation between the biomass

concentration measured by filtration and the cell volume obtained from image analysis. The best fit curve to the data gave a healthy fungus density of 0.334 g dry weight/cm^3.

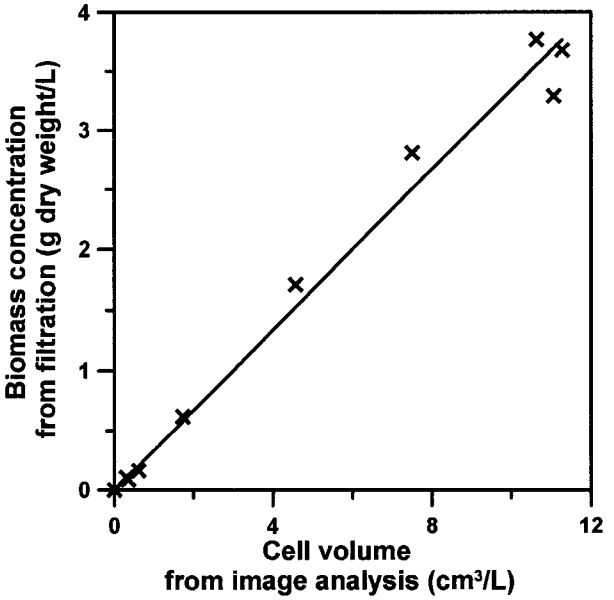

Figure 6.3 – Relationship between the dry weight biomass concentration of *T. reesei* and the cell volume estimate from image analysis. A cell density of 0.334 g dry weigth/cm^3 is found from the best fit curve.

This value compares to cell densities that were found for other filamentous fungi. The density of *Penicillium crysogenum* determined by a filter cake assay was found to be of 0.35 g dry weight/cm^3 (Nestaas and Wang, 1981) at early stages of the fermentation. Similarly, cell densities ranging from 0.32 to 0.45 g dry weight/cm^3 were measured for organisms such as *Streptomyces griseus*, *Steptomyces tendae* and *Penicillium crysogenum* (Oolman and Liu, 1991) at the beginning of the fermentation. Although the overall cell density decreases as the age of the fermentation increases, the healthy cell density can be used throughout the fermentation with the image analysis algorithm since lactophenol blue does not stain degenerated regions.

6.3.2 Biomass Quantification

To verify the efficacy of the method as a tool to estimate the biomass concentration, image analysis measurements were performed during a batch fermentation and compared to the values obtained from dry weight filtration. Figure 6.4 shows the growth curve of *T. reesei* in a stirred tank bioreactor. The image analysis algorithm combined with lactophenol blue staining gave a good estimate of the actual biomass concentration. Five

replicates were analyzed at 45.25 h for both the image analysis and filtration methods. Biomass concentrations of 2.3 ± 0.4 and 2.85 ± 0.03 g dry weight/L (mean ± standard deviation) were obtained respectively. A t-test showed that there was no significant difference between the values at 98% confidence level. The proposed image analysis technique is not as precise as the conventional dry weight filtration but it has the advantage of being suitable for fermentations containing particles such as corn steep solids. As part of complex medium, the amount of solid particles bigger than the pore sizes of the filter changes throughout a fermentation and interferes with the measure from dry weight filtration. To verify the robustness of the image analysis technique, samples were also analyzed after centrifugation and replacement of the supernatant (defined media) by corn steep solids containing media. The image analysis algorithm eliminated efficiently corn steep solids from the volume calculation. Corn steep solids tend to adhere to the cells which make it difficult to separate particles from the cells and obtain an accurate biomass concentration using conventional technique. The image analysis method offers the advantage of diluting the sample thereby minimizing interactions with cells and solid particles. For most samples, lower concentrations were obtained in the presence of solid particles. This observation can be explained by the loss of microorganisms during the supernatant removal. However, this step was performed to compare the results with the dry weight by filtration and would not be required to analyze the biomass in a fermentation containing corn steep solids.

The proposed image analysis technique has the advantage of being rapid compared to the conventional dry weight filtration which requires at least 24 h of dehydration. The image acquisition for each sample was done in 45 minutes and the image analysis took less than 15 minutes. The accuracy of the technique has limitations depending on the biomass concentration. The estimate is based on the hypothesis that the sample is homogeneous. It was demonstrated that the lactophenol blue staining protocol with the image analysis algorithm was suitable for batch fermentations but the data tend to become less accurate and more variable at higher concentrations. In the case of filamentous fungi fed-batch fermentation, clumps form as the biomass concentration increases and samples become less homogeneous (Tucker et al., 1992). Intensive mixing would be required to use the image analysis technique in this case. Nevertheless, the

proposed technique offers an alternative method to estimate the biomass concentration that is especially useful when complex medium with solid particles is employed.

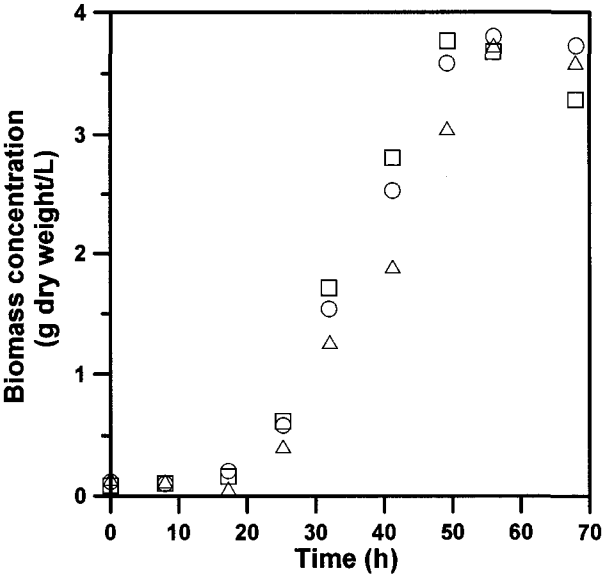

Figure 6.4 – Batch growth curve of *T. reesei* in a stirred tank bioreactor. Biomass concentrations measured by dry weight filtration (□), image analysis in the absence of solid particles (○), and image analysis in the presence of corn steep solids (Δ) are shown.

6.4 CONCLUSIONS

An image analysis algorithm based on lactophenol blue staining was used to estimate the hyphal density of *T. reesei*. Knowing this value for healthy filamentous fungi, the method is successful in estimating the biomass concentration during the course of batch fermentation. This rapid tool is especially powerful for fermentations with complex medium because it has the advantage of excluding solid particles from the measurement. Moreover, the method could easily be extended and combined with existing morphological algorithms (Lecault et al., 2007, Packer and Thomas, 1990) to study relationship between the biomass concentration and the morphology of filamentous fungi during the course of fermentation.

6.5 REFERENCES

Bittner, C., Wehnert, G., and Scheper, T., In Situ Microscopy for on-Line Determination of Biomass. Biotechnology and Bioengineering, *60*: 24-35, 1998.

Guez, J. S., Cassar, J. P., Wartelle, F., Dhulster, P., and Suhr, H., Real Time in Situ Microscopy for Animal Cell-Concentration Monitoring During High Density Culture in Bioreactor. Journal of Biotechnology, *111*: 335-343, 2004.

Lecault, V., Patel, N., and Thibault, J., Morphological Characterization and Viability Assessment of *Trichoderma reesei* by Image Analysis. Biotechnology Progress, *23*: 734-740, 2007.

Lejeune, R., Nielsen, J., and Garon, G. V., Morphology of *Trichoderma reesei* QM 9414 in Submerged Cultures. Biotechnology and Bioengineering, *47*: 609-615, 1995.

Lynd, L. R., Weimer, P. J., and van Zyl, W. H., Microbial Cellulose Utilization: Fundamentals and Biotechnology. Microbiology and Molecular Biology Reviews, *66*: 506-577, 2002.

Maras, M., van Die, I., Contreras, R., and van den Hondel, C. A., Filamentous Fungi As Production Organisms for Glycoproteins of Bio-Medical Interest. Glycoconjugate Journal, *16*: 99-107, 1999.

Mohseni, M. and Allen, D. G., The Effect of Particle Morphology and Concentration on the Directly Measured Yield Stress in Filamentous Suspensions. Biotechnology and Bioengineering, *48*: 257-265, 1995.

Nestaas, E. and Wang, D. I. C., A New Sensor, the Filtration Probe, for Quantitative Characterization of the Penicillin Fermentation. Biotechnology and Bioengineering, *23*: 2803-2813, 1981.

Nestaas, E. and Wang, D. I. C., Computer Control of the Penicillin Fermentation Using the Filtration Probe in Conjunction With a Structured Process Model. Biotechnology and Bioengineering, *95*: 317-326, 2006.

Oolman, T. and Liu, T. C., Filteration Properties of Mycelial Microbial Broths. Biotechnology Progress, *7*: 534-539, 1991.

Packer, H. L., Keshavarz-Moore, E., and Lilly, M. D., Estimation of Cell Volume and Biomass of *Penicillium chrysogenum* Using Image Analysis. Biotechnology and Bioengineering, *39*: 384-391, 1992.

Packer, H. L. and Thomas, C. R., Morphological Measurement on Filamentous Microorganisms by Fully Automatic Image Analysis. Biotechnology and Bioengineering, *35*: 870-881, 1990.

Papagianni, M., Fungal Morphology and Metabolite Production in Submerged Mycelial Process. Biotechnology Advances, *22*: 189-259, 2004.

Riley, G. L., Tucker, K. G., Paul, G. C., and Thomas, C. R., Effect of Biomass Concentration and Mycelial Morphology on Fermentation Broth Rheology. Biotechnology and Bioengineering, *68*: 160-172, 2000.

Sarra, M., Ison, A. P., and Lilly, M. D., The Relationships Between Biomass Concentration, Determined by a Capacitance-Based Probe, Rheology and Morphology of *Saccharopolyspora erythraea* Cultures. Journal of Biotechnology, *51*: 157-165, 1996.

Tucker, K. G., Kelly, T., Delgrazia, P., and Thomas, C. R., Fully-Automated Measurement of Mycelial Morphology by Image Analysis. Biotechnology Progress, *8*: 353-359, 1992.

CHAPTER 7

Estimation of Biomass Concentration of *Trichoderma reesei* RUT C-30 in Insoluble Medium Through DNA Quantification

Raseeka Rahumathulla, Nilesh Patel, and Jules Thibault

Department of Chemical and Biological Engineering

University of Ottawa

Ottawa (ON), K1N 6N5, Canada

Abstract

Trichoderma reesei is a fungus widely used for cellulase production. Estimating growth rate for such fungal species in submerged culture fermentations in the presence of solid particles is important for better monitoring and understanding of the process. A method for estimating the biomass concentration in presence of insoluble medium during the fermentation (solka floc cellulose and corn steep solids, respectively) based on DNA quantification is described. Interference from both types of suspended solids (corn steep and solka floc cellulose) is negligible for samples which undergo the full extraction procedure due to the removal of most interfering components during acid extraction. In soluble medium, the measured DNA content (mg) per g biomass was found to be 26.1 ± 1.4. Results show that this method is suitable to estimate the fermentation parameter of biomass concentration in the presence of corn steep solids and solka floc cellulose in the biomass concentration ranges usually encountered in *T. reesei* fermentations. Further improvements such as larger sampling volumes in the lower biomass concentration range (less than 5.0 g/L) would allow for improved accuracy and application of this method across the range of biomass concentrations typical to the cellulase production industry.

Keywords: Biomass, Colorimetric, DNA, *Trichoderma reesei*.

7.1 INTRODUCTION

A cost-effective medium for production of cellulase is required for any large-scale conversion of waste cellulosic material into simple sugars (Ghose and Sahai, 1979). Such affordable mediums (i.e. corn steep solids) are often by-products of industrial processes and are composed of solid particles. Production of fungal cellulases, particularly from *Trichoderma reesei*, has held significant research interest in recent years due to the growing promise of cellulosic-derived fuels. Solid substrates are often used in submerged fermentation processes such as for cellulase production. However, a common problem in the analysis and control of these fermentation processes is the inability to determine biomass concentration due to the intertwining of the biomass and solid substrate during cultivation (Shuler and Kargi, 1992). Determination of the growth rate from biomass concentration is fundamental to the understanding of fermentation processes (Agar, 1985). Estimates for the biomass concentration are required for calculating the specific productivity, applying control strategies based on substrate consumption, analyzing and diagnosing the state of fermentation, developing models and making decisions during the culture cycle (Kennedy et al., 1992).

Several enhanced cellulase-producing mutants of *T. reesei* have been used for cellulase production using corn steep liquor and microcrystalline cellulose as substrates (Farid and El-Shahed, 1993). This practice has promoted interest in the ability to estimate biomass concentration in the presence of such solid substrates. Various compounds have been studied in order to indirectly quantify fungal biomass in solid cultures, including glucosamine, nucleic acids, ergosterol and gas phase CO_2 and O_2. However compared to the abundance of techniques devised to measure biomass concentration in soluble mediums, there are limited publications on estimating biomass concentration in the presence of solid particles (Kennedy et al., 1992).

The inference of biomass concentration from DNA quantification is a promising choice due to minor interference by medium substrates (May et al., 2006) and supporting evidence that the amount of DNA in any given organism is amazingly constant and does not alter due to environmental circumstances or by changes in the nutrition or metabolism of the cell (Lehninger, 1975). Further, DNA content in *Trichoderma* strain is also reported to be constant during the course of fermentation (Ghose and Sahai, 1979, Pitt

and Bull, 1982). In choosing a method to quantify the DNA content of a microorganism, the factors to consider include the effectiveness of DNA extraction, sensitivity of the DNA assay, discrimination between RNA and DNA, and the required time and cost for the analysis. The lack of current literature on *T. reesei* RUT C-30 DNA extraction and quantification illustrates the need for the further development of such methods.

Filamentous fungi have an exceptionally strong cell wall which impedes cell lysis and the recovery of DNA using conventional extraction methods. In the past, various lysis methods have been employed including chemical (Solomon et al., 1983), enzymatic and mechanical breakage (Nandakumar and Marten, 2002). The methods applied to filamentous fungi, such as *T. reesei*, are often laborious and time consuming (Cassago et al., 2002). Fungal nucleases, polysaccharides and pigments provide further difficulties in isolating DNA from filamentous fungi (Muller et al., 1998).

Therefore, the objective of this paper is to determine whether monitoring DNA concentration throughout the fermentation is a suitable method for estimating biomass concentration during the *T. reesei* fermentation. Details involved with extraction and quantification of DNA, and choosing sample volumes are presented while ensuring viable sample volumes and handling methods used in industry. Finally, the biomass concentration is estimated in the presence of suspended solids such as corn steep solids and solka floc cellulose, common substrates in the cellulase production industry.

7.2 MATERIALS AND METHODS

7.2.1 Cultivation of fungi

Glycerol stock solutions of *T. reesei* RUT C-30 spores (ATCC 56765) were supplied by Iogen Corporation, Ottawa. Shake flask culture medium contained: lactose, 13 g/l; $(NH_4)_2SO_4$, 1.4 g/l; KH_2PO_4, 2.0 g/l; $MgSO_4 \cdot 7H_2O$, 0.3 g/l; $CaCl_2 \cdot 2H_2O$, 0.3 g/l; $FeSO_4 \cdot 7H_2O$, 5.0 mg/l; $MnSO_4 \cdot 7H_2O$, 1.6 mg/l; $ZnSO_4 \cdot 7H_2O$, 1.4 mg/l; $CoCl_2 \cdot 6H_2O$, 2 mg/l, protease peptone, 2 g/l and yeast extract, 0.5 g/l. The pH of the medium was initially adjusted to 5.5 using 10N NaOH. Shake flask cultures were performed with a volume of 500 ml in a 1-l baffled Erlenmeyer flask. Flasks were kept in an orbital shaker at 200 rpm and 28°C for 55 h. The stainless steel stirred-tank bioreactor with a working volume of 17 l is sterilized and inoculated with shake flask culture medium.

Fermentation medium was similar to the shake flask medium with 50 g/l lactose and double the nutrient concentration. A one-sided pH control was performed by the addition of NH_4OH (15% v/v) to prevent the pH from dropping below 4.5. The pH was measured on-line by a pH FermProbe (Broadley-James Corporation, Irvine, CA) whereas the dissolved oxygen (DO) was continuously monitored by a DO Sensor (Broadley-James Corporation, Irvine, CA). The DO was kept about the critical DO limit of 20% by manipulating the agitation.

7.2.2 Biomass quantification

The biomass concentration in fermentation samples without solid substrate was quantified by dry weight analysis. Dry weights were determined by vacuum filtration of 10 ml fermentation samples through dried GF/A filter paper (Whatman) of known weight. The filter paper was then washed with 20 ml deionized distilled water under vacuum filtration. Filter paper samples were dried at 95°C for 24 h and then allowed to cool at room temperature without exposure to moisture. The filter paper with sample was measured and the biomass dry weight was determined representing the dry weight of biomass in 10 ml of fermentation broth. All samples were analyzed in triplicates.

7.2.3 Acid Extraction of DNA

Chemicals: 0.5 M $HClO_4$ and 0.25 M $HClO_4$ solutions were prepared from a 70% (w/w) perchloric acid (Sigma-Aldrich).

Procedure: An appropriate volume of culture sample was placed in a 50-ml centrifuge tube. The sample was then centrifuged for 15 min at 14 000 rpm, and 4°C (VS-550, Vision Scientific Co., Korea). The supernatant was disposed and the pellet is resuspended in 6 ml ice-cold 0.25 M $HClO_4$ (Sigma-Aldrich). The centrifuge tube was then placed in an ice-bath for 30 min with periodic shaking every 10 min. The sample was centrifuged again for 15 min at 14 000 rpm and 4°C. The supernatant was again disposed. The remaining pellet was resuspended in 4 ml 0.5 M $HClO_4$. The centrifuge tube was then placed in a water bath at 70°C for 20 min with periodic shaking every 10 min. Samples were centrifuged for 20 min at 14000 rpm and 22°C. The supernatant was then collected in a separate tube (Supernatant 1), and the pellet is resuspended in 3 ml 0.5 M $HClO_4$. The centrifuge tube was then placed in 70°C water bath for 20 min with periodic shaking every 10 min. Samples were centrifuged again for 20 min at 14000 rpm and 22°C.

Supernatant collected from this tube was then added to Supernatant 1. The Herbert method (Herbert et al., 1971) has been modified so that the supernatant was collected in two extractions as opposed to three extractions recommended in the original method.

7.2.4 Colorimetric Quantification of DNA

Chemicals: Diphenylamine reagent was prepared by dissolving 1.5 g of reagent-grade diphenylamine (Sigma-Aldrich) in 100 ml of glacial acetic acid and adding 1.5 ml concentrated H_2SO_4. Prior to use, 0.1 ml of aqueous acetaldehyde (16 mg/ml) was added to 20 ml of diphenylamine reagent as required.

Standard DNA solutions: Highly polymerized calf-thymus DNA preparation was used (Sigma-Aldrich). A stock solution of 0.4 mg DNA/ml was prepared by dissolving calf thymus DNA in 5 mM NaOH over a period of 48 h and then stored at 4°C. From this solution, working standards were prepared by mixing the stock standard with an equal volume of 1 M $HClO_4$ and heating at 70°C for 15 min.

Generating standard curve: Dilutions of calf-thymus DNA working standard were used to generate a DNA standard curve. A standard curve was determined between 3 and 100 μg DNA/ml from the 200 μg DNA/ml working stock solution. Tubes containing 2 ml of known amounts of DNA standard and a blank containing only 0.5 M $HClO_4$ were prepared. A 2 ml of diphenylamine reagent was added to each tube. Tubes were kept in a dark incubator for 17 h at 30°C. The standard curve was generated by measuring the absorbance of each tube at 600 nm against the blank.

Procedure: The total supernatant collected in the acid extraction method was used to prepare solutions (dilutions) such that DNA extracted was within the calibration range. A 2 ml freshly-prepared diphenylamine reagent was added to each 2 ml aliquot. The tubes were then covered with parafilm, mixed by inversion and placed in a dark incubator set at 30°C for 17 h. Absorbance of these samples at 600 nm was measured with a spectrophotometer (Perkin Elmer Lambda 25) with 1.0 cm polystyrene cells.

7.2.5 Sample Preparation

In order to ensure the amount of DNA extracted per sample was within the linear range of the assay, an adequate sampling volume must be pre-determined. Based on experiments in soluble medium where the biomass concentration was found by dry weight analysis, the sample volume used for DNA analysis were determined. The

samples collected from the fermentation were separated into three aliquots. The first aliquot represented the soluble medium. Corn steep solids (Sigma-Aldrich) and solka floc cellulose (Grade 1016, International Fiber Corp., USA) were added to the second and third aliquot to obtain a final concentrations of 6 g/l and 10 g/l respectively to represent the maximum substrate concentrations encountered in the industry.

7.3 RESULTS AND DISCUSSION

It has been found that RNA and protein levels, unlike DNA, tend to vary throughout the fermentation process and can be dependent on nutrient supply (Pitt and Bull, 1982; Mohagheghi et al., 1988). Thus, DNA appears to be the most appropriate component of biomass to be used in estimating biomass concentration. Several protocols have been proposed for the extraction of DNA from fungal tissues, such as SDS-based, CTAB-based, glass bead beating and various commercial DNA extraction kits. Although the first two methods are time-consuming, the others require the purchase of specialized instrumentation or have a high cost per sample (Guerrero et al., 2005). Thus, in the present study, a simple and cost effective technique based on a modified extraction method of Herbert (Herbert et al., 1971) coupled with the colorimetric method of Burton (Burton, 1956) is used to extract and quantify DNA during *T. reesei* fermentation.

A soluble medium was chosen to allow for the determination of biomass concentration during *T. reesei* fermentation by dry-weight analysis. Samples collected approximately every 4 h during the batch process of *T. reesei* fermentation were analyzed for biomass concentration using dry-weight analysis and also for the DNA content using the extraction and quantification technique described earlier. The calf thymus standard curve was used to estimate DNA concentration of fermentation samples based on their absorbance values at 600 nm. A linear correlation between the DNA content and the biomass concentration estimated by dry-weight was obtained as shown in Figure 7.1. These results support the notion that the DNA content of *T. reesei* remains constant throughout the fermentation process and can be used as a good indication of biomass concentration.

Although the standard curves in the presence of corn steep solids and solka floc cellulose require small correction factors based on the background noise of solid

particles, this interference effect was not included due to the disposal of the supernatant during the extraction procedure. Preliminary tests after the disposal of the supernatant indicate that the maximum absorbance error due to the presence of solids is ± 0.044 A600 units and ± 0.039 A600 units for corn steep and solka floc cellulose, respectively. This interference does not have a significant effect in the resulting biomass concentration estimate. Thus in this study, the standard curve was created without taking into account the interference due to solid particles.

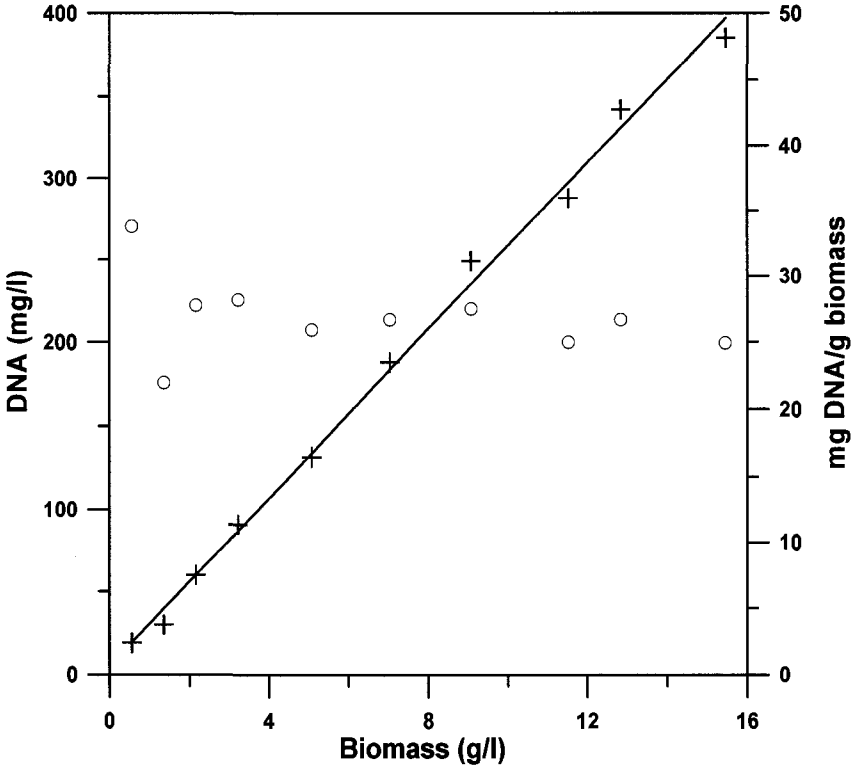

Figure 7.1 – Amount of DNA (+) extracted and mg DNA/g biomass (○) obtained for different biomass concentration in a stirred tank bioreactor.

It is evident from Figure 7.1 that above biomass concentrations of 5 g/l in soluble medium, the measured DNA content (mg) per g biomass was fairly consistent with a deviation of less than ± 1.4 (approximately 5%) from the mean value of 26.1 mg DNA/g biomass. Similarly in the presence of corn steep solids, the measured DNA content (mg) per g biomass was 25.6 mg DNA/g biomass. However, at lower biomass concentration in the presence of solka floc cellulose particles due to the sample handling difficulties and small sampling volume described later, only biomass concentrations above 7 g/l showed fairly consistent results with a deviation of less than ± 0.5 from the mean value of 25.4

mg DNA/g biomass. For another strain of *T. reesei*, Ghose and Sahai (1979) obtained a mean value of 20.3 mg DNA/g biomass during the cultivation of *T. reesei* QM 9414 at different dilution rates in a continuous culture.

The linear correlation determined from Figure 7.1 was then used to estimate the biomass concentration of samples with insoluble particles as shown in Figure 7.2 based on the measured DNA concentrations. Compared to the dry-weight estimates conducted with soluble medium, it is evident that the modified Herbert method yields fairly comparative estimates of biomass concentration throughout the fermentation in both soluble medium and in the presence of corn steep solids. However, in the presence of solka floc cellulose particles, there is a higher error in the estimation of biomass concentration below 7 g/l. After further testing and also taking into consideration the background absorbance of solka floc cellulose particles, this error appears to be connected with difficulties in handling (pipetting) the non-homogeneous cellulose.

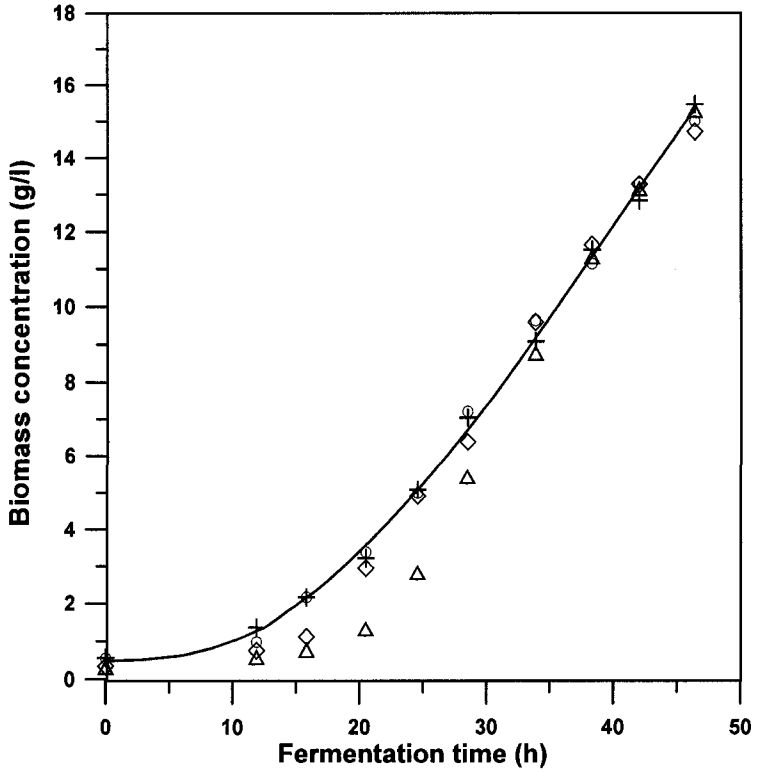

Figure 7.2 – Profile of dry weight (+) of fermentation samples and estimated biomass concentration of samples with no solid medium (○), with corn steep solids (◊) and with solka floc (Δ) using DNA measurements of the fermentation samples.

In addition to sample handling difficulties, another contributing factor in the error found at lower biomass concentrations was the sample volumes chosen in this range. In order to achieve results within the linear range of the diphenylamine assay, a minimum amount of biomass (about 8 mg) is required. In the case of earlier fermentation samples which have low biomass concentrations, the sample volumes chosen were in the lower region of the assay's linear range thus leading to inaccuracy. Although these sample volumes were chosen in the lower end of the calibration range in order to represent industrially-viable sample sizes, it is recommended that in the future larger sample volumes should be chosen to ensure sufficient biomass is present and that DNA extraction will be consistent across the whole range of biomass concentrations.

One of the advantages of this procedure is that several samples can be simultaneously processed. There has been support that the diphenylamine method measures the active biomass present in the reactor due to evidence that the decline in the measured DNA coincides with the start in the drop in CO_2 evolution rate (Lejeune and Baron, 1995). The concept of using DNA to estimate biomass concentration appears to be effective even in the presence of nutrient-limiting mediums as shown by Pitt and Bull (1982), who found that in contrast to RNA and protein, the DNA concentration of glucose-limited mycelia was comparatively stable over various dilution rates in fermentation.

Overall, the combination of the modified acid extraction procedure of Herbert and the colorimetric method of Burton shows reliable estimation of the biomass concentration above a critical biomass concentration of 5 g/l. Thus, biomass concentration can be effectively monitored when using cost-effective industrial mediums with solid particles since the biomass concentration is usually higher during the production phase. However the method could be further improved in lower biomass concentration range by including the background noise due to the insoluble substrate and also sampling larger volume.

Further modifications can be applied to this method which includes greatly decreasing the time required by incubating the samples in a dark incubator at 50°C for 3 h as opposed to 30°C for 17 h (Gendimenico et al., 1988). Although for this modification the sensitivity limit is partly sacrificed (3 μg as opposed to 1 μg detection limit), the significant savings in time may be beneficial for some applications that do not require increased sensitivity.

7.4 CONCLUSIONS

DNA appears to be superior to other intracellular components such as proteins, nitrogen, lipids or RNA when estimating biomass concentration due to the consistent DNA content of an organism despite varying nutrition and environmental factors. This work has shown that the modified method of Herbert (Herbert et al., 1971) for DNA extraction coupled with the Burton method (Burton, 1956) for DNA quantification is simple and effective in estimating biomass concentration in fermentations samples with or without insoluble particles such as corn steep and cellulose (solka floc). Sample volume size is a critical factor to ensure that the measured DNA amount lies within the linear range of the assay. Assuming an appropriate sample volume size is selected, this approach appears suitable over the range of industrially-relevant biomass concentrations common to *T. reesei* RUT C-30 fermentations. Further improvements to this procedure were also recommended.

7.5 REFERENCES

Agar, D. W., Microbial Growth Rate Measurement Techniques. Comprehensive Biotechnology, *4*: 305-327, 1985.

Burton, K., A Study of the Conditions and Mechanism of the Diphenylamine Reaction for the Colorimetric Estimation of Deoxyribonucleic Acid. Biochemical Journal, *62*: 315-323, 1955.

Cassago, A., Panepucci, R. A., Baião, A. M. T., and Henrique-Silva, F., Cellophane Based Mini-Prep Method for DNA Extraction From the Filamentous *Trichoderma reesei* . BMC Microbiology, *2*: 1-4, 2002.

Farid, M. A. and El-Shahed, K. Y., Cellulase Production on High Levels of Cellulose and Corn Steep Liquor. Zentralblatt für Mikrobiologie, *4*: 277-283, 1993.

Gendimenico, G. J., Bouquin, P. L., and Tramposch, K. M., Diphenylamine-Colorimetric Method for DNA Assay: A Shortened Procedure by Incubating Samples at 50°C. Analytical Biochemistry, *173*: 45, 1988.

Ghose, T. K. and Sahai, V., Production of Cellulase by *Trichoderma reesei* QM 9414 in Fed-Batch and Continuous-Flow Culture With Cell Recycle. Biotechnology and Bioengineering, *21*: 283-296, 1979.

Guerrero, R. T., Goes-Netoi, A., and Loguercio-Leitea, C., DNA Extraction From Frozen Field Collected and Dehydrated Herbarium Fungal Basidiomata: Performance of SDS and CTAB-Based Methods. Biotemas, *18*: 19-32, 2005.

Herbert, D., Phipps, P. J., and Strange, R. E., Chemical Analysis of Microbial Cells. Methods in Microbiology, *5*: 209-344, 1971.

Kennedy, M. J., Thakur, M. S., and Wang, D. I. C., Techniques for the Estimation of Cell Concentration in the Presence of Suspended Solids. Biotechnology Progress, *8*: 375-381, 1992.

Lehninger, A. L. Biochemistry: The Molecular Basis of Cell Structure And Function. Worth Publishers, New York, 1975.

Lejeune, R. and Baron, G. V., Effect of Agitation on Growth and Enzyme Production of *Trichoderma reesei* in Batch Fermentation. Applied Microbiology and Biotechnology, *43*: 249-258, 1995.

May, B. A., VanderGheynst, J. S., and Bumsey, T., The Kinetics of *Lagenidium giganteum* Growth in Liquid and Solid Cultures. Journal of Applied Microbiology, *101*: 807-814, 2006.

Mohagheghi, A., Grohmann, K., and Wyman, C. E., Production of Cellulase on Mixtures of Xylose and Cellulose. Applied Biochemical and Biotechnology, *17*: 263-277, 1988.

Muller, F. M. C., Werner, K. E., Kasai, M., Francesconi, A., Chanock, S. J., and Walsh, T. J., Rapid Extraction of Genomic DNA From Medically Important Yeasts and Filamentous Fungi by High-Speed Cell Disruption. Journal of Clinical Microbiology, *36*: 1625-1629, 1998.

Nandakumar, M. P. and Marten, M. R., Comparison of Lysis Methods and Preparation Protocols for One- and Two-Dimensional Electrophoresis of *Aspergillus oryzae* Intracellular Proteins. Electrophoresis, *23*: 2216, 2002.

Pitt, D. E. and Bull, A. T., Influence of Culture Conditions on the Physiology and Compositon of *Trichoderma aureoviride*. Journal of General Microbiology, *128*: 1517-1527, 1982.

Shuler, M. L. and Kargi, F. Bioprocess Engineering Basic Principles. Prentice Hall PTR, New Jersey, 1992.

Solomon, B. O., Erickson, L. E., and Yang, S. S., Estimation of Biomass Concentration in the Presence of Solids for the Purpose of Parameter Estimation. Biotechnology and Bioengineering, *25*: 2469-2477, 1983.

SECTION - III

Trichoderma reesei RUT C-30 FERMENTATION

CHAPTER 8

Growth of *Trichoderma reesei* RUT C-30 in a Stirred Tank and Reciprocating Plate Bioreactor

Nilesh Patel, Viviane Choy, Philippe Malouf, and Jules Thibault*

Department of Chemical and Biological Engineering

University of Ottawa

Ottawa (ON), K1N 6N5, Canada

Abstract

The objective of the present study was to understand the close relationship that exists between the shear field within a bioreactor, the morphology of the microorganism, the rheology of fermentation broth, and the process performance. To achieve this objective, a series of fed-batch fermentation runs at different agitation speeds were performed using the industrially important strain *Trichoderma reesei* RUT C-30 in two different bioreactors. The two bioreactors, stirred tank bioreactor (STB) and reciprocating plate bioreactor (RPB) are characterized by significantly different shear field to which microorganims are exposed. Highest biomass concentration (ca. 15 g/L) was obtained at higher agitation rates in both bioreactors due to better oxygen supply. However, better filter paper activities per mg of protein were obtained at lower agitation in both bioreactors. Foaming problems were severe in experiments performed in the STB, especially at lower agitation. On the other hand for the runs in the RPB, biomass accumulation on the top plate of the mixing system caused operational difficulties at lower agitation. In both bioreactors, newer and healthier fungi in the batch phase were not affected even at higher agitation rates. However, during the fed-batch phase, higher degree of fragmentation at high agitation intensity was confirmed by image analysis.

Also, the rheological analysis showed an increase in apparent viscosity during the batch phase and early fed-batch phase. During the late stages of fermentation, the apparent viscosity decreased due to cell lysis and spore formation.

Keywords: cellulase, fed-batch, image analysis, rheology, *Trichoderma*

8.1 INTRODUCTION

The global energy demand is rising rapidly due to population growth, increased standards of living, and rapid industrial development of emerging countries. It has become crystal clear that the world's reliance on rapidly depleting reserves of fossil fuels is unsustainable. Among the various alternatives that can make a difference right away, bioethanol appears to be the most promising. Bioethanol is obtained from a fermentation process whereby simple sugars are converted to ethanol. There is mounting evidence that biofuels may lead to new problems for the planet if large portions of food crops are diverted to produce biofuels. Worldwide, millions of motorists wanting to maintain their mobility at all costs are competing with two billion of the poorest people who are simply trying to survive. The most viable route to meet the current challenge is to use lignocellulosic feedstocks including agricultural residues (straw and corn stovers) and forestry wastes, as well as residues from high-biomass energy crops, such as poplar trees and switchgrasses.

Even though bioethanol production from cellulosic biomass is incontestably the future, especially through a judicious integration of food and chemical production (known as biorefinery), major scientific advances in biotechnology and processing are necessary. In particular, to recover the fermentable sugars from lignocellulosic biomass via hydrolysis is much more difficult than from sugarcane and corn. This hydrolysis step, whereby the biopolymers from lignocellulosic materials are separated into fermentable sugar, requires a large quantity of enzymes, and represents one of the major expenses associated with the utilization of cellulosic biomass. The production of a low-cost cellulase enzyme is a critical step in the development of a sustainable process for the conversion of cellulosic biomass to fermentable sugars (Schell et al., 2001).

Cellulase is most efficiently produced by the filamentous microorganisms *Trichoderma reesei*. *T. reesei* strains are also widely used for the production of enzymes employed in

the laundry and pulp and paper industry (Maras et al., 1999). *T. reesei* fermentations are performed in submerged or solid state aerobic conditions. Submerged fermentation is the preferred choice and it is important to determine the operating conditions that will lead to good biomass growth and efficient protein production. A submerged fungal fermentation is recognized as a complex multiphase, multicomponent process where cell growth and product formation are influenced by a large number of operating parameters such as culture broth composition, temperature, pH, shear stress, initial inoculum, dissolved oxygen and fungal morphology. All these parameters are varying during the course of the fermentation, and, due to the complex interrelationship of operating parameters, it is important to consider all of them simultaneously (Schügerl et al., 1998).

Lejeune and Baron (1995) have studied the effect of agitation on growth and enzyme production of *T. reesei* and shown that, in a 20-L bioreactor, the optimal agitation rate for enzyme activity was 200 rpm whereas it was 300 rpm for fastest growth. They also found that, at 400 rpm, the extracellular protein concentration was at its lowest. Ganesh et al. (2000) clearly showed that a loss in cellulase activity increased with an increase in agitation speed in a stirred tank bioreactor. These results point to the delicate compromise between the necessary shear that is required for homogenization of the fermentation broth and high oxygen mass transfer coefficient (K_La), and the detrimental impact of shear on growth and production.

Rushton turbines are most often employed to achieve adequate mixing and good oxygen mass transfer. However, Rushton turbines lead to non uniform mixing with higher shear at the tips of the blades whereas much lower shear exists in the periphery of the bioreactor (Reuss et al., 2000). Other geometries of mixing devices, such as the reciprocating plate bioreactor (Lounes and Thibault, 1993), provide a more uniform mixing and are well-suited for highly viscous fermentations. Compared to unicellular microbes, the unique morphology of filamentous fungi presents special challenges during the optimization and scale-up of fermentation. An understanding of the growth and morphological complexity of the filamentous fungi is paramount for developing consistent, scalable, productive and efficient fungal fermentation processes (Wang et al., 2005). Morphological characteristics of submerged mycelial cultures have been established as one of the key bioprocess parameters (Žnidaršic and Pavko, 2001).

The overall objective of this investigation is to understand the intimate relationship that exists between the key process parameters, rheology and the morphological characteristics of *T. reesei* during the course of fermentation in a stirred tank and reciprocating plate bioreactor. In this paper, the impact of the type of mixing device and the intensity of agitation on the growth of *T. reesei* and cellulase production is reported. The results are analyzed in terms of biomass, protein, morphology and rheology.

8.2 MATERIALS AND METHODS

8.2.1 Microorganism

The strain used in this work was *T. reesei* RUT C-30 (ATCC 56765) supplied by Iogen Corporation, Ottawa. The glycerol stock solutions of spores were maintained at -80°C and were transferred on potato dextrose agar plates. New plates were prepared every month and kept at 4°C.

8.2.2 Bioreactor

The two bioreactors, a stirred tank bioreactor (STB) with three Rushton turbines and a reciprocating plate bioreactor (RPB) with six plates, were used in these experiments. These bioreactors, built in our laboratories, are identical except for the mixing mechanism. The experimental setup is similar to the one used by Patel et al. (2004). Both bioreactors have a total volume of 22 L and a maximum working volume of 17 L. The bioreactors are made of stainless steel and have an inner diameter of 228 mm and a column height of 550 mm. The cover plates of the bioreactors have ports for sampling, pH probe, dissolved oxygen probe, substrate and base addition, and a thermocouple. The gas sparger at the bottom of the bioreactor consists of thin stainless steel plate containing 100 uniformly distributed 1-mm diameter holes.

A schematic view of the plate stack used in the RPB is shown in Appendix A.1 (a). The plate stack consists of 6 perforated stainless steel plates, 221 mm in diameter and 1.25 mm thick. Each plate was spaced 50 mm apart from one another. The perforations have a diameter of 19 mm and holes are distributed on an equilateral triangular pitch. The plate fractional free area, including the 3.5-mm annular space between the plate edge and bioreactor wall, is 0.36.

A schematic view of the mixing device used in the STB is shown in Appendix A.1 (b). The three identical Rushton turbines were mounted on the central shaft. The locations of the impellers, measured from the bottom of the column, are 54, 132 and 210 mm. Each turbine has 6 blades mounted on the periphery of a 50-mm diameter disk. Each blade is 25 mm long, 15 mm high and 1.5 mm thick. Four baffles, 375 mm high, 16 mm wide and 1 mm thick, were placed inside the mixing vessel.

8.2.3 Cultivation Method

The volume of the culture medium was 10 L and contained: glucose, 13 g/L; $(NH_4)_2SO_4$, 1.4 g/L; KH_2PO_4, 2.0 g/L; $MgSO_4 \cdot 7H_2O$, 0.6 g/L; $CaCl_2 \cdot 2H_2O$, 0.3 g/L; $FeSO_4 \cdot 7H_2O$, 5.0 mg/L; $MnSO_4 \cdot 7H_2O$, 1.6 mg/L; $ZnSO_4 \cdot 7H_2O$, 1.4 mg/L; $CoCl_2 \cdot 6H_2O$, 2 mg/L and corn steep solids, 6.0 g/L. The pH of the medium was initially adjusted to 5.5 using 10N NaOH. Medium was autoclaved for 20 minutes. Shake flask cultures were performed with a volume of 500 mL in a 1-L Erlenmeyer flask with three baffles. A spore solution in sterilized water was prepared from the plates. The spore concentration was calculated using a Petroff Hausser counting chamber (Hausser Scientific, Horsham, PA) and an appropriate volume was inoculated in the flask to obtain an initial concentration of 5×10^3 spores/mL. Flasks were kept in an orbital shaker at 200 rpm and 28°C for 55 h before inoculation.

8.2.4 Control Strategies

The pH was measured on-line by a pH FermProbe (Broadley-James Corporation, Irvine, CA) whereas the dissolved oxygen was continuously monitored by a dissolved oxygen Sensor (Broadley-James Corporation, Irvine, CA). When the initial glucose was consumed, corresponding to the end of the batch phase, 150 g/L lactose monohydrate solution (without nutrients) was added such that the dissolved oxygen was maintained in the vicinity of the 30% set point that is well above the critical dissolved oxygen (Schafner and Toledo, 1992). If the dissolved oxygen was above 30%, a preset amount of lactose medium was added to the bioreactor whereas no solution was fed if the dissolved oxygen was below 30%. The comparison was done every 20 s. The preset amount of lactose added was changed manually as the fermentation progressed. This control strategy was also used to control the pH at 4.5 by the addition of 15 vol% NH_4OH. Foam was controlled by automatic addition of Sigma 204 antifoam.

8.2.5 Analysis

A 45-mL sample was collected approximately every 4 - 6 h during the batch phase and 12 h during the fed-batch. One mL of this sample was used for image analysis and the remaining sample was stored at 4°C pending further analysis. The amount of biomass was quantified by dry weight analysis. Sample was filtered through a pre-dried and pre-weighted glass fibre filter (grade A/E, Gelman Sciences, MI). One volume of the sample was washed with two volumes of deionised distilled water and dried for 24 h at 95°C. The weight of the sample was measured after a 24-h period of cooling in a desiccator.

Glucose concentration was determined using YSI glucose analyzer (YSI Incorporated, USA) and protein concentration was determined with Bradford assay using Bovine Serum Albumin (BSA) as standard. Filter paper (FPA) and carboxymethyl cellulose (CMC) activities were determined as per the IUPAC protocol (Ghose, 1987).

For image analysis measurements, a monochrome camera (CoolSnap ES, Roper Scientific, Tucson, AZ) mounted on an Olympus IX81 microscope (Olympus, Melville, NY) was used. The automated stage of the microscope was controlled by the Image-Pro® Plus software (Image-Pro® Plus version 5.1, Media Cybernetics, Silver Spring, MD). Morphology of *T. reesei* was classified into branched, unbranched, entangled and clumped. Viability was measured by staining microorganisms with FDA (fluorescein diacetate) solution since active mycelia exhibit bright fluorescence whereas dead mycelia appear dark on the picture taken under fluorescence microscopy. Both morphological parameters and viability were determined according to protocol described by Lecault et al. (2007).

Rheological analysis of the fermentation broth samples were performed with the AR-G2 Rheometer, controlled by a computer with AR Instrument Control and Data Analysis software (TA Instruments, New Castle, Delaware, USA). The concentric cylinder fixture (545012.001 HA Aluminium Conical DIN Rotor, 14-mm radius, TA Instruments, Delaware, USA) was used for samples collected in the first 12 h of the fermentation runs when the broth had properties close to water. As biomass concentration increased with time, the vane and cup fixture (545025.001 Stainless Steel, Vane Rotor, 14-mm radius, TA Instruments, Delaware, USA) was used because this geometry prevented sedimentation and wall slip and the integrity of the morphology was maintained. All

samples were brought to reactor operating temperature of 28°C and pre-sheared to erase sample handling history and equilibrated before rheology measurement. The apparent viscosity was obtained for shear rates at 30 s^{-1}. A more detailed explanation on the rheological analysis can be found in Malouf (2008).

8.3 RESULTS

Seven fermentation runs were performed using *T. reesei* Rut C-30 strain in STB and RPB. Samples collected during the experiments were analyzed for the biomass concentration, protein production, rheology of the broth, and the morphology of the microorganism. Profiles of biomass, dissolved oxygen, pH, and protein production are shown in Figure 8.1 (a) for STB at 400 rpm and in Figure 8.1 (b) for RPB at 1.0 Hz.

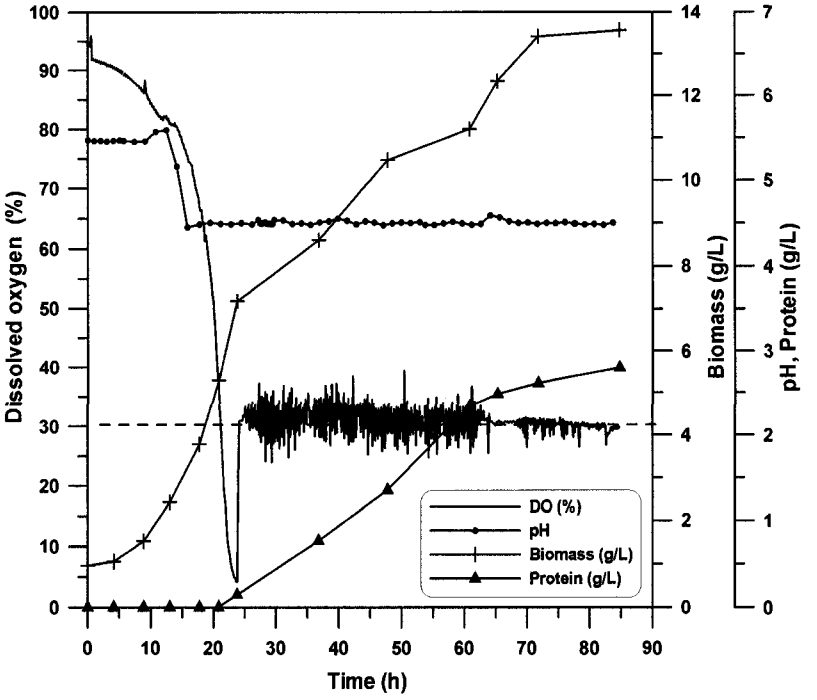

Figure 8.1 (a) – Profile of biomass, dissolved oxygen, pH and protein production in STB operating at 400 rpm.

As the fermentation progressed, the pH of the fermentation broth increased and later dropped to 4.5 where a one-sided pH control was activated using NH_4OH (15 vol%) addition as the manipulated variable. During the batch phase, only glucose was used as a substrate for biomass growth. When glucose was completely consumed and dissolved oxygen rose to 30%, lactose feeding was initiated. A solution containing only lactose

(without nutrients), which is a good inducer of cellulase (Domingues et al., 2001), was used during the fed-batch phase. These represent typical profiles obtained in all experiments that were performed except that the rate of change and concentration levels of all variables varied with the type of mixing device and agitation intensity. These will be examined in the following sections.

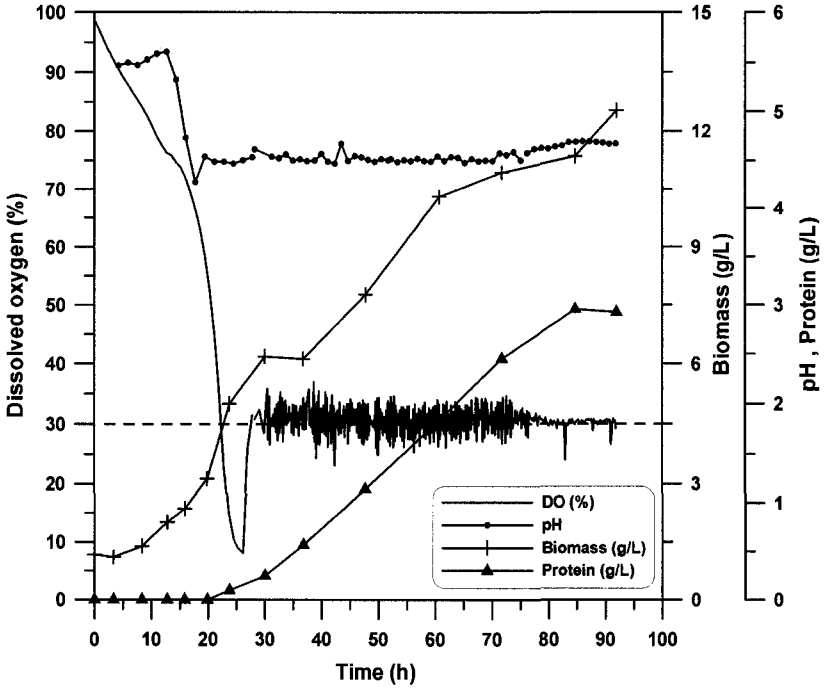

Figure 8.1 (b) – Profile of biomass, dissolved oxygen, pH and protein production in RPB operating at 1.0 Hz.

8.3.1 Effect of Agitation on Biomass Growth, Sugar Consumption and Protein Production

Figure 8.2 presents the biomass and glucose concentration profiles during fermentation runs that were performed in the two bioreactors under different intensities of agitation. The initial biomass concentration for all experiments was approximately 0.9 g/L. However, since biomass is measured by dry weight and a portion of the corn steep solids that is an ingredient of the culture medium is insoluble, the initial biomass concentration is somewhat inflated. Indeed, samples analysed under the microscope showed the presence of insoluble corn steep solids at the beginning of fermentation whereas complete consumption was observed before the end of the batch process. This can explain the

apparent lag phase observed in Figure 8.2 that was probably caused by an increase in biomass accompanied by a consumption of corn steep solids.

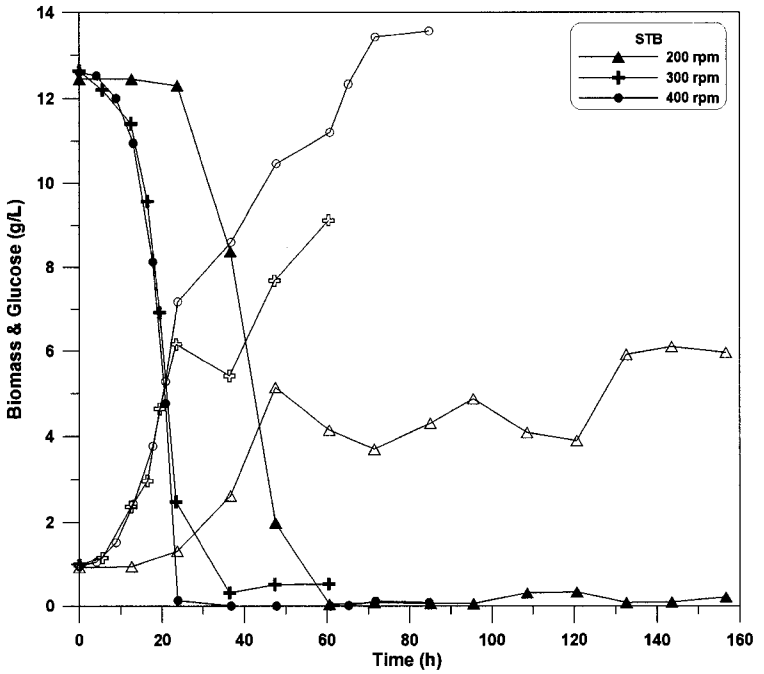

Figure 8.2 (a) – Profile of biomass production (open symbols) and glucose concentration (filled symbols) as a function of time in STB at different agitation.

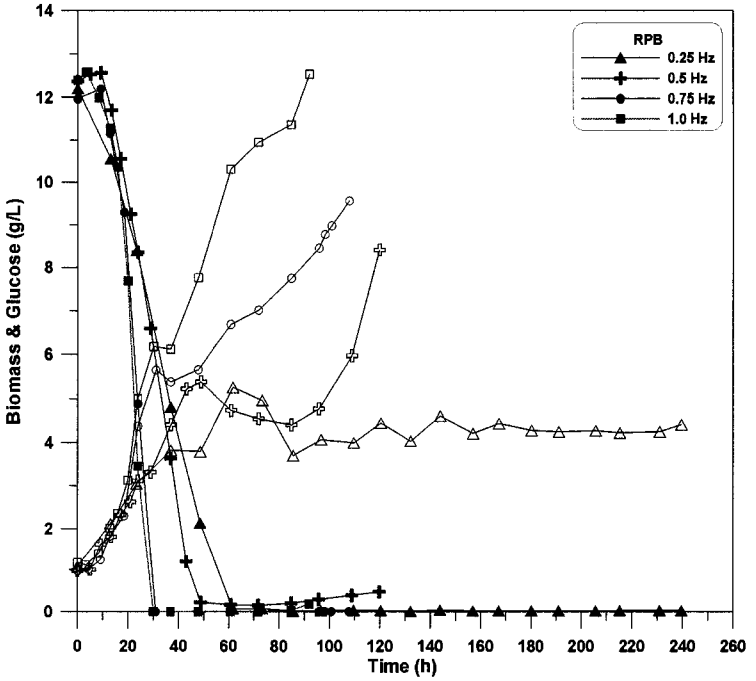

Figure 8.2 (b) – Profile of biomass production (open symbols) and glucose concentration (filled symbols) as a function of time in RPB at different agitation.

As shown in Figure 8.2, the maximum biomass concentration was obtained at higher agitation speeds: 400 rpm in the STB and 1.0 Hz in the RPB. During the batch phase, the dissolved oxygen dropped and stayed close to 0% (data not shown) causing oxygen limitation for all experiments except at 400 rpm and 1.0 Hz. The period of growth below the critical dissolved oxygen level decreased with the increase in agitation intensity due to better oxygen supply. When glucose was completely consumed, the mode of operation was switched from batch to fed-batch. In the fed-batch phase, lactose serving as the inducer for protein production was added in a way to control the dissolved oxygen concentration in the vicinity of 30%. The time at which the fed-batch phase was initiated is reported in Table 8.1 for each experiment.

Table 8.1 – Transition time from batch to fed-batch cultivation phase and time at which spore formation occurs.

Experiment	End of Batch phase (h)	Spore formation (h)
STB – 200 rpm	54.81	120.66
STB – 300 rpm	26.07	47.35
STB – 400 rpm	24.51	71.46
RPB – 0.25 Hz	68.41	-
RPB – 0.50 Hz	51.54	95.76
RPB – 0.75 Hz	34.07	84.77
RPB – 1.0 Hz	27.14	71.72

However, there were some operational difficulties associated with both bioreactors. Foaming issues during *T. reesei* fermentation have been well documented (Nystrom and Allen, 1976). Foam control was difficult at lower agitation for experiments performed in

the STB. At 200 rpm, agitation was increased for short periods of time in order to mix the foam with the medium and to create a more uniform mixture. However at 300 rpm, foam control was more difficult even with brief periodic higher agitation. In this case, foam formed a separate stable layer above the fermentation broth and the addition of antifoam was not effective. Similar foaming problems associated with *Trichoderma* strain were encountered by other researchers (Weber and Agblevor, 2005). For this reason, the experiment at 300 rpm was stopped earlier. At 200 rpm, most likely due to the slower growth, it was still possible to control the foam. On the other hand at 400 rpm, the medium was well mixed and the addition of antifoam was able to mitigate the formation of foam. Therefore, as suggested by McLean et al. (1985), for a particular STB at given operating conditions, there is an upper limit of biomass concentration where fermentation can be performed without foaming problems.

This problem was not encountered in the RPB due to the more uniform mixing that is achieved with the axial motion of plates that occupy the whole cross-sectional area of the fermenter. However, fermentation conducted in the RPB had its own operational disadvantage. Operating the RPB in fed-batch mode implies that some of the upper plates are not initially immersed in the fermentation broth. Because of the reciprocation of the plate stack, an upper plate could be immersed a short time during its downward motion and carry with its biomass that was allowed to build on its surface. This accumulation of biomass would eventually return to the medium as the volume of the fed-batch fermentation increases and the plate has a longer or total contact with the medium. This problem was more predominant at lower agitation speed where the rate of substrate consumption was lower and, as a result, the broth volume increase was lower. For the experiment conducted in the RPB at 0.5 Hz, the biomass accumulation on the top plate detached and was suddenly mixed with the bioreactor medium, causing a sudden increase in biomass concentration in the medium (Figure 8.2 (b)). This sudden biomass increase had a repercussion in the substrate requirement and the controller feed rate had to increase to maintain the dissolved oxygen around 30% (Figure 8.3 (b)). For higher agitation, the medium level increase was faster and therefore the biomass accumulation on the top plate was not significant. On the other hand, due to both the low growth rate

and substrate feeding at 0.25 Hz, the liquid level did not increase sufficiently even after 240 h of operation to dislodge the biomass on the top plate and to mix with the medium.

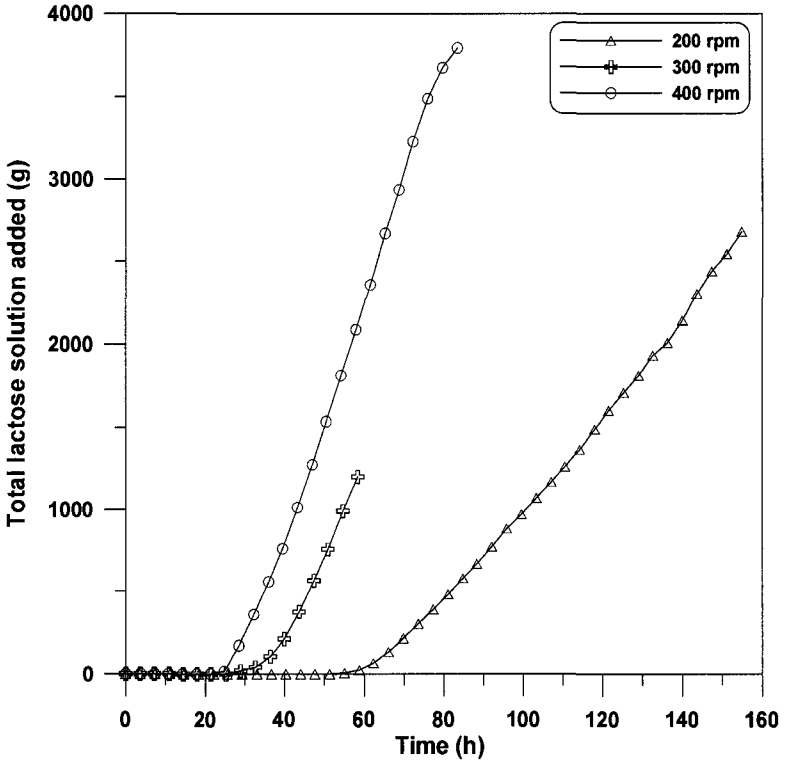

Figure 8.3 (a) – Total lactose solution added as a function of time for experiments performed in STB.

During the fed-batch phase, the rate of lactose feeding (Figure 8.3) was adjusted to maintain the dissolved oxygen in the vicinity of 30%. No other manipulated variables, such as the agitation or air flow rate, were used. Because the lactose feeding relied only on the dissolved oxygen concentration, the growth rate was thereby limited. The amount of lactose fed during the fed-batch process remained on the average nearly constant. In addition, no additional nutrients were added with lactose during the fed-batch process. Therefore, although biomass concentration continued to increase, the viability started to drop as discussed later. At the end of the fermentation, spore formation was observed in all fermentation runs except for the experiment conducted in the RPB at 0.25 Hz where the growth rate was very low. Therefore, an increase in biomass concentration at the end of fed-batch was mainly due to spores. The times at which spores were first observed in the samples when analyzed under the microscope are also reported in Table 8.1.

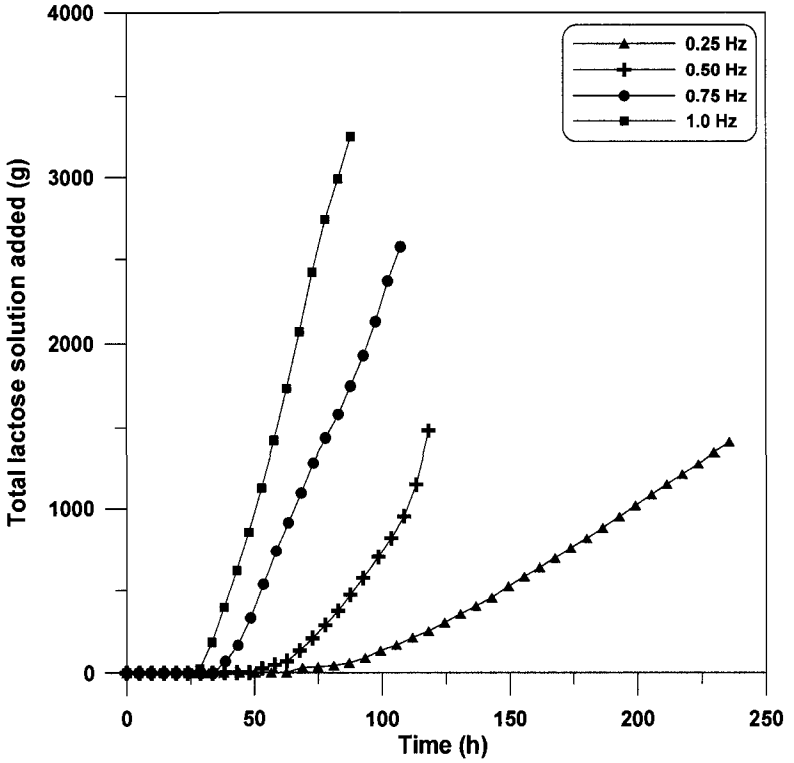

Figure 8.3 (b) – Total lactose solution added as a function of time for experiments performed in RPB.

Protein production started in the last portion of the batch phase when sugar concentration became low. The protein production commenced earlier as the speed of agitation was increased (Figure 8.4). However, relatively low protein concentrations, in the range of 2 to 3 g/L, were obtained. This low concentration was probably due to the lactose feeding controller strategy used in this study and nutrient limitation discussed above. There was no effect of dissolved oxygen on the protein production since the dissolved oxygen was maintained well above the limiting concentration of 20% during the fed-batch process. Further, there was no cellulase inhibition due to glucose since the glucose concentration during the fed-batch was very low as shown in Figure 8.2 (Velkovska et al., 1997).

Figures 8.5 (a) and 8.5 (b) show the protein activity (FPU & CMC) per mg of protein produced for all experiments conducted in both bioreactors. A higher filter paper activity was obtained at low agitation (200 rpm and 0.25 Hz) in both bioreactors. However, lower CMC activity was obtained for the experiment performed in the STB at 200 rpm in the

early production phase but higher CMC activity similar to FPA activity was obtained for experiments performed in the RPB.

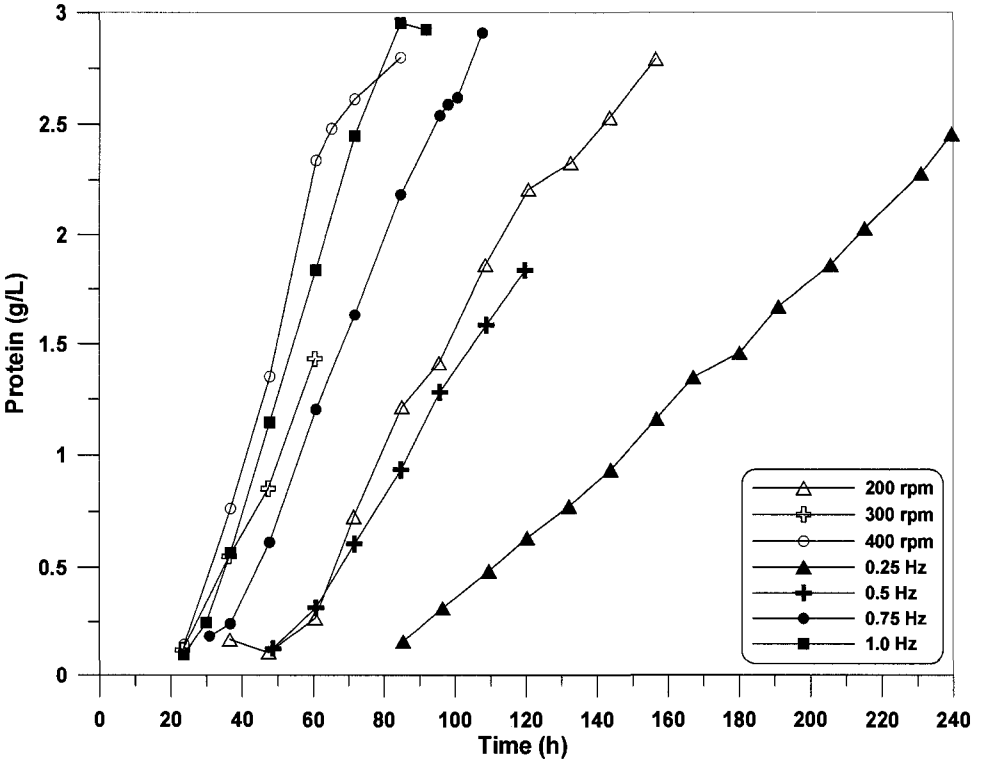

Figure 8.4. Extracellular protein produced as a function of time in STB and RPB at different agitation.

A higher activity obtained at lower agitation could be due to a few reasons such as better induction of cellulase at slower growth rate (Hendy et al., 1984), better secretion of complete enzyme complex especially β-glucosidase at low growth rate (Allen and Andreotti, 1982, Pakula et al., 2005) and/or protein degradation at higher agitation (Ganesh et al., 2000, Lejeune and Baron, 1995, Weber and Agblevor, 2005). Nevertheless, the protein productivity was very low to justify operating experiments at low agitation. Therefore, experiments at 400 rpm for STB and 0.75 HZ for RPB were found to be optimum under the conditions used in this study. An agitation rate greater than 400 rpm may lead to better optimum but such operating conditions were not evaluated in the present study. Higher agitation could have a detrimental effect on the growth and protein production (Lejeune and Baron, 1995).

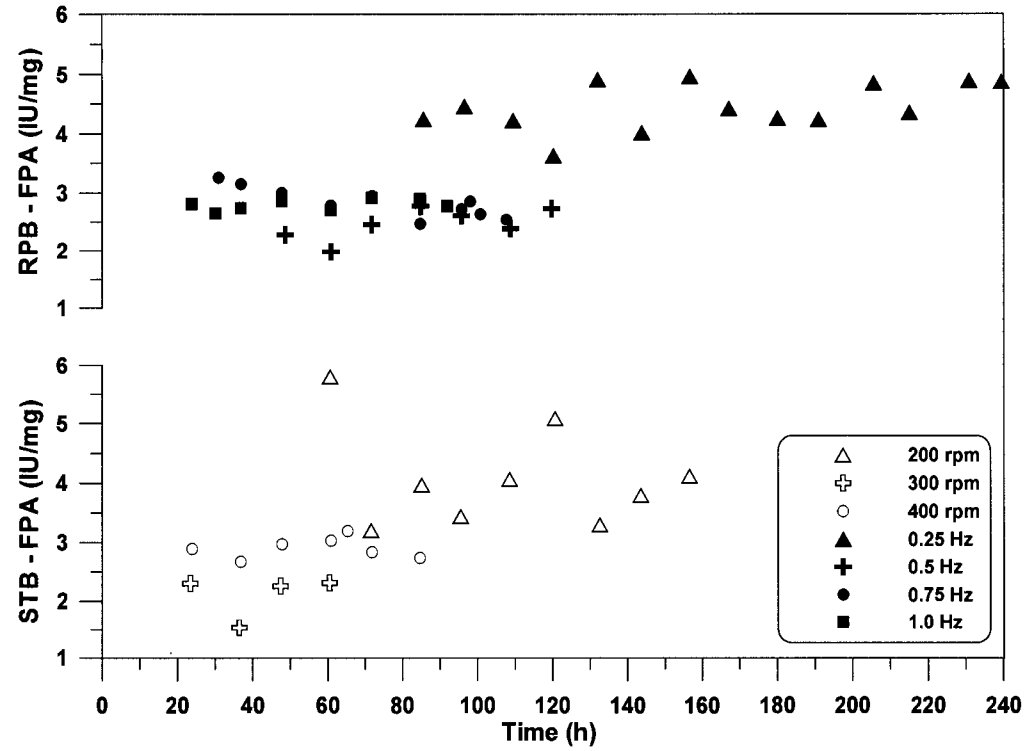

Figure 8.5 (a) – Filter paper activity (FPA) per mg of protein produced for experiments performed in STB and RPB.

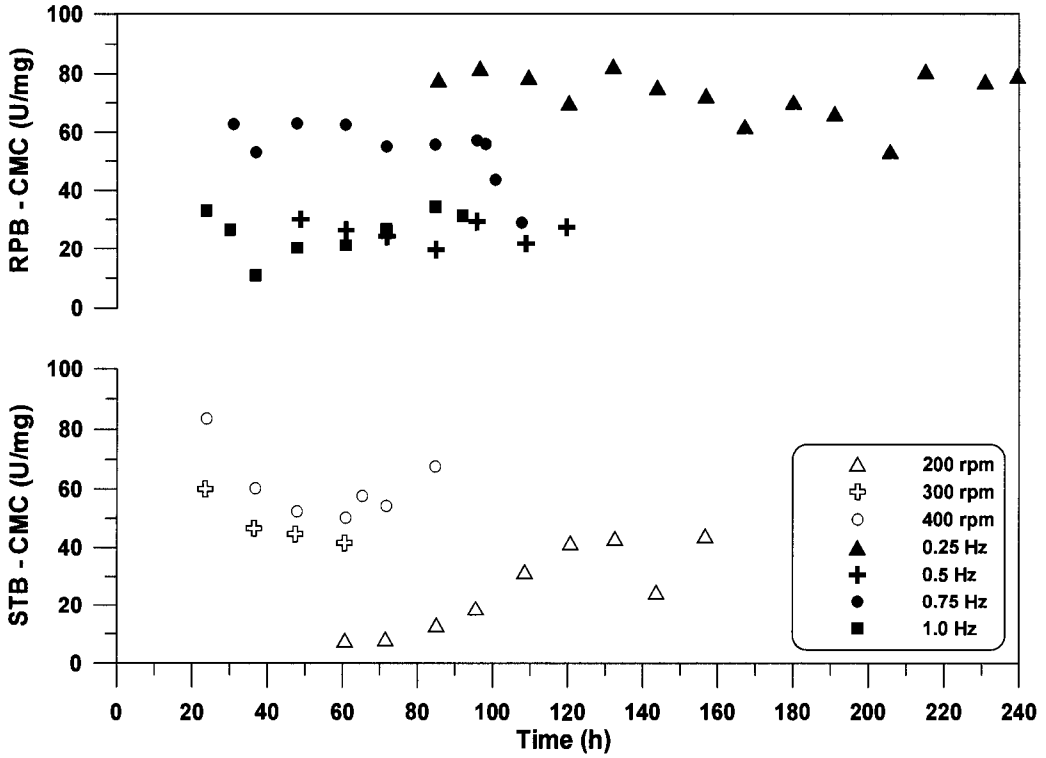

Figure 8.5 (b) – Carboxymethyl cellulose activity (CMC) per mg of protein produced for experiments performed in STB and RPB.

8.3.2 Effect of Agitation on Morphology and Viability

The effect of agitation on the morphology of *T. reesei* is shown in Figures 8.6 (a) and 8.6 (b) for STB and RPB, respectively. These figures present the fraction of the microorganisms on an area basis that were classified as branched, unbranched, entangled or clumped.

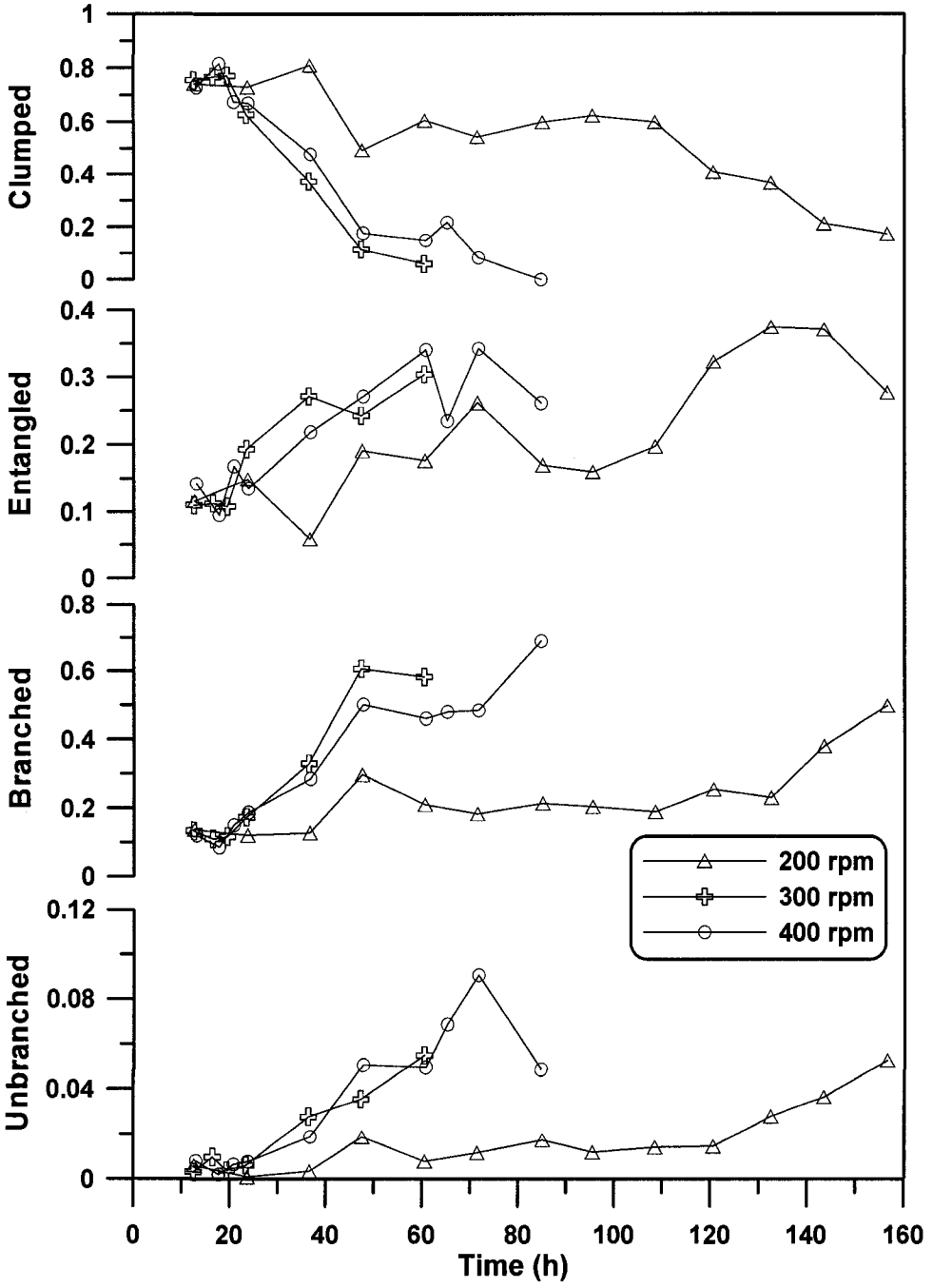

Figure 8.6 (a) – Classification of microorganism as branched, unbranched, entangled or clumped for experiments performed in STB.

The initial high clump percentage observed for all experiments was due to the growth of the inoculum in shake flask cultivations under low shear conditions. Similar observations were made during the characterization of *Streptomyces olindensis* in submerged fermentation (Pamboukian et al., 2002).

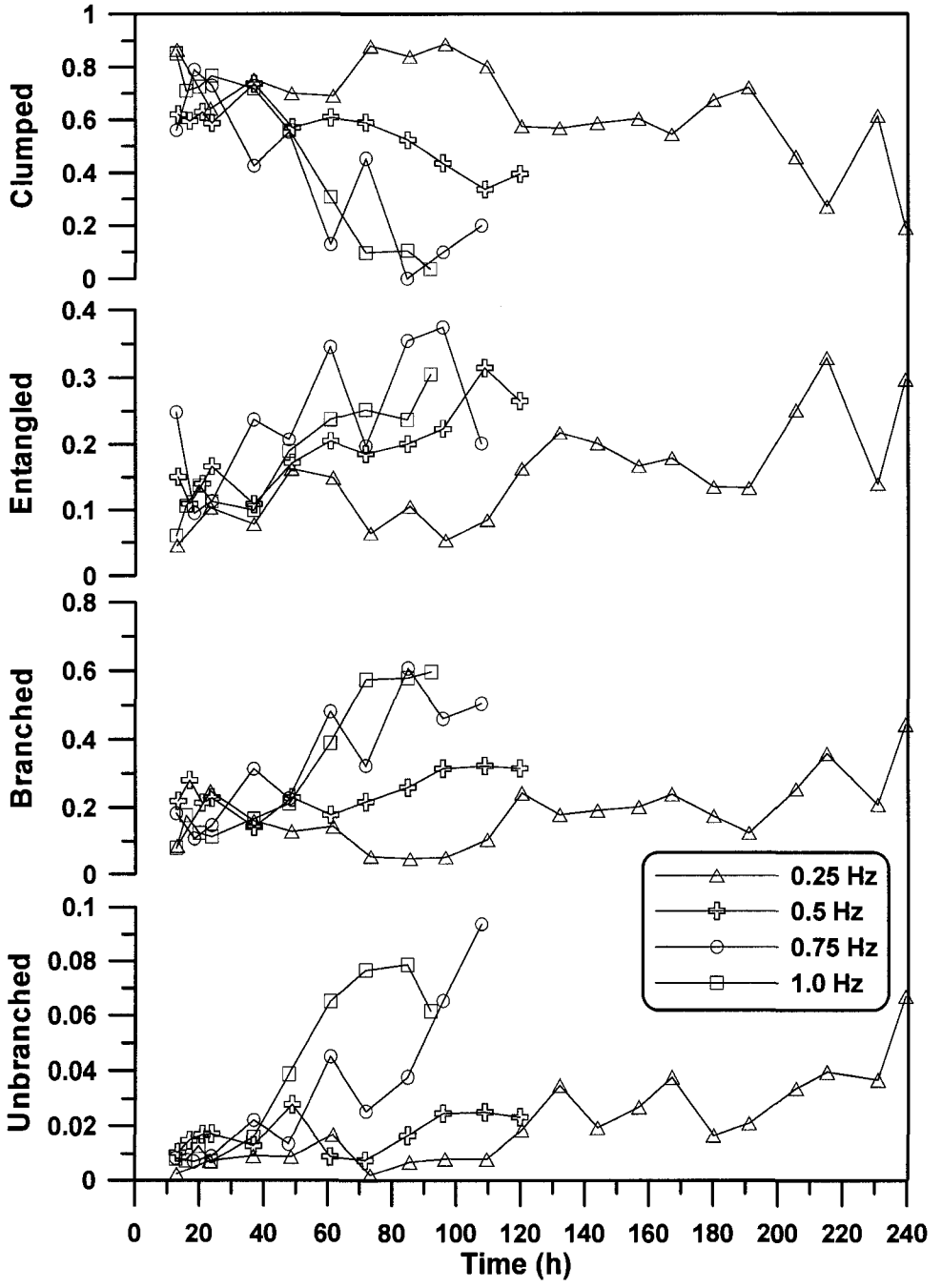

Figure 8.6 (b) – Classification of microorganism as branched, unbranched, entangled or clumped for experiments performed in RPB.

Significant fragmentation was observed only during the fed-batch process indicating that during the growth in batch phase, young and growing mycelia are very resistant to the shear stress even at very high agitation (Lejeune et al., 1995). During the fed-batch in the STB, low agitation at 200 rpm resulted in a significantly slower fragmentation of the microorganism. The rate of increase in the percentages of unbranched, branched, and entangled morphological states as well as the rate of decrease in clumped microorganism observed at 300 and 400 rpm were nearly identical. Similarly in the RPB, slower fragmentation occurred at 0.25 Hz followed by progressively faster fragmentation for 0.50 Hz, 0.75 and 1.0 Hz.

The fraction average viability of the microorganism for the fermentations conducted in the STB and RPB under different agitation is presented in Figures 8.7 (a) and 8.7 (b). The viability during the early portion of the batch phase was not the same for all fermentations. However, at the beginning of the fed-batch, the viability was nearly the same for all fermentations in the range of 80-90%. During the batch phase, viability increased and remained high due to the growth of fungi. Lejeune et al. (1995) also found no significant effect of agitation on the early growth of *T. reesei* QM 9414. Only for the experiment at 0.25 Hz, a decrease in viability at the end of the batch phase was more apparent.

When the switch from batch to fed-batch mode was made and the lactose feeding starts, the percentage viability increased again or remained at a higher level during the first portion of the fed-batch phase. After this initial high viability level in the fed-batch mode, the viability started to progressively decrease. However, in some fermentation, an increase in viability was observed near the end of the experiment. One possible cause of this increase in viability is the disintegration of dead and weaker fungi. These empty microorganisms along with spores are not considered during the microscopic image analysis and, therefore, the increase in viability is attributed to the measurement of only healthy and live fungi.

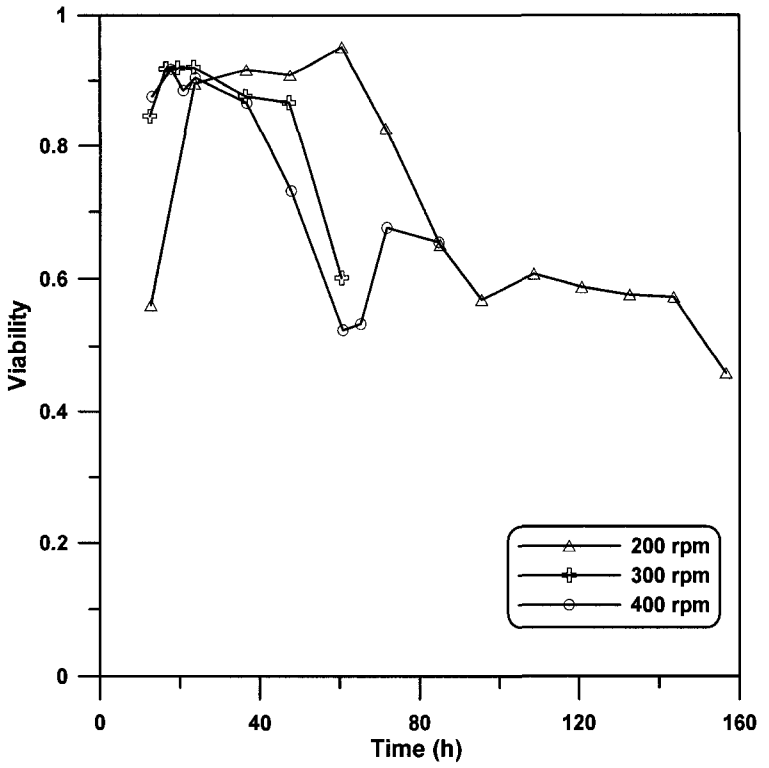

Figure 8.7 (a) – Viability of microorganism for experiments performed in STB.

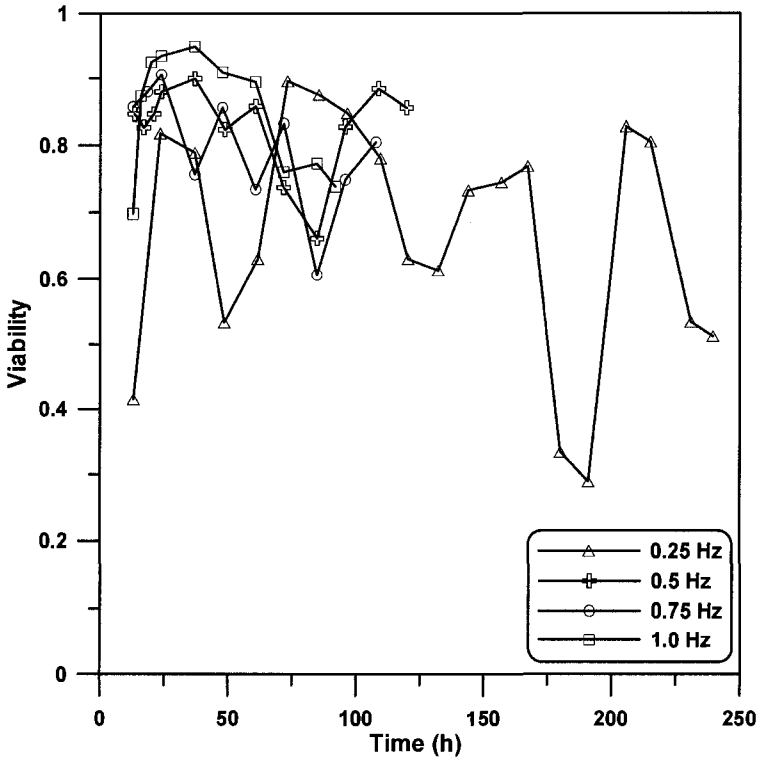

Figure 8.7 (b) – Viability of microorganism for experiments performed in RPB.

8.3.3 Effect of Agitation on Rheology

The apparent viscosity of the fermentation broth for each experiment conducted in the STB and RPB under different agitation is presented in Figures 8.8 (a) and 8.8 (b).

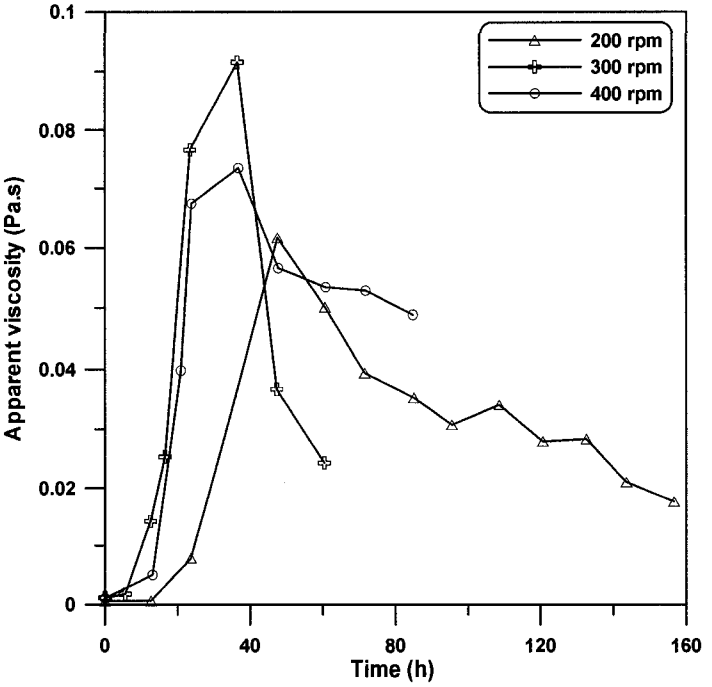

Figure 8.8 (a) – Profile of the apparent viscosity as a function of fermentation time at 200, 300 and 400 rpm in STB. The apparent viscosity was measured at a shear rate of 30 s^{-1} and a temperature of 28°C.

These figures clearly show that the growth of fungi during the batch phase caused a significant increase in apparent viscosity of the fermentation broth. This significant increase in apparent viscosity is attributed to the increase in biomass concentration. A maximum apparent viscosity is achieved during the early fed-batch phase although the biomass concentration continues to increase. This phenomenon was also observed in other filamentous fungi fermentations (Cho et al., 2002, Gupta et al., 2007, Riley et al., 2000, Marten et al., 1996). In addition, Riley et al., (2000) showed that the area and maximum dimension decreased as a function of fermentation time. After the maximum apparent viscosity, the observed change in morphology produced a decrease in apparent viscosity thus counteracting the effect of increasing biomass concentrations.

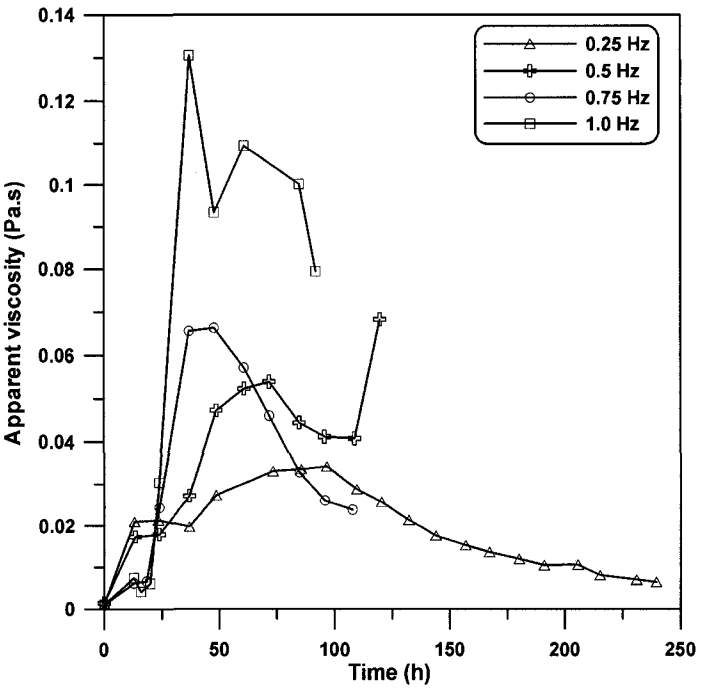

Figure 8.8 (b) – Profile of the apparent viscosity as a function of fermentation time at 0.25, 0.5, 0.75 and 1.0 Hz in RPB. The apparent viscosity was measured at a shear rate of 30 s^{-1} and a temperature of 28°C.

Indeed, it was observed in fermentations performed in this investigation that the area of *T. reesei* was mostly greater than 5000 μm^2 in the batch phase whereas, in the fed-batch, the area was much smaller. It was also suggested that the viscosity decrease could be attributed to weaker microorganism, the formation of spores and the decrease in dispersed form of filamentous microorganisms or to cell lysis (Gupta et al., 2007, Pamboukian et al., 2002). Spores have the same properties of spherical suspensions, which have a lower viscosity than other types of morphology. The only exception was at 0.5 Hz experiment in the RPB where biomass from the top plate mixed with medium causing an increase in both biomass concentration and viscosity of broth at the end of fermentation.

8.4 DISCUSSION

Experiments performed in this study using *T. reesei* can be divided into three parts: batch phase, early fed-batch phase and spore formation phase. The time at which each phase occurs during the fermentation is shown in Table 8.1. During the batch phase, biomass increase due to microorganism growth was the main cause of an increase in the

apparent viscosity of the fermentation broth. Viability increased or remained high during the batch phase and the morphological analysis showed that the fragmentation was not significant, which is most likely due to the young and healthy microorganism. As glucose was exhausted at the end of the batch phase, the growth rate decreased and only for the experiment at 0.25 Hz a decrease in viability was observed. This occurrence is more apparent for the run at 0.25 Hz due to the slower growth rate and longer stationary and death phase. However, the apparent viscosity continues to increase and peaks shortly after the maximum biomass concentration obtained in the batch phase.

During the fed-batch, biomass concentration continues to rise but the apparent viscosity starts to decline. During this phase, fragmentation also occurred causing a decrease in the percentage of clumps and an increase in branched, unbranched and entangled microorganisms. As mentioned earlier, due to the feeding strategy employed, viability increased briefly for experiments with low growth rate as fed-batch started but then decreased as fermentation progresses. Also during fed-batch, the apparent viscosity starts to drop perhaps due to the change in the morphology and weaker microorganism. However, at the end of fermentation, the apparent viscosity drop was caused by an increase in spore concentration and a decrease in filamentous microorganism due to the cell lysis (Marten et al., 1996).

At the end of fermentation, spores were formed for all fermentations except at the lower agitation of 0.25 Hz in the RPB. Empty objects formed due to the disintegration of weaker and dead fungi along with spores are not analysed and therefore the viability of sample increases due to analysis of only healthy filamentous microorganism.

8.5 CONCLUSIONS

Trichoderma reesei fermentations were performed in identical bioreactors but using two different types of mixing systems: stirred tank bioreactor and reciprocating plate bioreactor. The effect of the mixing system and agitation speed were studied on the biomass, protein, viscosity, and morphology of microorganism. Higher growth rate and faster protein production were achieved as the agitation was increased. However, except for CMC activity per mg of protein in STB, highest protein activities per mg of protein were obtained at lower agitation for both STB and RPB. Agitation speed also had significant effect on the morphology. Higher agitation caused a faster decrease in the

clump percentage and an increase in the percentage of branched, unbranched and entangled microorganisms. In the early stages of fermentation, biomass growth resulted in an increase in viscosity. However during the fed-batch, viscosity most likely decreased due to weaker microorganisms and change in the morphology. Late in fed-batch phase, the decrease was largely due to spore formation and decrease in filamentous microorganism. The results presented here provide a better understanding of the intimate relationship that exists between the key process parameters, rheology and the morphological characteristics of *T. reesei* during the course of the fermentation.

8.6 REFERENCES

Allen, A. L. and Andreotti, R. E., Cellulase Production in Continuous and Fed-Batch Culture by *Trichoderma reesei* MCG-80. Biotechnology and Bioengineering Symposium, *12*: 451-459, 1982.

Cho, Y. J., Hwang, H. J., Kim, S. W., Song, C. H., and Yun, J. W., Effect of Carbon Source and Aeration Rate on Broth Rheology and Fungal Morphology During Red Pigment Production by *Paecilomyces sinclairii* in a Batch Bioreactor. Journal of Biotechnology, *95*: 13-23, 2002.

Domingues, F. C., Queiroz, J. A., Cabral, J. M. S., and Fonseca, L. P., Production of Cellulases in Batch Culture Using a Mutant Strain of *Trichoderma reesei* Growing on Soluble Carbon Source. Biotechnology Letters, *23*: 771-775, 2001.

Ganesh, K., Joshi, J. B., and Sawant, S. B., Cellulase Deactivations in Stirred Reactor. Biochemical Engineering Journal, *4*: 137-141, 2000.

Ghose, T. K., Measurement of Cellulase Activity. Pure & Applied Chemistry, *59*: 257-268, 1987.

Gupta, K., Mishra, P. K., and Srivastava, P., A Correlative Evaluation of Morphology and Rheology of *Aspergillus terreus* During Lovastatin Fermentation. Biotechnology and Bioprocessing Engineering, *12*: 140-146, 2007.

Hendy, N. A., Wilke, C. R., and Blanch, H. W., Enhanced Cellulase Production in Fed-Batch Culture of *Trichoderma reesei* C-30. Enzyme and Microbial Technology, *6*: 73-77, 1984.

Lecault, V., Patel, N., and Thibault, J., Morphological Characterization and Viability Assessment of *Trichoderma reesei* by Image Analysis. Biotechnology Progress, *23*: 734-740, 2007.

Lejeune, R. and Baron, G. V., Effect of Agitation on Growth and Enzyme Production of *Trichoderma reesei* in Batch Fermentation. Applied Microbiology and Biotechnology, *43*: 249-258, 1995.

Lejeune, R., Nielsen, J., and Garon, G. V., Morphology of *Trichoderma reesei* QM 9414 in Submerged Cultures. Biotechnology and Bioengineering, *47*: 609-615, 1995.

Lounes, M. and Thibault, J., Hydrodynamics and Power Consumption of a Reciprocating Plate Gas-Liquid Column. Canadian Journal of Chemical Engineering, *71*: 497-506, 1993.

Malouf, P., Relationship Between Morphology and Rheology During *Trichoderma reesei* RUT C-30 Fermentations, MASc Thesis, University of Ottawa, Ottawa, 2008.

Maras, M., van Die, I., Contreras, R., and van den Hondel, C. A., Filamentous Fungi as Production Organisms for Glycoproteins of Bio-Medical Interest. Glycoconjugate Journal, *16*: 99-107, 1999.

Marten, M. R., Velkovska, S., Khan, S. A., and Ollis, D. F., Rheological, Mass Transfer, and Mixing Characterization of Cellulase-Producing *Trichoderma reesei* Suspension. Biotechnology Progress, *12*: 602-611, 1996.

McLean, D. D., Abear, K., and Podruzny, M. F., Fed-Batch Production of Cellulases Using *Trichoderma reesei* Rutgers C-30. Canadian Journal of Chemical Engineering, *64*: 588-597, 1985.

Nystrom, J. M. and Allen, A. L., Pilot Scale Investigation and Economics of Cellulase Production. Biotechnology and Bioengineering Symposium, *6*: 55-74, 1976.

Pakula, T. M., Salonen, K., Uusitalo, J., and Penttilä, M., The Effect of Specific Growth Rate on Protein Synthesis and Secretion in the Filamentous Fungus *Trichoderma reesei.* Microbiology, *151*: 135-143, 2005.

Pamboukian, C. R. D., Guimarães, L. M., and Facciotti, M. C. R., Applications of Image Analysis in the Characterization of *Streptomyces olindensis* in Submerged Culture. Brazilian Journal of Microbiology, *33*: 17-21, 2002.

Patel, N. and Thibault, J., Evaluation of Oxygen Mass Transfer in *Aspergillus niger* Fermentation Using Data Reconciliation. Biotechnology Progress, *20*: 239-247, 2004.

Reuss, M., Schmalzriedt, S., and Jenne, M. Application of Computational Fluid Dynamics (CFD) to Modeling Stirred Tank Bioreactors. *In* K. Schügerl and K. H. Bellgardt (eds.), Bioreaction Engineering. Modelling and Control, pp. 207-246. Springer, 2000.

Riley, G. L., Tucker, K. G., Paul, G. C., and Thomas, C. R., Effect of Biomass Concentration and Mycelial Morphology on Fermentation Broth Rheology. Biotechnology and Bioengineering, *68*: 160-172, 2000.

Schafner, D. W. and Toledo, R. T., Cellulase Production in Continuous Culture by *Trichoderma reesei* on Xylose-Based Media. Biotechnology and Bioengineering, *39*: 865-869, 1992.

Schell, D. J., Farmer, J., Hamilton, J., Lyons, B., McMillan, J. D., Saez, J. C., and Tholudur, A., Influence of Operating Conditions and Vessel Size on Oxygen Transfer During Cellulase Production. Applied Biochemistry and Biotechnology, *91-93*: 627-642, 2001.

Schügerl, K., Gerlach, S. R., and Siedenberg, D., Influence of the Process Parameters on the Morphology and Enzyme Production of *Aspergilli*. Advances in Biochemical Engineering and Biotechnology, *60*: 195-266, 1998.

Velkovska, S., Marten, M. R., and Ollis, D. F., Kinetic Model for Batch Cellulase Production by *Trichoderma reesei* Rut C30. Journal of Biotechnology, *54*: 83-94, 1997.

Wang, L., Ridgway, D., Gu, T., and Moo-Young, M., Bioprocess Strategies to Improve Heterologous Protein Production in Filamentous Fungal Fermentation. Biotechnology Advances, *23*: 115-129, 2005.

Weber, J. and Agblevor, F. A., Microbubble Fermentation of *Trichoderma reesei* for Cellulase Production. Process Biochemistry, *40*: 669-676, 2005.

Žnidaršic, A. and Pavko, A., The Morphology of Filamentous Fungi in Submerged Cultivations As Bioprocess Parameter. Food Technology and Biotechnology, *39*: 237-252, 2001.

CHAPTER 9

Design of a Novel Couette Flow Bioreactor to Study the Growth of Fungal Microorganism

Nilesh Patel[1], Viviane Choy[1], Theresa White[2], Glenn Munkvold[2], and Jules Thibault[1]*

[1]Department of Chemical and Biological Engineering,

University of Ottawa, Ottawa (ON), K1N 6N5, Canada

[2]Iogen Corporation, Ottawa, Ontario, Canada, K1V 1C1

Abstract

Fermentations using *Trichoderma reesei* Rut C-30 were performed in a 5-L Couette Flow Bioreactor (CFB) which was designed and built to perform experiments in batch and continuous modes. Process parameters such as dissolved oxygen, pH and temperature were measured and controlled without disturbing the shear profile inside the bioreactor. Effect of shear on the growth, protein production and morphology was studied by performing runs at 100, 200, 300 and 400 rpm. Morphological characterization was performed by classifying *T. reesei* as clumped, entangled, branched and unbranched microorganisms. At higher shear rates, lower protein production rate and activity, and higher rate of fragmentation were observed. Also, the cell thickness decreased with increasing speed, going from 8.3 μm for the experiment at 100 rpm to 4.3 μm at 400 rpm.

The effect of substrate, lactose (an inducer) or glucose, was investigated by switching the feed medium during the two runs performed at 300 and 400 rpm. When glucose was used as a substrate, an increase in biomass concentration and a drop in protein production were observed, as expected. However, higher fragmentation and thicker cells were also observed compared to experiments performed using only lactose as a substrate.

The novel design of the CFB used in the present study includes a large volume that allows growing larger size microorganisms (e.g. fungi) than plant cells and permits larger sampling volumes without affecting the fermentation. It also has the ability to carry out experiments for long periods of time, both in batch and continuous modes. Finally, experiments in the CFB can also be performed while measuring and controlling important process parameters.

Keywords: cellulase, Couette flow bioreactor, fermentation, morphology, shear, *Trichoderma reesei*

9.1 INTRODUCTION

Achieving adequate mixing is very important in submerged fermentation. Higher mixing intensity will certainly improve mass transfer. However, higher mixing intensity may adversely affect the growth of microorganism and product formation in addition to higher energy requirements. To find a judicious intensity of mixing for a particular fermentation and type of mixing devices, it is thus important to study the effect of shear on the growth, productivity and morphology of microorganisms. However, most of the studies reported in the literature were performed in conventional bioreactors such as a stirred tank bioreactor with Rushton turbines where microorganisms are subjected to non-uniform shear fields (Reuss et al., 2000). Also, gas sparging required for oxygen supply may cause shear damage to the microorganism (Cherry and Hulle, 1992) due to the shear forces associated with bubbles rising through the fermentation medium and bubbles bursting at the liquid surface. Further, it is difficult to evaluate the effect of shear due to mixing and gas sparging in these types of bioreactors.

In order to overcome these limitations, several studies have been performed in a Couette flow bioreactor (CFB) (Janes et al., 1987, O'Connor et al., 2002, Sahoo et al., 2003, Sun and Linden, 1999). In a CFB, the fermentation broth is entrapped in the small annular section of the two concentric cylinders with inner or outer cylinder rotating at a constant speed. For a thin annular space, almost constant shear rate can be assumed (Bird et al., 2006). Indeed, operating coaxial cylinder bioreactors with the outer cylinder rotating leads to laminar Couette flow and thus uniform shear stresses within the annulus (Curran and Black, 2005a). A bioreactor with an outer rotating cylinder provides

operations at higher Reynolds number (Schlichting, 1955) compared to bioreactors with an inner rotating cylinder.

Another important design consideration is the method used to provide oxygen to the fermentation broth. As mentioned earlier, it is very difficult to separate the effect of shear caused by mixing and that caused by bubble formation and coalescence during gas sparging. Therefore, in this study, aeration is provided by diffusing air through a membrane fixed to the external surface of the inner cylinder. Oxygen flux to the fermentation broth can be varied by manipulating the pressure or by changing the oxygen content of the feed gas.

CFBs have been successfully used in the past to study the effect of shear on the growth of different microorganisms, particularly in culture suspensions of plant or animal cells (Sahoo et al., 2003, Wong et al., 2001). However, these bioreactors were small in size, typically less than 1 L, and usually run in batch mode. Another constraint in the study of shear effect on microorganisms lies in the fact that its effect is time-dependent (O'Connor et al., 2002) and, therefore, it is important to perform these studies by exposing the cells to similar residence times as would prevail during the fermentation.

Considering all of the above-mentioned characteristics and constraints, the novelty in the CFB designed for this investigation consists in its larger volume (5 L) compared to previous studies and that it can be operated in batch or continuous mode for days. Process parameters such as pH, dissolved oxygen and temperature are also measured and controlled throughout the fermentation without disturbing the shear field.

In the present study, the application of CFB for the study of shear stress on filamentous microorganism was done by performing experiments using the industrially important fungi *Trichoderma reesei* used for the production of cellulase enzyme. Mitard and Riba (1988) performed experiments in a CFB using *A. niger* but oxygen was provided by sparging air and the morphology analysis in their study was performed on the pellet form instead of filamentous form encountered as in *T. reesei* fermentation. Previous studies have shown that growth and enzyme production of *T. reesei* are influenced by shear stress. However, these experiments were performed in bioreactors with non-uniform mixing and gas sparging (Lejeune et al., 1995). Even in such conditions, thorough investigations have been performed involving biomass and protein production but very

few studies have been done involving correlating morphology, growth and enzyme production. Therefore in the present study, samples were analyzed for biomass, protein production and activity, and the influence of shear on the morphology of microorganism was also examined.

9.2 MATERIALS AND METHODS

9.2.1 Microorganism

The strain used throughout this work was *T. reesei* RUT C-30 (ATCC 56765). The glycerol stock solutions of spores were maintained at -80°C and were transferred on potato dextrose agar plates. New plates were prepared every month and kept at 4°C.

9.2.2 Cultivation method

The culture medium (5 L) contained: lactose, 5 g/L; $(NH_4)_2SO_4$, 1.4 g/L; KH_2PO_4, 2.0 g/L; $MgSO_4 \cdot 7H_2O$, 0.3 g/L; $CaCl_2 \cdot 2H_2O$ (autoclaved separately), 0.3 g/L; $FeSO_4 \cdot 7H_2O$, 5.0 mg/L; $MnSO_4 \cdot 7H_2O$, 1.6 mg/L; $ZnSO_4 \cdot 7H_2O$, 1.4 mg/L; $CoCl_2 \cdot 6H_2O$, 2 mg/L, peptone, 2 g/L and yeast extract, 0.5 g/L. The pH of the medium was initially adjusted to 4.0. Medium was autoclaved for 20 minutes and then transferred to the bioreactor under sterile conditions. Shake flask cultures were performed with a volume of 250 mL in a 1-L Erlenmeyer flask with three baffles. The spore concentration was calculated using a Petroff Hausser counting chamber (Hausser Scientific, Horsham, PA) and an appropriate volume was inoculated in the flask to obtain an initial concentration of 5×10^3 spores/mL. Flasks were kept in an orbital shaker at 200 rpm and 28°C for 55 h.

9.2.3 Analysis

A 25-mL samples was collected approximately every 12 h. One mL of each sample was used immediately for image analysis and the remaining sample was stored at 4°C pending further analysis. The amount of biomass was quantified by dry weight analysis. Samples of the culture broth were filtered through a pre-dried and pre-weighted glass fiber filter (grade A/E, Gelman Sciences, MI) and washed with two parts of deionised distilled water and oven dried for 24 h at 95°C. The weight of the sample was then measured after a 24-h period of cooling in a desiccator. Protein concentration was determined using the Bradford assay with bovine serum albumin (BSA) as standard. Filter paper (FPA) and carboxymethyl cellulose (CMC) activities were determined as per

the IUPAC protocol (Ghose, 1987). Glucose and lactose concentrations were determined using YSI glucose analyzer (YSI Incorporated, USA) and enzymatic kit (Boehringer Mannheim, Germany), respectively.

For image analysis measurements, a monochrome camera (CoolSnap ES, Roper Scientific, Tucson, AZ) mounted on an Olympus IX81 microscope (Olympus, Melville, NY) was used. The automated stage of the microscope was controlled by the Image-Pro® Plus software (Image-Pro® Plus version 5.1, Media Cybernetics, Silver Spring, MD). Image analysis was performed according to protocol described by Lecault et al. (2007).

9.2.4 Design of Couette Flow Bioreactor

The main objective of growing microorganisms in a CFB is to provide uniform and defined shear conditions. Therefore, the two cylinders of the reactor should be very well aligned and have smooth surfaces. Additional design considerations for fungal fermentation included the larger size of microorganism compared to plant and animal cells, their ability to grow on the bioreactor wall and the formation of foam, especially in *T. reesei* fermentations.

9.2.4.1 REACTOR VOLUME

It is very important that the total volume collected during sampling in the batch phase does not significantly affect the fermentation. Based on this consideration, the CFB was designed to operate with a volume of 5 L such that it will be possible to retrieve a 25-mL sample every 12 h during the batch phase which represents less than 5% of the reactor volume.

9.2.4.2 SHEAR FIELD

Shear rate at any radial position 'r' in the annular section between two concentric cylinders with a rotating outer wall can be calculated by Equation (9.1).

$$\dot{\gamma}(r) = 2\ \Omega\ \frac{\left(\frac{k\, r_o}{r}\right)^2}{1 - k^2} \tag{9.1}$$

where k is the ratio of inner to outer radii (r_o) and Ω is the angular velocity of the outer cylinder. For a small annular space, k tends to one and as shown in Equation (9.1), the shear rate is nearly constant (Sahoo et al., 2003). Therefore, the inner and outer radii were selected such that k was close to 1 but leaving enough volume for the desired reactor size.

An inner radius of 8.89 cm (3.5") and an outer radius of 10.16 cm (4") were selected to give a value of k equal to 0.875. Table 9.1 shows the average shear rate at different rpm in the CFB designed in the present study. The effective working height of the reactor was approximately 66 cm to provide a working reactor volume of 5 L. As shown in Table 9.1, the CFB designed in the present study can achieve shear rates typically encountered in a stirred tank bioreactor (Metzner and Taylor, 1960).

Table 9.1 – Shear rate in Couette Flow Bioreactor

rpm	Shear Rate $\dot{\gamma}$ (s^{-1})
100	78.15
200	156.30
300	234.45
400	312.60

The rheological behaviour of filamentous microorganism changes from Newtonian to non-Newtonian as the viscosity increases due to either an increase in biomass concentration, a change in morphology or product formation. In this work, shear rate has been calculated on the assumption that the medium is Newtonian, which is acceptable (based on the previous studies performed in our laboratory (Malouf, 2008) due to the relatively low biomass concentration (maximum 3.0 g/L) of *T. reesei* obtained in the CFB. Similar observation and assumption have been made at low biomass concentration for other filamentous microorganisms such as *Penicillium chrysogenum* (Jüsten et al., 1996).

9.2.4.3 OXYGEN SUPPLY AND REQUIREMENT

There are two main design considerations regarding oxygen supply. First, the oxygen supply should be able to meet the oxygen demand of the microorganisms and, second, the oxygen needs to be supplied by diffusion through the membrane rather than bubbling in order to minimize disruption of the shear field.

In a hydrophobic microporous membrane such as polypropylene (PP), polysulfone (PS) and polytetrafluoroethylene (PTFE), the pores are filled with gas and water does not wet its surface. This is preferred in membrane bioreactors since it decreases the attachment of microorganism on the membrane surface (bio-fouling) and also, the mass transport resistance is considerably smaller than in a hydrophilic membrane, where the pores are filled with water (Côté et al., 1988, Schneider et al., 1995). However, one of the disadvantages of these membranes is that the pressure on the gas phase cannot be increased above the bubble point because gas bubbles may appear in the liquid (low bubble point). This limits the selection of an operating gas pressure with porous membranes (Côté et al., 1988, Reij et al., 1998). On the other hand, in a dense hydrophobic membrane such as silicone based, the gas is absorbed on the membrane material and diffusion takes place within the dense polymer. This type of membrane allows operation at higher gas pressure to achieve adequate aeration without forming air bubbles. These membranes have been used in many applications such as waste water treatment (Suzuki et al., 1993) and gas permeable bioreactors (Schwarz and Anderson, 1998). However, the gas film resistance of microporous membrane is 10-150 times smaller than the resistance of dense membrane (Reij et al., 1998).

To take advantage of both types of membranes, a composite membrane consisting of a thin top layer (<1-30 μm) of dense material over a highly porous support layer such as non-woven polyester or a microfiltration membrane (PS or polyvinylidine fluoride (PVDF)) can also be used. Though Schwarz and Anderson (1998) have suggested that if the pore size is 1 μm or less, a coating of dense material is not preferred.

Therefore in the present study, a commercially available microporous hydrophobic PTFE membrane with 0.2 μm pore size and 139 μm thickness (TF-200, 10" x 10", Pall Corporation, USA) was used in the CFB. This membrane does not have any coating of dense polymer but has a polypropylene (PP) backing for support. Advantages of a PTFE membrane are its high chemical resistance and mechanical strength. Also, the PTFE membranes have been successfully used in the past to provide sufficient oxygen for cell growth (Sahoo et al., 2003, Schneider et al., 1995). In order to eliminate as much as possible cell attachment, the backing was facing the gas side to avoid cell attachment. Reij et al. (1998) cite that during long operations, polysaccharides might absorb on the

membrane causing a decrease in critical pressure and subsequently allow liquid to flow through the pores.

9.2.4.4 COUETTE FLOW BIOREACTOR

Based on the above considerations, a CFB was designed and built as shown in Figures 9.1 and 9.2. It consists of a stainless steel inner cylinder with holes, an outer cylinder made of Plexiglas and a top cover plate (Figure 9.1). As mentioned earlier, the annular space between the inner and outer cylinders where the microorganism are grown is ca. 1.27 cm and the ratio of radii of inner to outer cylinder is 0.875. The inner cylinder has a total of 756 holes with a diameter of 1 cm, thus providing a total aeration surface area of 0.0594 m^2.

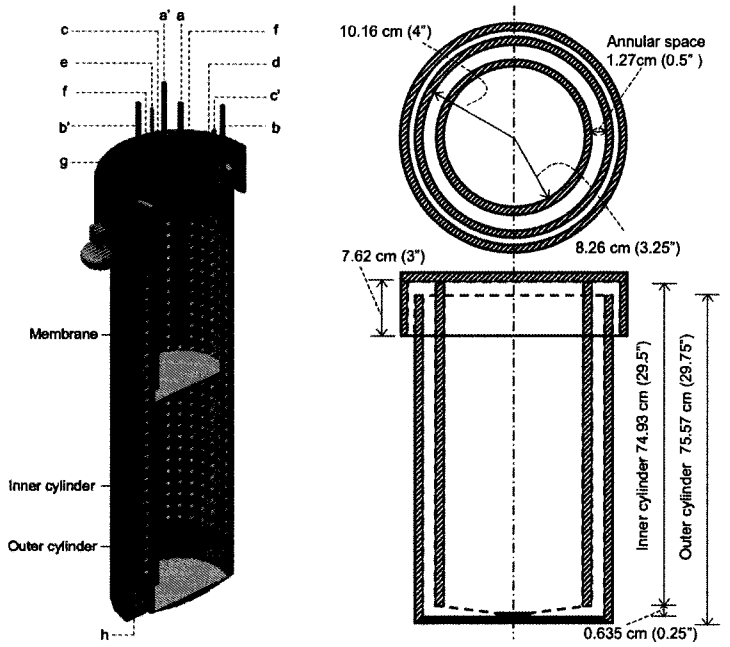

Figure 9.1 – Dimensions and schematic diagram of CFB with ports for air supply and removal from the top (a & a') and the bottom chamber (b & b'), sample recirculation (c and c'), substrate addition (d), NH_4OH addition (e), sterile N_2 flow over the medium surface (f), antifoam or water addition (g), and drainage at the bottom (h).

The PTFE membrane was cut into small pieces and smoothly attached to the external surface of the inner cylinder (Appendix C). Different adhesives such as Contact Cement (LePage, Henkel Canada Corporation, ON) applied using rollers, Super 77 adhesive (3M Corporation, USA) applied by spraying and silicone based sealant (Silicone II, GE, USA) were tested. Silicone presented good results perhaps due to its hydrophobic nature.

Rollers attached on the top plate were adjusted to centrally align the outer Plexiglas cylinder. The outer cylinder was rotated using a motor connected at the bottom of the reactor. Due to the hydrostatic pressure of the fermentation medium and given that only a small pressure gradient can be applied across the membrane, the inner cylinder was divided into two chambers with separate air flow and pressure regulators. Also, as shown in Figure 9.2, the medium was continuously circulated through a probe holder where pH and dissolved oxygen (DO) were measured. A 3-way valve in the circulating system was used to periodically collect samples.

9.2.4.5 CONTROL AND MEASURMEMENT

As indicated on the schematic diagram of the CFB shown in Figure 9.1, there are two ports for air inlet and two ports for air exhaust for each chamber. Air flow was kept constant using mass flow controllers and the air pressure inside both chambers was maintained just below the bubble point using pressure relief valves (Straval, NJ, USA). As mentioned earlier, the bubble point at the bottom part of the reactor was higher than at the top section due to the effect of the hydrostatic pressure and, thus, a higher pressure was maintained in the bottom chamber.

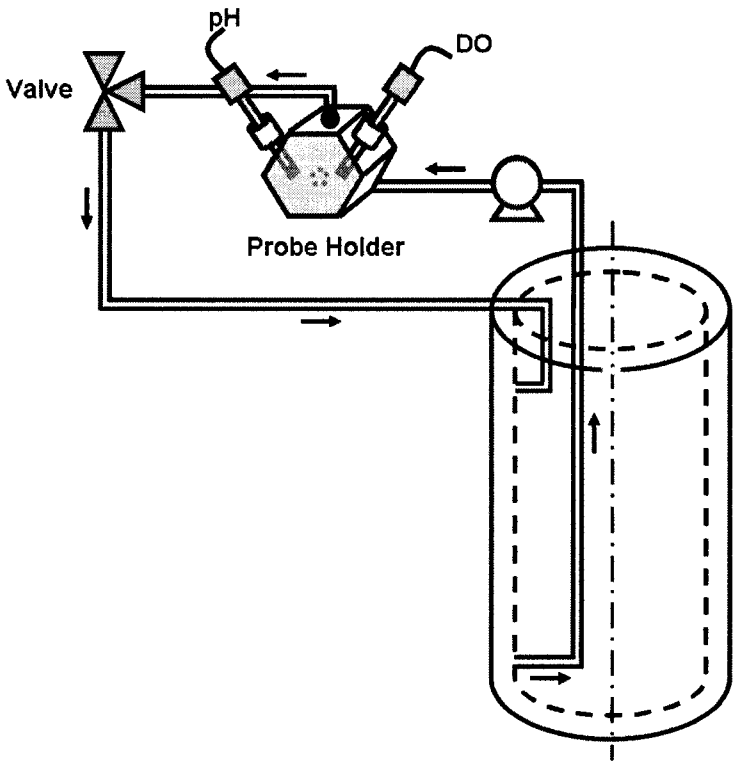

Figure 9.2 – Schematic diagram of the recirculation system in the CFB.

As previously mentioned, one of the objectives of using a CFB was to perform experiments in continuous mode. Therefore, the reactor includes ports for acid/base and substrate addition. Both pH (Van London pHoenix Company, Texas, USA) and DO (Broadley-James Corporation, Irvine, CA) probes were calibrated before connecting them to the probe holder through which the medium was continuously circulated. Also, the reactor has an opening on the top for the addition of an anti-foaming agent as well as water to compensate for any loss by evaporation. Finally, the complete reactor setup, including the measurement and control system, was enclosed in a chamber with temperature controlled at 28°C. The temperature of the fermentation medium was verified using the dissolved oxygen probe which could also measure temperature

9.2.4.6 STERILIZATION

The sterilization of the CFB could not be done in an autoclave and therefore chemical sterilization was performed instead. The stainless steel inner cylinder and the top cover plate as well as the PTFE membrane are chemical resistant and did not present a concern regarding the type of sterilizing product. Furthermore, the PTFE membrane acts as sterile filter for air diffusing from the inner cylinder to the annular space. However, the outer cylinder is made of Plexiglas and it is more prone to damage by the chemical sterilization. Ethanol, methanol and bleach (sodium hypochlorite) were tested as sterilization solvents. The latter was selected as it was found to be suitable even after long exposure times. Commercially available bleach (Javex, 5.25% sodium hypochlorite) was diluted by adding 1 part bleach to 6 part water. The annular space was filled with bleach and all but the air flow ports were sterilized as well by passing bleach through them. Bleach was also circulated through the sampling tube and probe holder. Sterile filters were connected to the air and nitrogen ports and air flow was started during the chemical sterilization process. After approximately 10 minutes, the bleach solution was removed from the bottom port which has a quick connect and the reactor was completely rinsed with sterile water before the addition of medium and inoculum.

9.2.4.7 EXPERIMENT

Following the CFB sterilization, the autoclaved medium was added to the reactor through the feeding port under sterile conditions and the rotation of the outer cylinder was started. Later, the feeding port was connected to the lactose solution reservoir and

ammonium hydroxide (NH_4OH) solution was connected to the pH port for a one-sided pH control. The inoculum was then added to the bioreactor through the 3-way valve. Throughout the experiment, the medium was continuously circulated and samples were collected approximately every 12 h. The pressure in the top and bottom chambers was monitored regularly and kept below the bubble point as explained previously. A small flow of sterile nitrogen or air was also passed in the headspace of fermenter to create a positive pressure relative to ambient pressure in order to prevent contamination. During the batch phase, additional water was added to compensate for evaporation. For all experiments in the CFB, the addition of antifoam was not required.

9.2.5 Control Strategies

When the initial lactose was consumed at the end of the batch phase, a 5 g/L of lactose monohydrate solution was then continuously added such that the DO could be maintained above the critical dissolved oxygen of 20% (Schafner and Toledo, 1992). The pH was kept above 3.5 by addition of a 3.5% v/v solution of NH_4OH so that the pH does not affect negatively the protein production and growth of *T. reesei* (Gallo et al., 1981, Sternberg, 1976).

9.3 RESULTS AND DISCUSSION

9.3.1 Oxygen mass transfer coefficient

Prior to performing fermentation in the CFB, the ability of the membrane aeration system to provide an adequate oxygen supply to sustain the biochemical reaction has been investigated by estimating the overall oxygen mass transfer coefficient (K_La) with distilled deionized water at various speeds of rotation of the outer cylinder. For each experiment, the level of dissolved oxygen was reduced to zero by gassing out using nitrogen with the outer cylinder rotating. When the DO concentration was nearly zero, a set pressure of air was maintained on the inner side of the membrane. The DO level was recorded as a function of time until nearly saturation was achieved. Figure 9.3 presents the four plots that were obtained at the four rotation speeds.

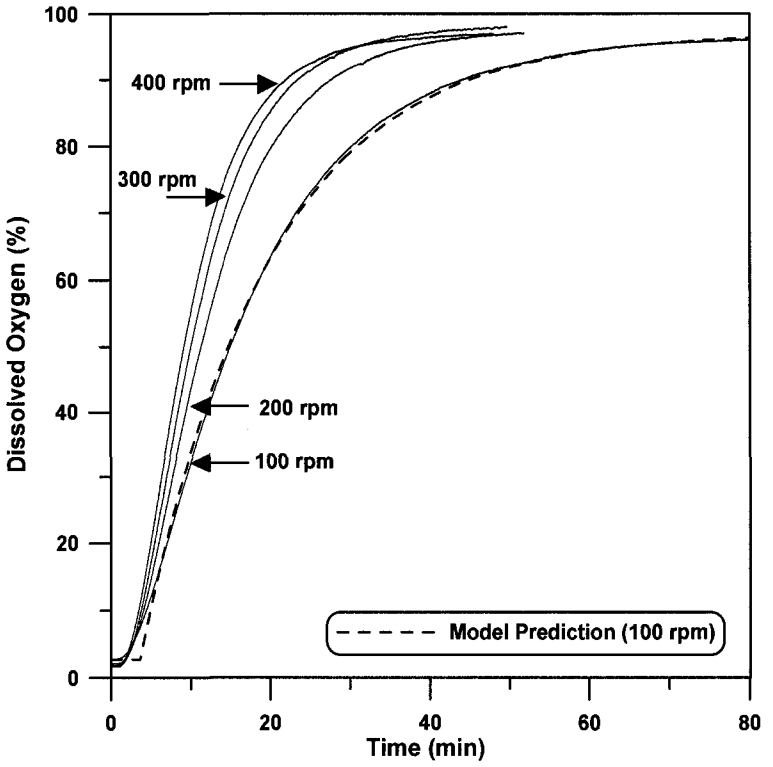

Figure 9.3 – Profile of dissolved oxygen concentration as a function of time at different rpm. Predicted dissolved oxygen concentration for run at 100 rpm is also shown.

Performing an oxygen mass balance on the system and assuming the mass transfer resistance on the gas side is negligible compared to the resistances due to the liquid side and the membrane, the oxygen flux density (N_{O_2}) across the active part of the membrane can be expressed by the following equation:

$$N_{O_2} = \frac{C_L^* - C_L}{\frac{1}{K_L} + \frac{1}{P_M}} = K_{L,e}\left(C_L^* - C_L\right) \tag{9.2}$$

Knowing the oxygen flux density across the membrane, it is possible to calculate the change of the dissolved oxygen in the liquid medium. Assuming a uniform concentration in the liquid, the following dynamic mass balance applies:

$$\frac{dC_L}{dt} = N_{O_2}\left(\frac{A}{V_L}\right) = K_{L,e}a\left(C_L^* - C_L\right) \tag{9.3}$$

It is therefore possible to determine the value of K_La that will minimize the sum of squares of the errors between the experimental DO concentration and the predicted one. The fit can be performed individually for each speed of rotation to determine the effective

$K_{L,e}a$ or for the four speeds of rotation simultaneous to determine the four K_La values and the membrane permeability (P_M). The results obtained are presented in Figure 9.4. It is observed that the oxygen mass transfer increases with the speed of rotation, as expected.

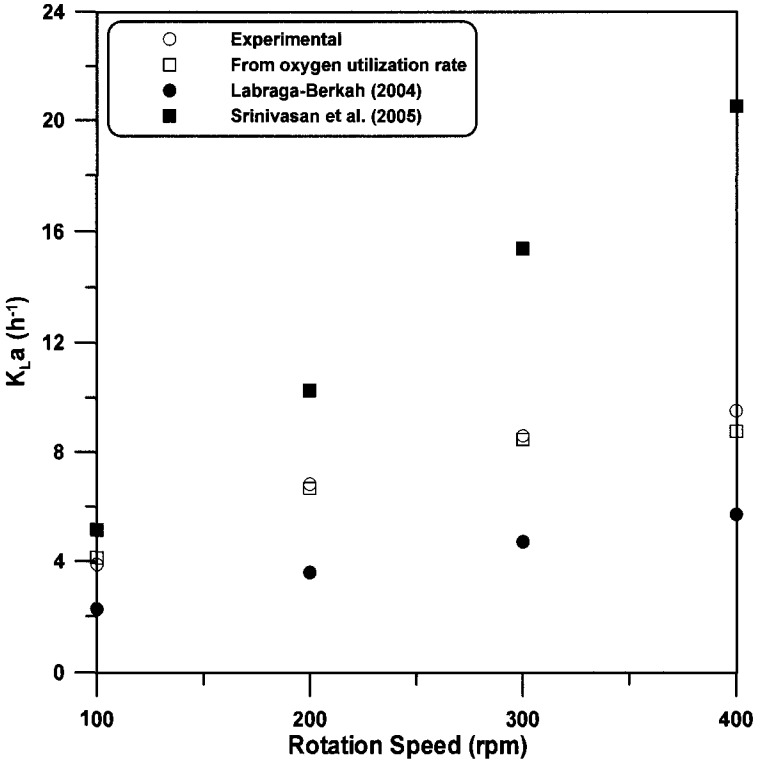

Figure 9.4 – Experimental and predicted oxygen mass transfer coefficient at different speeds of rotation of the outer cyliner.

The results were compared with available correlations for similar systems. However, it was not possible to find a correlation to predict the oxygen mass transfer coefficient that would apply directly to the present bioreactor. Two Sherwood-Reynolds-Schmidt type correlations were retained: Srinivasan et al. (2005) (equation 9.4) and Labraga and Berkah (2004) (equation 9.5).

$$Sh = \frac{12}{\ln\left(r_o/r_i\right)}\frac{\left(r_o - r_i\right)}{\left(2\times r_i\right)} + 0.0048\ Re\ Sc^{1/3}\left[\frac{r_i}{r_o}\right]^{-1.25} \tag{9.4}$$

$$Sh = 0.135\left[\left(0.5\ Re^2\right)\ Sc\right]^{1/3} \tag{9.5}$$

The predictions of K_La with these two correlations using the appropriate definition of Re number are presented in Figure 9.4. On the average, the first correlation over predicts by a factor of 1.6 whereas the second one under predicts by a factor of 1.78. Correlations

proposed by Curran and Black (2005a, 2005b) for K_La in a coaxial bioreactor with the inner cylinder rotating could not be used because these correlations were derived for a bioreactor working volume of more than two orders of magnitude smaller that our 5-L CFB leading to Re number far outside the range of applicability of these equations. These correlations over predicted K_La by one order of magnitude. Similarly, K_La predicted by the correlation of Sherwood et al. (1975) that was used by Sahoo et al. (2003) in their study in a 0.25 L CFB were 7 times smaller than the experimental one. To obtain this prediction, it was also necessary to extrapolate outside the range of validity of this correlation.

Finally, it was decided to also use the average substrate feed rate and DO concentration during the continuous phase for experiments performed at the four speeds of agitation to estimate the oxygen utilization rate and in turn the value of K_La that had to prevail to maintain the average DO within the CFB.

$$K_La = \frac{OUR}{C_L^* - C_L} \tag{9.6}$$

The oxygen uptake rate (OUR) under steady state was calculated based on the assumption that 55 % of the carbon fed to the bioreactor is combusted. The results of this analysis are presented in Figure 9.4. The results obtained are very close to the experimental K_La values that were obtained in water which tend to confirm that the oxygen mass transfer coefficients obtained in this investigation do indeed apply.

9.3.2 *T. reesei* Fermentations in CFB

Four experiments at 100, 200, 300 and 400 rpm were performed in the CFB using *T. reesei* RUT C-30. One of the concerns during the fermentation experiments, especially those carried out for long periods of time, was the effect on the membrane. The membrane proved to be resistant and fermentations at the four shear rates were performed without having to replace the membrane. Another concern during the fermentation runs involved biomass attachment to the membrane. In the current study, it was observed that at 100 rpm, a small amount of biomass adhered at a few sites on the membrane. However, there was no biomass growth either on the membrane or on the reactor surface during the fermentation runs at 200, 300 and 400 rpm.

To study the effect of the type of substrate on the growth, protein production and morphology of microorganism, the lactose solution was replaced by a glucose solution (5 g/L) after 95 h and 97 h for experiments performed at 300 and 400 rpm, respectively. Only for the fermentation carried out at 400 rpm, the glucose solution was replaced again by a lactose solution (5 g/L) at 143 h in order to examine the effect of switching back to the substrate (lactose) used previously in the first part of the fermentation run.

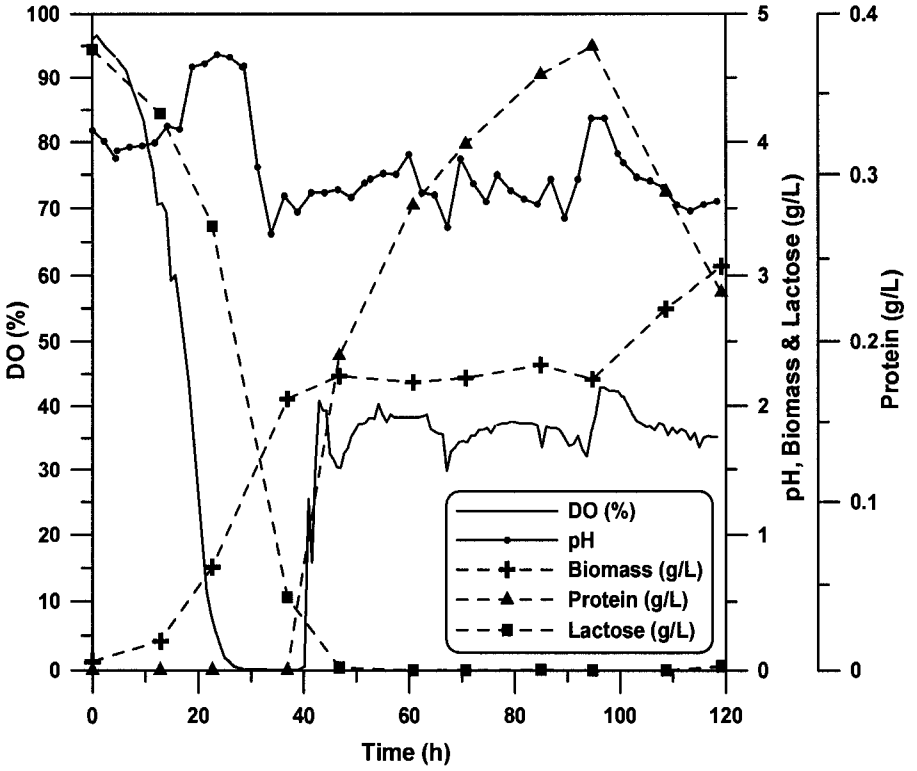

Figure 9.5 – Profile of biomass, DO, lactose, pH and protein production in CFB operating at 300 rpm.

Figure 9.5 shows the profile of biomass concentration, DO, lactose concentration, pH and protein production for the experiment performed at 300 rpm. When the lactose solution supplied during the batch phase was completely consumed, the DO started to increase and the continuous mode of operation was started. At this point, the same substrate as the one used in batch phase was fed such that the DO would be maintained above 20%. The pH initially increased and then dropped to 3.5, where a one-sided pH control was initiated using a 3.5% v/v NH_4OH solution. These represent typical profiles obtained in all experiments that were performed except that the rate of change and

concentration levels of all variables changed with the shear rate. These profiles will be examined in the following sections.

9.3.2.1 EFFECT OF SHEAR ON GROWTH AND PROTEIN PRODUCTION

Figure 9.6 (a) shows the biomass concentration obtained during the growth of *T. reesei* in the CFB at different speed of rotation and, consequently different shear rates. During the batch phase of the four runs, the biomass concentration was between 2 to 2.5 g/L. Biomass concentration was almost constant during the continuous phase for all runs except for the one carried out at 100 rpm, where a decrease in biomass concentration was observed. This decrease could be due to the lower oxygen mass transfer at 100 rpm and therefore, under the continuous phase, biomass concentration progressively decreased until it reached steady state where biomass was removed at the same rate that it was produced.

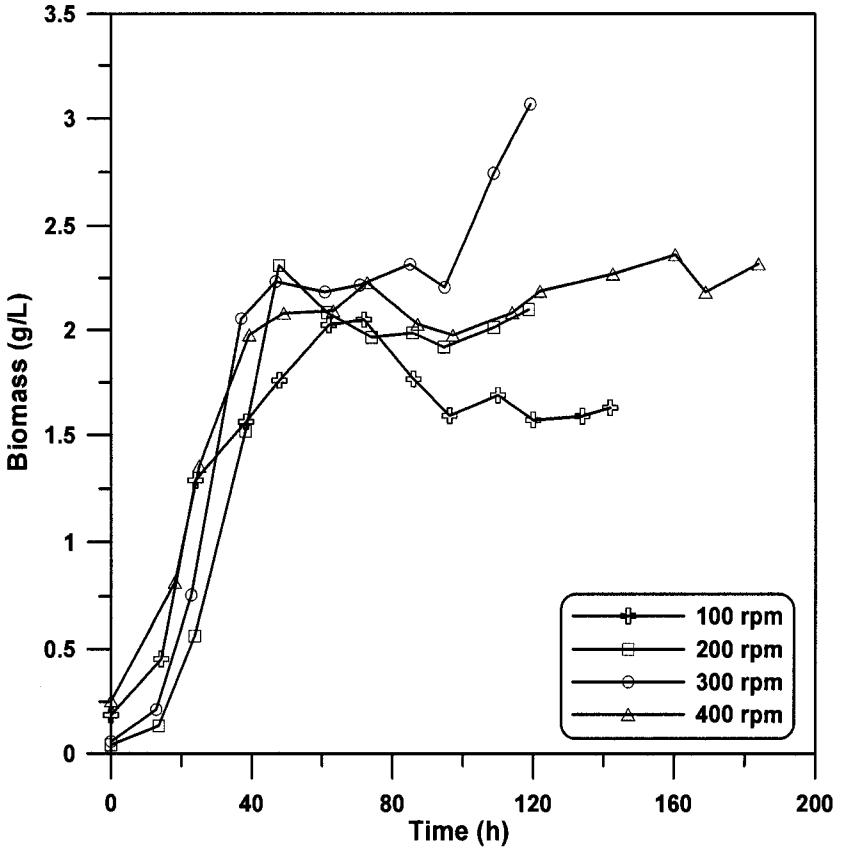

Figure 9.6 (a) – Profile of biomass production as a function of fermentation time in CFB.

The effect of shear on protein production is shown in Figure 9.6 (b). Protein production started when the lactose concentration reached a low value (data not shown). For the run

at 400 rpm, the protein production started earlier but the production rate decreased as fermentation progressed. Although highest FPA activity was obtained at 200 rpm, there was no specific trend on the FPA activity as shear rate was increased. However, the CMC activity (Figure 9.7) was lower during the run at 400 rpm compared to other fermentation runs. These results are similar to the finding of Mukataka et al. (1988) who performed experiments with *T. reesei* QM9414 to study the effect of agitation intensity on the cellulase components. As the agitation intensity was increased, both FPA and CMC activities increased. However, when the speed of the tip of the impeller was 1.0 m/s, the CMC activity was 25% lower than at 0.7 m/s. On the other hand, for a speed range of the tip of the impeller of 0.7 to 1.4 m/s, the difference in FPA activities was not significant.

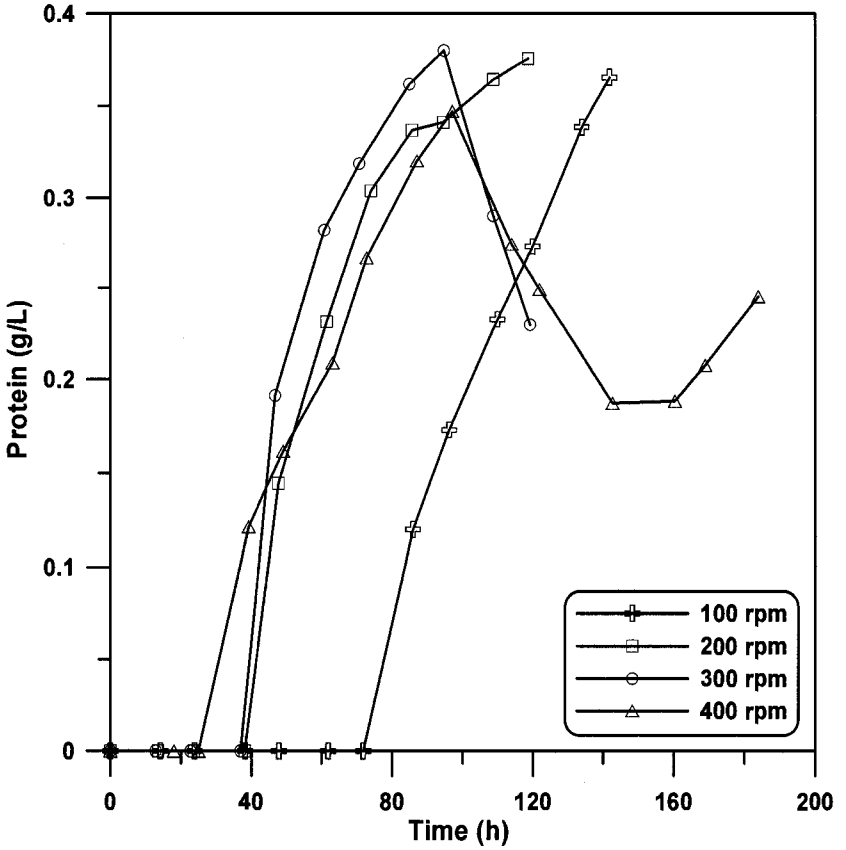

Figure 9.6 (b) – Extracellular protein produced as a function of fermentation time in CFB.

When the substrate was changed from lactose to glucose in the runs carried out at 300 and 400 rpm (after 95 and 97 h, respectively), an increase in biomass production and decrease in protein concentration were observed. These changes were expected since glucose is not an inducer for cellulase production (Kubicek and Penttilä, 1998) similar to

lactose (Domingues et al., 2001). It is important to stress that a continuous mode of operation prevailed in the CFB such that, following the growth in the lactose medium, a decrease in the production rate resulted in a progressive decrease in the protein production of the fermentation broth. Protein production resumed when the substrate feeding was switched back to lactose after 143 h for the experiment carried out at 400 rpm. Similar trends were observed for FPA and CMC activity as shown in Figure 9.7.

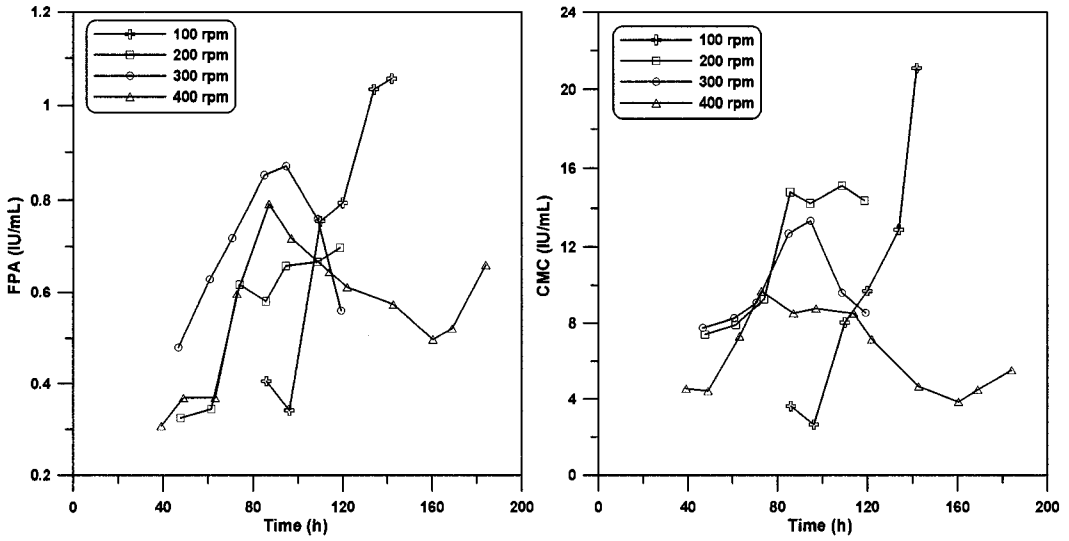

Figure 9.7. Filter paper (FPA) and carboxymethyl cellulose (CMC) activity as a function of fermentation time.

9.3.2.2 EFFECT OF SHEAR ON MORPHOLOGY

The effect of shear on the morphology of *T. reesei* is shown in Figure 9.8. This figure displays the percentage area fraction of the microorganism that was classified as either unbranched, branched, entangled or clumped. It should be pointed out that the high clump percentage area fraction observed at the start of all experiments is due to the inoculum growth in the shake flask cultivation under low shear conditions. These trends were similarly observed during the characterization of *Streptomyces olindensis* in submerged fermentation (Pamboukian et al., 2002).

It is clear from Figure 9.8 that shear had a significant impact on the fragmentation of the microorganism during the continuous phase but little impact during the growth phase indicating that young and growing cells are very resistant to high shear (Lejeune et al., 1995). Fragmentation leading to the formation of unbranched microorganism was higher for the run performed at 400 rpm compared to other experiments, which could be a sign

of negative impact of excessive shear on the microorganism. The latter could also explain the decrease in protein production rate for the run carried out at high shear rate (400 rpm). Another interesting observation is the increase in fragmentation when the substrate was switched from lactose to glucose for the runs at 300 and 400 rpm.

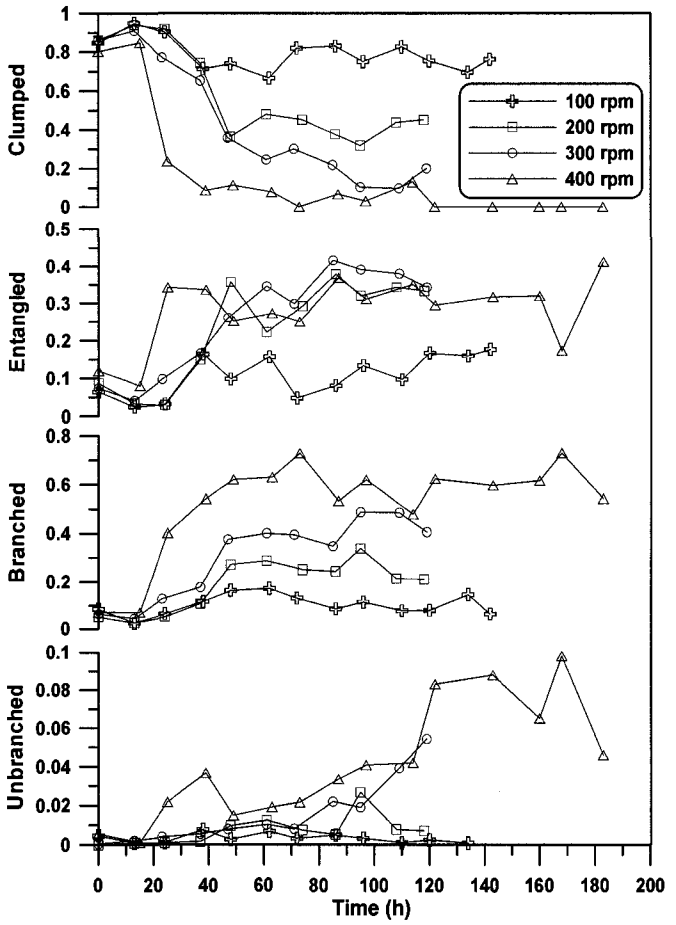

Figure 9.8 – Morphological classification of microorganism as unbranched, branched, entangled or clumped as a function of fermentation time on area basis.

The effect of shear on the fragmentation can also be shown by the dentritic length, which is the total length of a microorganism. Figure 9.9 shows the dentritic length for the branched microorganisms. Higher dentritic lengths were obtained when the experiment was performed at 100 rpm indicating that longer fungi grow at lower shear rates. Marten et al. (1996) also observed shorter mycelium at higher agitation (high shear) rates using the same strain as used in this study. Shorter filaments due to higher shear rates do not necessarily mean a negative effect on the product formation. During the fermentation with *Aspergillus niger*, shorter filaments were found to be appropriate for citric acid

production (Papagianni et al., 1994). Further, Marten and coworkers (1996) found that shorter mycelium obtained at higher agitation led to higher yield stress and viscosity. Therefore, along with morphology, rheological characterization will help to further improve our understanding of the complex interrelationship that exists between various process parameters in a submerged fermentation.

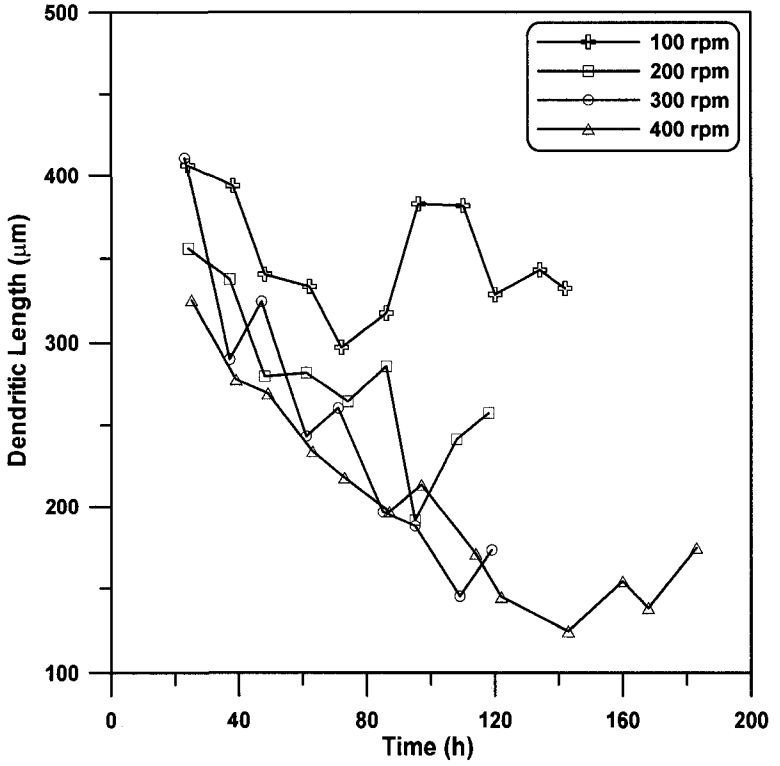

Figure 9.9 – Dentritic length of branched microorganism as a function of fermentation time for different rotation speeds.

Interestingly, the microorganism thickness was influenced by both the shear rate and the type of substrate used (Figure 9.10). During the course of the batch phase, the thickness of the cells increased except for the run carried out at 400 rpm. Subsequently, in the continuous phase, the cell thickness presented two trends. In those experiments performed at 100 and 200 rpm, the cell thickness decreased but in the experiments carried out at 300 and 400 rpm, it remained constant. In summary, when there was protein production and the biomass concentration was constant, the cell thickness either decreased or remained constant suggesting secondary metabolism related to cellulase production. Velkovska et al. (1997) divided the *T. reesei* RUT C-30 fermentation using solka floc as substrate into 5 stages and also observed thinner filament morphology in the

later stages (fourth) corresponding to both rapid product formation and substrate depletion. This conclusion was also supported when the substrate was switched from lactose to glucose. As mentioned earlier, this substrate change was only performed during the continuous phase for experiments carried out at 300 and 400 rpm. During this period, the cell thickness increased as the protein production decreased and biomass concentration increased. Finally, the cell thickness started to decrease again when substrate feeding was switched back to lactose for run at 400 rpm. Similar trends in cell thickness were found during the fermentation of *Trichoderma harzinium* in a stirred tank bioreactor (Serrano-Carreón et al., 1997).

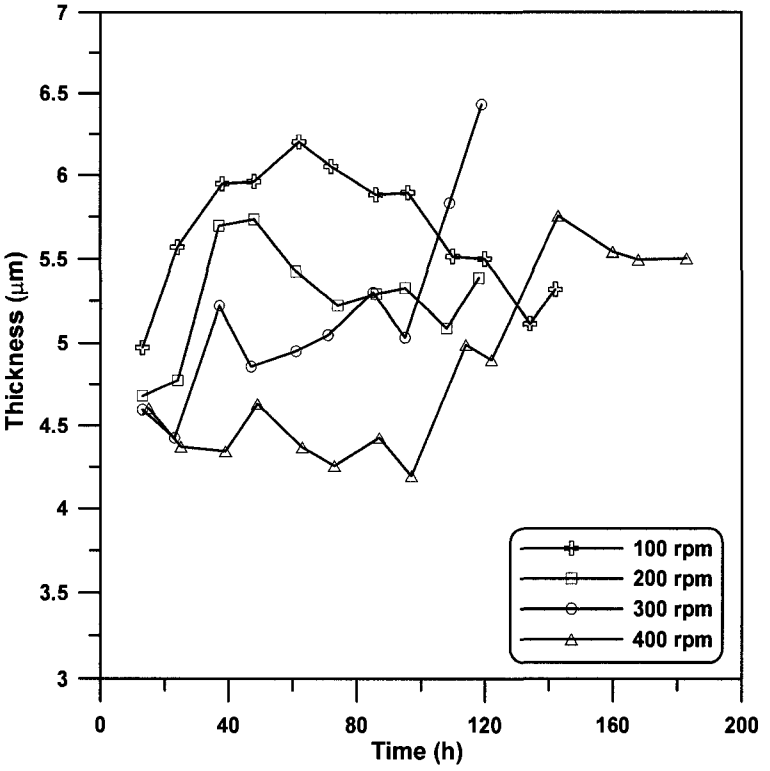

Figure 9.10 – Average thickness of microorganism as a function of fermentation time for different rotation speeds.

The increase in cell thickness and biomass concentration is due to the accumulation of storage material such as lipids during the early growth phase and later due to the degradation of the storage material causing a decrease in cell thickness. Although, for experiment performed using *Aspergillus niger*, higher agitation caused smaller but thicker hyphae which was advantageous to the citric acid production (Papagianni et al., 1994). Similarly Matsumura et al. (1981) developed a model for the fermentation of

Cephalosporium acremonium which was based on the assumption that swollen hyphal fragments formed during gradual substrate limitation were preferred for antibiotic production. For the experiments performed in this study using *T. reesei* Rut C-30, thinner hyphae were observed during the production phase.

9.4 CONCLUSIONS

A CFB was designed and successfully used to study the impact of shear on the growth, protein production and morphology of the filamentous microorganism *T. reesei* Rut C-30. The CFB presented in this study differs from similar bioreactors used to study the effect of shear on microorganism in its large volume, ability to conduct experiments in batch and continuous modes for days (as opposed to hours in previous studies) and perform measurement and control of various process parameters such as DO, pH and temperature. Shear was found to impact protein production and activity at higher shear rates (400 rpm). Also, morphological characterization revealed that shear had a significant influence on the fragmentation and thickness of the microorganism. Length of the filaments (dentritic length) decreased with the increase in shear rate but was not found to have any significant link with either protein production or the type of substrate for the operating conditions used in this study. On the other hand, thickness was found to be an important morphological parameter to monitor during the *T. reesei* fermentation. Thinner hyphae were observed during the growth in lactose medium and also during the protein production phase.

Further modification to the current CFB design could be done to improve the performance. In the present study, a commercially available membrane was used. Further research on the selection or design of newer membranes will help to achieve more oxygen supply to the microorganism. Wong et al. (2001) spun an oxygen permeable silicon-layer on a porous ceramic bowl to overcome oxygen limitation during cultivation of carrot cell cultures. However, the bowl diameter was only 101.6 mm. The CFB presented here can be further used to study the influence of shear on many other important parameters. Rocha-Valadez et al. (2007) during *T. harzianum* experiments found smaller clump diameter for runs performed under higher specific energy dissipation rate and also a strong relationship between rheology and fungal morphology

(clump diameter). Therefore, further studies in *T. reesei* in CFB could be performed to better understand the effect of process parameters. For example, it could be used to investigate the effect of shear on the individual cellulase components, sporulation response (Sahoo et al., 2004), rheology of fermentation broth (Mitard and Riba, 1988, O'Connor et al., 2002), viability (Abu-Reesh and Kargi, 1989), and intracellular metabolite content which could influence the growth and product formation. Further, this information can be used to better design large scale bioreactors since the average shear field is an important consideration during the scale-up of bioreactors.

9.5 NOMENCLATURE

A surface area available for aeration (m^2)

C_L dissolved oxygen concentration (mol/m^3)

C_L^* dissolved oxygen concentration in equilibrium with mean gaseous oxygen concentration (mol/m^3)

CFB Couette flow bioreactor

DO dissolved oxygen (%)

k ratio of inner to outer radii of the concentric cylinders (–)

K_L oxygen mass transfer coefficient (m/s)

$K_{L,e}$ effective oxygen mass transfer coefficient (m/s)

K_La overall oxygen mass transfer coefficient (s^{-1})

$K_{L,e}a$ overall effective oxygen mass transfer coefficient (s^{-1})

N_{O_2} oxygen flux density ($mol/m^2.s$)

OUR oxygen uptake rate (mol/L.s)

P_M membrane permeability (m/s)

r radial distance in the annular section between two concentric cylinders (m)

r_o radius of the outer cylinder (m)

r_i radius of the inner cylinder (m)

Re Reynolds number (–)

RPM revolution per minute

Sc Schmidt number (–)

Sh Sherwood number (–)

t time (s)

V_L liquid volume in the fermenter (m^3)

GREEK LETTERS

$\dot{\gamma}$ shear rate (s^{-1})

Ω angular velocity (rad/s)

9.6 REFERENCES

Abu-Reesh, I. and Kargi, F., Biological Responses of Hybridoma Cells to Defined Hydrodynamic Shear Stress. Journal of Biotechnology, *9*: 167-178, 1989.

Bird, R. B., Stewart, W. E., and Lightfoot, E. N. Transport Phenomena, 2nd edition, John Wiley and Sons, New York, 2002.

Cherry, R. S. and Hulle, C. T., Cell Death in the Thin Films of Bursting Bubbles. Biotechnology Progress, *8*: 11-18, 1992.

Côté, P., Bersillon, J. L., Huyard, A., and Faup, G., Bubble-Free Aeration Using Membranes Process Analysis. Journal WPCF, *60*: 1986-1992, 1988.

Curran, S. J. and Black, R. A., Oxygen Transport and Cell Viability in an Annular Flow Bioreactor: Comparison of Laminar Couette and Taylor-Vortex Flow Regimes. Biotechnology and Bioengineering, *89*: 766-774, 2005a.

Curran, S. J. and Black, R. A. Taylor-Vortex Bioreactors for Enhanced Mass Transport. In J. B. Chaudhuri and M. Al-Rubeai (eds.), Bioreactors for Tissue Engineering, pp. 47-85, Springer, Netherlands, 2005b.

Domingues, F. C., Queiroz, J. A., Cabral, J. M. S., and Fonseca, L. P., Production of Cellulases in Batch Culture Using a Mutant Strain of *Trichoderma reesei* Growing on Soluble Carbon Source. Biotechnology Letters, *23*: 771-775, 2001.

Gallo, B., Tassinari, T., Spano, L., and Ryu, D. D. Y., Cellulase Process Improvement and its Economics. *In* M. Moo-Young (ed.), Advances in Biotechnology, Vol. 3, pp. 281-288, Pergamon Press, 1981.

Ghose, T. K., Measurement of Cellulase Activity. Pure & Applied Chemistry, *59*: 257-268, 1987.

Janes, D. A., Thomas, N. H., and Callow, J. A., Demonstration of a Bubble-Free Annular-Vortex Membrane Bioreactor for Batch Culture of Red Beet Cells. Biotechnology Techniques, *1*: 257-262, 1987.

Jüsten, P., Paul, G. C., Nienow, A. W., and Thomas, C. R., Dependence of Mycelial Morphology on Impeller Type and Agitation Intensity. Biotechnology and Bioengineering, *52*: 672-684, 1996.

Kubicek, C. P. and Penttilä, M. E. Regulation of Production of Plant Polysaccharide Degrading Enzymes by *Trichoderma*. *In* C. P. Kubicek, G. E. Harman, and K. L. Ondik (eds.), *Trichoderma* and *Gliocladium*, Enzymes, Biological Control and Commercial Applications, pp. 49-67, Taylor & Francis, Bristol, UK, 1998.

Labraga, L. and Berkah, T., Mass Transfer From a Rotating Cylinder With and Without Crossflow. International Journal of Heat and Mass Transfer, *47*: 2493-2499, 2004.

Lecault, V., Patel, N., and Thibault, J., Morphological Characterization and Viability Assessment of *Trichoderma reesei* by Image Analysis. Biotechnology Progress, *23*: 734-740, 2007.

Lejeune, R., Nielsen, J., and Garon, G. V., Morphology of *Trichoderma reesei* QM 9414 in Submerged Cultures. Biotechnology and Bioengineering, *47*: 609-615, 1995.

Malouf, P. Relationship Between Morphology and Rheology During *Trichoderma reesei* RUT C-30 Fermentations. MASc Thesis, University of Ottawa, Ottawa, Canada, 2008.

Marten, M. R., Velkovska, S., Khan, S. A., and Ollis, D. F., Rheological, Mass Transfer, and Mixing Characterization of Cellulase-Producing *Trichoderma reesei* Suspension. Biotechnology Progress, *12*: 602-611, 1996.

Matsumura, M., Imanaka, T., Yoshida, T., and Taguchi, H. Optimal Conditions for Production of Cephalosporin C in Fed-Batch Culture. *In* M. Moo-Young (ed.), Advances in Biotechnology, Vol. 1, pp. 297-302, Pergamon Press, 1981.

Metzner, A. B. and Taylor, J. S., Flow Patterns in Agitated Vessels. AIChE Journal, *6*: 109-114, 1960.

Mitard, A. and Riba, J. P., Morphology of *Aspergillus niger* Cultivated at Several Shear Rates. Biotechnology and Bioengineering, *32*: 835-840, 1988.

Mukataka, S., Kobayashi, N., Sato, S., and Takahashi, J., Variation in Cellulase-Constituting Components From *Trichoderma reesei* With Agitation Intensity. Biotechnology and Bioengineering, *32*: 760-763, 1988.

O'Connor, K. C., Cowger, N. L., De Kee, D. C. R., and Schwarz, R. P., Prolonged Shearing of Insect Cells in a Couette Bioreactor. Enzyme and Microbial Technology, *31*: 600-608, 2002.

Pamboukian, C. R. D., Guimarães, L. M., and Facciotti, M. C. R., Applications of Image Analysis in the Characterization of *Streptomyces olindensis* in Submerged Culture. Brazilian Journal of Microbiology, *33*: 17-21, 2002.

Papagianni, M., Mattey, M., and Kristiansen, B., Morphology and Citric Acid Production of *Aspergillus niger* PM 1. Biotechnology Letters, *16*: 929-934, 1994.

Reij, M. W., Keurentjes, J. T. F., and Hartmans, S., Membrane Bioreactor for Waste Gas Treatment. Journal of Biotechnology, *59*: 155-167, 1998.

Reuss, M., Schmalzriedt, S., and Jenne, M. Application of Computational Fluid Dynamics (CFD) to Modeling Stirred Tank Bioreactors. *In* K. Schügerl and K. H. Bellgardt (eds.), Bioreaction Engineering. Modelling and Control, pp. 207-246. Springer, 2000.

Rocha-Valadez, J. A., Galindo, E., and Serrano-Carreón, The Influence of Circulation Frequency on Fungal Morphology: A Case Study Considering Kolmogorov Microscale in Constant Specific Energy Dissipation Rate Cultures of *Trichoderma harzianum*. Journal of Biotechnology, *30*: 394-401, 2007.

Sahoo, S., Rao, K. K., Suresh, A. K., and Suraishkumar, G. K., Intracellular Reactive Oxygen Species Mediate Suppression of Sporulation in *Bacillus subtilis* Under Shear Stress. Biotechnology and Bioengineering, *87*: 81-89, 2004.

Sahoo, S., Verma, R. K., Suresh, A. K., Rao, K. K., Bellare, J., and Suraishkumar, G. K., Macro-Level and Genetic-Level Responses of *Bacillus subtilis* to Shear Stress. Biotechnology Progress, *19*: 1689-1696, 2003.

Schafner, D. W. and Toledo, R. T., Cellulase Production in Continuous Culture by *Trichoderma reesei* on Xylose-Based Media. Biotechnology and Bioengineering, *39*: 865-869, 1992.

Schlichting, H. Boundary Layer Theory. McGraw Hill, New York, 1955.

Schneider, M., Reymond, F., Marison, W., and von Stockar, U., Bubble-Free Oxygenation by Means of Hydrophobic Porous Membranes. Enzyme and Microbial Technology, *17*: 839-847, 1995.

Schwarz, R. P. and Anderson, C. D. Gas Permeable Bioreactor and Method of Use. US Patent: 5,763,279, USA, 1998.

Serrano-Carreón, L., Flores, C., and Galindo, E., γ-Decalactone Production by *Trichoderma* Harzianum in Stirred Bioreactors. Biotechnology Progress, *13*: 205-208, 1997.

Sherwood, T. K., Pigford, R. L., and Wilke, C. E. Mass Transfer, McGraw Hill, New York, 1975.

Srinivasan, R., Jayanti, S., and Kannan, A., Effect of Taylor Vortices on Mass Transfer From a Rotating Cylinder. AIChE Journal, *51*: 2885-2898, 2005.

Sternberg, D., Production of Cellulase by *Trichoderma*. Biotechnology and Bioengineering Symposium, *6*: 35-53, 1976.

Sun, X. and Linden, J. C., Shear Stress Effects on Plant Cell Suspension Cultures in a Rotating Wall Vessel Bioreactor. Journal of Industrial Microbiology and Biotechnology, *22*: 44-47, 1999.

Suzuki, Y., Miyahara, S., and Takeishi, K., Oxygen Supply Method Using Gas-Permeable Film for Wastewater Treatment. Water Science Technology, *28*: 243-250, 1993.

Velkovska, S., Marten, M. R., and Ollis, D. F., Kinetic Model for Batch Cellulase Production by *Trichoderma reesei* Rut C30. Journal of Biotechnology, 54: 83-94, 1997.

Wong, V., Williams, D., and Colby, C. B., Ensuring Oxygenation of Carrot Cell Cultures in a Couette Viscometer During Investigation of Shear Effects. Biotechnology Letters, *23*: 1841-1847, 2001.

CHAPTER 10

Continuous *Trichoderma reesei* Fermentations Using Different Control Strategies

Nilesh Patel, Amanollah Baloochzehi, and Jules Thibault

Department of Chemical and Biological Engineering

University of Ottawa

Ottawa (ON), K1N 6N5, Canada

Abstract

The growth of *Trichoderma reesei* RUT C-30 and the associated enzyme production were investigated using different substrate feeding strategies. The experiments were carried out in two stages: an initial batch phase with glucose or lactose as the carbon source and a second continuous phase with lactose as the enzyme-inducing carbon source. The substrate feeding strategies were classified into two main categories: (1) based on dissolved oxygen (DO) and (2) based on NH_4OH requirements to maintain the pH above a threshold value. The DO strategy was further subdivided into strategies based on growth and starvation cycles and based on continuous feed. Higher enzyme activites per mg of protein were obtained for runs performed using the control strategies based on DO with growth and starvation cycles. On the other hand, lower enzyme activities were observed in the experiments based on the continuous feeding strategy and when the DO was controlled by manipulating agitation. However, excessive foam and spore formation during the experiments with resulted in early termination of fermentations with cyclic feeding compared to runs performed by the continuous feeding strategy

Keywords: bioreactor, cellulase, dissolved oxygen, fermentation, monitoring and control, *Trichoderma reesei*

10.1 INTRODUCTION

Monomeric sugars, glucose for instance, could be used as feedstock in a number of biotechnological processes such as ethanol or hydrogen production. Such sugars could potentially be produced through degradation of lignocellulosic material such as cellulose. However, hydrolysis of cellulose into glucose is usually achieved using cellulase enzyme complexes as catalyst. These enzyme complexes are primarily produced by both bacteria and fungi (Reczey et al., 1996). *Trichoderma reesei,* a soft rot fungus, is one of the most common classes of fungi used in the production of cellulolytic enzymes such as cellulase. *T. reesei* RUT C-30 is a mutant strain of the fungus with improved cellulase production and highly resistant to catabolite repression.

Most of the current control strategies for enzyme production are designed to keep a low substrate concentration in the bioreactor, which promotes higher enzyme production. Phenylalanine production by recombinant *E. coli* (Konstantinov et al., 1990) glucoamylase production by recombinant *S. cerevisia* (Oh et al., 1998), and cellulase production by *T. reesei* (Esterbauer et al., 1991) are some of the processes in which a low substrate concentration is maintained for maximum prodict formation. Additionally, in many fermentation reactions, an inducer is added to enhance productivity. For *T. reesei* fermentation, lactose is found to be a good inducer of cellulase (Domingues et al., 2001, Morikawa et al., 1995). High substrate concentration in the fermentation medium often results in overgrowth or by-product formation by forcing the microorganisms towards the undesired fermentative path and away from the desired enzyme producing path. For example, acetic acid is formed, instead of phenylalanine, in *E. coli* cultures with excess glucose concentration (Konstantinov et al., 1990). In the case of *T. reesei*, unwanted sporulation or unproductive cell growth results if an optimal substrate concentration is not maintained.

In the present work, various substrate feeding strategies for the continuous production of cellulase by *T. reesei* RUT C-30 were implemented. Although continuous fermentation with *T. reesei* results in low enzyme concentrations (Persson et al., 1991), it is advantageous to perform further studies to improve such processes due to various benefits such as low down-time compared to batch and fed-batch fermentations. Given that the cost associated with the production of cellulase is one of the most important

considerations in cellulose hydrolysis processes, a continuous cellulase production process with a high specific activity will greatly reduce the cost of the enzyme. A robust and dynamic control strategy which ensures a continuous cellulase production by the microorganisms is therefore required. The main problem in a continuous fermentation is maintaining an optimum enzyme production rate for long periods of time. Currently, *T. reesei* fermentations in fed-batch and continuous mode are operated using continuous feeding of the substrate. However, Bailey and Tahtiharju (Bailey and Tahtiharju, 2003) have shown that runs performed under growth and starvation cycles are beneficial if an optimal balance between the two cycles can be maintained. Such a feeding technique leads to pulsed addition of substrate which was also found to be beneficial during *Aspergillus niger* fermentation due to improved oxygen mass transfer, because of the low viscosity broth achieved compared to the continuous feeding strategy (Bhargava et al., 2003). However, the viscosity of the broth was not measured in this study.

Dissolved oxygen (DO) and pH of the medium could be used to infer the substrate concentration within the fermentation. The use of DO as a parameter for substrate concentration arises from the fact that when the carbon source in the bioreactor is depleted, a marked increase in DO value is observed. Similarly, the pH of the medium could be used as an indicator for carbohydrate exhaustion because a decrease in the culture pH during growth and an increase in pH upon exhaustion of the carbon source are observed for filamentous fungi such as *T. reesei*. Therefore, for the first few runs presented in this study, the DO concentration was used to control the substrate feeding rate. Later, to account for disturbances in dissolved oxygen concentration arising from external sources such as antifoam addition, a dual loop control scheme based on dissolved oxygen and agitation speed was employed. Finally, the rate of base addition for maintaining the pH above a threshold value was used to control the substrate feeding rate.

10.2 MATERIALS AND METHODS

10.2.1 Microorganism

The strain used in this work was *T. reesei* RUT C-30 (ATCC 56765). The glycerol stock solutions of spores were maintained at -80°C and were transferred on potato dextrose agar plates. New plates were prepared every month and kept at 4°C.

10.2.2 Bioreactor

A stirred tank bioreactor (STB) with three Rushton turbines was used in these experiments. The experimental setup is similar to the one used by Patel and Thibault (Patel and Thibault, 2004). The bioreactor is made of stainless steel and has an inner diameter of 228 mm and a column height of 550 mm. The cover plates of the bioreactor have ports for sampling, pH probe, dissolved oxygen probe, substrate and base addition, and a thermocouple. The gas sparger at the bottom of the bioreactor is a thin plate perforated with one hundred uniformly distributed holes, 1 mm in diameter. A mechanical foam breaker was installed on the central shaft at 440 mm from the bottom of the reactor. The three identical Rushton turbines were mounted on the central shaft. The locations of the impellers, measured from the bottom of the column, are 54, 132 and 210 mm. Each turbine has 6 blades mounted on the periphery of a 50-mm diameter disk. Each blade is 25 mm long, 15 mm high and 1.5 mm thick. Four baffles, 375 mm high, 16 mm wide and 1 mm thick, were placed inside the mixing vessel. Air flow rate to the bioreactor was maintained at 7 SLPM for Runs 1 through 7, whereas it was decreased to 5 SLPM in Run 8 (Table 10.1). A constant agitation speed of 400 rpm was maintained throughout the fermentation runs except when variable agitation was used to control the DO. A cooling jacket around the bioreactor controlled the temperature of the broth at 28°C throughout the experimental runs. A mass spectrometer (Proline, Ametek, Pittsburgh, PA) was used to measure the concentration of O_2 and CO_2 in the exhaust gas. All pumps with speed control, electronic balances, mass flow meter, mass spectrometer and, probes for pH, DO and temperature, were connected to the computer using a data acquisition card. The control schemes presented in this study were developed using the LabVIEW® measurement and control software (National Instrument, Austin, USA) installed on a computer. Also, the measurement and control of process variables such as off-gas analysis, pH and agitation were performed using this software.

10.2.3 Cultivation Method

The volume of the culture medium during the batch phase was 10 L and contained: glucose, 13 g/L; $(NH_4)_2SO_4$, 1.4 g/L; KH_2PO_4, 2.0 g/L; $MgSO_4 \cdot 7H_2O$, 0.6 g/L; $CaCl_2 \cdot 2H_2O$, 0.3 g/L; $FeSO_4 \cdot 7H_2O$, 5.0 mg/L; $MnSO_4 \cdot 7H_2O$, 1.6 mg/L; $ZnSO_4 \cdot 7H_2O$, 1.4 mg/L; $CoCl_2 \cdot 6H_2O$, 2 mg/L, protease peptone (2.0 g/L) and yeast extract (0.5 g/L). All

the experiments performed in this study are listed in Table 10.1. Only for Run 8, glucose was replaced by lactose (40 g/L) and the nutrient concentration was doubled. The pH of the medium was initially adjusted to 5.5 using 10N NaOH solution. Medium was autoclaved for 20 minutes.

Table 10.1 List of experiments with operating and control paramters

Experiment	Controlled Variable	Agitation	Feeding rate (mL/min)	Lactose (g/L)
Run 1	DO	Constant	$F_{UL} = 4.0$ $F_{LL} = 0.0$	60
Run 2	DO	Constant	$F_{UL} = 4.0$ $F_{LL} = 0.8$	60
Run 3	DO	Constant	Continuous w/adjustment	60
Run 4	DO	Variable	$F_{UL} = 4.0$ $F_{LL} = 0.8$	60
Run 5	DO	Constant	$F_{UL} = 4.0$ $F_{LL} = 0.0$	120
Run 6	DO	Constant	Continuous w/adjustment	120
Run 7	NH_4OH rate	Variable	$F_{UL} = 4.0$ $F_{LL} = 0.8$	60
Run 8	NH_4OH rate	Variable	$F_{UL} = 4.0$ $F_{LL} = 0.8$	60

Shake flask cultures were performed with a volume of 500 mL in a 1-L Erlenmeyer flask with three baffles. A spore solution in sterilized water was prepared from the plates. Flasks were kept in an orbital shaker at200 rpm and 28°C for 55 h. The pH was measured on-line by a pH FermProbe (Broadley-James Corporation, Irvine, CA) whereas the dissolved oxygen (DO) was continuously monitored by a DO Sensor (Broadley-James Corporation, Irvine, CA). During the continuous phase, 60 g/L lactose monohydrate

solution with a nutrient concentration three times the batch phase was used. Only for Runs 4 and 5, a lactose concentration of 120 g/L with a nutrient concentration six times the batch phase was used.

10.2.4 Analysis

A 45-mL sample was collected approximately every 4-6 h during the batch phase and 12 h during the continuous phase. The amount of biomass was quantified by dry weight analysis. Samples were filtered through a pre-dried and pre-weighted glass fibre filter (grade A/E, Gelman Sciences, MI). One volume of the sample was washed with two volumes of deionised distilled water and dried for 24 h at 95°C. The weight of the samples was measured after a 24-h period of cooling in a desiccator.

Glucose and lactose concentrations were determined using YSI glucose analyzer (YSI Incorporated, USA) and enzymatic kit (Boehringer Mannheim, Germany), respectively. Extracellular protein concentration was determined by the Bradford assay using bovine serum albumin (BSA) as standard. Filter paper (FPA) and carboxymethyl cellulose (CMC) activities were determined as per the IUPAC protocol (Ghose, 1987).

10.2.5 Control Strategies

The present paper focuses on two substrate feeding strategies for continuous cellulase production: dissolved oxygen (DO) and base requirements for controlling the pH above a minimum threshold. As noted earlier, the depletion of the carbon source in the bioreactor could be detected through the increasing DO values and consequently a control strategy could be implemented to utilize the DO readings to manipulate the substrate feeding rate to the bioreactor. Similar to DO readings, a marked increase in reaction pH could signal substrate exhaustion. In this case, however, the rate of base requirements to the bioreactor was used as opposed to actual pH values. The decrease in the rate of base addition is an indication of impending pH increase linked to substrate exhaustion.

Control schemes based solely on substrate feeding rate for DO control may lead to excessive alteration of the feeding rate and, as a consequence, may create a stressful growth environment. Due to their low time constant, DO responds rapidly to changes in air flow rate, antifoam addition and pressure. The variations in DO values resulting from such disturbances can be managed by a change in the agitation speed. Changes in metabolism, nutrient limitation, and population activity have a much higher time constant

and the DO responds rather slowly to these changes (Konstantinov et al., 1990). These changes can be controlled using the lactose feeding rate. The scheme was based on two independent loops. The first loop was based on either DO or base requirement control strategies discussed below. To account for any changes with low time constants, the second loop used the agitation speed to regulate the DO. If the DO value exceeded 35% (D_{UL}), the agitation speed was lowered by a value of 5 rpm (ΔA). Similarly, the agitation speed was increased by 5 rpm if the DO was below the lower limit of 25% (D_{LL}). These step changes were followed by a 20 s wait time. The lower limit of agitation was set at 400 rpm to avoid mixing and foaming issues associated with further decrease in agitation. The upper limit was set at 500 rpm for Run 4 and 7, and it was set at 600 rpm for Run 8 due to the lower air flow rate compared to other runs. The variable agitation control scheme is shown in Figure 10.1. Agitation control was only performed for Runs 4, 7 and 8. For the remaining runs, agitation was kept constant at 400 rpm. Experiments where the agitation control was not used, the upper and lower limits of the feeding rate are changed manually such that the DO is maintained between 25 and 35%.

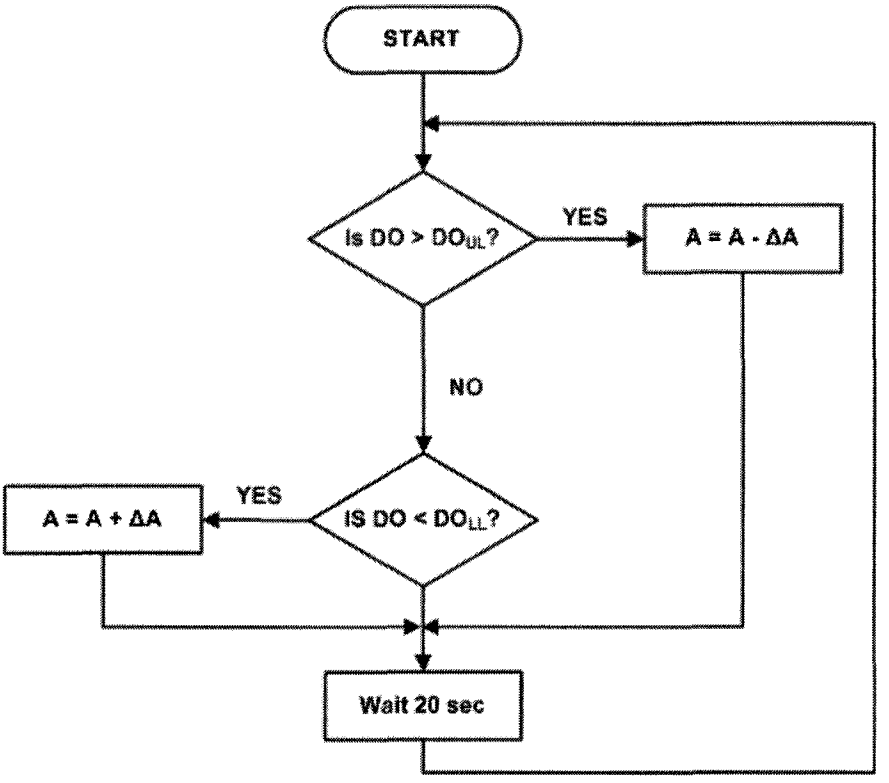

Figure 10.1 – Dissolved oxygen control based on the variable agitation speed.

10.2.5.1 DISSOLVED OXYGEN

Three different control strategies were used to maintain the dissolved oxygen (DO) concentration at the desired set point using the substrate feeing rate: (1) an on/off control strategy, (2) a two-level control strategy similar to the on/off control strategy except that the substrate feeding rate was not completely stopped, and (3) a continuous control strategy. Each of these control strategies will be briefly described in turn. The DO readings were averaged over a sampling period of 30 s to filter out small disturbances and inherent noise in the probe reading.

10.2.5.1.1 On/off control strategy

In the on/off control strategy (Figure 10.2), the DO set point (DO_{SP}) was 30%. The control strategy was relatively simple. If the DO was lower or equal to the predetermined set point of 30%, no substrate was added (F_{LL} = 0), whereas when the DO was greater than 30%, the lactose feeding rate was set to its upper limit of 4.0 mL/min (F_{UL}).

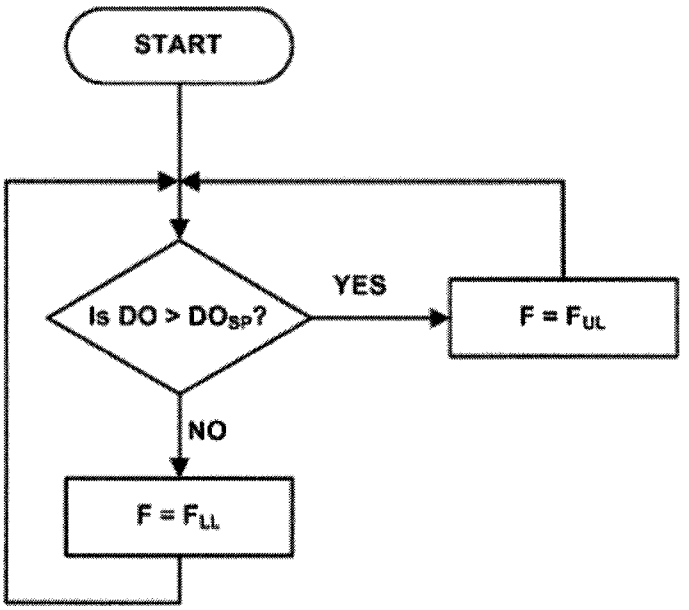

Figure 10.2 – Feeding strategy based on the on/off and two-level control scheme.

10.2.5.1.2 Two-level control strategy

The two-level control strategy is similar to that of the on/off scheme except in this case the lower feeding rate (F_{LL}) was not zero, but was set to 0.8 mL/min, while maintaining the upper limit (F_{UL}) at 4.0 mL/min. Setting the lower feeding rate to zero, might create extended periods in which the carbon source is completely depleted and as a result the microorganisms may experience undesired stress. To avoid the prolonged periods of

carbohydrate exhaustion, the feeding was continued at a lower value when the dissolved oxygen was below or equal to the set point of 30%.

10.2.5.1.3 Continuous feeding with adjustment strategy

In the continuous feed strategy (Figure 10.3), the set point of the DO was kept in the range of 25 (DO_{LL}) to 35% (DO_{UL}) to avoid frequent manipulation of substrate feeding when the DO set point is fixed. When this control was started at the end of batch phase, the substrate feeding rate (F) was set close to 3.0 mL/min. After 5 minutes, if the DO was between 25% and 35%, no change to the current feeding rate was made. For cases where the DO was greater than 35%, the feeding rate was increased by an increment of 0.1 mL/min (ΔF). Also, if the DO was less than 25%, the feeding rate was decreased by 0.1 mL/min (ΔF). This control loop was peformed every five minute as shown in Figure10.3.

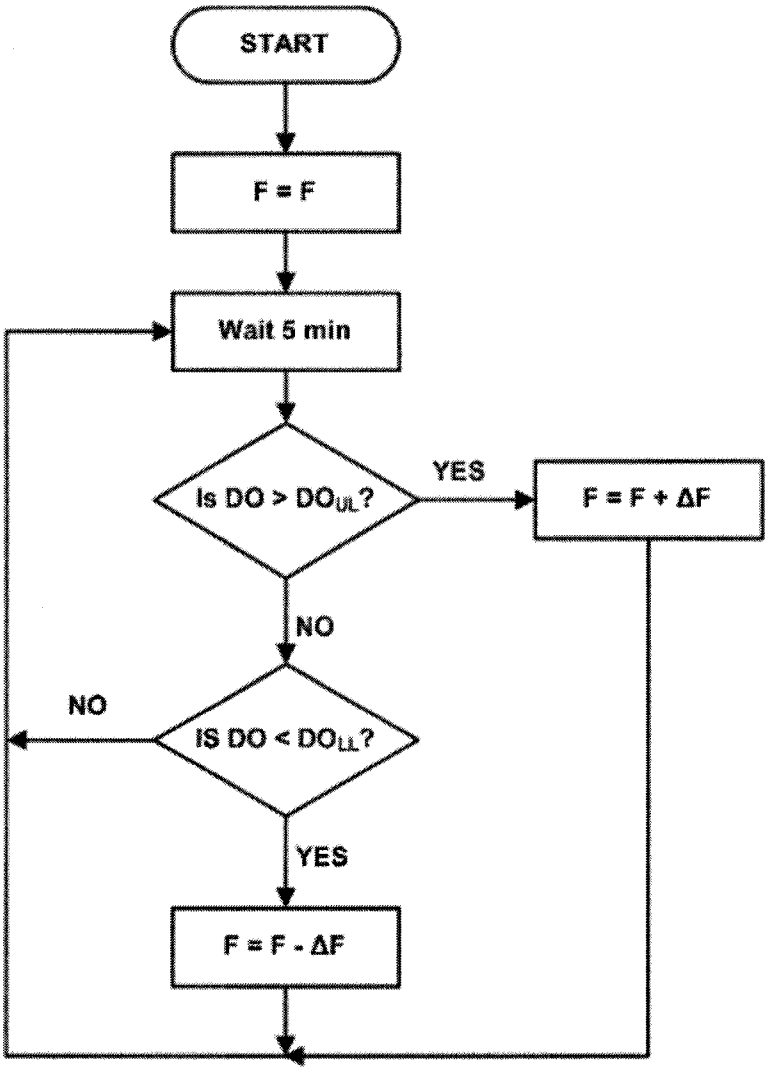

Figure 10.3 – Feeding strategy based on the continuous feed scheme.

10.2.5.1 BASE REQUIREMENT

As mentioned earlier, the pH of the fermentation broth can be used as an indicator to infer the substrate concentration within the fermentation broth and then to use this measurement to manipulate the substrate feeding rate to the bioreactor. More precisely, the changes in the rate of addition of NH_4OH solution were used as an indicator for the growth activities of the fungus. As the decreasing trend of base addition is indicative of declining growth, new medium was fed to the bioreactor when the rate of addition of the base decreased below a certain threshold. Conversely, an increase in the amount of base added was an indication of increased growth and the substrate feeding rate was thereby decreased. The control scheme based on the base requirement is shown in Figure 10.4.

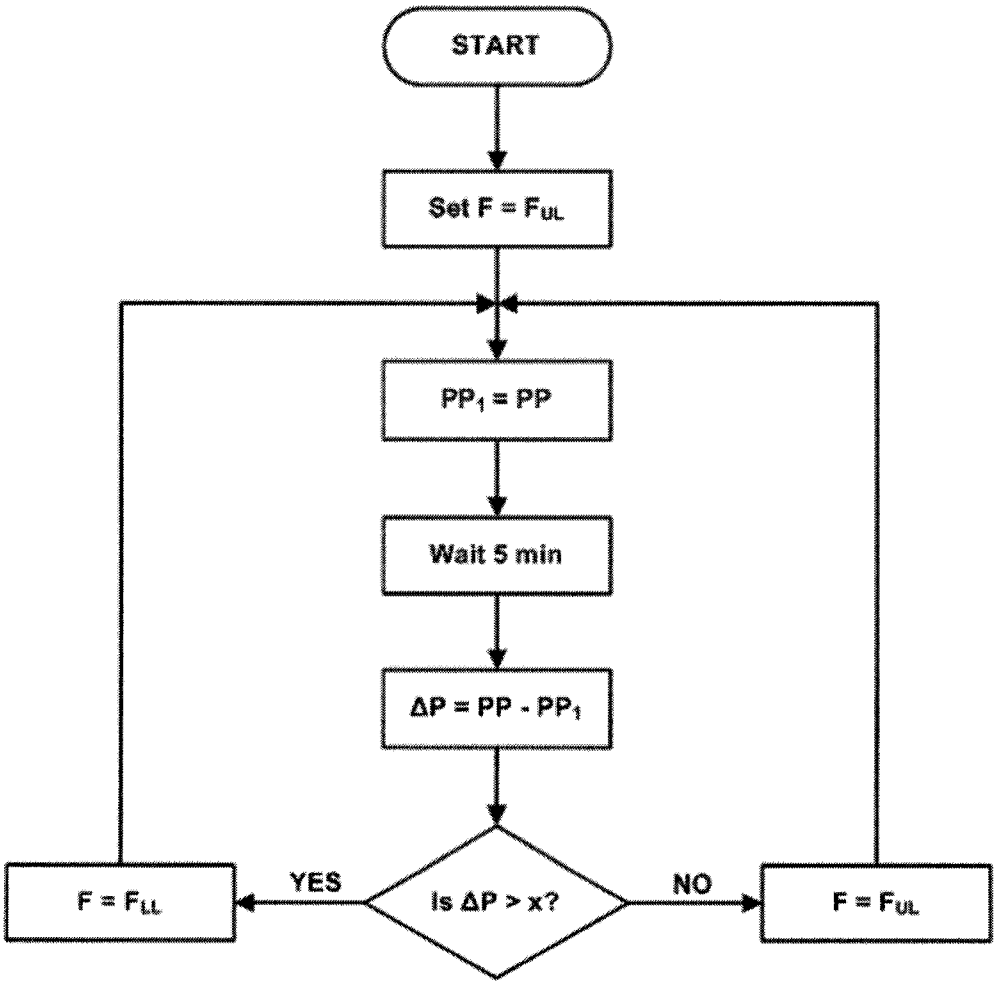

Figure 10.4 – Feeding strategy based on the NH_4OH requirements.

When the feeding control was initiated, the substrate feeding rate was set to the upper limit (F_{UL}) of 4.0 mL/min and the total amount of NH_4OH added thus far is stored (PP_1).

At each 5-minute time interval, a new value of total amount of NH_4OH added (PP) was obtained. The difference between the current value and the previous value was calculated to obtain the net NH_4OH added (ΔP) in the last 5 minutes. Values greater than the preset value signify an increase in the rate of base addition resulting from higher growth of the fungi. Therefore, if the difference exceeded the preset value (x) of 1.5 mL, the lactose feeding would switch to the lower limit (F_{LL}) of 0.8 mL/min. In cases where the NH_4OH feeding rate was less than or equal to the preset value (x), the lactose feeding would switch to the upper limit of 4.0 mL/min. This comparison was performed every 5 minutes using new values of total NH_4OH added. The amount of NH_4OH added was calculated from the equation relating the voltage sent to pump and the amount of NH_4OH added. The dissolved oxygen was controlled only by the agitation control scheme (Figure 10.1).

10.3 RESULTS AND DISCUSSION

In a typical *T. reesei* fermentation, the microorganisms are grown during the batch phase to a sufficient level for an efficient enzyme production occurring subsequently in fed-batch or continuous mode. Substrate suitable for the growth such as glucose can be used during the growth phase. In the fed-batch or continuous phase, carbon sources such as lactose which induce cellulase production are typically used. It is during this phase where several control strategies were employed for the continuous production of the cellulase enzyme complex in *T. reesei* RUT C-30. All the experiments performed in this study are listed in Table 10.1. Runs 1 through 6 were performed using DO as the controlled variable while Runs 7 and 8 were based on NH_4OH addition rate. The lactose concentration and agitation speed were similar for Runs 1 to 3 and only the feeding scheme were different for each run. In Run 4, lactose solution at 60 g/L was fed using the two-level control strategy but agitation was manipulated as shown on Figure 10.1 to keep the DO between 25 and 35%. Runs 5 and 6 were performed by feeding a lactose solution with a higher concentration of 120 g/L during the continuous phase. In Runs 7 and 8, the feeding strategy based on NH_4OH addition rate and a variable agitation scheme as depicted on Figure 10.1 was implemented.

Figure 10.5 shows the results of experimental Run 1 performed initially in batch mode and later in a continuous mode. The DO decreased rapidly due to the growth of the fungi

in the first 24 h of the batch phase. The pH of the medium increased during the early batch phase but later decreased and was controlled around 4.5 using NH_4OH solution. After approximately 24 h, the DO started to increase due to the complete consumption of glucose supplied in the initial medium. The fermentation in continuous mode was started when the DO rose to 30%. An on/off control strategy (Figure 10.2) discussed earlier was used in this experiment to control the DO in the vicinity of 30% by adjusting the lactose feeding rate. All feeding strategies were successful in controlling the DO close to its set-point similar to the Run 1 as shown in Figure 10.5. Given that the protein production is a secondary metabolism, it started when the substrate concentration in the batch phase was low. The maximum protein concentration after 95 h of fermentation was 3.1 g/L. The experiment had to be stopped after 96 h due to excessive foaming and sporulation. The biomass concentration, on the other hand, increased until 48 h after which it stabilized around 11 g/L. A small decrease in the biomass concentration at the end is due to the cell lysis and formation of spores.

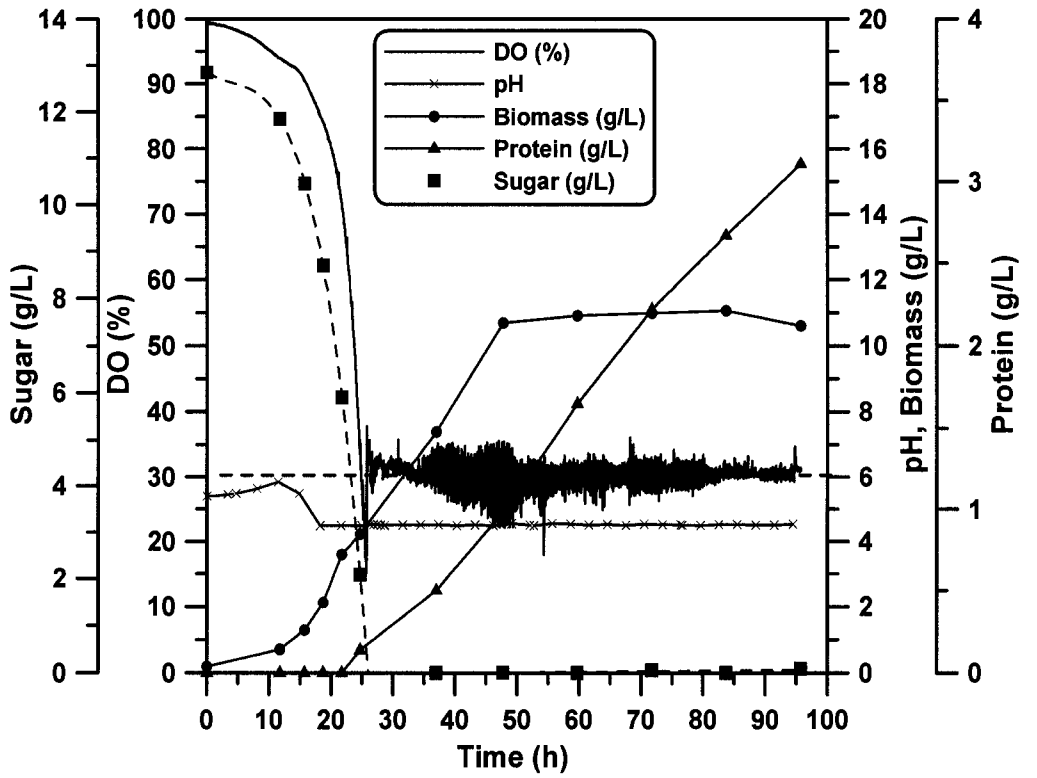

Figure 10.5 – Profile of biomass growth, DO level, pH, sugar and protein concentrations during Run 1.

The substrate feeding rate profile for Run 1 between 36 and 40 h is presented in Figure 10.6 along with the associated profiles of the percentage CO_2 in the exit gas, the pH and the DO concentration. It is evident that pH and DO are consistently controlled around their respective set points. In the later stages of the experiment, the lactose feeding rate (F_{UL}) was manually adjusted to stabilize the DO around its set point of 30%. This adjustment in feeding rate also helped to stabilize the increasing trend in CO_2 cycles observed in Figure 10.6.

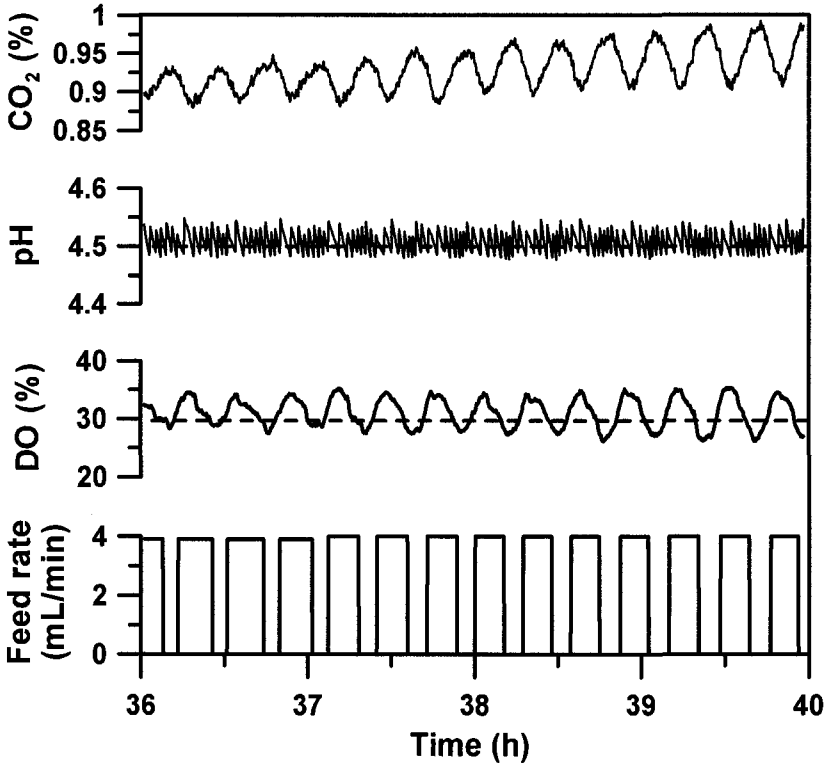

Figure 10.6 – Profile of CO_2 production rate, DO level, lactose feeding rate and pH for Run 1.

Biomass and protein production obtained during Runs 1, 2 and 3 are shown in Figure 10.7. All three runs had similar feed composition and agitation rates. Three control strategies, on/off, two-level, and continuous feed with adjustment, were used for Runs 1, 2, and 3, respectively. Lactose was added at an average feeding rate of 2.21 ± 0.14 mL/min throughout these three fermentations. The biomass concentration between these runs was not significantly different during the early stages of continuous phase. Only for Run 1 there was more biomass growth during the later stages of the fermentation. At the

end of fermentation, the protein concentration for Runs 1 and 2 was close to 3.2 g/L and for Run 3 it was 4.1 g/L. The protein production in Runs 1 and 2 was close to Run 3 in around 80 h but later decreased due to the sporulation. It is hypothesized that the lower protein concentrations and shorter experiments in Runs 1 and 2 are due to the microorganisms being placed under higher stress conditions in growth and starvation cycles. It is important to note that although the biomass concentration reached steady state, the protein production was still increasing before the experiment had to be stopped due to the sporulation.

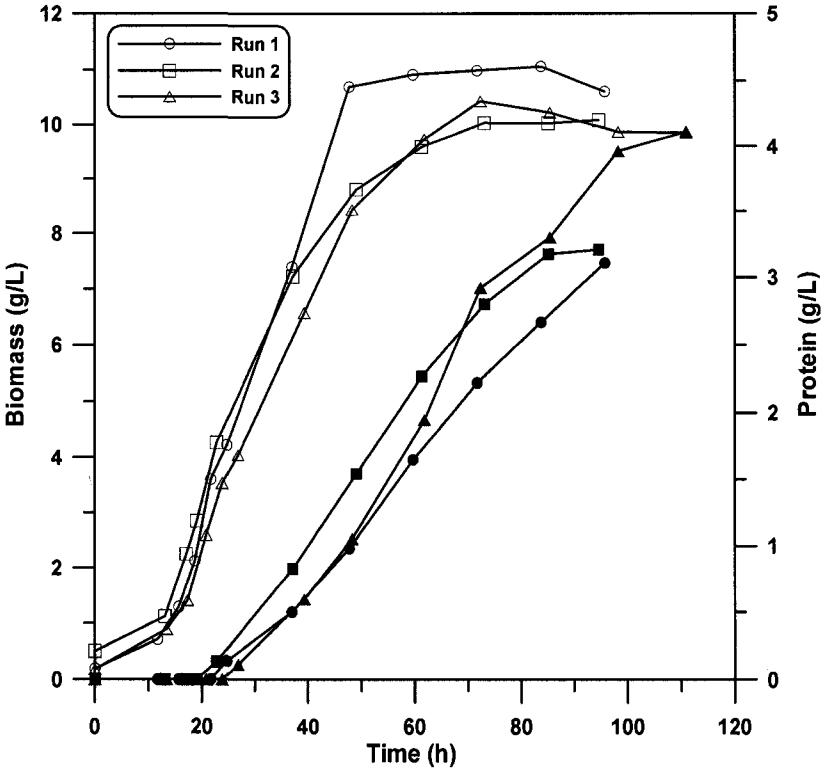

Figure 10.7 – Profile of biomass (empty symbols) and protein (filled symbols) for Runs 1, 2 and 3.

To compare the activity between the three runs, FPA and CMC activities per mg of protein are shown in Figure 10.8. It is clear that higher protein activity per mg of protein is obtained when substrate feeding is performed in the cyclic mode (Runs 1 and 2). The enzyme activity of Run 3 was the lowest in terms of both FPU and CMC activity per mg of protein. The results indicate that the growth of the microorganisms in cyclic growth and starvation leads to better secretion of the complete enzyme complex and thus higher activity per mg of protein. Thus, scarcity of substrate during the starvation cycle probably

leads to stronger induction and thus higher enzyme activity (Hendy et al., 1984). The increase in enzyme activity towards the end of some experiments is most likely due to the release of the enzymes from mycelia, particularly the cell walls, upon the death of microorganisms (Watson and Nelligan, 1983).

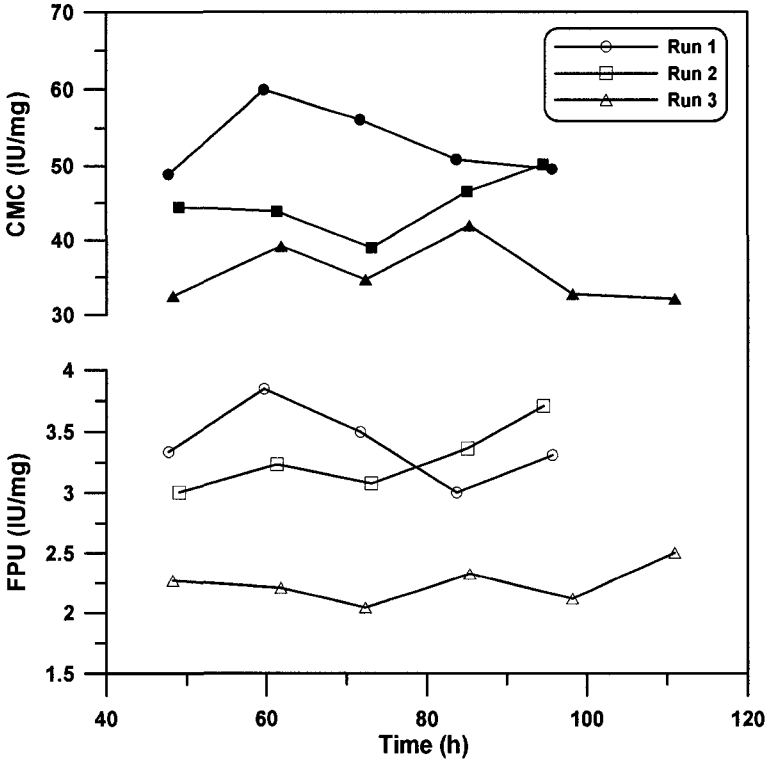

Figure 10.8 – Profile of activity per mg of protein for Runs 1, 2 and 3.

Based on the two-level feeding strategy, a new experiment (Run 4) was performed except the agitation was manipulated before the feeding rate was adjusted manually if the DO went outside the range of 25 to 35%. Due to higher agitation and subsequently better oxygen transfer, a higher biomass concentration of 13 g/L was obtained at the end of the fermentation (95.33 h). However, the experiment was stopped due to sporulation. The protein concentration of 3.2 g/L with activities of 3 IU/mg protein and 35 IU/mg protein for FPA and CMC respectively were achieved.

Due to difficulties encountered in operating the fermentations discussed above, two runs (5 and 6) at a higher lactose concentration (120 g/L) were performed to evaluate its effect on the growth and protein production. Runs 5 and 6 were performed with the on/off and continuous feed control strategies, respectively. Figure 10.9 presents the evolution of protein and biomass concentrations for Runs 5 and 6, respectively. As expected,

increasing the lactose concentration enhanced the protein concentration. At the end of the fermentation, 7.1 g/L of protein concentration could be achieved when using a higher lactose concentration of 120 g/L (Run 6) as opposed to a protein concentration of 4.1 g/L when using a lower lactose concentration of 60 g/L (Run 3). Nevertheless, similar problems of foam formation and sporulation towards the end of the experiment were observed in both runs regardless of lactose concentration. Also, similar to earlier runs (1 and 2), the total fermentation time was shorter for Run 5 with feeding strategy based on growth and starvation cycle (on/off control) compared to Run 6 which was based on the continuous feeding. It is evident from Runs 1, 2 and 3 that a higher protein activity could be achieved by operating *T. reesei* fermentation in cycles of growth and starvation. However, the feeding strategy based on dissolved oxygen with repeated cycles of growth and starvation (Runs 1, 2 and 5) caused more foaming problems and sporulation compared to experiments based on a continuous feeding strategy (Runs 3 and 6). Therefore a new feeding strategy based on the NH_4OH addition rate (Figure 10.4) was used to grow the microorganism in similar cycle of growth and starvation.

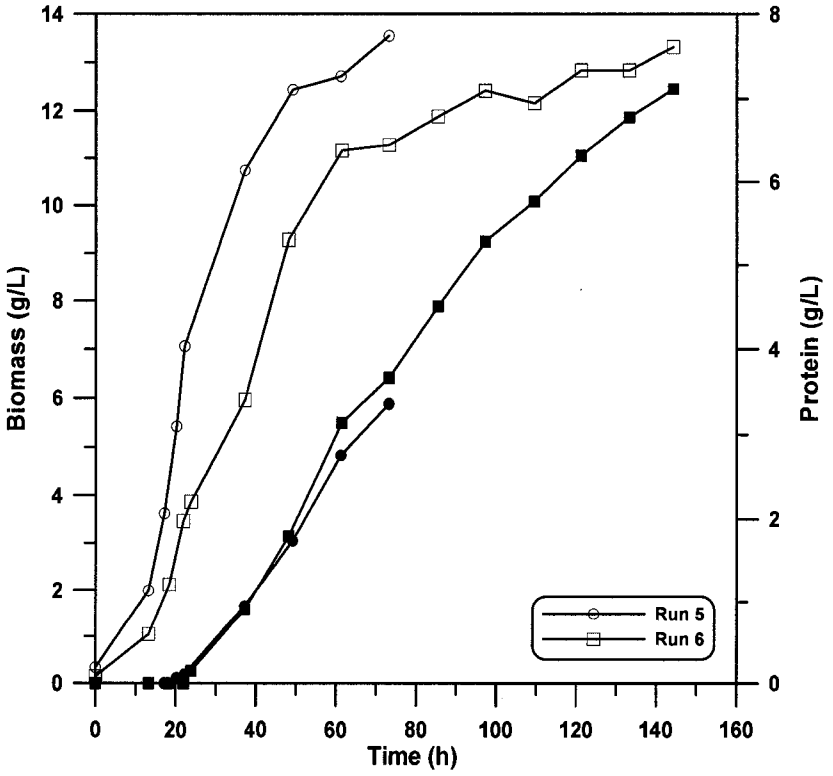

Figure 10.9 – Profile of biomass (empty symbols) and protein (filled symbols) for Runs 5 and 6.

In Runs 7 and 8, the controlled variable was switched from DO to the rate of NH_4OH addition. The DO was controlled via the variable agitation scheme presented in Figure 10.1 and a lactose concentration of 60 g/L was used during the continuous phase. In Run 8, the aeration rate was also decreased to 5 SLPM to reduce foaming in the bioreactor. Meanwhile, to counterbalance the decrease in oxygen transfer rate associated with lower aeration rates, the agitation upper limit was increased to 600 rpm from its previous value of 500 rpm. Moreover, compared to Run 7 in which 13 g/L of glucose was used during the batch phase, lactose with a concentration of 40 g/L was used in Run 8. The average lactose feeding rate during the continuous phase for Runs 7 and 8 was 2.27 and 2.44 mL/min, respectively. A higher feeding rate for Run 8 is due to additional biomass production (Figure 10.10) because of higher initial substrate (lactose) concentration in the batch phase.

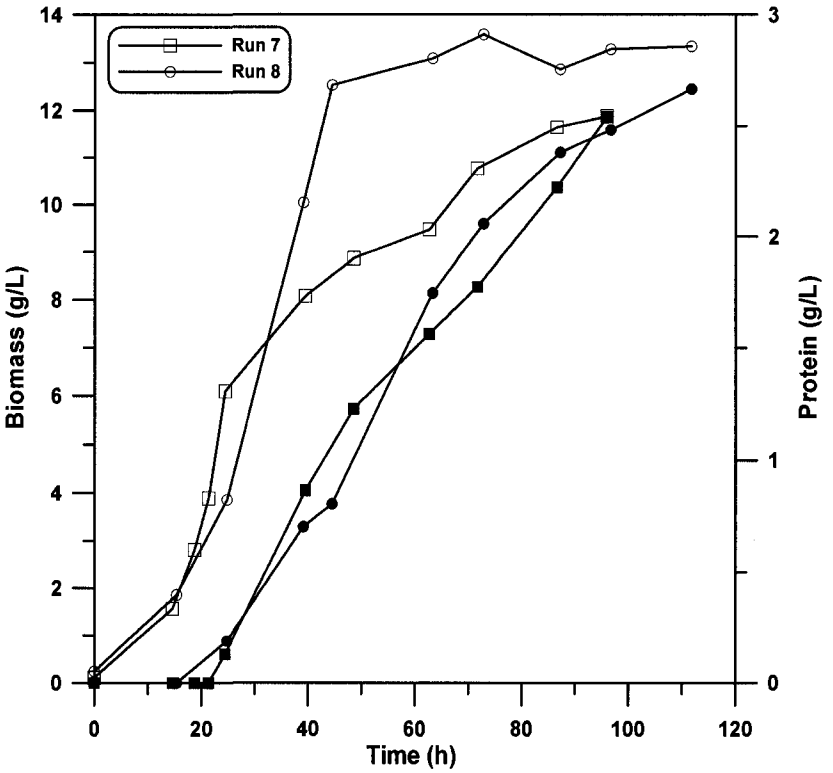

Figure 10.10 – Profile of biomass (empty symbols) and protein (filled symbols) for Runs 7 and 8.

Change in substrate during the batch phase and lower aeration had no significant effect on the foaming and spore formation since the period of continuous phase was similar for Runs 7 and 8. Also, the protein concentrations in both runs were similar at 96 h

(Figure 10.10) and, similar spore formation was observed for both cases at the end of fermentation. This was not expected since the preset value (x) used to switch between the growth and starvation was set to 1.5 mL which is equivalent to NH_4OH feeding of 0.03 mL/min per litre of bioreactor volume, which is greater than the value of 0.01 used by Bailey and Tahtiharju (2003) for a similar cycle time of 5 min. Therefore, microorganisms in the current feeding strategy were subjected to less stress during the starvation cycle. However, it is important to point out that the strain used in the previous study was a low-foaming hydrophobin II deletant of *T. reesei* strain Rut C-30. FPU and CMC activities per mg of protein for both runs are shown in Figure 10.11.

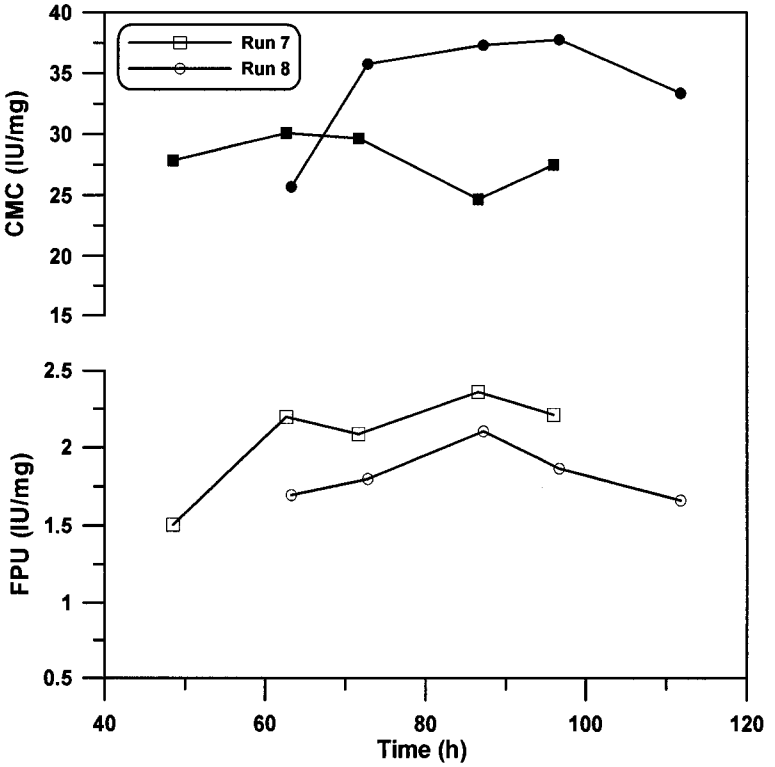

Figure 10.11 – Profile of activity per mg of protein for Runs 7 and 8.

A lower activity for Runs 7 and 8 compared to other experiments performed using the growth and starvation cycle (Runs 1 and 2), could be due to higher agitation speeds. It has been shown in the past that the cellulase activity is affected by higher agitation (Ganesh et al., 2000, Lejeune and Baron, 1995, Weber and Agblevor, 2005).

10.4 CONCLUSIONS

It has been suggested that oscillations between growth and starvation enhances enzyme production during the *T. reesei* RUT C-30 fermentation (McLean et al., 1985). Therefore, various control strategies involving both cyclic and continuous feeding were implemented in the production of cellulase enzyme complexes by the fungus *T. reesei* RUT C-30. The control schemes were successful in avoiding substrate accumulation during the continuous phase for all experimental runs. The activities (FPA and CMC) per mg of protein indicate that the growth and starvation cycles based on DO control strategies tend to give better enzyme activities. Although a higher activity was obtained in Runs 1 and 2, unfortunately optimal conditions for enzyme production could not be maintained and excessive foam formation and sporulation were observed in both cases forcing the termination of the fermentation after 95 h of operation. Usually the spore formation in *T. reesei* RUT C-30 grown on solid substrate such as cellulose is attributed to local spots of nutrient limitation (Olsson et al., 2003). However in the current study, a soluble medium (glucose, lactose and nutrients) was used throughout the fermentation and therefore the cause of sporulation is probably due to the stress associated with growth limitations imposed during the feeding strategies used in this study. Enzyme production and activity results obtained in this study suggest that the adopted DO and NH_4OH rate control strategies could inherently be used. However, the amount of substrate added during the growth and starvation cycle needs to be optimized along with the utilization of better foaming control techniques to perform continuous fermentations for long periods of time. Genetic modification of the microorganism could assist in eliminating foaming issues (Bailey and Tahtiharju, 2003). Other techniques such as operating under a backpressure of 135-170 kPa (5-10 psig) (Kadam, 1996), using of draught tube (Nystrom and Allen, 1976), using a lower aeration rate and a richer oxygen concentration in the inlet gas to the fermentation broth could potentially reduce foam formation and consequently allow running the cultivation for a longer period of time. Another process variable which could be used to control the substrate feeding rate is the use of the CO_2 concentration in the exit gas (Allen and Mortensen, 1981). As shown in Figure 10.6, the CO_2 concentration in the exit gas responds rapidly to the exhaustion and presence of substrate in the medium.

10.5 NOMENCLATURE

A agitation rate (rpm)

ΔA change in agitation rate (rpm)

DO dissolved oxygen concentration measured by the oxygen probe (%)

DO_{LL} lower limit of dissolve oxygen (%)

DO_{SP} dissolved oxygen set point (%)

DO_{UL} upper limit of dissolve oxygen (%)

F substrate feeding rate (mL/min)

ΔF change in substrate feeding rate (mL/min)

F_{LL} lower limit of substrate feeding rate (mL/min)

F_{UL} upper limit of substrate feeding rate (mL/min)

ΔP net amount of NH_4OH added in preset time interval (mL)

PP total amount of NH_4OH added (mL)

x parameter used to determine the substrate feeding rate (mL)

10.6 REFERENCES

Allen, A. L. and Mortensen, R. E., Production of Cellulase From *Trichoderma reesei* in Fed-Batch Fermentation From Soluble Carbon Sources. Biotechnology and Bioengineering, *23*: 2641-2645, 1981.

Bailey, M. J. and Tahtiharju, J., Efficient Cellulase Production by *Trichoderma reesei* in Continuous Cultivation on Lactose Medium With a Computer-Controlled Feeding Strategy. Applied Microbiology and Biotechnology, *62*: 156-162, 2003.

Bhargava, S., Wenger, K. S., and Marten, M. R., Pulsed Feeding During Fed-Batch *Aspergillus oryzae* Fermentation Leads to Improved Oxygen Mass Transfer. Biotechnology Progress, *19*: 1091-1094, 2003.

Domingues, F. C., Queiroz, J. A., Cabral, J. M. S., and Fonseca, L. P., Production of Cellulases in Batch Culture Using a Mutant Strain of *Trichoderma reesei* Growing on Soluble Carbon Source. Biotechnology Letters, *23*: 771-775, 2001.

Esterbauer, H., Steiner, W., Labudova, I., Hermann, A., and Hayn, M., Production of *Trichoderma* Cellulase in Laboratory and Pilot Scale. Bioresource Technology, *36*: 51-65, 1991.

Ganesh, K., Joshi, J. B., and Sawant, S. B., Cellulase Deactivations in Stirred Reactor. Biochemical Engineering Journal, *4*: 137-141, 2000.

Ghose, T. K., Measurement of Cellulase Activity. Pure & Applied Chemistry, *59*: 257-268, 1987.

Hendy, N. A., Wilke, C. R., and Blanch, H. W., Enhanced Cellulase Production in Fed-Batch Culture of *Trichoderma reesei* C-30. Enzyme and Microbial Technology, *6*: 73-77, 1984.

Kadam, K. L. Cellulase Production. *In* C. E. Wyman (ed.), Handbook on Bioethanol: Production and Utilization, pp. 213-252, Taylor & Francis, Washington DC, 1996.

Konstantinov, K., Kishimoto, M., Seki, T., and Yoshida, T., A Balance DO-Stat and Its Application to the Control of Acetic Acid Excretion by Recombinant *Escherichia Coli*. Biotechnology and Bioengineering, *36*: 750-758, 1990.

Lejeune, R. and Baron, G. V., Effect of Agitation on Growth and Enzyme Production of *Trichoderma reesei* in Batch Fermentation. Applied Microbiology and Biotechnology, *43*: 249-258, 1995.

McLean, D. D., Abear, K., and Podruzny, M. F., Fed-Batch Production of Cellulases Using *Trichoderma reesei* Rutgers C-30. Canadian Journal of Chemical Engineering, *64*: 588-597, 1985.

Morikawa, Y., Ohashi, T., Mantani, O., and Okada, H., Cellulase Induction by Lactose in *Trichoderma reesei* PC-3-7. Applied Microbiology and Biotechnology, *44*: 106-111, 1995.

Nystrom, J. M. and Allen, A. L., Pilot Scale Investigation and Economics of Cellulase Production. Biotechnology and Bioengineering Symposium, *6*: 55-74, 1976.

Oh, G., Moo-Young, M., and Chisti, Y., Automated Fed-Batch Culture of Recombinant *Saccharomyces cerevisiae* Based on On-Line Monitored Maximum Substrate Uptake Rate. Biochemical Engineering Journal, *1*: 211-217, 1998.

Olsson, L., Christensen, T. M. I. E., Hansen, K. P., and Palmqvist, E. A., Influence of Carbon Source on Production of Cellulases, Hemicellulases and Pectinases by *Trichoderma reesei* Rut C-30. Enzyme and Microbial Technology, *33*: 612-619, 2003.

Patel, N. and Thibault, J., Evaluation of Oxygen Mass Transfer in *Aspergillus niger* Fermentation Using Data Reconciliation. Biotechnology Progress, *20*: 239-247, 2004.

Persson, I., Tjerneld, F., and Hahn-Hägerdal, B., Fungal Cellulolytic Enzyme Production: A Review. Process Biochemistry, *26*: 65-74, 1991.

Reczey, K., Szengyel, Z., Eklund, R., and Zacchi, G., Cellulase Production by *T. reesei*. Bioresource Technology, *57*: 25-30, 1996.

Watson, T. G. and Nelligan, I., Pilot Scale Production of Cellulase by *Trichoderma reesei* (RUT C-30). Biotechnology Letters, *5*: 25-28, 1983.

Weber, J. and Agblevor, F. A., Microbubble Fermentation of *Trichoderma reesei* for Cellulase Production. Process Biochemistry, *40*: 669-676, 2005.

CHAPTER 11

Conclusions

The importance of products derived from biological sources is expected to increase tremendously worldwide. There is a net impetus by many governments to shift from a petroleum-based economy to a bio-based economy. In an effort to reduce its dependence on petroleum, the US Government committed to take the necessary actions in order to triple the amounts of chemicals produced from biomass by 2010. As Canada is now following in the same direction (Hanson and Edwards, 2002), innovative ways must be devised in order to achieve the objectives set by this goal. This transition will strongly depend on a wider use of enzymes as catalysts for the production of chemicals from biomass. The present project has the intention to contribute to a better understanding of the operating conditions that favour and enhance the production of enzymes. This understanding not only applies to the specific microorganism considered herein but also to other similar fermentation systems.

The application targeted by this research project is the production of enzymes for the saccharification process to convert agricultural wastes into bioethanol. One of the major expenses associated with the transformation of biomass is the cost of the enzyme. Therefore, the production of low-cost cellulase is a critical step in the development of a sustainable enzyme-based process for the conversion of cellulosic biomass to fermentable sugars (Schell et al., 2001).

This research project was concerned with one of the species of filamentous fungi, *Trichoderma reesei*. Filamentous fungi are eukaryotic microorganisms that are widely used in the manufacturing of protein products used in many aspects of our daily lives, including agricultural and food industries. They have been employed for a long time and will continue to be the principal sources of industrial enzymes. Industrial *T. reesei* strains have the capacity to secrete large amount of cellulase during fermentation. Also, the cellulase produced by *T. reesei* is a complete enzyme system which can successfully break the cellulose to simple sugars. As a result, *T. reesei* strains are widely used for the

production of enzymes employed in the laundry and pulp and paper industry (Maras et al., 1999).

A series of fermentation runs in different bioreactors (RPB, STB and CFB) were performed in the present project to study the influence of process parameters on the growth, protein production, morphology and rheology of the *T. reesei* fermentation broth (Appendix E).

11.1 MAIN ACCOMPLISHMENTS AND FINDINGS

Based on the above discussion, a brief summary of the thesis accomplishments and an assessment of the objectives are presented next. The reader could refer to Chapter 1 where the objectives were introduced.

(1) Couette Flow Bioreactor (CFB): A 5-L CFB was successful designed, built and tested by performing fermentations using *T. reesei*. The CFB reactor is, to our knowledge, the largest of its kind and it includes features that allow conducting fermentations of filamentous microorganism under defined shear fields in batch and continuous mode. The results show a strong correlation between the morphology (thickness) and protein production. As well, the shear was found to have a significant effect on the fragmentation of the microorganism.

(2) Fermentation Control and Measurement System: A completely automated control and measurement system was developed to perform batch, fed-batch and continuous operations in the different types of bioreactors used in this study. An important feature of this control and measurement system is its flexibility in implementing new feeding strategies to optimize the cellulase production.

(3) Image Analysis Technique: A semi-automated image analysis protocol was successfully developed and applied in *T. reesei* fermentation to characterize the morphology of the microorganism. The morphology and viability of the cells were monitored throughout the fermentations performed in STB, RPB and CFB.

(4) Evaluation of Stirred Tank and Reciprocating Plate Bioreactors: The performance of STB and RPB was studied by conducting fed-batch experiments at different agitation rates. Both bioreactors offered certain advantages and disadvantages during the *T. reesei* fermentation. The type of mixing devices had a significant influence on

the cell growth and protein production during the fermentation. The findings presented herein need to be considered while designing fermentation processes in this type of bioreactors.

(5) Feeding Strategies: A series of experiments were performed using different feeding strategies based on the dissolved oxygen and NH_4OH addition rate. Cellulase activity was enhanced when *T. reesei* was grown under repeated cycles of growth and starvation. However, the additional stress due to this cyclic growth caused large amount of foam and spore formation leading to decrease in the fermentation time. A higher agitation rate was also found to affect the protein activity.

(6) Biomass Estimation Techniques: Two new techniques to estimate biomass concentration in the presence of solid substrate were presented. The first technique is based on the measurement of cell density (0.334 g dry weight/cm^3) to estimate the biomass concentration. The second technique is based on the measurement of DNA content of the biomass to estimate the biomass concentration based on the calculated DNA content (mg) per gram of *T.reesei* of 26.1. Both techniques were successfully applied in the *T. reesei* fermentation in presence of insoluble substrates commonly used in the industry.

(7) Oxygen Mass Transfer Coefficient (K_La): A review of the K_La measurement techniques currently available during the solid state and submerged fermentations was performed. Two new estimation techniques were presented: (1) a technique based on the change in agitation and air flow rate and (2) a data reconciliation method using a neural network. Both techniques were used to estimate K_La in different types of fermentation systems.

(8) Publications: The research project also contributed with a total of twelve peer-reviewed articles. Nine of them are presented herein as part of the present thesis. The remainder three papers are part of a parallel project linked to this thesis and are listed below:

   a. Choy, V., Patel, N. and Thibault, J., Application of Image Analysis in the Fungal Fermentation of *Trichoderma reesei* RUT C-30.

   b. Malouf, P., Patel, N., Rodrigue, D. and Thibault, J., Relationship Between Morphology and Rheology During *Trichoderma reesei* RUT C-30

Fermentations. In this study, a rheological characterization protocol was developed to follow the rheology of the fermentation medium. As mentioned earlier, the rheological characterization protocol was developed and some results used in the present study to better understand the interrelationship among all process variables.

c. Choy, V., Patel, N., and Thibault, J., Blood Glucose Monitor: An Alternative Off-line Method to Measure Glucose Concentration During Fermentations with *Trichoderma reesei*, Biotechnology Letters, 29, 1075–1080, 2007.

11.2 FUTURE WORK

Biofuels will certainly become an important alternative to the conventional fuels in this century. However to become successful, there is still a need for more research in this area. The following list offers various recommendations and future work that would need to be looked into to better understand fungi fermentations at the bench and industrial scale.

(1) Apply Image analysis, rheology analysis and oxygen mass transfer estimation techniques developed in this study to the large scale industrial fermentation to optimize the production of cellulase.

(2) As mentioned in Chapter 9 that Rocha-Valadez et al. (2007) during *T. harzianum* experiments found smaller clump diameter for runs performed under higher specific energy dissipation rate and also a strong relationship between rheology and fungal morphology (clump diameter). Therefore, further studies in *T. reesei* especially in CFB with more detailed sample analysis (example rheological characterization) to relate shear stress and other process parameters, such as DO and pH, to the growth and protein production during the *T. reesei* fermentation is required.

(3) The developed feeding strategies based on dissolved oxygen and NH_4OH addition rate needs to be further investigated to develop successful and profitable cellulase fermentation process.

(4) The experiments performed in this study used *T. reesei* strain but the techniques and protocols developed herein can be extended to industrial and proprietary strains of *T. reesei* as well as to other filamentous microorganisms such as *A. niger*. Similar

studies can be carried out using other microorganisms in order to have a better understanding and for further process optimization.

(5) It was observed during this study that there are certain characteristics of *T. reesei* fungi, such as excessive foam formation during the production phase, which could be modified by genetic mutation. This would help in further optimization of the cellulase production. Bailey and Tähtiharju (2003) deleted the genes responsible for foam formation and were able to perform an experiment at high-cellulase productivity for long periods of time without foaming problems.

11.3 FINAL REMARKS

It is forecasted that the proportion of bio-ethanol will increase in Canada and thus, any step at reducing its cost will contribute to boost its use and help meeting the Kyoto protocol targets since emissions due to the fuels used in transportation represent more than 25% of all GHG emissions. It has been suggested that biobased products will change the economics of agriculture around the world (Singh et al., 2003). A greater use of bio-ethanol will also favour the Canadian agriculture economy, as an increase in ethanol use will bring additional sources of revenue for farmers.

The results presented in this thesis attempt to provide a better understanding of the *T. reesei* fermentation process used for cellulase production. It was the main interest of the authors that the techniques developed can be successfully implemented in large scale industrial bioreactors and help in improving the productivity of the cellulase fermentation.

11.4 REFERENCES

Bailey, M. J., Tahtiharju, J., Efficient Cellulase Production by *Trichoderma reesei* in Continuous Cultivation on Lactose Medium with a Computer-Controlled Feeding Strategy. Applied Microbiology and Biotechnology, *62*, 156-162, 2003.

Hanson, J. and Edwards, S., Towards a Biobased Economy: Issues and Challenges Paper. Pollution Probe, 2002.

Maras, M., van Die, I., Contreras, R., and van den Hondel, C. A., Filamentous Fungi As Production Organisms for Glycoproteins of Bio-Medical Interest. Glycoconjugate Journal, *16*: 99-107, 1999.

Rocha-Valadez, J. A., Galindo, E., and Serrano-Carreón, The Influence of Circulation Frequency on Fungal Morphology: A Case Study Considering Kolmogorov Microscale in Constant Specific Energy Dissipation Rate Cultures of *Trichoderma harzianum*. Journal of Biotechnology, *30*: 394-401, 2007.

Schell, D. J., Farmer, J., Hamilton, J., Lyons, B., McMillan, J. D., Saez, J. C., and Tholudur, A., Influence of Operating Conditions and Vessel Size on Oxygen Transfer During Cellulase Production. Applied Biochemistry and Biotechnology, *91-93*: 627-642, 2001.

Singh, S. P., Ekanem, E., Wakefield, T., and Corner, S. Emerging Importance of Bio-Based Products and Bioenergy in the U.S. Economy: Information Dissemination and Training of Students. World Food and Agribusiness Symposium and Forum. 2003. Cancun, Mexico.

APPENDIX

A.1 Schematic diagram of the RPB (a) and STB (b).

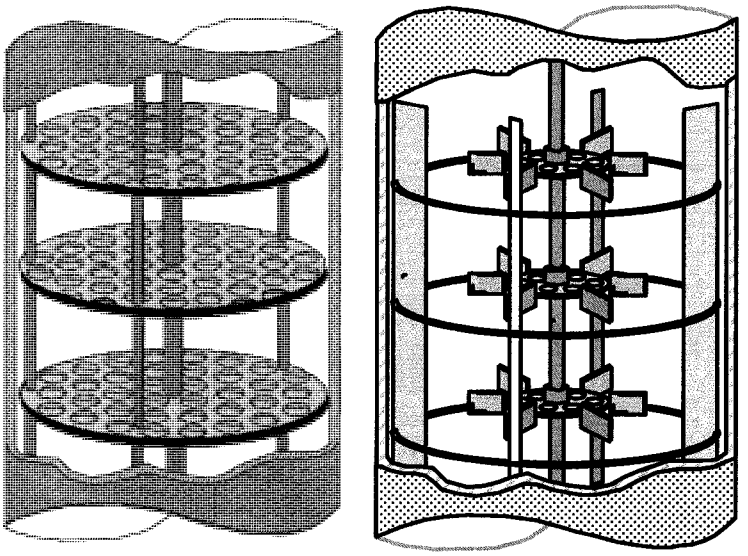

(a) (b)

A.2 Picture of the Couette flow bioreactor set-up.

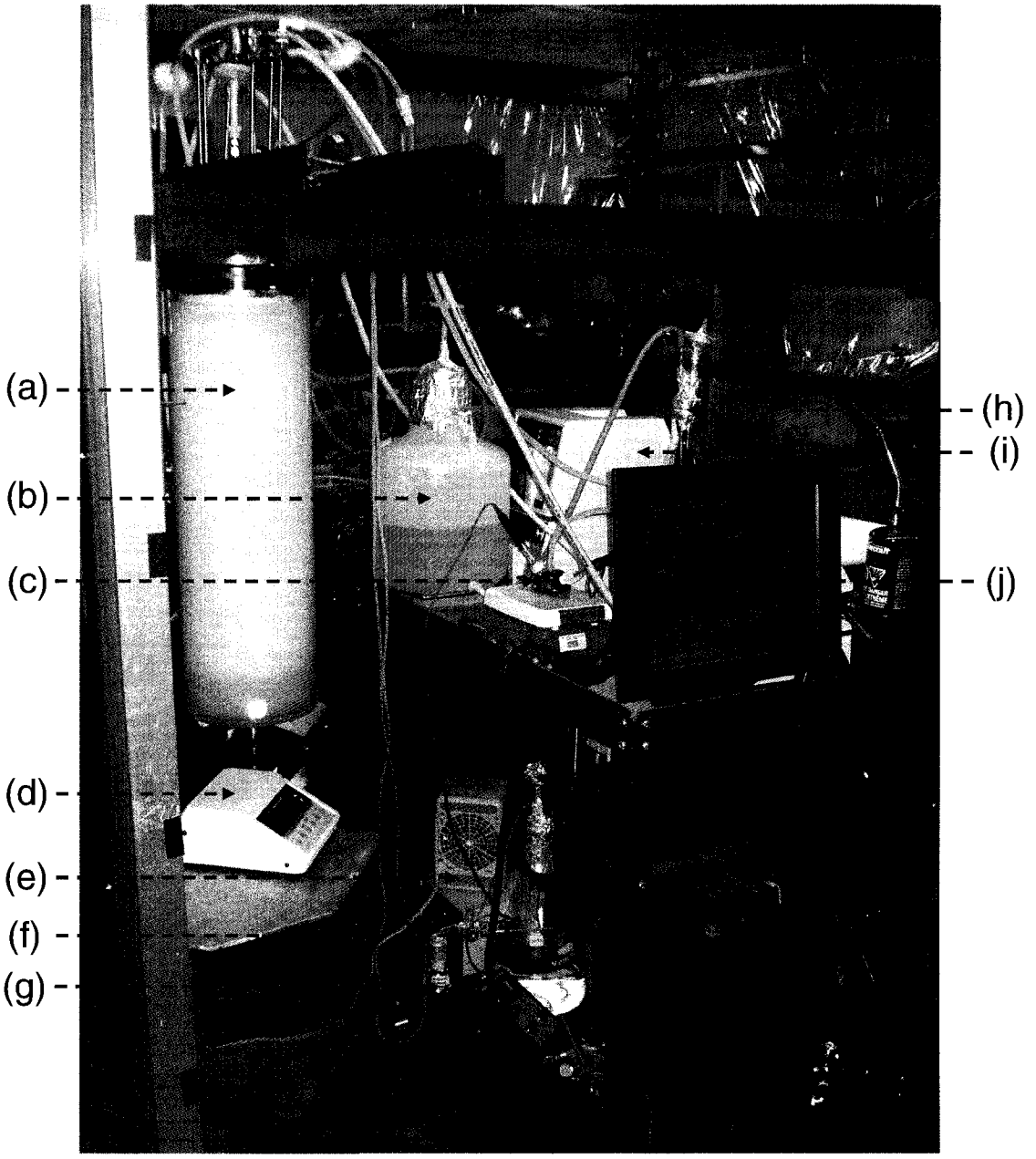

(a) Couette Flow Bioreactor, (b) Substrate, (c) DO & pH probe holder, (d) Agitation controller, (e) Heater, (f) Water, (g) Antifoam, (h) NH_4OH, (i) Pump, and (j) Computer system for control and measurement

A.3 Layout of the LabVIEW program.

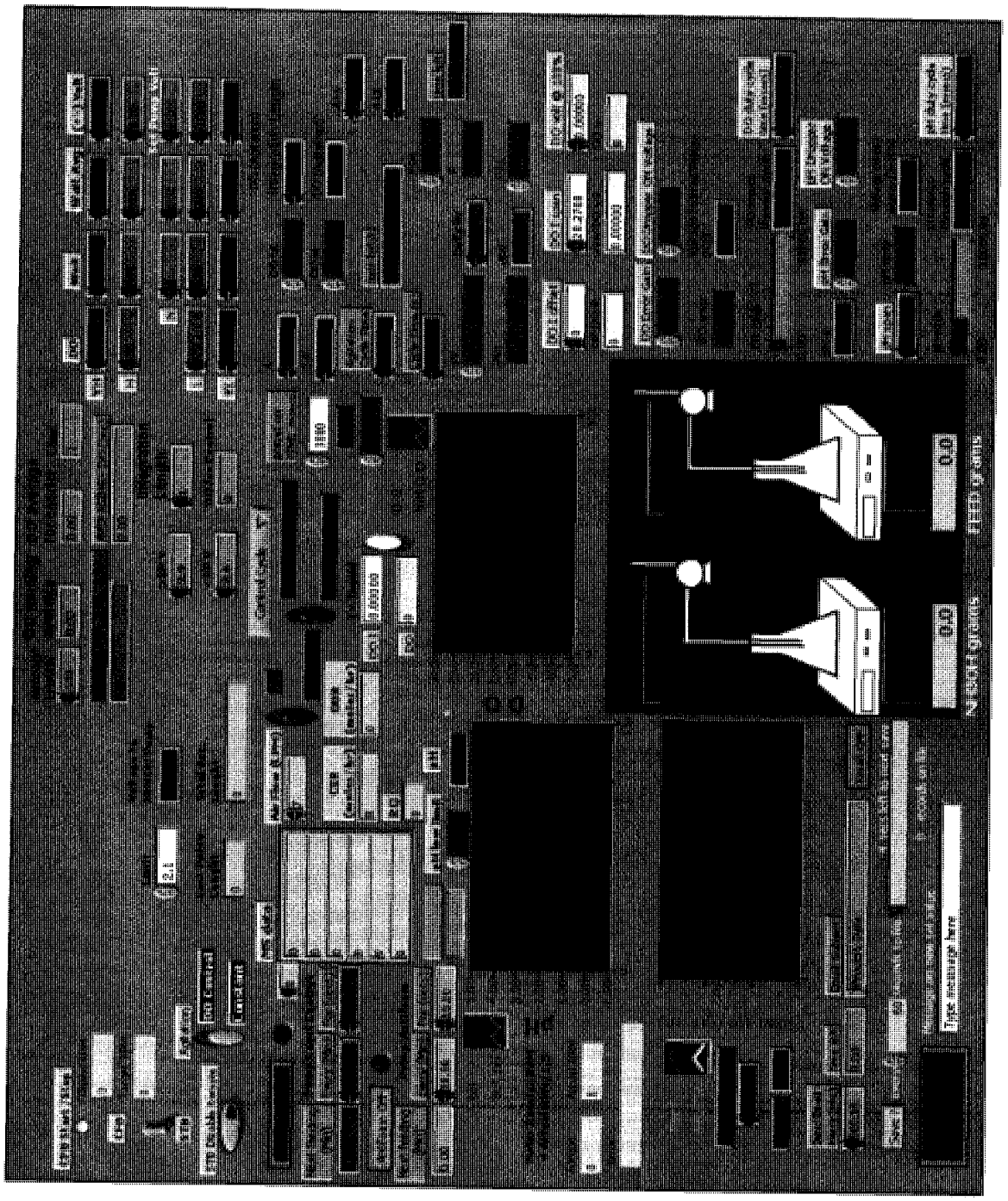

A.4 Schematic diagram of the set-up.

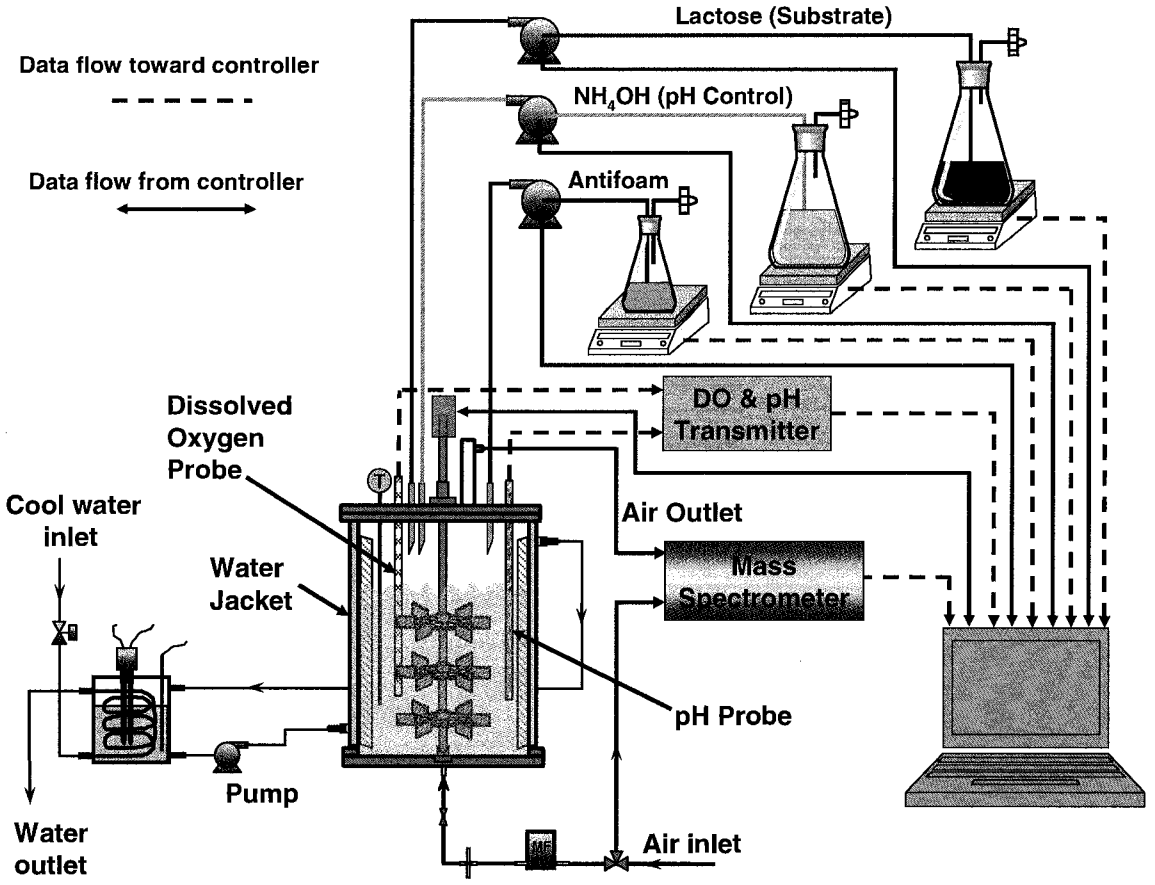

A.5 Picture of the stirred tank bioreactor set-up.

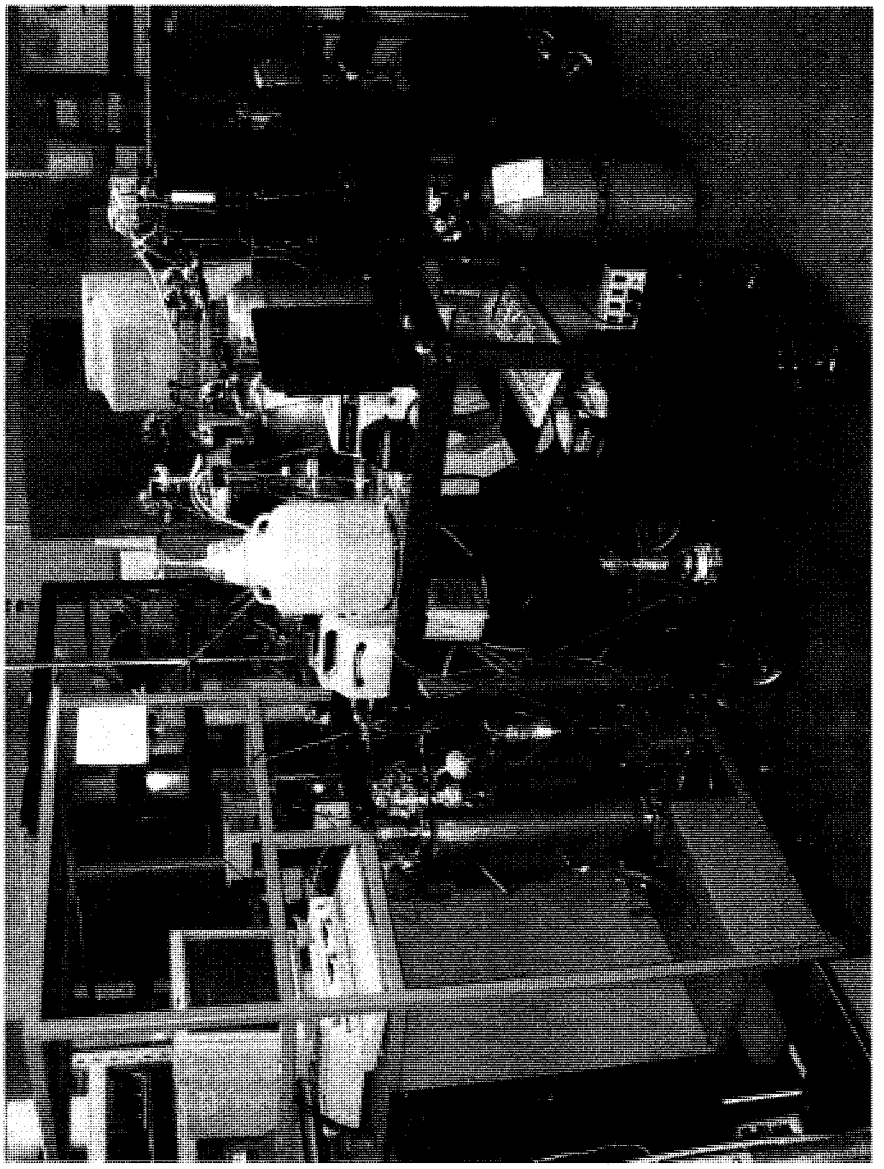

B.1 Medium composition during *T. reesei* fermentation.

Details	Iogen (2006)	Modified (for 17 L)	Mandels 1957	Tangnu 1981	Mandels 1969	Olsson 2003	Juhász 2005
Microorganism	-	RUT C-30	QM 6a	RUT C-30	QM 6a	RUT C-30	RUT C-30
Substrate & Inducer (g/L)	Glucose (13) Lactose	Lactose	Glucose (0.5%)	Cellulose (10, 25, 50%)	Solkafloc (1%)	Cellulose	Solkafloc (7.5)
$(NH_4)_2SO_4$ (g/L)	2.2	2.49	1.4	1.4	1.4	1.4	1.4
KH_2PO_4 (g/L)	1.39	3.6	2	2	2	2	2
$MgSO_4.7H_2O$ (g/L)	0.7	0.53	0.3	0.3	0.3	0.3	$MgSO_4$ (0.3)
$CaCl_2.2H_2O$ (g/L)	0.185	0.33	0.3	0.4	$CaCl_2$ (0.3)	0.4	$CaCl_2$ (0.3)
$FeSO_4.7H_2O$ (mg/L)	1.75	2.975	Fe (1 ppm)	5	5	5	5
$MnSO_4.H_2O$ (mg/L)	0.56	0.952	Mn (0.5 ppm)	1.6	1.56	1.6	$MnSO_4$ (1.6)
$ZnSO_4.7H_2O$ (mg/L)	0.49	0.833	Zn (0.8 ppm)	1.4	1.4	1.4	$ZnSO_4$ (1.4)
$CoCl_2.6H_2O$ (mg/L)	-	-	Co (0.5 ppm)	$CoCl_2$ (2)	$CoCl_2$ (2)	20	$CoCl_2$ (20)
Others (g/L) & Antifoam	CSL (6) Mazu 6000	CSL (10.2) Mazu 6000	Urea (0.3) Yeast Ext. (0.1)	Urea (0.3) T-80 (0.2 mL) Peptone (1) GE-60(0.1%)	Urea (0.3) T-80 (0.1%) Peptone (0.1-0.2%) DowAF (25mg/ml)	Urea (0.3) Yeast Ext. (0.25) Peptone (0.75) Sigma S2121	Urea (0.3) Peptone(0.75) Yeast Ext. (0.25) Dow AF (25mg/ml)

Details	Domingues 2000 & 2001	Weber 2005	Sternberg 1976	Lejeune 1995	Lejeune 1998	Watson 1984	UOttawa 2006**
Microorganism	Rut C30	Rut C30	QM 6a/9123/9414	QM 9414	QM 9414	RUT C30	RUT C30
Substrate & Inducer (g/L)	Lactose (10) / Solkafloc (10)	Glucose Avicel (45)	Cellulose 0.75%	Lactose (10) Avicel (10)	Glucose (20) Lactose (20)	Cellulose (10)	Glucose (13) Lactose
$(NH_4)_2SO_4$ (g/L)	5	1.4	1.4	1.4	4	1.4	1.4
KH_2PO_4 (g/L)	15	2	2	2	2	2	2
$MgSO_4.7H_2O$ (g/L)	1.23	0.6	0.3	0.3	0.6	0.3	0.6
$CaCl_2.2H_2O$ (g/L)	0.8	0.3	0.3	0.3	0.3	0.4	0.3
$FeSO_4.7H_2O$ (mg/L)	2.71	5	5	5	5	9.2	5
$MnSO_4.H_2O$ (mg/L)	1.6	1.6	1.6	1.6	1.6	2	1.6
$ZnSO_4.7H_2O$ (mg/L)	1.4	1.4	1.4	1.4	1.4	2.7	1.4
$CoCl_2.6H_2O$ (mg/L)	3.6	2	2	2	2	2	2
Others (g/L) & Antifoam	Yeast Ext (0.3) Peptone (0.75) T-80 (0.5) Silicone Oil	Urea (0.3) Peptone (1) Tween80 (0.15) Rhodorsil (5mL)	Urea (0.3) Peptone (0.075%) T-80 (0.2%)	Urea (0.3) Peptone (1) Tween80 (0.2) Rhodorsil (5mL)	Urea (0.3) Peptone (1) Tween80 (0.2) Rhodorsil 426R	Urea (0.3) Peptone (1), T-80 (0.1-0.2ml/L)	CSL (6) or Yeast Ext. (0.5) & Peptone (2) Sigma 204

** Nutrient concentration during the fed-batch and continuous mode was adjusted based on the lactose concentration.

C.1 Schematic representation of image processing.

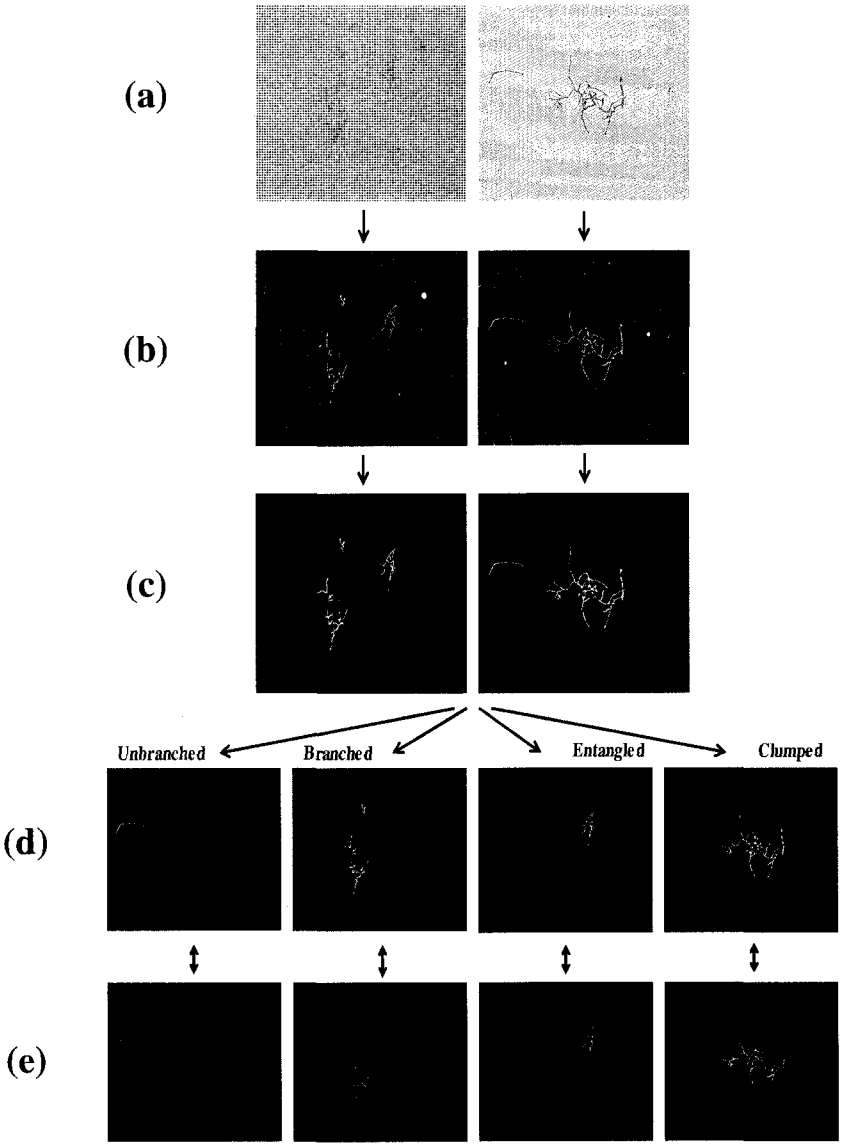

Pictures taken under (a) light microscopy were first transformed into (b) binary images. They were then (c) cleared of artefacts and microorganisms were (d) classified into unbranched, branched, entangled and clumped cells. The viability of the cells was determined by (e) FDA staining under fluorescence microscopy. Pictures were taken with an Olympus IX-81 microscope under x10 original magnification.

D.1 Various steps in CFB set-up.

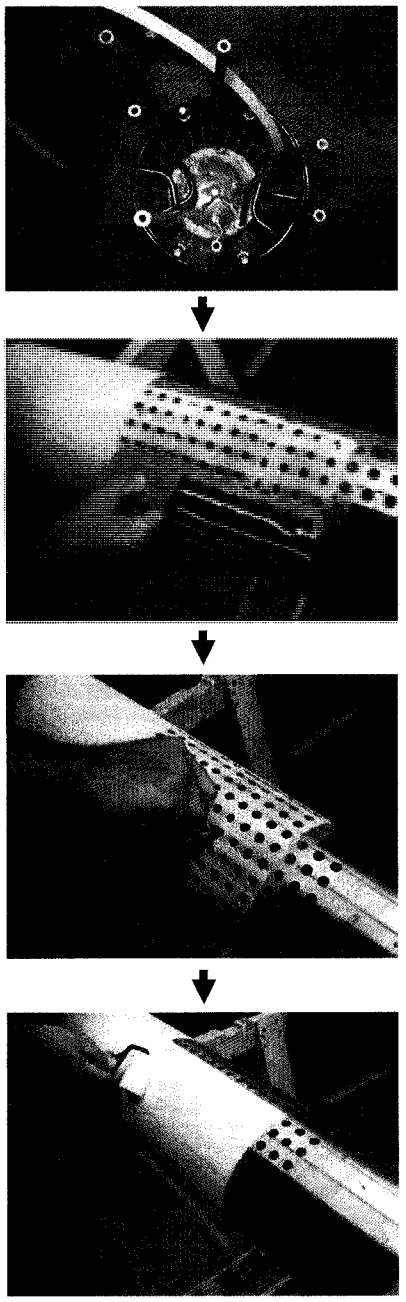

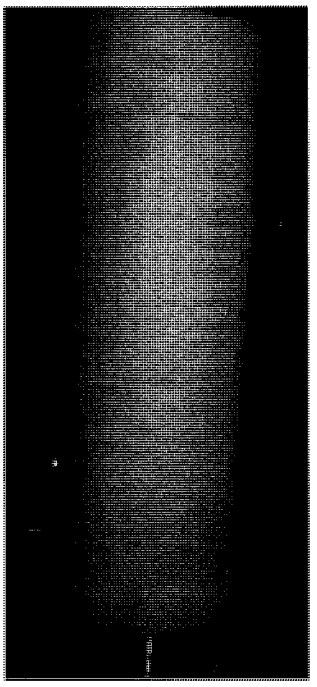

Inner Cylinder with Membrane

Top Ports

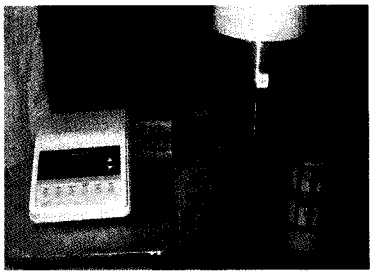

Motor System

E.1 List of experiments performed in RPB.

Date		Run	Operating Conditions
From	To		
26-Jan-2006	02-Feb-2006	RPB 1	0.25 Hz; Batch
17-Feb-2006	20-Feb-2006	RPB 2	0.5 Hz; Batch
20-Apr-2006	22-Apr-2006	RPB 3	0.75 Hz; Batch
01-May-2006	04-May-2006	RPB 4	0.25 Hz; Fed-Batch
01-Jun-2006	06-Jun-2006	RPB 5	0.5 Hz; Fed-Batch
15-Jun-2006	29-Jun-2006	RPB 6	0.25-075 Hz; Fed-Batch
06-Jul-2006	10-Jul-2006	RPB 7	0.75 Hz; Fed-Batch
12-Jul-2006	15-Jul-2006	RPB 8	0.75 Hz; Fed-Batch
17-Jul-2006	18-Jul-2006	RPB 9	0.75 Hz; Fed-Batch
20-Jul-2006	21-Jul-2006	RPB 10	0.75 Hz; Fed-Batch
23-Jul-2006	24-Jul-2006	RPB 11	0.75 Hz; Fed-Batch
21-Feb-2007	22-Feb-2007	RPB 12	0.25 Hz; Fed-Batch
27-Feb-2007	28-Feb-2007	RPB 13	0.25 Hz; Fed-Batch
08-Mar-2007	09-Mar-2007	RPB 14	0.25 Hz; Fed-Batch
15-Mar-2007	15-Mar-2007	RPB 15	0.25 Hz; Fed-Batch
16-Mar-2007	26-Mar-2007	RPB 16	0.25 Hz; Fed-Batch
27-Mar-2007	27-Mar-2007	RPB 17	0.5 Hz; Fed-Batch
31-Mar-2007	06-Apr-2007	RPB 18	0.5 Hz; Fed-Batch
05-May-2007	10-May-2007	RPB 19	0.75 Hz; Fed-Batch
21-May-2007	25-May-2007	RPB 20	1.0 Hz; Fed-Batch
01-Jun-2007	04-Jun-2007	RPB 21	0.75 Hz; Fed-Batch
04-Jun-2007	09-Jun-2007	RPB 22	0.75 Hz; Fed-Batch; Constant Feed/Level
11-Jun-2007	11-Jun-2007	RPB 23	0.75 Hz; Fed-Batch
16-Jun-2007	22-Jun-2007	RPB 24	0.75 Hz; Fed-Batch; Constant-Feed/Level

E.2 List of experiments performed in STB.

Date		Run	Operating Conditions
From	To		
07-Sep-2006	09-Sep-2006	STB 1	300 rpm; Batch
13-Sep-2006	18-Sep-2006	STB2	300 rpm; Fed-Batch
26-Oct-2006	29-Oct-2006	STB 3	500 rpm; Fed-Batch
17-Oct-2006	29-Oct-2006	STB 4	500 rpm; Fed-Batch
30-Oct-2006	04-Nov-2006	STB 5	500 rpm; Fed-Batch
29-Jan-2007	03-Feb-2007	STB 6	300 rpm; Fed-Batch
21-Feb-2007	22-Feb-2007	STB 7	200 rpm; Fed-Batch
24-Feb-2007	26-Feb-2007	STB 8	400 rpm; Batch
27-Feb-2007	28-Feb-2007	STB 9	200 rpm; Fed-Batch
03-Mar-2007	5-Mar-2007	STB 10	500+475 rpm; Fed-Batch
08-Mar-2007	09-Mar-2007	STB 11	200 rpm; Fed-Batch
14-Mar-2007	21-Mar-2007	STB 12	200 rpm; Fed-Batch
27-Mar-2007	30-Mar-2007	STB 13	300 rpm; Fed-Batch
31-Mar-2007	01-Apr-2007	STB 14	400 rpm; Fed-Batch
10-Apr-2007	-	STB 15	400 rpm; Fed-Batch
13-Apr-2007	18-Apr-2007	STB 16	500 rpm; Fed-Batch
05-May-2007	09-May-2007	STB 17	400 rpm; Fed-Batch
21-May-2007	25-May-2007	STB 18	400 rpm; Fed-Batch; Constant Feed
01-Jun-2007	04-Jun-2007	STB 19	400 rpm; Fed-Batch; Constant Feed
05-Jun-2007	09-Jun-2007	STB 20	400 rpm; Fed-Batch
11-Jun-2007	12-Jun-2007	STB 21	400 rpm; Fed-Batch
15-Jun-2007	21-Jun-2007	STB 22	400 rpm; Fed-Batch; Constant Feed/Level
14-Jul-2007	19-Jul-2007	STB 23	400 rpm; Continuous; On/Off/Level Control
28-Jul-2007	31-Jul-2007	STB 24	400 rpm; Continuous; Constant Feed based on DO%
01-Aug-2007	07-Aug-2007	STB 25	400 rpm; Continuous; Constant Feed based on DO%

Date		Run	Operating Conditions
From	To		
19-Aug-2007	22-Aug-2007	STB 26	400 rpm; Continuous; On/Off (control duty cycle)
26-Aug-2007	31-Aug-2007	STB 27	400 rpm; Continuous; Varying feed rate
01-Sep-2007	04-Sep-2007	STB 28	400 rpm; Continuous; Constant Feed based on DO%
10-Sep-2007	14-Sep-2007	STB 29	400 rpm; Continuous; Constant Feed based on DO%
14-Oct-2007	18-Oct-2007	STB 30	400 rpm; Continuous; Varying feed rate
20-Oct-2007	21-Oct-2007	STB 31	400 rpm; Continuous
24-Oct-2007	25-Oct-2007	STB 32	400 rpm; Continuous
26-Oct-2007	30-Oct-2007	STB 33	400 rpm; Continuous; On/Off
11-Dec-2007	14-Dec-2007	STB 34	350-400 rpm; Continuous
17-Jan-2008	22-Jan-2008	STB 35	400 rpm; Continuous
08-Feb-2008	12-Feb-2008	STB 36	400+ rpm; Continuous; DO control → Agitation; Varying feed rate
02-Mar-2008	06-Mar-2008	STB 37	400+ rpm; Continuous; DO control → Agitation; Feed rate → NH_4OH
11-Mar-2008	15-Mar-2008	STB 38	400+ rpm; Continuous; DO control → Agitation; Feed rate → NH_4OH
21-Mar-2008	26-Mar-2008	STB 39	400+ rpm; Continuous; DO control → Agitation; Feed rate → NH_4OH

E.3 List of experiments performed in CFB.

Date		Run	Operating Conditions
From	To		
18-Feb-2007	21-Feb-2007	CFB 1	150 rpm; Batch + Fed-Batch
22-Jul-2007	24-Jul-2007	CFB 2	250 rpm; Batch
16-Sep-2007	-	CFB 3	200 rpm; Batch
05-Nov-2007	-	CFB 4	400 rpm; Batch
08-Nov-2007	09-Nov-2007	CFB 5	400 rpm; Batch
27-Nov-2007	28-Nov-2007	CFB 6	200 rpm; Batch
01-Dec-2007	06-Dec-2007	CFB 7	200 rpm; Continuous
24-Jan-2008	29-Jan-2008	CFB 8	300 rpm; Continuous
31-Jan-2008	06-Feb-2008	CFB 9	100 rpm; Continuous
27-Feb-2008	07-Mar-2008	CFB 10	400 rpm; Continuous